SCANNING METHODS AS MONITORING, VERIFICATION, AND ACCOUNTING TOOLS FOR CO_2 SEQUESTRATION IN UNCONVENTIONAL GAS RESERVOIRS

Joseph David Amante

Thesis submitted to the faculty of Virginia Polytechnic Institute and State University in partial fulfillment of the requirements for the degree of

Master of Science

In

Mining and Minerals Engineering

Nino S. Ripepi, Chair

Mario G. Karfakis

Steven Keim

May 29th, 2015

Blacksburg, Virginia

Keywords: Coal, X-ray computed tomography, permeability, echometer, sequestration

SCANNING METHODS AS MONITORING, VERIFICATION, AND ACCOUNTING TOOLS FOR CO_2 SEQUESTRATION IN UNCONVENTIONAL GAS RESERVOIRS

Joseph David Amante

ABSTRACT

Unconventional gas reservoirs in carbon dioxide sequestration activities is a relatively new and unexplored concept currently undergoing pilot scale testing. Sequestration has the potential for enhancing gas recovery while mitigating carbon dioxide to long term storage structures. Due to the extremely complex systems associated with these unconventional reservoirs, modeling becomes difficult to predict accurately. This thesis presents methods to increase the confidence of inferred parameter testing for unconventional reservoir sequestration in both seam coal bed methane wells and a shale wells. Various tests include the use of computed tomography coupled with Avizo modeling software, inductively coupled mass spectrometer fluid transport analysis, pressure transient build tests, liquid level detection, and desorption analysis coupled with cleat image analysis. Analyses of coals performed by both environmental scanning electron microscope (ESEM) and μCT demonstrate that distributions of cleat porosity in coals are anisotropic and not correlated to the seam depth or location. ESEM is used with μCT scanning to verify the results before and after the impregnation of the carbonic acid. The μCT data in *Avizo Fire*© was used calculate an increase in cleat permeability by 25%. The increase of major flow pathways is caused by the dissolution of carbonates. Changes in the structures were observed qualitatively through ESEM and μCT and quantitatively through Avizo™ and inductively coupled mass spectrometry. The results of comparative study between the cleat structures and the desorption of various seams indicate a trend in the cleat porosity and the desorption rate of the coals as well as the cleat porosity and the total gas in various seams.

ACKNOWLEDGEMENTS

None of this research would be possible without the guidance of my principle investigator, Dr. Nino Ripepi, who has guided me and my crazy ideas into something that produces results. Dr. Ripepi takes research to a whole new level at Virginia Polytechnic Institute and State University by incorporating technologies of other departments. In a day, I could go from ICTAS II computed tomography lab to an off campus Civil Engineering Structures building, to the water quality testing lab in Durham. Every conversation with Dr. Ripepi feels like a brainstorming session rather than a lecture. He leads by example; his dedication to science makes him unafraid to venture out to the field sites in 40 degree weather, pouring rain, and install survey moments by pounding holes into solid rock for other researchers at the Virginia Center for Coal and Energy Research. It has been an absolute privilege to work alongside him and I feel lucky to have acquired a vast amount of knowledge from our time and experiences together. The work presented in this thesis is performed in conjunction with other graduate students and researchers at Virginia Tech. Some of the data presented is a combination of the work from, but not limited to: Andrew Kyle Louk, Charles Scholosser, Cigdem Keles, Ellen Gilliland, Xu Tang, Dr. Nino Ripepi, and various associates at Cardno. The testing occurred with equipment from multiple engineering departments within the university such as the Computed Tomography Lab in ICAST II run by Dr. Rolf Mueller, the ICTAS Nanoscale Characterization and Fabrication Laboratory with the help of Stephen McCartney, and the Civil and Environmental Engineering water lab run by Jeffery Parks. I also want to thank the Department of Energy for funding the project through contract number DE-FE0006827.

TABLE OF CONTENTS

Contents

LIST OF FIGURES

LIST OF TABLES

PREFACE

The results and progression of the thesis is based on the findings in chronological order. The first chapter proves the merits of computed tomography as tool for identifying cleats and other minerals present in various coals. This CT scanning coupled with both electron scanning microscope results and inductively couple mass spectrometry proves that mineral transport is possible and has the potential to greatly influence the reservoir. The next chapter examines the cleat structure from a recently drilled core hole with desorption testing done on select seams to determine the gas in place per seam. This data is also used to predict the possible flow pathways for the sequestration of carbon dioxide. The final chapter is an examination of a piece of equipment called an Echometer and test the precision of the unit and possible benefits and techniques that can be used to measure in the field conditions.

LITERATURE REVIEW

1. INTRODUCTION

The effect of increasing atmospheric carbon dioxide (CO_2) concentrations on global climate change is an important issue facing global society today. In attempt to counteract and mitigate the release of carbon dioxide emission, the U.S Department of Energy established energy research and development programs in carbon sequestration and storage. Long term storage options of CO_2 in thin, unmineable coal seams are just one option of possible geologic structures under investigation (Figueroa et al., 2008). Other options include storage of these CO_2 emissions in: active or depleted oil/gas fields with enhanced oil recovery, gas shales, methane hydrate formations, and deep saline aquifers (Klara et al., 2003). While various options are viable for sequestration projects, ones that allow for the production or enhanced gas recovery of a value based product such as oil, heavy condensates, methane, ethane, and/or propane are preferred to increase economic feasibility of potential projects (Oldenburg et al., 2001). Coal seam sequestration with the recovery of natural gases is an appealing way of addressing the anthropogenic generation of carbon dioxide as it could potentially offset some of the cost of capture, transportation, and storage of carbon dioxide produced from natural gas electrical generation (Rubin et al., 2004).

The technology and practice of injecting CO_2 into geologic formations currently exists and has been practiced for years in conventional oil and gas reservoirs (Malik and Islam, 2000). In December of 1993, BP Amoco performed a small pilot CO_2 injection experiment in the San Juan basin coal from Fruitland Formation in Colorado (Oudinot et al., 2011) to attempt to enhance recovery.

Understanding, quantifying, and qualifying the gas/coal interaction is important to better understand the potential of the reservoirs but is difficult to replicate in the laboratory setting due to complex factors. Predictions concerning stability, internal structure, how the gas is held in place, transportation, and desorption can help provide more reliable input parameters that further refine estimates of gas in place and storage capacity of a reservoir. Investigations of methane production from coal have led to extensive research because of the importance of degasing of underground coal mines for safety (Jackson and Kershaw, 1996. Karacan et al., 2011). The study of the carbon dioxide's capacity in coal seams under in-situ conditions is limited due to difficulties replicating conditions in a laboratory setting (Mirzaeian and Hall, 2006. Gathitu et al., 2009).

When CO_2 interacts with coal, multiple processes occur: first, methane absorbed onto coal is displaced by CO_2 and creates swelling in the coal matrix. Methane then travels into the cleat system of the coal where it begins to move toward an area of lower pressure, normally a production well. Methane desorption causes the coal to shrink, whereas CO_2 absorption causes the coal to swell (White, 2003). In general, coal swelling due to CO_2 absorption is greater than the shrinking caused by methane desorption (Pan and Connell, 2007). The net effect is coal swelling that is larger than the original matrix (White, 2003. Reeves, 2004). The amount of CO_2 absorbed on a particular coal is found to directly coincide with the amount of water present as seen from adsorption isotherms as described by Ekrem Ozdemir in 2009.

The mechanisms for gas flow in coal involves the following: desorption of the gas from the coal surface inside the micropores, diffusion of the gas through the micropores governed by Fick's law, and Darcy flow through the cleat system/natural fracture network in the coal to the wellbore (Liu and Rutqvist, 2010). Once the pressure in the coalbed reservoir is reduced, the coal

becomes less capable of retaining the methane in adsorbed locations. At this point the gas molecules start detaching themselves from the surface of the pore structure and fractures, which begins the process of desorption.

The rate at which these gas molecules desorb is based on the permeability. This permeability is commonly broken into three components: desorption from the internal coal surface, diffusion through the matrix and micropores, and fluid flow in the natural fracture network seen in Figure 1 (Crosdale et al., 1998).

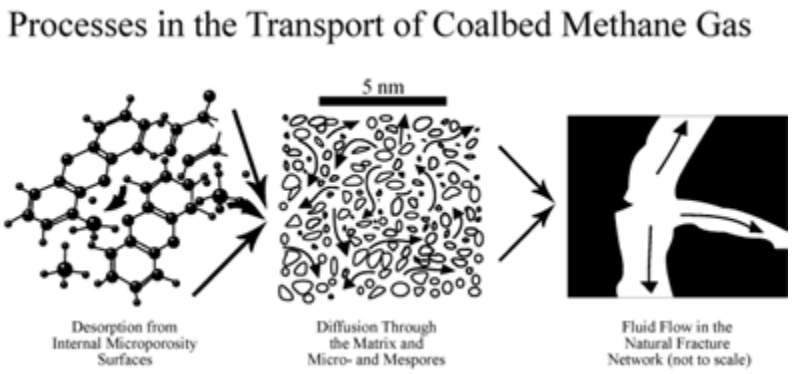

Figure 1: Coalbed methane transport ("How Do You Get Coalbed Methane?" http://www.tridentexploration.ca/how-do-you-get-coalbed-methane/details. Web. 31 Mar. 2015 Used under fair use, 2015)

Most numerical models use the spacing of the butt and face cleat to create units or blocks to determine how far the gas has to diffuse before reaching the fracture network. The desorption of the gas in the coal causes the permeability to increase due to the shrinkage (Harpalani and Chen, 1997). Most modeling studies assume that cleats are small in terms of length, height, and aperture (Crosdale et al., 1998). Cleat structures can be extremely heterogeneous in nature within the same seam over a small area. Cleat spacing changes with coal rank significantly with the smallest spacing in lignite, increasing through medium volatile bituminous coal. A very detailed analysis of cleat structures was made by Laubach et al. (1998).

Fractures and cleats are the critical parameters for economic viability of coalbed methane and CO_2 sequestration. At the initial stage of production, the cleats are under pressure, methane gas desorbs, and the released gas diffuses through the coal matric until it reaches a cleat system, and then flows through the cleat network to the wellbore (Mandal et al., 2004). This permeability directly relates to the feasibility of a well or oil field.

2. CARBON CAPTURE, STORAGE, AND UTILIZATION

Reducing the levels of anthropogenic carbon dioxide emission has been a concern of the public for many years as concerns of global temperatures show "trends". Carbon dioxide is an important greenhouse gas listed by the Environmental Protection Agency due to the dependence on fossil fuels as an energy source. Thirty-eight percent of emissions in the United States are produced by electrical generation from the combustion of fossil fuels (Carbon Dioxide Emissions EPA, 2014). This process of storage and utilization may be broken into three parts: capture, storage, and utilization. Carbon capture, storage, and utilization is a major player in technological advances to attempt to reduce these CO_2 emissions (Azar et al., 2006). The storage mainly discussed in these projects is by the capture of CO_2 from fossil fuel electrical generation stations.

The technology presently used to capture the emissions from the electrical generation plants and can reduce emissions by as much as 80-90% (Metz et al., 2005). This capture comes at a cost to the consumer and the electrical power generation station. Christian Azar conducted an economic study of carbon capture in 2006 and concluded that from the process of capturing the carbon dioxide would reduce the efficiency of coal, natural gas, oil, and biomass plants by 10% while raising the price of electricity dramatically. CO_2 capture can be implemented in three

stages of the combustion cycle: post combustion, pre combustion, and oxy-fuel capture. However, each process presents challenges and advantages. The most common methods of capture are: absorption, separation by membranes, and cryogenic separation (Pires et al., 2011. Steeneveldt et al., 2006).

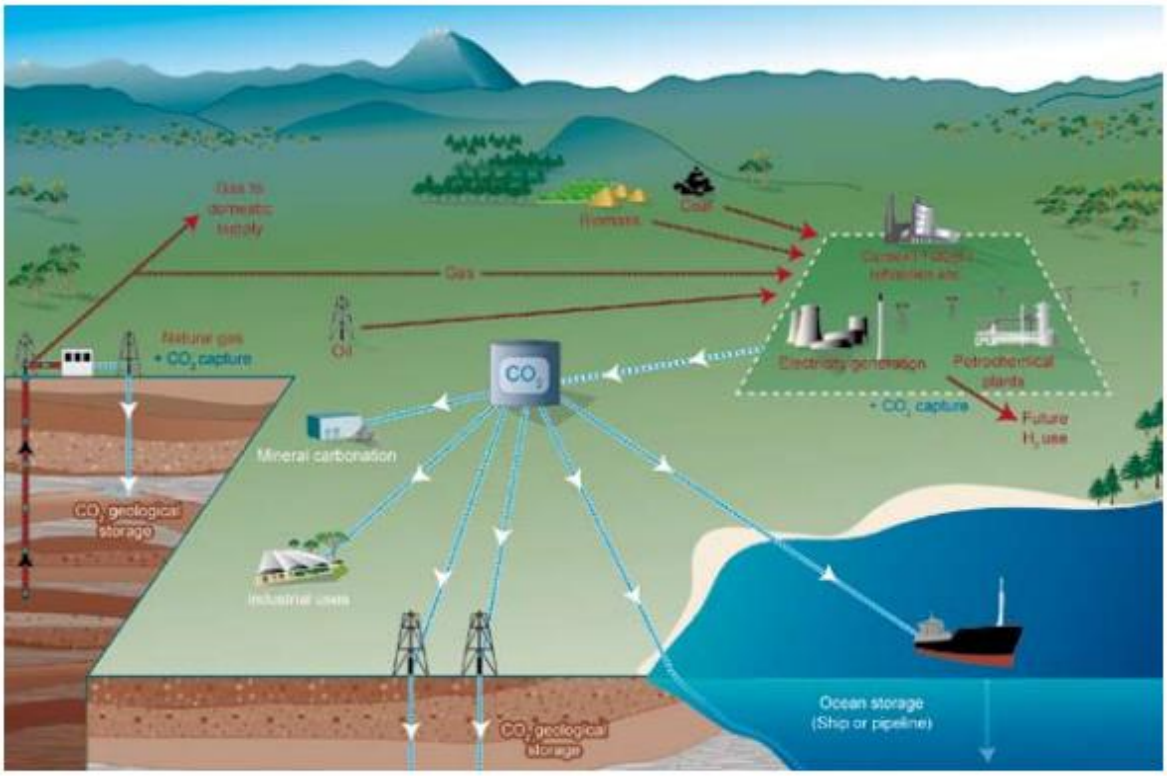

Figure 2: Sequestration Methods and Options (Metz, Bert, et al. "IPCC special report on carbon dioxide capture and storage. Prepared by Working Group III of the Intergovernmental Panel on Climate Change." *IPCC, Cambridge University Press: Cambridge, United Kingdom and New York, USA* 4 (2005)) used under fair use, 2015

Depending upon the location of the capture facility, several options are available for transportation to potential storage options; the most mature market is pipelines to oil fields while others including trucking (Metz et al., 2005). The injection of CO_2 for enhanced oil recovery is a proven mechanism for oil recovery and is commonly used (Metz et al., 2005. Pires et al., 2011). Other options for storage include:

1). Geologic storage in:

A). Gas/Oil fields

B). Saline formations

C). Enhanced Coal Bed Methane Recovery

2). Ocean Storage

A). Direct injection (dissolution type)

B). Direct injection (lake type)

3). Mineral carbonation

A). Natural silicate minerals

B). Waste materials

While mineral carbonation and ocean storage are still in the research and demonstration phase, short term geologic storage studies show potential for long term storage options and implementation through the oil industry. Geologic storage relies on injection at great depths to maintain temperature and pressure above the critical temperature of carbon dioxide (Gibbins and Chalmers, 2008). CO_2 can be injected into suitable saline formations or oil fields at depths below 2,000 feet that have appropriate geochemical trapping formations to prevent leakages to the surface (Ennis-King and Patterson, 2003).

3. ENHANCED RECOVERY ON COAL BED METHANE WELLS

In the past decade, new technologies have been proposed to enhance the recovery potential of coal bed methane through two main concepts: stripping and displacement. Stripping of methane gas through the use of nitrogen (N_2-ECBM) is capable of recovering 90% more gas in place than conventional means (Reeves and Oudinot, 2004). Nitrogen stripping works by lowering the partial pressure of methane to promote the desorption process. Rapid injection of nitrogen will increase methane production rates. The timing and quantity of nitrogen needed to effectively

increase rates depends on a vast quantity of parameters such as: well spacing, thickness of seam, permeability, pore network, gas composition, etc. Nitrogen injection is normally halted when gas content of offset wells reaches 50% nitrogen in composition (Reeves and Oudinot, 2004).

In CO_2 enhanced recovery, the injected CO_2 is preferentially adsorbed which then shears the methane molecule out of the coal. This molecule of methane is then considered free gas. Laboratory isotherm testing demonstrates that coal can roughly adsorb twice the volume of CO_2 as methane (Jikich et al., 2008). The production increase associated with CO_2 enhanced recovery takes longer than nitrogen injection. This can be accounted for due to the absorption of the CO_2 relatively near the well bore with the absorbed CO_2/methane front growing elliptically out from the injection well in the hydraulic fracture direction or the face cleat direction. This CO_2 plume will be present in significant quantities in the offset wells and the injection will be terminated. When CO_2 breakthrough is seen early in the injection phase it may be stripped and reinjected into the formation. CO_2 enhanced recovery has the potential for providing a storage mechanism for anthropogenic carbon dioxide, as well as improving production of coal bed methane wells. If the area is left undisturbed, it is likely that the sequestrated carbon dioxide would be stored on geologic time scale. If the area is disturbed, this could potentially to void the benefit of the sequestration event by venting the carbon dioxide to the atmosphere.

The concept of sequestration of carbon dioxide into coal seams is not a new concept. In the late 1980s Amoco Corporation developed the concept for nitrogen enhanced coal bed methane. In 1993, Amoco successfully demonstrated the process in a pilot project in the San Juan Basin in Colorado. Later that year 1993, Amoco undertook a CO_2 enhanced coal bed methane pilot project but the performance results were unreleased to the public. Since 1996,

Burlington Resources and Amoco have been operating a proof of concept on a 13 well CO_2 ECBM in the San Juan Basin. The project is located in the Allison production unit. The wells tested were sub-average producers averaging around 23000 m^3/day. The Allison pilot test injected 85,000 m^3/day of naturally occurring CO_2 from the McElmo Dome, which was piped through the area to West Texas to aid in enhanced oil recovery (Reeves, 2004). The 13 wells for the project consist of nine producer wells and four injections wells. Production was based on using conventional pressure depletion methods for about five years prior to injection. The four injection wells were not hydraulically stimulated to potentially reduce the risk of CO_2 leakage. Pilot performance varies depending on the well. Severe water encroachment was present in the wells during the shut in period of six months after the injection phase. The theory behind the shut in period was to encourage CO_2 methane transfer in the desired reservoir and limit CO_2 breakthrough. When production finally resumed after the CO_2 injection, the rates were less than the pre-injection rates. Water production increased dramatically and the enhancement was strongest in the only well that had not been shut in. A positive indication of sequestration or no CO_2 breakthrough is that the CO_2 content of the produced gas remained unchanged throughout the injection period despite the injection of 57 million cubic meters of CO_2. The Allison project suggests that enhanced recovery is possible with the injection of CO_2 into coal seams based on results published at various conferences (Reeves, 2004). It does not demonstrate the potential for long-term geologic storage since a monitoring program was not implemented around the area.

4. ENHANCED RECOVERY OF SHALE WELLS

Shale wells, compared to their counterpart coal bed methane wells, present additional challenges and mechanisms for natural gas transport. Unconventional gas reservoirs can be characterized

with complex geologic systems and petrophysical systems that typically consist of very fine grain textures. These textures and carbon content exhibit gas storage and flow characteristics that interact on the nano-scale level which serve as gas sorption sites (Sondergeld et al., 2010). Gaseous shale has free gas stored in the pores of the rock matrix as well as gas adsorbed on the surface area of the organic content and clays (Dahaghi, 2010). Shale gas has ultra-low permeability compared to conventional resources which rendered this resource uneconomic until hydraulic fracturing and horizontal drilling successfully stimulated an area around the well. Most prolific shale exploited in the United States are flat, thick, and predictable which attributes to long predictable rates of gas production (Dahaghi, 2010).

Carbon dioxide is used in conventional gas wells due to its preferential adsorption. The same mechanism can be employed in unconventional reservoirs to adsorb to the primary pore system, driving the methane to the secondary pore, increasing the pressure and causing the methane to flow to the production well (Shi and Durucan, 2003). Upon adsorption of the carbon dioxide molecule the shale matrix swells which affects the pore pressure, pore volume, and permeability. This occurrence has been modeled using a modified Pamer-Mansoori Method published by Mavor and Gunter (2006).

5. EQUIPMENT UTILIZED FOR INTERNAL INVESTIGATIONS

Computed tomography (CT) is a non-destructive radiographic imaging technique for producing three dimensional computerized models of objects. CT scanners reconstruct digital data in cross sectional slices, which can be stacked to create a three-dimensional rendering (Masschaele, 2012). The CT scanning device used in this experiment is the SkyScan model 1172. Electromagnetic radiation passes through the specimen and attenuation of signal is

received by the detector. The specimen rotates 180-360 degrees, depending on the level of accuracy required, while being scanned and with each angle the detector obtains a corresponding signal. Image reconstruction is made by mathematical transformation of all these angles' signals. The X-ray is a cone beam with a specific width, and the images obtained from every layer have a certain scanning thickness. Every image reflects average value of the linear attenuation coefficient inside the material with a specific thickness (Mao et al., 2007). The linear attenuation coefficient of a sample is composed by several materials, regardless of whether it is a compound, mixture, or solid solution, and has no relationship with the material aggregation. The linear attenuation coefficient is equal to sum of the linear attenuation coefficient of different components contained in the material multiplied by mass percentage of the same ingredient in the sample (Jikich et al., 2008). It is difficult to measure the material's attenuation coefficient directly, and CT number is used to quantitatively describe the attenuation. With reference to a certain proportion, the CT number can be converted into grey values, which are shown as CT images (Abel et al., 2012). The material linear attenuation coefficient has an approximate linear relationship with the density of the material, so the CT images will reflect the changes in material density (Zhang et al., 2009).

Medical CT scanning has been utilized in the past to scan coals (Yao et al., 2009). The resolution of the CT scanner used by Yanbin Yao does not provide adequate resolution to observe smaller cleat structures. This may be achieved through the use of a μCT scanner. The μCT scanner provides a smaller focal spot with a reduced electron current to provide higher resolution of scans. The typical current of a micro-focus tube is 100 μA, which is a 1000 times less powerful than a medical scanner. The lower X-ray flux results in longer scan times. As μCT is never applied to humans the object that is rotated in the path of the X-ray beams which

requires uniform circular samples for best accuracy. Besides a clearer distinction between pores and material, some bright spots occur in the reconstruction images. The difference is apparent, however, it remains difficult to identify possible minerals due to artifacts occurring (star-artifacts, beam-hardening, and ring artifacts) due to a partial volume effect. With no prior knowledge of the composing minerals this method of identification is not powerful, since not only is the atomic number responsible for the attenuation, but also the density. To identify these 'spots', a scanning electron microscope is used in conjunction with back scatter electron images (Cnudde et al., 2006).

Scanning Electron Microscope (SEM) is an automated image analysis system which uses back scattered electron and energy dispersive X-ray signals from a scanning electron microscope to create digital images across the sample surface. Each pixel in these images contains information, derived from BSE and energy dispersive spectrometry (EDS) data, on the chemistry of the mineral, matrix, or organic component that make up an individual small region under the electron beam (Danilatos, 1990). The unit is coupled to a computer, which controls the movement of the sample stage and the electron beam and also collects and analyses the data from the various measurement devices. In particular, data on the chemistry of each pixel site are converted by the computer to qualitative data on mineralogy due to the association of chemical elements present (Creelman and Ward, 1996).

Samples are typically sputter-coated which is a technique of depositing a metal coating on specimen surfaces to be examined with an environmental scanning electron microscope (ESEM). The dried samples are attached to support stubs with a variety of materials (colloidal silver, colloidal carbon, double sided tape, or conductive carbon tape) prior to coating with precious metals such as gold-palladium to ensure the electrical conductivity of the specimen

surface. In modern sputter coating, the temperature rise during the evaporation process increases to less than 10˚C and in many cases is stronger for a very sensitive sample that is free of heat damage (Cnudde et al., 2006)). By using a more simple procedure for ESEM preparation, the sample requires fewer hours before reaching the electron microscopy phase (Muscariello et al., 2005). Another option, which is more common, is to grind coal samples and then mount them via epoxies or carbon support films. While this method does not present the results with the internal structure of the coal it does have advantages. The most notable advantages are the ease of preparation and lack of artifacts introduction from the milling process. In addition, since nearly all the particles clinging to the coating have some area transparent to the electron beam, a much greater amount of thin area more randomly dispersed from within the whole coal sample is potentially available for examination than would be found in specimens thinned from bulk. Results obtained from powdered coal specimens in theory should contain a more representative sample of the bulk composition of the coal in question (Creelman and Ward, 1996).

Currently, ESEM is a widely applied method for determining the size, association, composition and abundance of minerals in coal. The mineral constituents appear in differences in back scatter electron emission coefficient of the mineral analyzed. The higher the atomic number, the greater the contrast is in back scatter electron emission (Galbreath et al., 1996).

6. REFERENCES

Abel, R. L., Laurini, C. R., & Richter, M. (2012). A palaeobiologist's guide to 'virtual'micro-CT preparation. Palaeontologia Electronica, 15(2), 15-2.

Azar, Christian, et al. "Carbon capture and storage from fossil fuels and biomass–Costs and potential role in stabilizing the atmosphere." *Climatic Change* 74.1-3 (2006): 47-79.

"Carbon Dioxide Emissions." EPA. Environmental Protection Agency, 2 July 2014. Web. 17 Jan. 2015. http://www.epa.gov/climatechange/ghgemissions/gases/co2.html

Cnudde, V., Masschaele, B., Dierick, M., Vlassenbroeck, J., Van Hoorebeke, L., & Jacobs, P. (2006). Recent progress in X-ray CT as a geosciences tool.Applied Geochemistry, 21(5), 826-832.

Creelman, R. A., & Ward, C. R. (1996). A scanning electron microscope method for automated, quantitative analysis of mineral matter in coal.International Journal of Coal Geology, 30(3), 249-269.

Crosdale, Peter J., B. Basil Beamish, and Marjorie Valix. "Coalbed methane sorption related to coal composition." *International Journal of Coal Geology*35.1 (1998): 147-158.

Dahaghi, Amirmasoud Kalantari. "Numerical simulation and modeling of enhanced gas recovery and CO2 sequestration in shale gas reservoirs: A feasibility study." *SPE International Conference on CO2 Capture Storage and Utilization*. Society of Petroleum Engineers, 2010.

Danilatos, G. D. (1990). Theory of the gaseous detector device in the environmental scanning electron microscope. Advances in Electronics and Electron Physics, 78, 1-102.

Ennis-King, Jonathan, and Lincoln Paterson. "Role of convective mixing in the long-term storage of carbon dioxide in deep saline formations." *SPE annual technical conference and exhibition*. Society of Petroleum Engineers, 2003.

Figueroa, José D., et al. "Advances in CO 2 capture technology—the US Department of Energy's Carbon Sequestration Program." International Journal of Greenhouse Gas Control 2.1 (2008): 9-20.

Galbreath K, C. Zygarlicke, G. Casuccio, T. Moore, P. Gottlieb, N. Agron-Olshina, G. Huffman, A. Shah, N. Yang, J. Vleeskens, and G. Hamburg. (1996) 'Collaborative study of quantitative coal mineral analysis using computer-controlled scanning electron microscopy'. *Fuel* Vol. 75 No. 4, pp. 424-430

Gathitu, Benson B., Wei-Yin Chen, and Michael McClure. "Effects of coal interaction with supercritical CO2: physical structure." *Industrial & Engineering Chemistry Research* 48.10 (2009): 5024-5034.

Gibbins, Jon, and Hannah Chalmers. "Carbon capture and storage." *Energy Policy* 36.12 (2008): 4317-4322.

Harpalani, Satya, and Guoliang Chen. "Influence of gas production induced volumetric strain on permeability of coal." *Geotechnical & Geological Engineering* 15.4 (1997): 303-325

"How Do You Get Coalbed Methane?" Http://www.tridentexploration.ca/how-do-you-get-coalbed-methane/details. Web. 31 Mar. 2015.

Jackson, P., and S. Kershaw. "Reducing long term methane emissions resulting from coal mining." Energy conversion and management 37.6 (1996): 801-806.

Jikich, S, R. Lendon, K. Seshadri, G. Irdi, and D. Smith. (2008) 'Carbon Dioxed Transport and Sorption Behavior in Confined Coal Cores for Enhanced Coalbed Methane and CO2 sequestration". *National Energy Technology Laboratory and Department of Energy*, IR-2008-029

Karacan, C. Özgen, et al. "Coal mine methane: a review of capture and utilization practices with benefits to mining safety and to greenhouse gas reduction." International Journal of Coal Geology 86.2 (2011): 121-156.

Klara, Scott M., Rameshwar D. Srivastava, and Howard G. McIlvried. "Integrated collaborative technology development program for CO 2 sequestration in geologic formations—United States Department of Energy R&D." Energy Conversion and Management 44.17 (2003): 2699-2712.

Laubach, S. E., et al. "Characteristics and origins of coal cleat: a review."International Journal of Coal Geology 35.1 (1998): 175-207

Liu, Hui-Hai, and Jonny Rutqvist. "A new coal-permeability model: internal swelling stress and fracture–matrix interaction." *Transport in Porous Media* 82.1 (2010): 157-171.

Malik, Qamar M., and M. R. Islam. "CO2 Injection in the Weyburn field of Canada: optimization of enhanced oil recovery and greenhouse gas storage with horizontal wells." *SPE/DOE improved oil recovery symposium*. Society of Petroleum Engineers, 2000.

Mandal, Dipak, D.C. Tewari, and M.S. Rautela, "Analysis of Micro-fractures in Coal for Coal Bed Methane Exploitation in Jharia Coal Field". *5th Conference & Exposition on Petroleum Geophysics,* Hyderabad-2004, India p 904-909

Mao, L, P. Shi, H. Tu, L. An, Y. Ju, and N. Hao. (2012) 'Porosity Analsysis Based on CT Images of Coal under Uniaxial Loading', *Advances in Computed Tomography*, pp. 5-10

Masschaele, Bert. (2007) 'High resolution computed tomography at the Ghent University: measuring, visualizing and analyzing the internal structure of objects with sub-micron precision.' Proceedings of Science 46: 1-8.

Mavor, Matthew J., and William D. Gunter. "Secondary porosity and permeability of coal vs. gas composition and pressure." *SPE Reservoir Evaluation & Engineering* 9.02 (2006): 114-125.

Metz, Bert, et al. "IPCC special report on carbon dioxide capture and storage. Prepared by Working Group III of the Intergovernmental Panel on Climate Change." *IPCC, Cambridge University Press: Cambridge, United Kingdom and New York, USA* 4 (2005)

Mirzaeian, Mojtaba, and Peter J. Hall. "The interactions of coal with CO2 and its effects on coal structure." *Energy & fuels* 20.5 (2006): 2022-2027.

Muscariello L., F. Rosso, G. Marino, A. Giordano, M. Barbarisi, G. Cafiero, and A. Barbarisi. (2005) 'A Critical Overview of ESEM Applications in the Biological Field'. *Journal of Cellular Physiology* 205:328-334

Oldenburg, C. M., Karsten Pruess, and Sally M. Benson. "Process modeling of CO2 injection into natural gas reservoirs for carbon sequestration and enhanced gas recovery." Energy & Fuels 15.2 (2001): 293-298.

Oudinot, Anne Y., et al. "CO2 Injection Performance in the Fruitland Coal Fairway San Juan Basin: Results of a Field Pilot." *SPE Journal* 16.04 (2011): 864-879

Ozdemir, Ekrem, and Karl Schroeder. "Effect of moisture on adsorption isotherms and adsorption capacities of CO2 on coals." *Energy & Fuels* 23.5 (2009): 2821-2831.

Pan, Zhejun, and Luke D. Connell. "A theoretical model for gas adsorption-induced coal swelling." *International Journal of Coal Geology* 69.4 (2007): 243-252.

Pires, J. C. M., et al. "Recent developments on carbon capture and storage: An overview." *Chemical Engineering Research and Design* 89.9 (2011): 1446-1460

Reeves, Scott R. "The Coal-Seq project: Key results from field, laboratory and modeling studies." *Proceedings of the 7th International Conference on Greenhouse Gas Control Technologies (GHGT-7)*. 2004.

Reeves, Scott, and Anne Oudinot. *The Tiffany Unit N2-ECBM Pilot: A Reservoir Modeling Study*. Advanced Resources International, Incorporated, 2004.

Rubin, Edward S., Anand B. Rao, and Chao Chen. "Comparative assessments of fossil fuel power plants with CO2 capture and storage." (2004): 285.

Shi, J. Q., and S. Durucan. "A bidisperse pore diffusion model for methane displacement desorption in coal by CO2 injection." *Fuel* 82.10 (2003): 1219-1229.

Sondergeld, Carl H., et al. "Petrophysical considerations in evaluating and producing shale gas resources." *SPE Unconventional Gas Conference*. Society of Petroleum Engineers, 2010.

Steeneveldt, R., B. Berger, and T. A. Torp. "CO 2 Capture and Storage: Closing the Knowing–Doing Gap." *Chemical Engineering Research and Design* 84.9 (2006): 739-76

White, Curt, "An Initail Set of Working Hypotheses Concerning Some Chemical and Physical Events When CO2 is Injected into a Coalbed", *Fuel Chemistry Division Preprints* 2003, 48(1), 114.

Yao, Y, D. Liu, Y. Che, D. Tang, S. Tang, and W Huang. (2009) 'Non-destructive characterization of coal samples from China using microfocus X-ray computed tomography'. *International Journal of Coal Geology* 80 113-123

Zhang, C.Z., Z.P. Guo, P. Zhang, *et al.* (2009) 'Industrial Computer Tomography Technique & Theory,' *Science Press House*, Beijing .

COAL CLEAT ALTERATION DUE TO CO_2 SEQUESTRATION

Results and summary presented for 2014 Pittsburgh Coal Conference and submitted to the International Journal of Oil, Gas and Coal Technology

1. ABSTRACT

Computed tomography (CT) is used in characterizing coal fractures and permeability. The introduction of carbonic acid from the sequestration of carbon dioxide reacting with water is a mechanism for dissolution of minerals in coals. The spatial distribution of fractures and mineralization are semi-quantitatively evaluated by μCT using computer-aided design. Analyses of coals performed by both environmental scanning electron microscope (ESEM) and μCT demonstrate that distributions of cleat porosity in coals are anisotropic and not correlated to the seam depth or location. ESEM is used with μCT scanning to verify the results before and after the impregnation of the carbonic acid. The μCT data in *Avizo Fire*© was used calculate an increase in cleat permeability by 25%. The increase of major flow pathways is caused by the dissolution of carbonates. Changes in the structures were observed qualitatively through ESEM and μCT and quantitatively through Avizo™ and inductively coupled mass spectrometry.

2. INTRODUCTION

Coal is an intricate polymeric material with multifaceted porous structures. The main physical constituents of coal include coal matrix which is made up of the organic carbon components, void-space volume occupied by pore sand fractures, and mineral inorganic constituents (Ritz and Klika, 2010). The organic components influence the methane adsorption capacity and diffusion, while pores, fractures, and cleats are the important flow pathways that determine the permeability and producibility of coalbed methane (Stock and Muntean, 1993).

Moreover, the permeability and producibility would be reduced when the void-space is filled with minerals such as calcite, quartz, and siltstones. Quantification of the volume and spatial disposition of pores, fractures and minerals in coals is a primary and fundamental requirement for carbon dioxide sequestration reservoir evaluation (Yao et al., 2009).

Previous methods for determining porosity and surface area are deficient for evaluating internal coal heterogeneity in three dimensions. At the same time, some methods are destructive to the samples, and may result in some misleading information on the pores, fractures, or internal pathways with is caused by grinding, drilling, and processing. New non-destructive techniques are needed to evaluate pores, fractures, and cleats in coals that can realistic provide repeatable results.

Computed tomography (CT) is a non-destructive technique that can provide quantitative detection of interior configuration of samples in 3D, and it has been broadly used in geological research of various coals to characterize zones of adsorption in a sample (Karacan and Okandan, 2000, 2001) (Karacan and Mitchell, 2003). The μCT scanner utilizes a microfocal source that makes it possible to scan small objects with a spatial resolution down to 3 micrometers (μm). Recently, CT techniques have shown promising prospects for applications in coal petrological and petrophysical researches (Golab et al., 2013).

The presence of high pressure CO_2 and water can have a profound effect on the mineral matter present in coal. Many minerals present in coal are soluble in acidic aqueous solutions. The solubility of CO_2 in water is substantial at high pressures. Calcite, dolomite, and other carbonate minerals are removed from coal at room temperature by extraction under acidic conditions with aqueous CO_2 solutions (R. Jahnke and D. Jahnke, 2004).

This process of dissolving carbon dioxide in water to form carbonic acid is common in nature and is a driving factor for cave development, stalactites, and stalagmite growth. The chemical reaction is shown below.

$$CO_2(g) + H_2O(l) \rightarrow H_2CO_3(aq)$$

$$H_2C0_3(aq) + 2OH^-(aq) \rightarrow {CO_3}^{-2}(aq) + 4H_2O(l)$$

$$Ca^{2+}(aq) + {CO_3}^{-2}(aq) \rightarrow CaCO_3\ (s)$$

As calcium carbonate precipitates, more carbon dioxide can be added to the system and the system becomes slightly acidic again. The carbonate ion is converted into bicarbonate which produces a very soluble calcium salt.

$$CaCO_3\ (s) + H_2C0_3(aq) \rightarrow Ca^{2+}(aq) + 2HC0_3(aq)$$

The solubility of carbonate minerals in acidic aqueous solutions is dependent upon both water and CO_2 being present (Larsen, 2003). Calcium removal is also affected by the coal to water ratio where calcium removal decreases as the volume of water decreases (Hayashi et al., 1991). During CO_2 sequestration in coal, it is expected that the saturated water in the coal will decrease with time due to the plume movement expanding radially from the injection well due to the pressure differential between the injection well and the offset wells. This reduction in the water content reduces the formation of carbonic acid from the injected CO_2, but the leading edge of the plume will be a mixture of CO_2 and water carbonic acid mixture.

The aim of this study is to demonstrate the capabilities of µCT for nondestructive coal characterization and observe the effects of carbon dioxide sequestration on the disposition of pores, fractures and minerals within the coals. The quantification and three dimensional visualization of the spatial disposition of calcite, permeability, and fractures in coals with respect

to the change of the structures from contact with a weak carbonic acid solution. This carbonic acid solution has been simulated based on the interaction of CO_2 with produced formation water from a previous 'huff-and-puff' sequestration test in a coalbed methane well in Russell County, Virginia, USA where the pH in the produced water was measured at 5.8 after injection (Miskovic et al., 2011).

The design of the experiment is to allow the comparison of a control core and a core that has been subjected to carbonic acid and compare them using μCT, ESEM, and inductively coupled mass spectrometry. The experiment is divided into two main parts: mineralization verification and impregnation of carbonic acid to simulate sequestration events. The mineral verification is achieved through the use of μCT scanning of coals at various depths and then confirmed with the use of ESEM. Once calcium rich coals have been selected two competent coal cores were chosen for impregnation of carbonic acid.

3.0 SAMPLE PREPARATION

The donated core samples from various core drilling sites in Buchanan County, Virginia, USA. Samples were logged and high quality seams of strong structural integrity were noted. For this paper the 12-VA-361 drill site was the main focus for analysis. Target competent seams were selected and prepared in the laboratory for cutting to reduce the size to allow for various scanning techniques. Samples were marked per elevation and tensioned axially using duct tape and cut. The samples were cut to 5.8 to 10.2 centimeters in length using a wet tile saw and allowed to dry before the removal of duct tape. The samples were then wrapped in a plastic sheath and sealed to prevent coal dust being exposed to various scanning equipment. The

samples were then transported to a climate and humidity controlled lab for initial testing (21˚ C and a relative humidity of 45%).

3.1 VISUALIZATION TEST INSTRUMENTS

The two methods for visualization of the coal structure are of μCT and ESEM. The μCT provides a detailed rendering of the entire core with micron level resolution, but some clarity is lost in the center of the core. The μCT does not provide mineral composition but maps the regions of differing density. The ESEM limits the scanning area to a 2-3 square centimeters and requires cutting of thin sections in the desired area. The ESEM does provide back scatter detection which is used to determine the mineral composition of desired areas.

3.2 TEST METHOD DEVELOPMENT

Samples are scanned using SkyScan's μCT 1172 scanner. The initial data is rendered and basic determinations of cleat structure, cleat filling, cleat orientation, and other mineralization are recorded. Target areas are then selected for more detailed scanning and quantification. These areas include: complex cleat structures, cleat filling, mineralization bands, and/or attempts to reduce ring artifacts in the scan. The heterogeneous nature of the coal requires multiple scans to successfully map the seam with minimal background noise, ring artifacts, and beam hardening. Starting settings for scanning parameters include a resolution of 17.4 microns with a 100kV and 100 amps for a scanning area of less than five centimeters on the longitudinal axis of the core. Scanning time increases with smaller resolution and rotational steps. Typical scanning times exceed 24 hours per coal sample. Once the area of interest is defined further verification of the

area is needed. A scanning electron microscope is used to verify the mineral composition of the coal, but this is a destructive method and the sample is no longer applicable to μCT scanning.

A CT scan is a density map of a material or specimen. Since X-ray attenuation is related to density, the CT image gives the density distribution within every point of the object scanned. If the object is scanned at two different energy levels, the data is converted to a CT number. A CT number is a comparison of the linear attenuation of the media compared with the linear attenuation to water.

4. VERIFICATION OF BOTH SEM AND X-RAY CT APPROACHES

The initial scans from various elevations in borehole 12-VA-361 are shown. A major focus is on a one foot section at 334.7 meters in depth (*1098 feet* sample) of elevation 1098 feet in depth for verification part of the experiment and 496.2 meters in depth (*1682 feet* sample) in depth for impregnation due to the intense calcite filling of the cleat structure.

Previous analysis of 13 samples from varying elevations does not show a correlation between the depth of the sample and the cleat network. The cores are subject to deflections on dense regions such as pyrite. Figure 3(a) is an example of intense silica mineralization in a coal sample. The denser silica is seen in darker colors. This feature is found throughout the coal sample and hides the cleat structure because the scanner is separating coal from a form of silica rather than separating coal from slight void pockets and fractures. A large amount of beam deflection and hardening are present resulting in extreme difficulties with verifications of minerals and void space. The only major take away from this scan is that the coal has mineralization and if a cleat structure is present an alternate scanning method is needed.

The scan, as seen in Figure 3(b), is the rendering of scan desired to visualize the structure of the coal both in clarity and internal structure. The face and butt cleats are clearly shown and there is only slight deflection, beam hardening, or ring artifacts. The presences of calcium is verified using an ESEM.

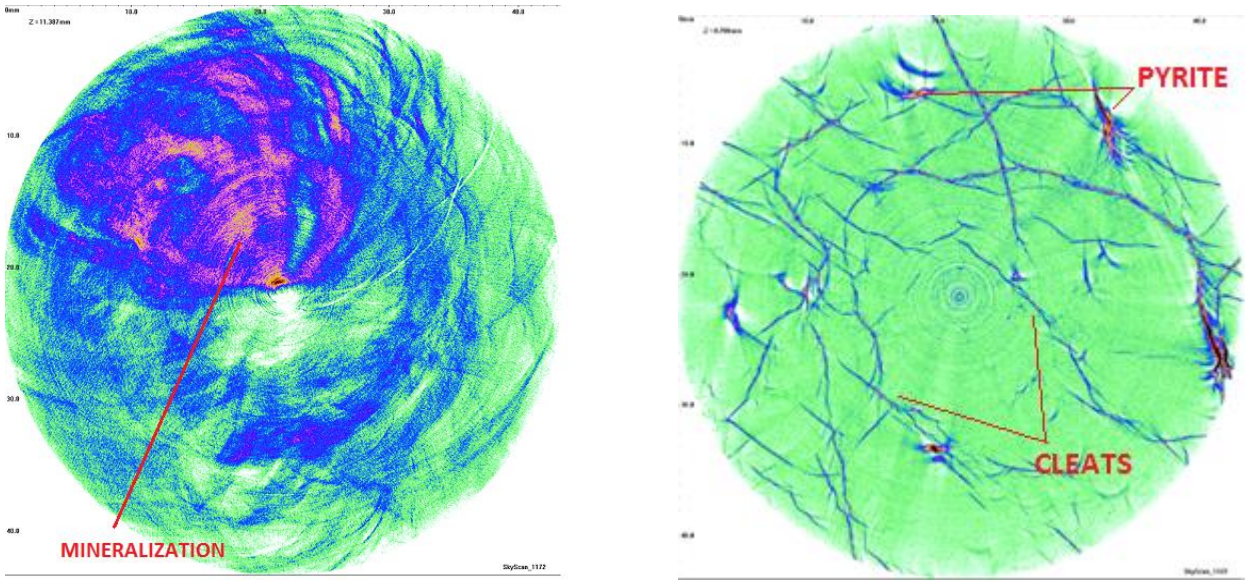

(a)Sample from VA elevation 1928 (587.6 meters) (b) Sample from VA elevation 1096

Figure 3:X-ray uCT results of bituminous coal samples from Buchanan

Figure 4(a) is an ESEM scan of a thin section sample 1098 (334.7 meters) and fifty times magnification. This cleat is filled with a calcium rich mineral (calcium carbonate) which is verified in Figure 4(b) using back scatter detection. The filled face cleat, in white, runs toward the bottom right with the butt cleat nearly 90 degrees to the face. A more detailed view of the filled cleat may be seen below in Figure 4(c) at one thousand times magnification. It is important to note that there is no space of gap between the edges of the calcite and the coal. This is examined after the impregnation of carbonic acid.

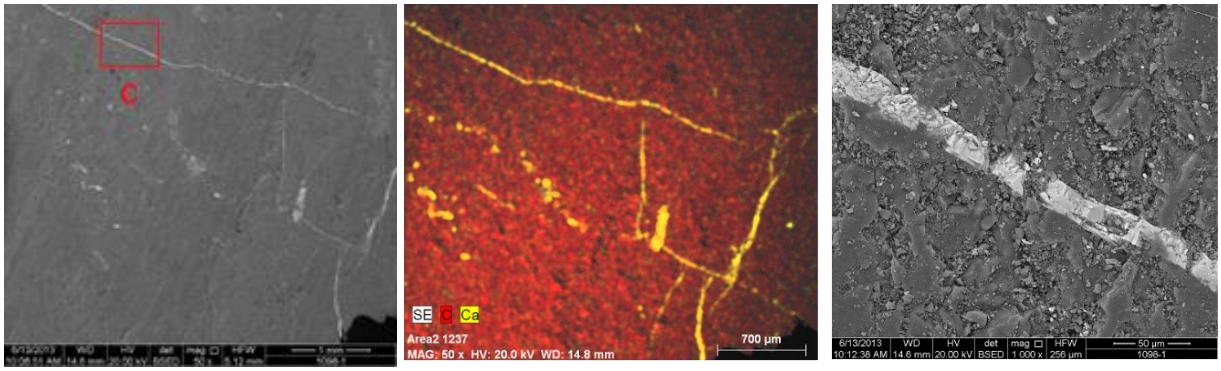

(a) 50x SEM SCAN **(b) 50x SEM SCAN Electron Detection** **(c) 1000x SEM SCAN**

Figure 4:ESEM test results of bituminous coal samples from Buchanan VA elevation 1098 (334.7 meters)

Sample 1098 also shows signs of general calcium mineralization not in cleat structures. The calcium intrusion may be seen below in Figure 5(a) on the right hand side of the image and throughout Figure 5(b). The precipitation may be caused by a hydrogenic event or introduced in the deposition event. It is likely that the presence of this mineralization has severely blocked the matrix pores, trapping or impeding matrix flow of the core.

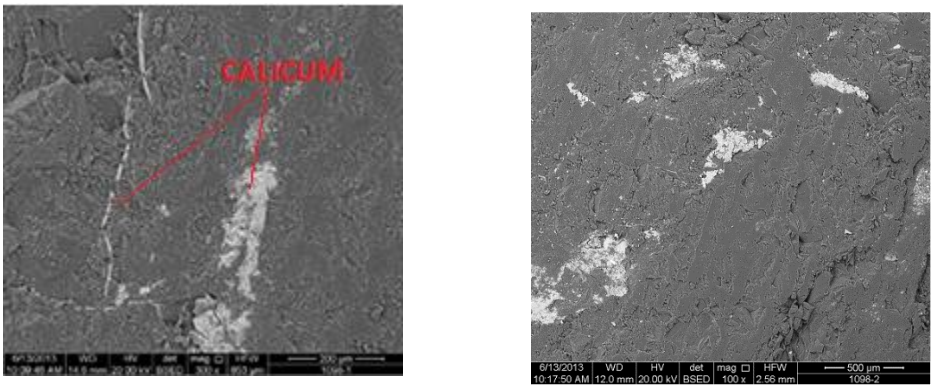

(a) 300x SEM SCAN (b) 100x SEM SCAN

Figure 5: ESEM test results of bituminous coal samples from Buchanan VA elevation 1098

5.1 VISUALIZATION OF CLEAT STRUCTURE

After the verification with the ESEM that the μCT scanner could detect both cleats voids and filled cleats, another sample of similar properties was prepared for the impregnation of carbonic acid in attempt to open the cleat structure. The 1682 core sample was then saturated in a solution of 5.7 pH carbonic acid under vacuum of 66.66 kPa for seven days at room temperature of 22.2 ˚C. Each day the system was allowed to restore to atmospheric pressure before the vacuum was reset to 66.66 kPa to help liberate any air bubbles from the sample and encourage the weak acidic solution to fill the pore space. A water sample was taken before the sample was rinsed with deionized water and the coal core sample was set in a drying oven on the lowest setting (32.2 ˚C) for a period of 72 hours. The justification for selecting the 1682 sample was due to the calcite filled cleats shown in the initial μCT scanning and a greater structural integrity and volume compared to the 1098 sample. The majority of the 1098 sample was destroyed in an attempt to cut a thin section for ESEM scanning. A small structurally damaged sample was impregnated for permeability testing. The μCT image in Figure 6 shows calcite in the cleats as a dark color. While this figure shows artifacts, the resolution is clear enough near the center of the sample to confirm that there is calcite present. Two ESEM samples will be compared: A ‘dry’ non-acidified sample and a ‘wet’ impregnated with a solution of carbonic acid. Figure 13(a,b,c) are from the dry sample SEM scans. The gap between the coal and the calcite is not as visible or just not present in some of the cleat structures. The figures progress from eighty times magnification to three hundred and fifty on two various regions of the coal scanning surface.

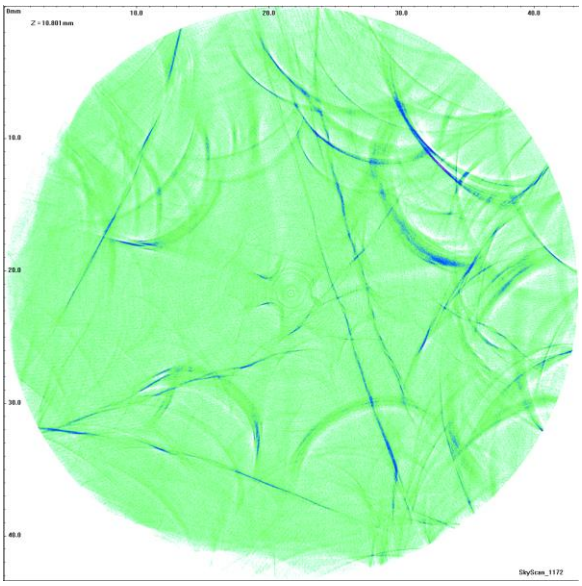

Figure 6: X-ray uCT results of bituminous dry coal samples from Buchanan VA elevation 1682

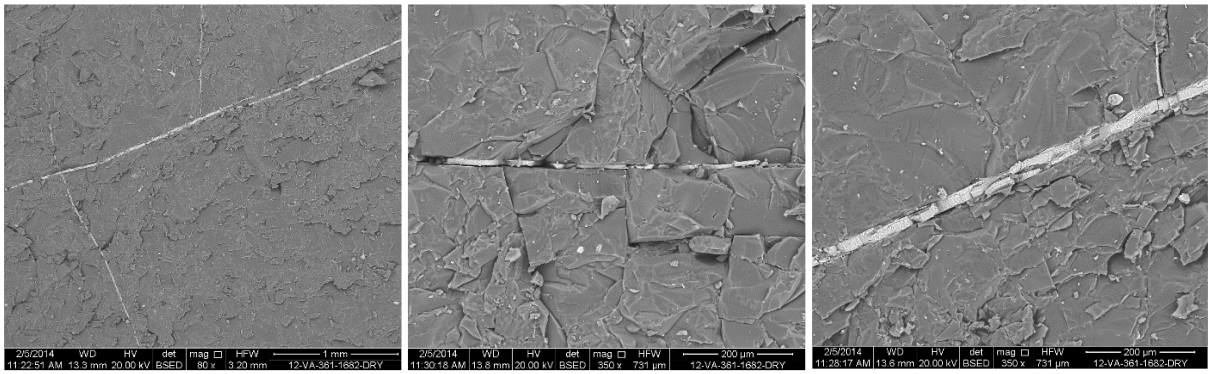

(a) 80x SEM SCAN (b) 350x SEM SCAN (c) 350x SEM SCAN

Figure 7: ESEM test results of bituminous dry coal samples from Buchanan VA elevation 1682

Figure 8(a) is the first image of the wet/impregnated sample. It has a major calcite intrusive cleat running along the sample. This cleat appears to have dissolved calcite by carbonic acid. A more magnified view of a different area is shown in Figure 8(b,c) show a dissolved flow path from fluid flow between the contact of the calcite and the coal. Figure 8(b) is magnified to 450x and shows a pathway for the acid to flow and an increased aperture between the coal in grey and the calcite in white. The calcite is also flaked along this pathway which can be seen in the upper left quadrant of the figure. This flaking is more evident in Figure 8(a) due to the

increased magnification to 1250x, and Figure 8(c) shows the most distinct path and separation between the calcium carbonate and the coal. The differences in the 'dry' and 'wet' samples are significant and quantified using Avizo™ software. The acidic solution had a significant effect on the cleat structure and matrix. It should also be noted that all of the sample were cut from internal sections of the coal after impregnation rather than exterior area of the sample.

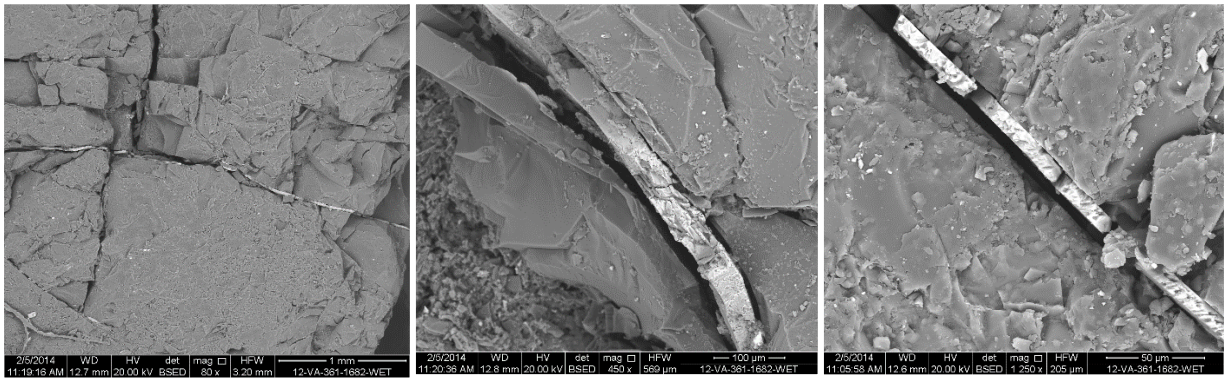

(a) 80x SEM SCAN **(b) 450x SEM SCAN** **(c)1250x SEM SCAN**

Figure 8: ESEM test results of bituminous wet coal samples from Buchanan VA elevation 1682

In comparison to the dry samples the wet ESEM scans show gaps between the calcium rich areas of the cleats. To further quantify the dissolution, the carbonic acid solution was tested before and after the impregnation in an inductively coupled plasma mass spectrometer (ICP-MS). The results are presented in Table A in two rows: pure carbonic acid and normalized results. The acid sample that was impregnated in the coal contains over orders of magnitude more calcium than the original sample of the acid.

Table A: Inductively plasma mass spectrometer results

	Na	Mg	Si	P	Cl	K	Ca	Mn	Zn	Sr	Ba
	ppb	ppb	ppb	ppb	ppm	ppb	ppb	ppb	ppb	ppb	Ppb
Carbonic Acid	214.3	19.1	5.6	17.3	0.7	30.4	134.9	1.1	10.3	0.4	1.7
Spent Carbonic Acid	3662.0	1121.0	432.0	51.8	4.4	934.2	16656.0	8.4	50.2	83.6	66.6

5.2 PERMEABILTY PREDICTION BASED ON SEM AND X-RAY CT RESULTS

With the conjunction of µCT scanning and ESEM visualization of the calcite cleat dissolution, further refinement and quantification of permeability is needed to help gauge the feasibility for future testing and/or large scale interaction. The software Avizo™ was used to visualize the data from the µCT scans.

5.2.1 PERMEABILITY CALCULATION METHOD

Both the original sample and the impregnated sample were scanned in the µCT scanner and the data was rendered in Avizo™. The pore structure was then mapped and absolute permeability calculations were performed based on single porosity and single permeability models. While this is not the most realistic model for coal, the platform does not allow for dual model calculations. If the aperture of the calcite cleat in the sample increases the software will be able to detect the increase through the increase in absolute permeability of the sample's cleat structure. The permeability measurements were performed perpendicular to the face cleats (in the butt cleat direction) and are derived below using equations in the FEI's Avizo™ software package and manual (FEI 2014).

5.2.2 ABSOLUTE PERMEABILTY

Absolute permeability is defined as the measure of the ability of a porous material to transmit a single phase fluid. Its SI unit is square meter (m^2), but square micrometer (μm^2) is more common since it is almost equivalent to one darcy (d): 1d = 0.9869233 (μm^2) . It is an intrinsic

property of a material, independant of any external condition. Absolute permeability appears in Darcy's law (Darcy 1856) as a constant coefficient relating fluid, flow and material parameters:

$$\frac{Q}{S} = -\frac{k}{\mu}\frac{\Delta P}{L}$$

Where:

- Q is the global flow rate that goes through the porous medium ($\frac{m^3}{sec}$)
- S is the cross section of the sample which the fluid goes through (m^2)
- k is the absolute permeability (m^2);
- μ is the dynamic viscosity of the flowing fluid ($Pa * s$ec);
- ΔP is the pressure difference applied around the sample (Pa);
- L is the length of the sample in the flow direction (m).

$\frac{Q}{S}$ is often noted as v ($\frac{m^3}{sec}$) and accounts for the superficial or mean fluid flow velocity through the porous medium or Darcy's velocity. Only single-phase fluids are considered for absolute permeability. Multi-phase flows are concerned by relative permeability

5.2.3 STOKES EQUATIONS AND FLOWS CONDITIONS

To numerically estimate absolute permeability, the Stokes equations are solved:

$$\begin{cases} \overrightarrow{\nabla_1} * \vec{V} = 0 \\ \mu\nabla^2\vec{V} - \vec{\nabla}P = \vec{0} \end{cases}$$

Where:

- $\overrightarrow{\nabla_1}$ is the divergence operator
- $\vec{\nabla}$ is the gradient operator
- $\vec{V}$ is the velocity of the fluid in the fluid phase of the material
- μ is the dynamic viscosity of the flowing fluid
- ∇^2 is the laplacian operator
- P is the pressure of the fluid in the fluid phase of the material

This equation system is a simplification of the Navier-Stokes equations, considering:

- an incompressible fluid, which means that its density is a constant
- a Newtonian fluid, which means that its dynamic viscosity is a constant
- a steady-state flow, which means that velocity does not vary over time
- a laminar flow, which means that the concerned velocities are small enough not to produce turbulence.

The last point is equivalent to considering flow at a low Reynolds number (Reynolds 1883) for the first appearance of Reynolds numbers). Once this equation system is solved, estimating the permeability coefficient consists of applying Darcy's law. All the values of this equation can be deduced from the solution of the equation system.

$(Q, \nabla P)$ or are external conditions (S, L, μ). It is computed by the Absolute Permeability Experiment Simulation module.

5.2.4 VOLUME AVERAGE FORM OF THE STOKES EQUATION

The effective permeability can be defined as the influence of the solid phase on the velocity of the fluid. A change of scale to get equations valid on the entire volume is necessary. The method of volume averaging is a technique that accomplishes a change of scale. Its main goal is to spatially smooth equations by averaging them on a volume (Whitaker, 1998). This very general theory leads to develop a closure problem which transforms the Stokes equations into a tensorial problem. It remains very similar to the Stokes equations, despite the fact it is a higher order problem:

$$\begin{cases} \vec{\nabla}_1 \vec{\vec{D}} = \vec{0} \\ \nabla^2 \vec{\vec{D}} - \vec{\nabla} \vec{d} = \vec{\vec{I}} \end{cases}$$

Where:

- $\vec{\vec{D}}$ is a tensor that can be considered as the source of the spatial deviation of the velocity, which can be referred to as velocity perturbation field

- $\vec{d}$ is a vector that can be considered as the source of the spatial deviation of the pressure, which can be referred to as pressure perturbation field
- $\vec{\vec{I}}$ is the unit tensor. The permeability tensor is extracted from the solution of the problem by calculating the mean value of $\vec{\vec{D}}$ over the volume V on which the system was solved

$$\vec{\vec{k}} = \frac{1}{V}\int_V \vec{\vec{D}}dV$$

This permeability tensor gives additional information about the intensity of permeability along any direction of space. It can give rise to the anisotropy of a porous media.

5.2.5 BOUNDARY CONDITIONS

Two approaches to estimate absolute permeability were utilized. The first is an experiment simulation based on Stokes equations resolution. The boundary conditions are specified as:

- A non-slip condition at fluid-solid interfaces.
- One voxel wide plane of solid phase (with no-slip condition) is added on the faces of the image that are not perpendicular to the main flow direction. This allows isolation of the sample from the outside, allowing no flow out of the system
- Experimental setups are added on the faces of the image that are perpendicular to the main flow direction. They are designed in a manner that creates a stabilization zone where pressure is quasi static, and the fluid can freely spread on the input face of the sample
- Two conditions can be chosen by the user: input pressure and flow rate and flow rate is estimated by the software.

The second approach solves the closure problem derived from Stokes equation by volume averaging. This is done in the Absolute Permeability Tensor Calculation module. The tensorial problem that is solved in this case is closed by imposing periodic boundary conditions to $\vec{\vec{D}}, \vec{d}$ and the geometry. A no-slip condition is imposed at the fluid-solid interfaces. The sample

represents a macroscopic, infinite material and must thus be representative of this porous medium.

5.3 PERMEABILITY OF DIFFERENT SAMPLES

Figure 9 and Figure 10 show the cleat structure mapped in Avizo™ without the carbon coal matrix. The Figures are a rectangular sub sample of the core. The color map in Figure 9(a,b,c) are based on the aperture of the cleat at different viewing planes.

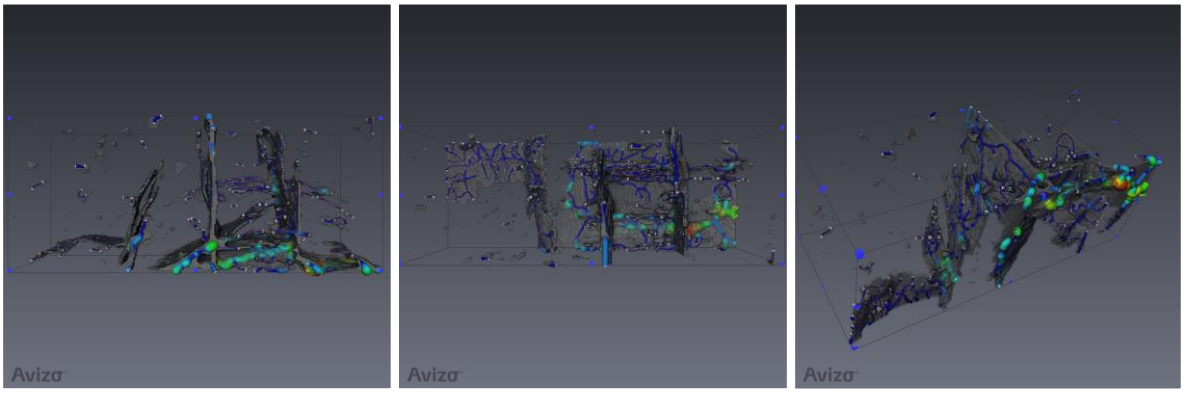

(a)View of XZ plane (b)View of XY plane (c) Isometric view

Figure 9:Three dimensional view of cleat system in bituminous dry coal samples from Buchanan VA elevation 1928 feet (587.6 meters)

Figure 10 shows the flow paths through the structure of the dry sample. The dry sample is the larger of the subsamples and is more complex in the mapping. It is almost double in size to the wet sample due to the concentration of cleats in the region. The flow paths are shown in red. The fluid viscosity is modeled off of carbon dioxide at a constant value of $8.30*10^{-5}$ pascal (Pa).

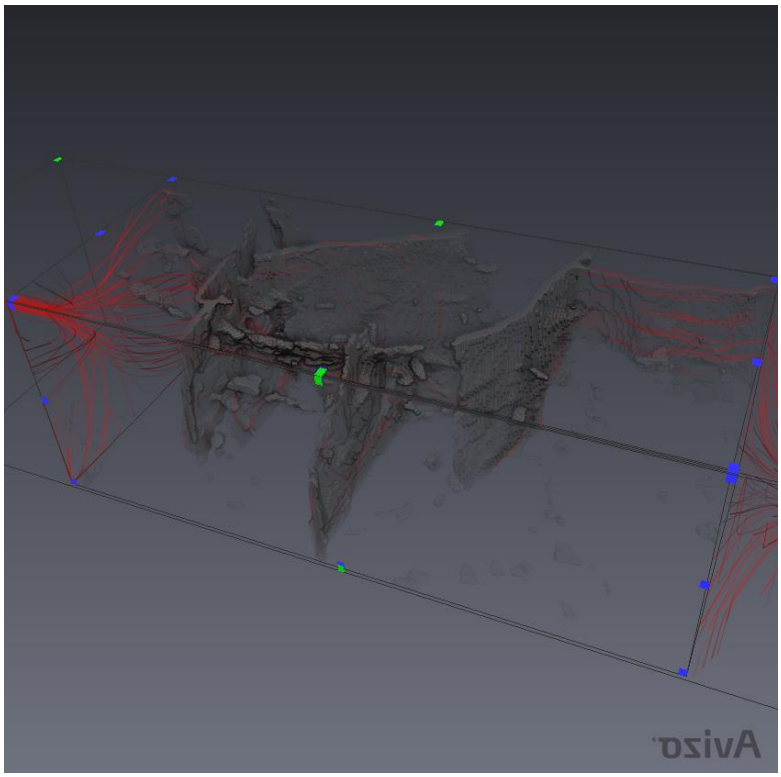

Figure 10: Flow through the cleat system

The structures for the wet samples are shown in Figure 11 and Figure 12(a,b). The area for the acid impregnated sample is smaller in attempt to decrease the time for permeability calculations. The results, of these tests can be seen in Table B. It should be noted that with a sample that only contained one major cleat and a small tertiary cleat the permeability of the sample still increased after the addition of the acid solution.

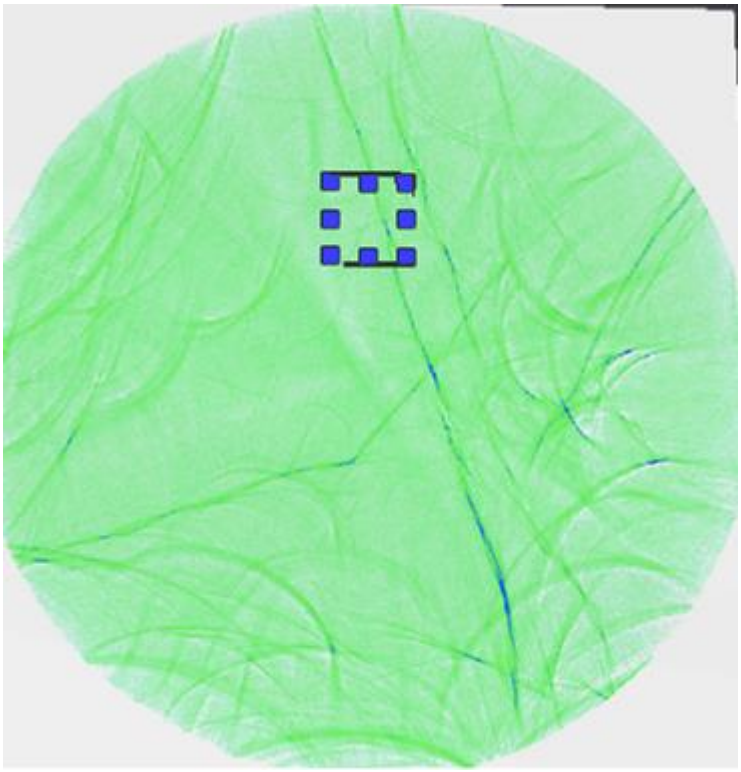

Figure 11:X-ray uCT results of bituminous dry coal samples from Buchanan VA elevation 1682 feet (492.6 meters)

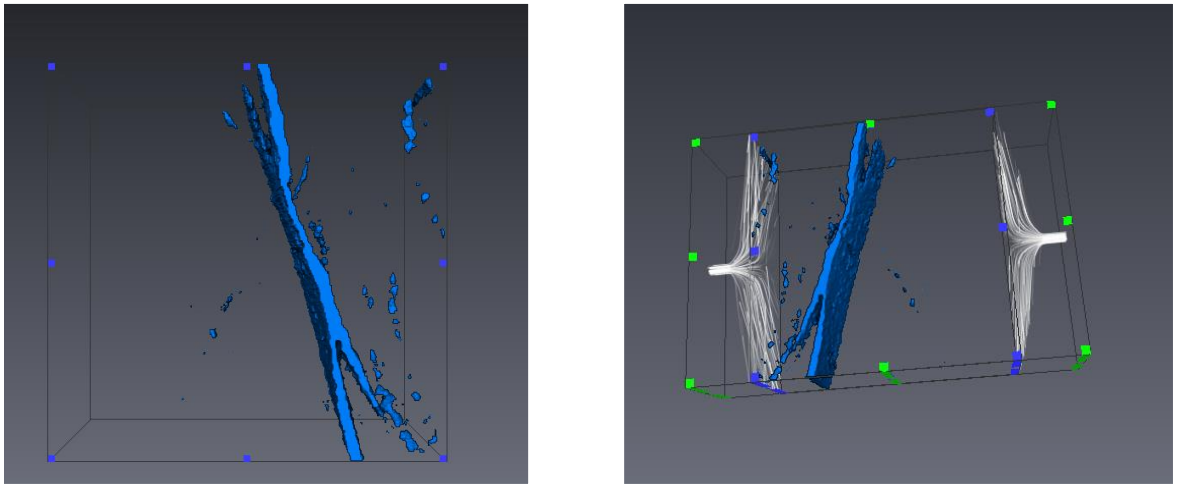

(a)Subsample cleat structure of wet sample (b)Permeability of subsample

Figure 12: X-ray uCT results of bituminous dry coal samples from Buchanan VA elevation 1682 (492.6 meters)

The single test with the 1682 feet (492.6 meters) and later with the 1082 (334.7 meters) sample indicate that the permeability increases with the addition of the carbonic acid based on the findings with Avizo™. The threshold value for Avizo™ is subjective to user error in assigning the peaks for the separation between the cleat structure, coal, and void space. For all the testing done in the laboratory the in-situ stress of the coal was not replicated. The aperture of the cleat and the corresponding permeability may be significantly less than what is modeled due to the overburden stress and stress associated with sequestration type injections. The ratio of the permeability before and after the carbonic injection is still noteworthy and clearly shows the dissolution of calcite results in an increase in permeability within the coal.

The dissolution of calcite in the coal is present through ESEM, inductively coupled plasma mass spectrometer (ICP-MS), and the permeability modeling with Avizo™. The Avizo™ results are shown in Table B. It should be noted that the 1082 feet (334.7 meters) dry sample had a substantial fracture or crack which causes the permeability to be significantly greater than the wet sample. There is no correlation between permeability and depth of the seam based on the limited testing in Avizo™. Though this laboratory test could not constrain all the variables to simulate in-situ conditions (confining pressure, temperature, saturation, etc.), the test shows that the transportation potential of calcium in the cleat structure is present and influences permeability of the well. This test with the carbonic acid was only a soaking test whereas the sequestration event will flow towards pressure sinks at offset production wells. This flow presents greater opportunity for the transport of calcium and other elements in a production field and the open system is less likely to reach an equilibrium state.

Table B: Permeability prediction results for different samples

Elevation (ft.)	(meters)	Permeability [um^2]	Permeability [micro Darcy]	Flow rate [$um^3.s^{-1}$]
1082-wet	**334.7**	0.018456	0.018701	5.89E+10
1082-dry*	**334.7**	3.882729	3.934175	1.15E+12
1509	**459.9**	0.006036	0.006116	1.17E+10
1582	**482.2**	0.032408	0.032837	1.93E+10
1682-wet	**512.6**	0.164637	0.166819	4.91E+10
1682-dry	**512.6**	0.123937	0.125579	4.91E+10
1747	**532.5**	0.02146	0.021744	4.40E+10
1837	**559.9**	0.012439	0.012604	2.24E+10
1873	**570.9**	0.016593	0.016813	1.43E+10
1950	**594.4**	0.007707	0.007809	9.84E+09
2282	**695.6**	0.024119	0.024439	1.71E+10

*represents a severely fractured sample that was scanned and should not be made in direct comparison to the wet sample. The viscosity modeled is a constant 8.30e-5 Pa.s with a constant input pressure of 5171070 Pa and out pressure of 4636160 Pa.

6. CONCLUSIONS

The results from the scanning electron microscope, the micro computed tomography, and inductively coupled plasma mass spectrometer, only qualify and quantify a laboratory setting and may not be indicative of in-situ conditions and reaction rates. The ESEM in conjunction with the inductively coupled plasma mass spectrometer provides a clear indication that calcite is being dissolved in coals and transport through the structure is indeed possible.

Sample 1682 feet (512.6 meters) shows a 25 percent increase in permeability in the cleat structures. This increase in permeability is observed in both the ESEM and the µCT scanner. The qualitative increase is observed in the ESEM in Figure 5 and quantitatively observed through Avizo™ modeling software and inductively couple mass spectrometry. The results warrant further investigation into carbon dioxide as a sequestration agent as well as an additive for enhanced gas recovery in calcium rich coals.

The formation of carbonic acid in this environment should produce permeability changes due to the calcite dissolving and attempting to reach equilibrium. Additional testing or use of CO_2 for stimulation in reservoirs contains great potential for enhanced oil, natural gas liquids, and gas recoveries due to the interaction of carbon dioxide with produced waters. This study only examined the flow through the cleat structure and not through the low permeability organic matrix structure.

7. REFERENCES

Darcy, H. (1856). Les fontaines publiques de la ville de Dijon: exposition et application... Victor Dalmont.

FEI. (2014). *Avizo 8: Avizo User's Guide*

Golab, Alexandra, et al. (2013) 'High-resolution three-dimensional imaging of coal using microfocus X-ray computed tomography, with special reference to modes of mineral occurrence.' *International Journal of Coal Geology* 113: 97-108.

Hayashi, Jun-ichiro, et al. (1991) 'Removal of calcium from low rank coals by treatment with CO 2 dissolved in water.' Fuel 70.10 :1181-1186.

Jahnke, Richard and Deborah B. Jahnke. (2004) 'Calcium carbonate dissolution deep sea sediments: Reconciling microelectrode, pore water and benthic flux chamber results'. *Geochimica et Cosmochimica Acta,*Vol. 68, No. 1 , pp. 47-59

Karacan, C. Ö., and E. Okandan. (2000) 'Fracture/cleat analysis of coals from Zonguldak Basin (northwestern Turkey) relative to the potential of coalbed methane production.' *International Journal of Coal Geology* 44.2:109-125.

Karacan, C. O., and E. Okandan.(2001) 'Adsorption and gas transport in coal microstructure: investigation and evaluation by quantitative X-ray CT imaging.' *Fuel* 80.4: 509-520

Karacan, C. Özgen, and Gareth D. Mitchell. (2003) 'Behavior and effect of different coal microlithotypes during gas transport for carbon dioxide sequestration into coal seams.' *International Journal of Coal Geology* 53.4: 201-217.

Larsen, John. (2003) 'Sorption of Carbon Dioxide by Coals'. *Fuel Chemistry Division Preprints*, 48(1), 112.

Miskovic, Ilija. (2014) 'A Data-Driven Approach for the Development of a Decision Making Framework for Geological Carbon Dioxide Sequestration in Unmineable Coal Seams.' Order No. DP19917 Virginia Polytechnic Institute and State University, 2011. Ann Arbor: *ProQuest.* Web. 11 Sep. 2014.

Reynolds, Osborne.(1883) 'An experimental investigation of the circumstances which determine whether the motion of water shall be direct or sinuous, and of the law of resistance in parallel channels.' Proceedings of the royal society of London35.224-226: 84-99.

Ritz, Michael, Zdenek Klika. (2010) 'Determination of minerals in coal by methods based on the recalculation of the bulk chemical analyses'. *Acta Geodyn. Geomater.,* Vol. 7, No. 4(160), pp. 453-460

Stock, Leon and John V. Muntea. (1993) 'Chemical Constitution of Pocahontas No. 3 Coal'. *Energy & Fuels*, 7, 704-709

Whitaker, Stephen (1998). '*The method of volume averaging*.' Vol. 13. Springer Science & Business Media,

Xiaojun, Cui, R. Marc Bustin, and Laxmi Chikatamarla. (2007) 'Adsorption-induced coal swelling and stress: Implications for methane production and acid gas sequestration into coal seams.' *Journal of Geophysical Research: Solid Earth (1978–2012)* 112.B10.

Yao, Y, D. Liu, Y. Che, D. Tang, S. Tang, and W Huang. (2009) 'Non-destructive characterization of coal samples from China using microfocus X-ray computed tomography'. *International Journal of Coal Geology* 80 113-123

COMPUTED TOMOGRAPHY TO QUANITIFY CO_2 SEQUESTRATION POTENTIAL PER SEAM IN UNCONVENTIONAL COAL RESERVOIRS

1. ABSTRACT

The basic use of computed tomography as a potential mapping tool has been previously examined in this thesis and determined to be a viable option for mapping cleat structures and permeability. The purpose of this study is to map the coal sections of core hole (C1) in the immediate area of a 20,000 ton CO_2 sequestration in a attempt to predict and interpret the results from the injection. Parameters considered for the study are: cleat structure, cleat filling, cleat aperture, permeability, cleat density, desorption, and mineralization. The results indicate a trend in the cleat porosity and the desorption rate of the coals as well as the cleat porosity and the total gas in various seams. While these results suggest a correlation, the analysis does not account for in-situ conditions and contains a small samples size.

2. INTRODUCTION AND OBJECTIVES

While methane gas is recognized and exploited as a resource in conventional gas wells, commercial utilization of coal bed resources have been limited to basins that have historical data and knowledge from long term production and development. While dual porosity models can be applied to coal reservoirs to model the historic production data, there is still a need to investigate reservoir properties to help in predicting storage and production potential. Difficulties arise due to the fact that coal seams are heterogeneous in terms of lithotypes, morphologies, structures, and mineral compositions even on a small geographic scale. This heterogeneity makes gas storage and production predications difficult when changing areas, while the seam remains constant, without extensive exploratory drilling. Further difficulties for Central Appalachian coals are the

number of seams and their ability to change thickness and/or presence in certain areas. In complex systems, such as the Central Appalachia coals, experiments are run on cores for desorbed gas from all the seams and represents an average gas in place for the area. This presents a problem, in that, all of the seams are not hydraulically fractured equally and the gas in place may be significantly misinterpreted. A nondestructive technique is needed to correlate the internal structure of each coal seam, while preserving the sample for other further testings, with the total gas content an desorption rate. In 1993, Gamson et al., investigated micrometer-sized structures in the Bowen Basin using a scanning electron microscope. They observed that the effectiveness of gas storage and drainage may vary according to the type of microstructure, its orientation, density, and the extent of filling in void space. Because of their observations they proposed a more complex four step model as opposed to the common two step model of diffusion at matrix then macrostructure transport.

As previously described, Karacan and Okandan (2000, 2001, 2003) demonstrated the structural heterogeneity effects on gas storage of seams and enhanced recovery potential during nitrogen, methane, carbon dioxide, and xenon injection in bituminous coals. Karacan and Okandan concluded that existing gas transport models are not appropriate for all lithotypes, since coal seams are heterogeneous in varying lithotypes and microstructures, which is seen Chapter 1. There is a need to further investigate each coal seam qualitatively through the use of computed tomography and quantitatively through image processing to better develop a predicting method for the sequestration flow.

3. SITE OVERVIEW

The site for the carbon dioxide injection is located in Buchannan County, VA shown in Figure 13. The majority of natural gas from Southwestern Virginia come from Buchannan County and Dickenson County (Virginia Natural Gas). The natural gas production started in advance of coal mining to reduce the potential for an explosive atmosphere in an underground environment (Virginia Natural Gas). In 2004, more than 85 million cubic feet of natural gas was produced as a result of expansion in these two counties (Virginia Natural Gas).

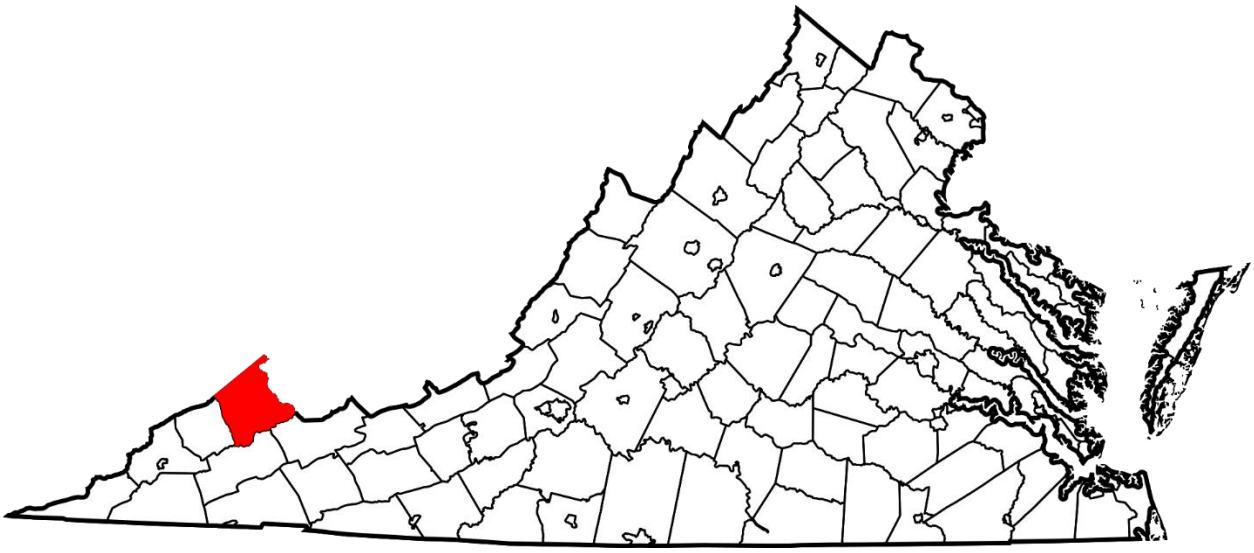

Figure 13: Buchannan County (https://en.wikipedia.org/wiki/Buchanan_County,_Virginia , 2015)

The test wells are located on CNX property in Vansant, Virginia. Figure 14, rendered in Google Earth™, displays the three injection wells in green hexagons (DD7, DD7A, and DD8), the newly drilled monitoring wells in blue hexagons, and the offset wells in yellow hexagons. The white outline is a forth of a mile area of influence and the red is 2400 feet^2 area of influence from the three injection wells. It should be noted that the hydraulic fracture direction is toward the Northeast. The monitoring wells M1 and M2 were drilled before the injection of the CO_2. C1 is a

monitoring well that was drilled using a coring bit. The core was logged by Cardno on site and eventually transported to the Virginia Department of Mining and Mineral Engineering in Charlottesville, Virginia. Select sections of the core were removed from the repository for laboratory testing.

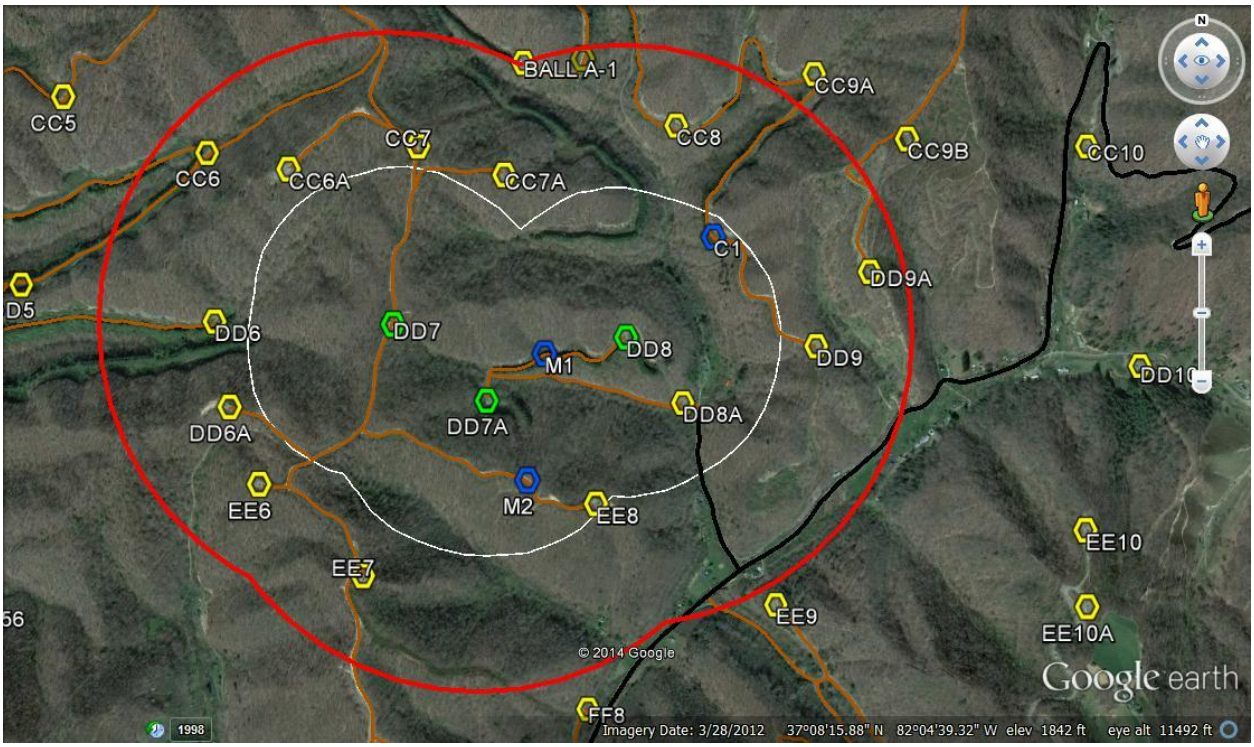

Figure 14: Site overview of CO2 injection site (https://www.google.com/maps, 2015)

4. CO_2 INJECTION PARAMETERS

The CO_2 injection is scheduled for the injection of 20,000 tons over a one year period followed by a one year soaking period. The CO_2 will be heated using propane to avoid the potential of freezing the liquid in the borehole. The CO_2 will be injected continuously at a rate of 60 tons per day with each injection well not to exceed 50 tons a day. The injection will be allowed to flow in the well that most readily accepts the gas.

5. SAMPLE PRESERVATION

Sample preservation and integrity starts on the core rig. Coal samples from the core rig that were greater than six inches were placed in sealed canisters to study desorption of the seams. The remainder of the core, both overburden and smaller coal seams, were placed in ten foot waxed core boxes for transport. Once the core arrived at the laboratory, select samples from the remaining seams were taken from the core boxes and sealed using a food grade vacuum sealer. The desorption testing was completed at Cardno's field office. Once desorption of the sample was completed the samples were returned to Virginia Polytechnic Institute and State University where the samples were again vacuum sealed. The pulled samples from the core box where sitting at atmospheric conditions for weeks and the vacuum sealing is an attempt to limit the oxidation and maintain moisture content of the sample. It should be noted that both the desorbed samples and the pulled samples are considered desorbed.

5.1 SAMPLING PREPARATION FOR SCANNING

The scanning in the SkyScan 1172 is required to have one flat surface to mount to the staging area of the machine. The 1.875" diameter core is wrapped in a plastic coating and then compressed using duct tape. This compression aids in the structural integrity of the core when cut and adds a small degree of prevention of water saturation. The samples were cut using a water cooled tile saw to lengths of 2-4 inches to allow them to be mounted in the micro computed tomography machine. The samples were allowed to dry overnight then they were wrapped in plastic cling wrap and taped axially. This wrapping is a dust prevention measure for the computed tomography machine. The samples were then mounted on a brass staging fixture

with modeling clay. The modeling clay is used to level the sample and provide a less drastic contrast in imaging than that of the brass near the ends of the samples.

5.2 SCANNING PARAMETERS

The scanning parameters stay constant in all aspects except for the resolution. Typically the sample was first scanned at 17.4 micron resolution. If further examination is required the resolution may be increased. The correlation between scanning time and resolution was exponential in nature. A single scan at 17.4 microns took over 20 hours to complete and render. A scan of 3.0 micron took between 72-96 hours depending on the size of the scanned area and had severe limitations due the thickness of the core. The upper limit of 100 kV would not penetrate the complete core and nor had the necessary resolution to provide meaningful results. These in-depth scans are not recommended due to memory restrictions, processing speed, and propensity to crash the entire system. The cores at 1.875" diameter were near the extremes of the staging area of 1.900" and the density of the coal requires the use of two filters: copper and aluminum. These filters filter out the lower energy X-rays and only allow the higher energy X-ray to penetrate the sample. This filtering helped to clear the resolution between materials such as between calcite and coal, coal and void, pyrite and coal, etc. A more in depth analysis of the scanning procedures may be found in the appendix.

5.3 X-RAY ATTENUATION, OPERATING CONDITIONS, AND VARIABLES

In X-ray computed tomography, materials are exposed to a concentrated beam of X-rays. In this technique, radiation is partly reflected, scattered, absorbed, and/or re-emitted as electromagnetic radiation or is transmitted through the material. The rays that make it through

the sample are received on a back plate located on the opposite side of the emission source. In the case of a micro-computed tomography machine, the sample is rotated, as compared to a traditional CT scan, the specimen is constant and the emission and detection source is moved around the orbit of the specimen. The basic unit of the µCT scanner is a pixel and is commonly expressed as a linear attenuation coefficient µ. This value is derived from Beer's equation:

$$\frac{I}{I_0} = \exp(-\mu h)$$

Where I_0 is the incident X-ray intensity and I is the intensity remaining after the ray has passed through the specimen of known thickness, h. Beer's equations assumes a well collimated beam and a monochromic source of X-ray which is true for the SkyScan 1172. The linear attenuation coefficient, µ, depends on the electron density and the atomic number from the equation below:

$$\mu = \rho(a + b\frac{Z^{3.8}}{E^{3.2}})$$

Where a is the Kline-Nishina coefficient, Z is the effective atomic number, E is the photon energy in keV, ρ is the density of the material, and b= 9.8 x 10^{-24}. Therefore, a µCT scan is just a density map of a material or specimen. Since X-ray attenuation is related to density, the µCT image gives the density distribution within every point of the object scanned. If the object is scanned at two different energy levels a new common unit may be renders which is referred to as a CT number. A CT number is a comparison of the linear attenuation of the media with the linear attenuation to water, similar to that of specific gravity.

6. SAMPLING

Sampling of core samples is limited to the cores not used for full desorption by Cardno. The samples that were received were scanned using SkyScan's µCT scanner. The figures can be viewed in in the appendix.

7. RESULTS

7.1. PRE-INJECTION: BASELINE

A pre-injection baseline of the injector wells was performed using the pressure build up method to determine the reservoir permeability. This test was conducted on the three producing wells and the permeability can be modeled with the Horner equation.

$$k(md) = 162.6\ \frac{(Production\ STB)(Formation\ Volume\ Factor)(viscosity\ of\ the\ gas)}{(Thickness\ of\ the\ target\ areas\ ft)\left(slope\ of\ \frac{psi}{cylce}\right)}$$

The buildup tests were conducted with the water pumps running during the normal scheduling using the Echometer. Figure 15 shows the buildup from the well DD7A. The two circled areas in red on the figure are the pumping cycles. The pressure on the figure starts to approach an azimuth and the slope of the psi per cycle can be calculated from the Horner equation.

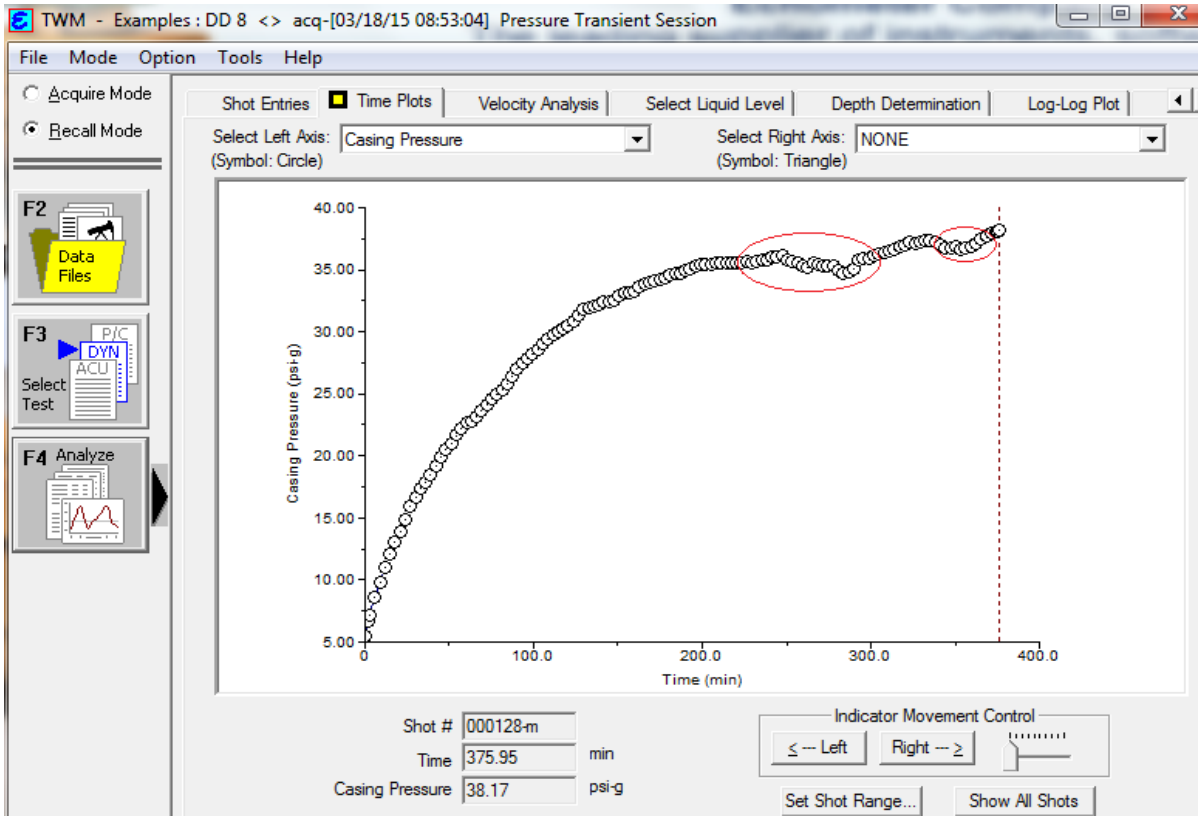

Figure 15: Echometer Buildup DD7A

The permeability of the three injection wells were determined to be:

DD7	= 9.65 md
DD7A	= 7.07 md
DD8	= 6.77 md

7.2. DESORPTION DATA FROM C1

Coal desorption techniques typically use the U.S. Bureau of Mines (USBM) canister-desorption method as described by Diamond and Levine (1981), Close and Erwin (1989), Ryan

and Dawson (1993), McLennan and others (1994), Mavor and Nelson (1997), and Diamond and Schatzel (1998). The coal desorption canister designs historically used with this method have an inherent flaw that allows a significant gas-filled headspace bubble to remain in the canister that later has to be compensated for by correcting the measured desorbed gas volume with a mathematical headspace volume correction (McLennan et al, 1994; Mavor and Nelson, 1997). This is compensated by filling the canister with as much inert material as possible to decrease the headspace. Cardno's Bluefield office preformed the desorption process and the raw data was received and processed. Figure 16 shows the normalized desorption data based on the dry mineral matter free by weight. There is no correlation between the depth of the seam and the cumulative gas desorbed. All of the seams have an ending spike or tail. This is the gas added from the crushing of the solid cores to release any trapped gas. It should be noted that the crushing of the cores does not contain a time component and is an addition of the previous interval which causes a drastic jump. Seam 1728 is the only seam with a negative tail because of the joining of two canisters that were completed in two different time intervals.

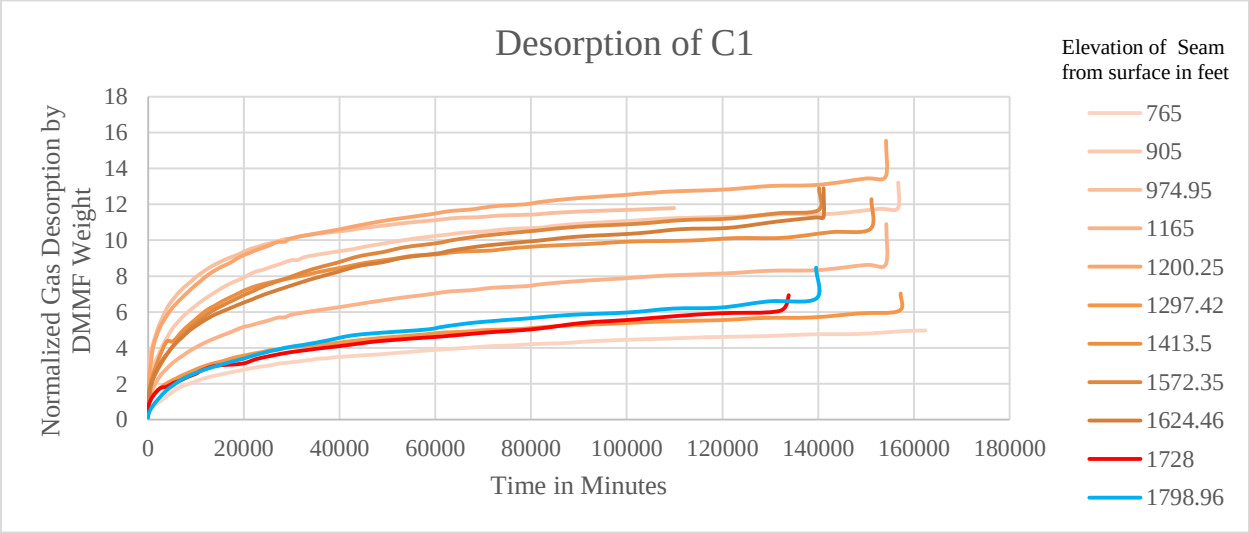

Figure 16: C1 Normalized Desorption Data

7.3. COMPUTED TOMOGRAPHY LINKED DESORPTION

The following section outlines an attempt to correlate µCT scanning with the desorption data to extract a working model to predict and help interpret the sequestration potential per seam.

The µCT scans are rendered as slices of the core samples. These samples are imported to an image software (ImageJ). The raw importation is seen in Figure 17.

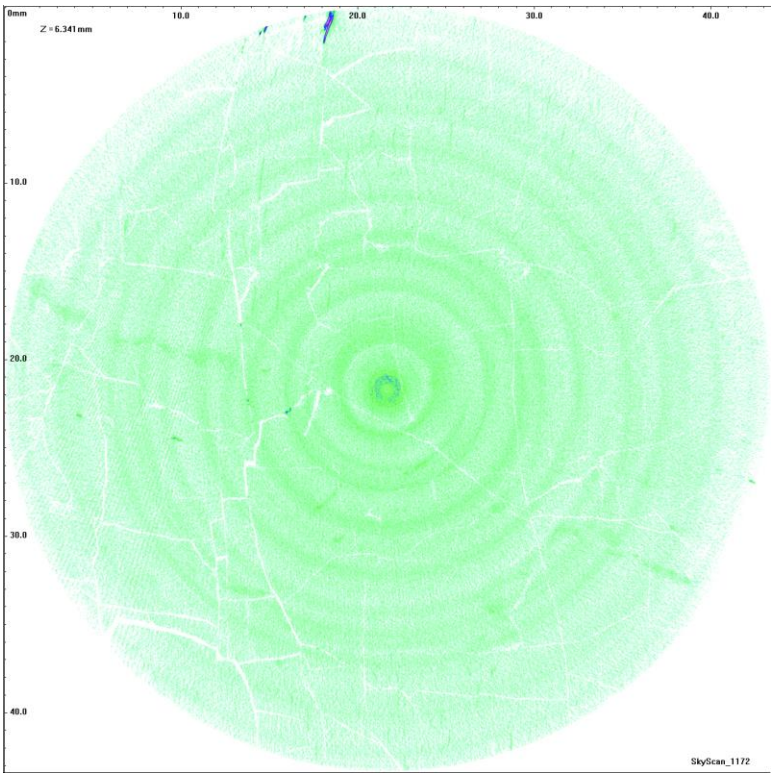

Figure 17: Elevation 1728 CT scan

The image is then scaled using photogrammetry to the outer grid lines for base line. The image is then converted to an 8 bit image in Figure 18.

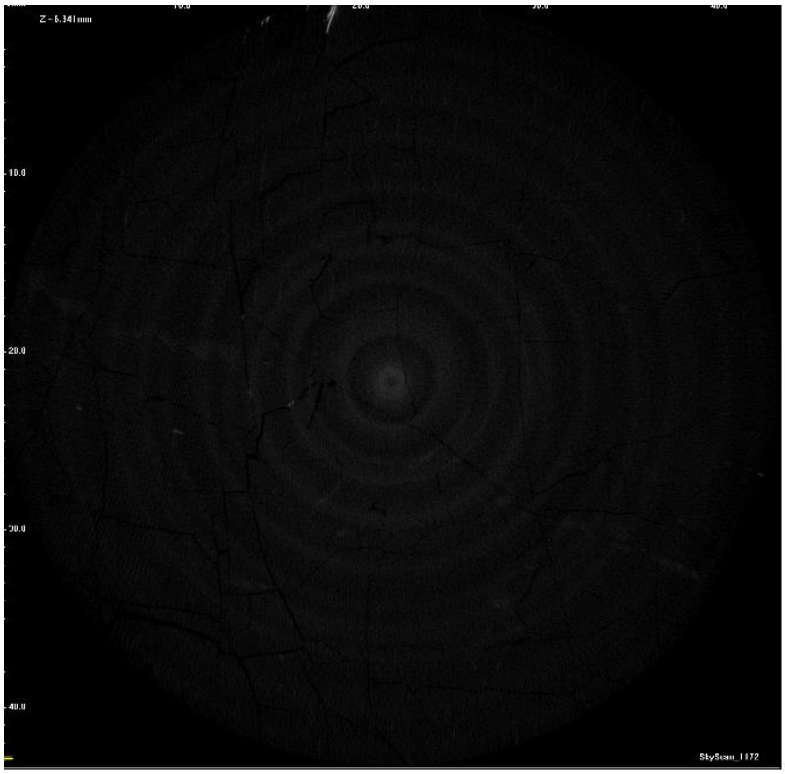

Figure 18: Elevation 1728 converted 8 bit

The 8 bit image is then process with a bandpass filter to filter down larger objects to 40 pixels and smaller objects to 3 pixels seen in Figure 19.

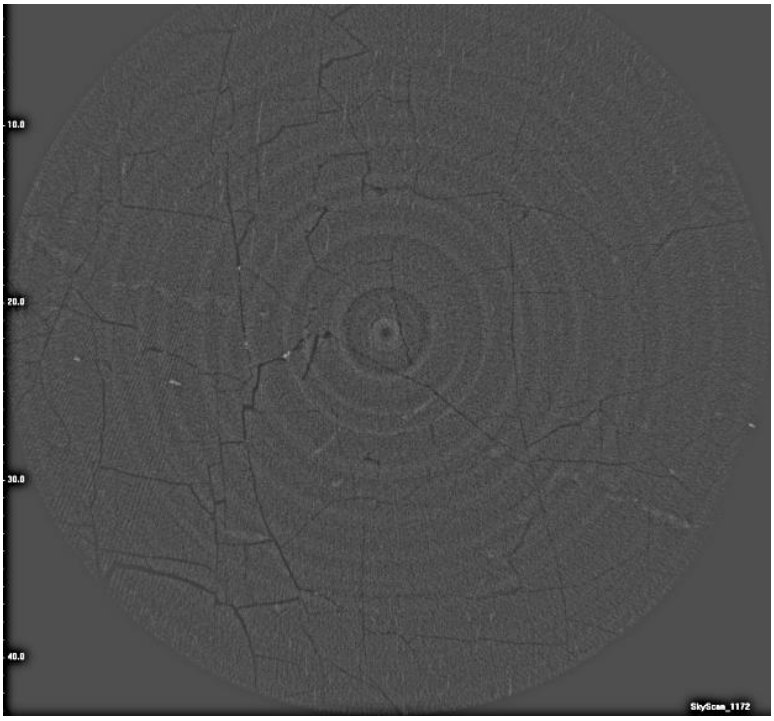

Figure 19: Elevation 1728 Bandpass filter

The image is now in the correct format to apply a threshold. The results are seen in Figure 20.

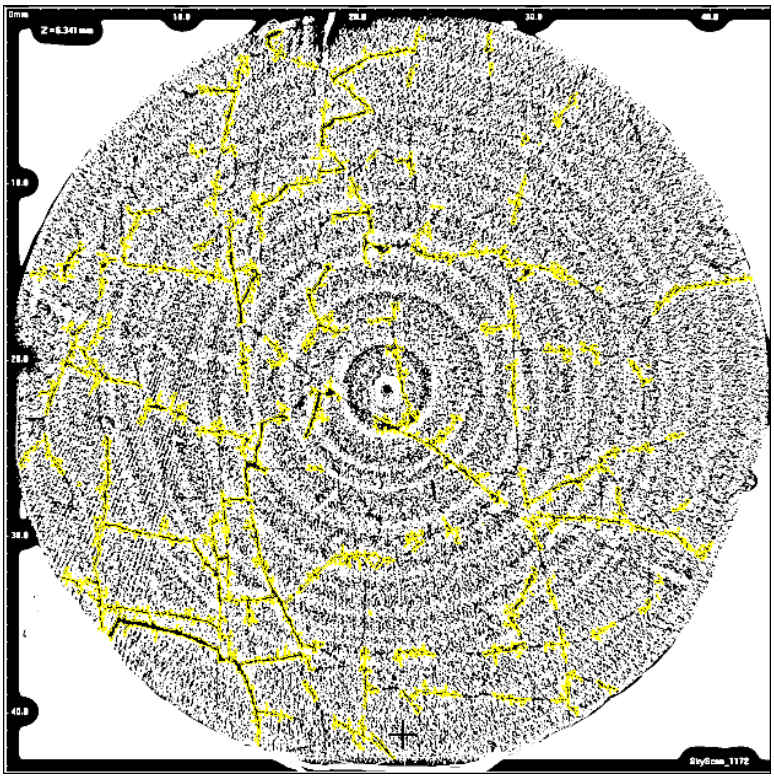

Figure 20: Elevation 1728 Threshold

The area highlighted in yellow is divided by the total area of the sample to obtain the cleat porosity for that seam, for that single image. Difficulties arise when the resolution of the sample blurs the edges of the cleat structure or completely shield them from the scan. It should be noted that the cleat porosities presented in the chapter are the average of multiple slices at different levels of the coal in the same seam. There is some user biases on the selection and interpretation of what constitutes a cleat and the boundary of the structure during the threshold event.

Data from five desorption test and five computed tomography scans are compared in Table C.

Table C: Desorption Data and Cleat Porosity

	Elevation (ft.)	**Max Slope**	**Total Gas Content (cc/g)**	**Moisture %**	**Ash %**	**Sulfur %**	**Cleat Porosity %**	**Residual Gas (cc/g)**
Greasy Creek	765	0.005941	6.38	0.71	15.71	0.86		
Lower Seaboard	905	0.014167	12.77	1.02	2.49	0.67		
U Horsepen	974.95	0.014168	10.95	1.03	16.3	3.16		
Poc 1	1165	0.006923	10.09	0.66	6.78	0.68		
Poc 10	1200.25	0.013235	14.51	0.78	7.59	1.35		
Poc 9	1297.42	0.004997	6.48	0.88	6.57	1.85	1.43	0.96
Poc 7	1413.5	0.007159	10.63	0.6	10.25	4.36	1.45	1.50
Poc 5 (10 bench)	1572.35	0.008231	12.03	0.63	6.14	1.24	1.68	1.28
Poc5 (20 bench)	1624.46	0.009152	11.84	0.57	6.35	1.74	1.964	1.5
Poc 3	1728	0.013736	3.37	1.04	7.14	1.48	4.30351	1.18
Poc 2	1798.96	0.003933	6.8	0.7	19.8	2.92		

The maximum slope in Table C is calculated from the first derivative of Figure 16 without the residual gas crushing.

7.4. DISCUSSION OF RESULTS FROM DESORPTION DATA WITH μCT SCANS

While five points from one well do not constitute a representative sample of the area, it does provide a qualitative analysis of inferences to attempt to predict sequestration events for these five seams and possibly the reservoir system as a whole.

One technique that is employed to graph the maximum desorption slope of each of the canisters versus the cleat porosity. The theory behind this phenomena is that the coal cleat can be modeled by Darcy flow mechanics. The seams with the largest cleat structures will desorb gas at a faster rate. The model does not take into account the total volume of gas or the gas lost from the tripping of the drill pipe, but the seams with larger cleat structures present a higher desorption slope than their counter parts. This rate is modeled exponentially in Figure 21 based on the dry mineral matter free content per weight.

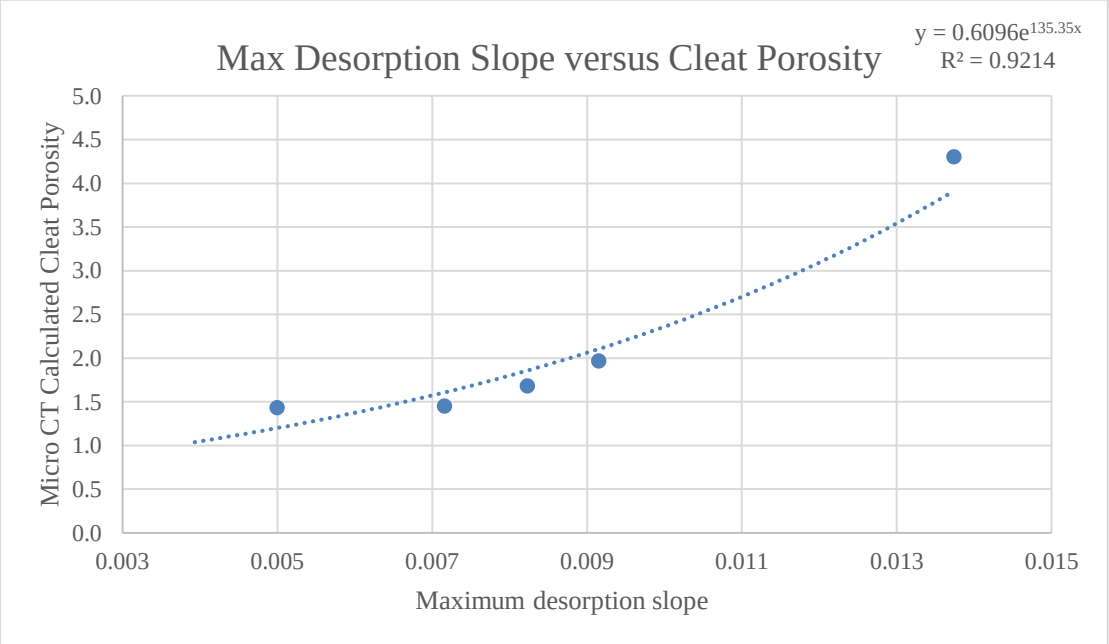

Figure 21: Max Desorption Slope versus Cleat Porosity

Since the coring well is in the gas production field, the cleat structure should correlate to the total gas in place based on the previous desorption theories previously discussed. This method of interpretation does not account for the depositional environments that formed the seam with varying amounts of gas but the effectiveness of the current facture nature in the system. Figure 22 shows the relationship with cleat porosity and total gas desorbed from the well. The highest cleat porosity (Pocahontas 3) is one of the deepest coal in the system. The following points increase in depth, gas content, and cleat porosity.

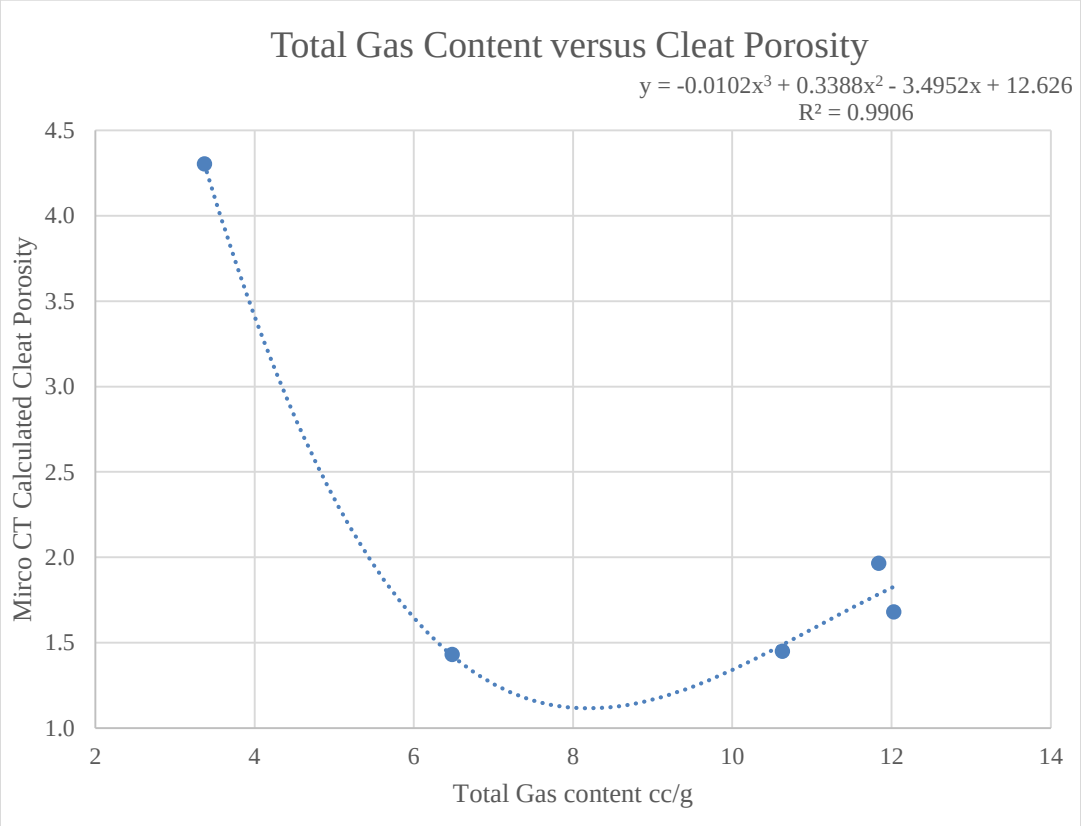

Figure 22: Total Gas Content versus Cleat Porosity

The results from Figure 22 are as expected. The Pocahontas 3 is the most cleated and therefore the most drained from gas production. The other four points increase in cleat porosity and also in

depth, which is common for deeper seams to contain more gas due to the in-situ stresses exerted on the seams. While this model is not an empirical model, it does provide useful information about the drainage of the reservoir and potential for sequestration.

8. CONCLUSIONS

With these two graphical representations and the data obtained from desorption testing, a prediction on the sequestration events per seam can be concluded. While both of these methods can be exploited for cleat porosity and potentially permeability, the model is too rudimentary to provide an empirical model. Table D attempts to correlate the cleat porosity from the two methods with the average permeability from three injection wells in the area (DD7, DD7A, and DD8 at 7.83 md). This number is a percent of the cleat porosity, it should not be used for modeling due to the low number of intact core samples from multiple wells in the reservoir. The more important number to consider is the percent of the cleat porosity in the system.

Table D: Model Calculations

		Gas Content Analysis		Desorption Slope Analysis	
	Elevation	Cleat Porosity (Gas Content)	Prediction of Permeability % of Reservoir	Cleat Porosity (Max slope)	Permeability % of Reservoir
Greasy Creek	765	1.47	7.09	1.36	5.12
Lower Seaboard	905	2.00	9.65	4.15	15.60
U Horsepen	974.95	1.58	7.65	4.15	15.60
Poc 1	1165	1.37	6.63	1.56	5.85
Poc 10	1200.25	2.08	10.04	3.66	13.75
Poc 9	1297.42	1.43	6.89	1.20	4.51
Poc 7	1413.5	1.50	7.26	1.61	6.04
Poc 5 (10 bench)	1572.35	1.85	8.94	1.86	6.99
Poc5 (20 bench)	1624.46	1.81	8.72	2.10	7.91
Poc 3	1728	4.30	20.77	3.91	14.72
Poc 2	1798.96	1.32	6.36	1.04	3.90

Both of the models predict that the Pocahontas 3 and 10 are significant contributors to the reservoir in terms of permeability percent. What permeability percent is representing is the storage potential for the various seams in questions because of the ability for CO_2 to flow. The modeled cleat porosity does not account for the in-situ stresses on the system and may overestimate the cleat porosity. It does provide a starting point for the potential flow networks of various seams.

Once the gaseous carbon dioxide has forced the liquids from the injection wells, it is believed that the carbon dioxide will flow in the coal structures that have a higher cleat porosity. The flow will follow the path of the least resistance which may change once a seam or group of seams have taken various amounts of carbon dioxide.

It is interesting to note the effect the carbon dioxide has on the well water in the system due to the formation of bicarbonate and carbonic acid. As calcium carbonate precipitates, more carbon dioxide can be added to the system and the system becomes slightly acidic. The carbonate ion is converted into bicarbonate which produces a very soluble calcium salt. The results indicate a trend in the cleat porosity and the desorption rate of the coals as well as the cleat porosity and the total gas in various seams. While these results suggest a correlation, the analysis does not account for in-situ conditions and contains a small samples size.

9. REFERENCES

Amante, Joseph D. "COAL CLEAT ALTERATION DUE TO CO2 SEQUESTRATION." Pittsburgh Coal Conference (2014): n. page. Web.

Close, J.C., and Erwin, T.M., 1989, Significance and determination of gas content data as related to coalbed methane reservoir evaluation and production implications: Proceedings of the 1989 Coalbed Methane Symposium, paper 8922, p. 37-55.

Diamond, W.P., and Levine, J.R., 1981, Direct method determination of the gas content of coal: procedures and results: U.S. Bureau of Mines Report of Investigations 8515, 36 p.

Diamond, W.P., and Schatzel, S.J., 1998, Measuring the gas content of coal: a review, in R.M. Flores, ed., Coalbed methane: from coal-mine outbursts to a gas resource: International Journal of Coal Geology, v. 35, p. 311-331

Gamson, Paul D., B. Basil Beamish, and David P. Johnson. "Coal microstructure and micropermeability and their effects on natural gas recovery."*Fuel* 72.1 (1993): 87-99

Karacan, C. Ö., and E. Okandan. "Fracture/cleat analysis of coals from Zonguldak Basin (northwestern Turkey) relative to the potential of coalbed methane production." *International Journal of Coal Geology* 44.2 (2000): 109-125.

Karacan, C. O., and E. Okandan. "Adsorption and gas transport in coal microstructure: investigation and evaluation by quantitative X-ray CT imaging."*Fuel* 80.4 (2001): 509-520

Karacan, C. Özgen, and Gareth D. Mitchell. "Behavior and effect of different coal microlithotypes during gas transport for carbon dioxide sequestration into coal seams." *International Journal of Coal Geology* 53.4 (2003): 201-217.

Reucroft, P. J., and A. R. Sethuraman. "Effect of pressure on carbon dioxide induced coal swelling." *Energy & Fuels* 1.1 (1987): 72-75

Ryan, B.D. and Dawson, F.M., 1993, Coalbed methane canister desorption techniques, in Geological fieldwork 1993, B.C. Ministry of Energy, Mines and Petroleum Resources, Paper 1994-1, pages 245-256.

Louk, Andrew K. Monitoring For Enhanced Gas and Liquids Recovery From CO2 'Huff-and-Puff' Injection Test in a Horizontal Chattanooga Shale Well. Thesis. Virginia Polytechnic Institute and State University, 2015. N.p.: n.p., n.d. Print.

Mavor, M. and Nelson, C.R., 1997, Coalbed reservoir gas-in-place analysis: Gas Research Institute Report no. GRI-97/0263, 134 p.

"Virginia Natural Gas." Virginia Natural Gas. N.p., n.d. Web. 20 Jan. 2015. <http://www.energy.vt.edu/vept/naturalgas/>.

UTILIZATION OF ACOUSTICS WELL WATER LEVEL TRACKING TO AID IN MONITORING SEQUESTRATION EVENTS AND TO REFINE RESERVIOR MODELING

1. ABSTRACT

The interaction of carbon dioxide sequestration in shale wells is not well understood. The interaction between sequestration shale wells and offset shale wells is even less understood without the use of microsesmic surveying. Due to the cost of microsesmic surveying and the limitations associated with this method, tracer gases were used as an alternative method to monitor arrival times and plume movement in a wellbore and in auxiliary wells. The tracer study is used in conjunction with gas chromatography from the wells and fluid level testing to monitor plume movement. This chapter will discuss the merits and results from liquid level testing in the Emory River 'huff-and-puff' sequestration project. The project injected 500 tons of carbon dioxide into a horizontal shale well to help interrupt sequestration events, determine parameters associated with horizontal well orientation, and overcome the limitations of down hole measurements through surface monitoring techniques.

2. INTRODUCTION

Most acoustic liquid level instruments measure the distance to the liquid level from a casing in an annulus. A single test is used and the acoustic signal is digitized and stored in a computer. The reflection time from the surface of the liquid at the bottom hole along with the gas composition is used to render an acoustic velocity that is used to calculate the total distance traveled (Podio 1990). Another method, if the tubing is still in place in the gas well, involves

counting reflections from the collars of the tubing o?f a known distance to the surface of the liquid (McCoy 1988).

Instrumentation of this practice was developed in the 1930's with three components: an acoustic pulse generator, a microphone, and a pressure gauge. The technology was primitive in nature with the acoustic pulse consisting of explosive materials such as blasting caps, 45 caliber blanks, and 10 gauge blanks (Rowland et al. 2003). This technique is a hazardous practice is no longer used due the damage to wells, the environment, and the propensity for an explosion if oxygen were to be introduced into a producing hydrocarbon well.

Currently, a gas gun has replaced the previously mentioned explosion detection style gun and offers versatility and economic benefits with the use of a pulse generator. A chamber of the acoustic gun is filled with a compressed gas in the gun and is suddenly released. The expansion of gas from the chamber into the well generates an acoustic pulse that is easily controlled by regulating the pressure in the gun's chamber. In most cases the compressed gas is CO_2 or N_2 and charged to pressure greater than that of the well pressure. The microphone within the wellhead converts the reflected acoustic signal into an electrical signal consisting of a series of pulses, which corresponds to a sequence of reflections that can be interrupted by a user (Rowan et al. 2003).

The percent of CO_2 in the annular gas requires special attention be given to the acquisition of acoustic fluid levels and to the calculations of the pump intake pressure. At low pressure carbon dioxide behaves as a hydrocarbon gas and the CO_2 gas column is easily calculated. If bottom hole pressure exceed 1000 psi and the temperature greater than 100° F (Figure 24) , the density of CO_2 increases rapidly to the the density of American Petroleum Institute(API) hydrocarbon liquids as seen below in figure Figure 23 (de Sa Neto et. Al 1999).

The CO_2, oil, and water may become miscible, and this mixture of the fluids can result in difficulties detecting the acoustic interface as there is no distinct interface. From 500 psi to 1500 psi, rapid changes in CO_2 density causing fluid gradients difficult to determine.

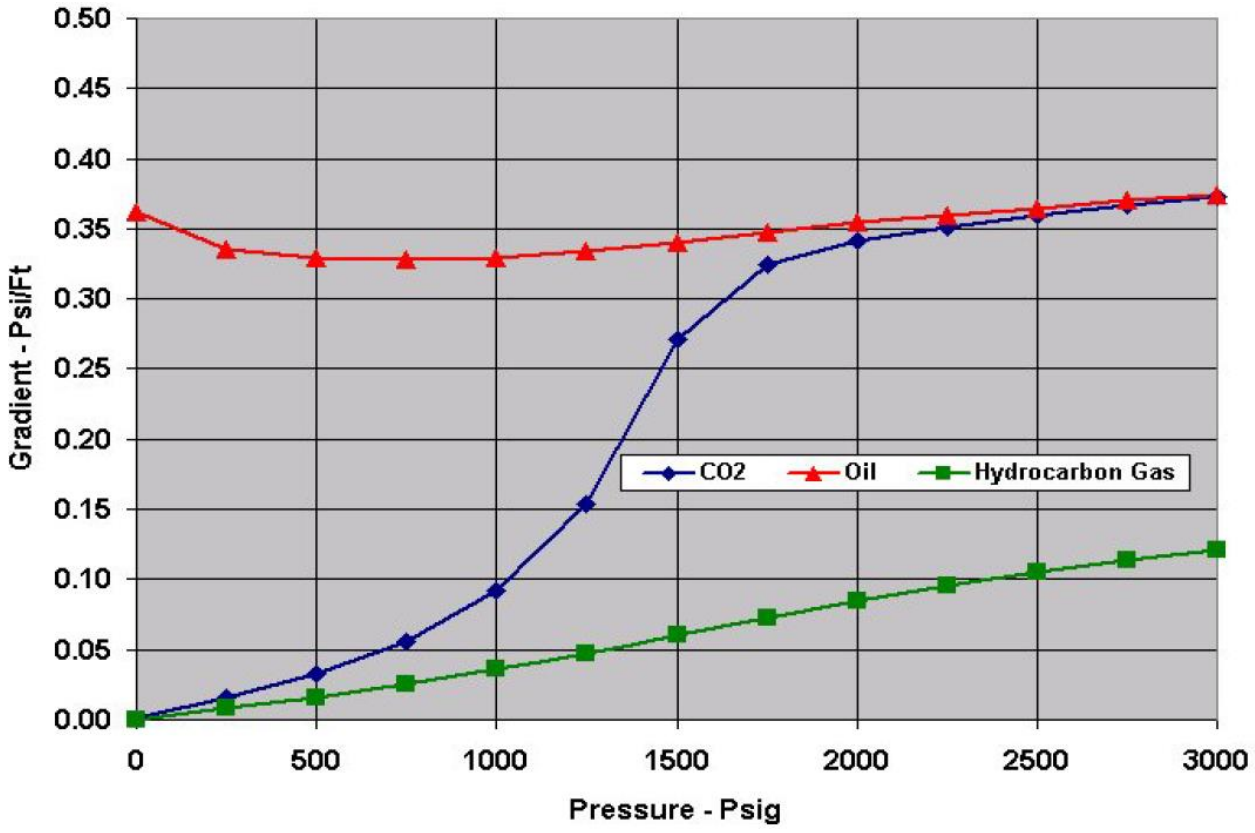

Figure 23: Comparison of Oil, CO2 and 0.85 SG Hydrocarbon Gas (API INDEX)

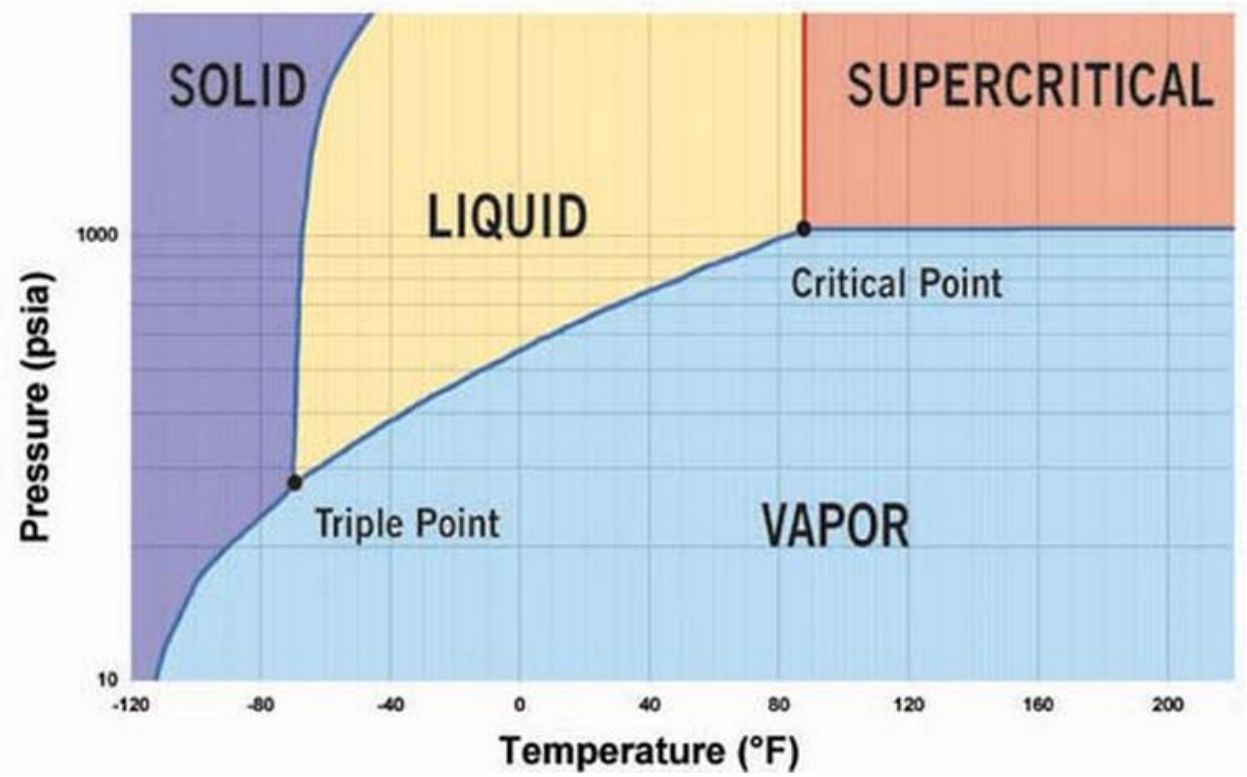

Figure 24: Phase diagram of CO2

3. SITE DEVELOPMENT

The target area for this test in Tennessee's Chattanooga shale located on CNX property in Wartburg Tennessee.

Gas well HW-1003 is a horizontal shale well which is characterized by figure Figure 25 model in Schlumberger Eclipse software by researchers Cidgem Keles of the Virginia Center for Coal and Energy Research. The well was sequestered with 500 tons of CO_2. During the injection phase, tracer gases were injected with the CO_2 plume to monitor movement and breakthrough at the offset production well. Sulfur hexafluoride (SF_6) and two perfluorocarbon tracers (PFTs), Perfluoromethylcyclopentane (PMCP), and Perfluoromethylcyclohexane (PMCH) were introduced at staggered times during the injection phase. Just over 3000ml of SF_6 and 500ml of PMCP were introduced, with the initial 50 tons of CO_2 injection and while the CO_2 was in gas

phase, to simulate the first plume movement through the geologic formations. This was also to test the arrival times of the much smaller molecule SF_6 versus PMCP. Later in the injection, 500 ml of PMCH were introduced when a total of 330 tons of CO_2 had been injected.

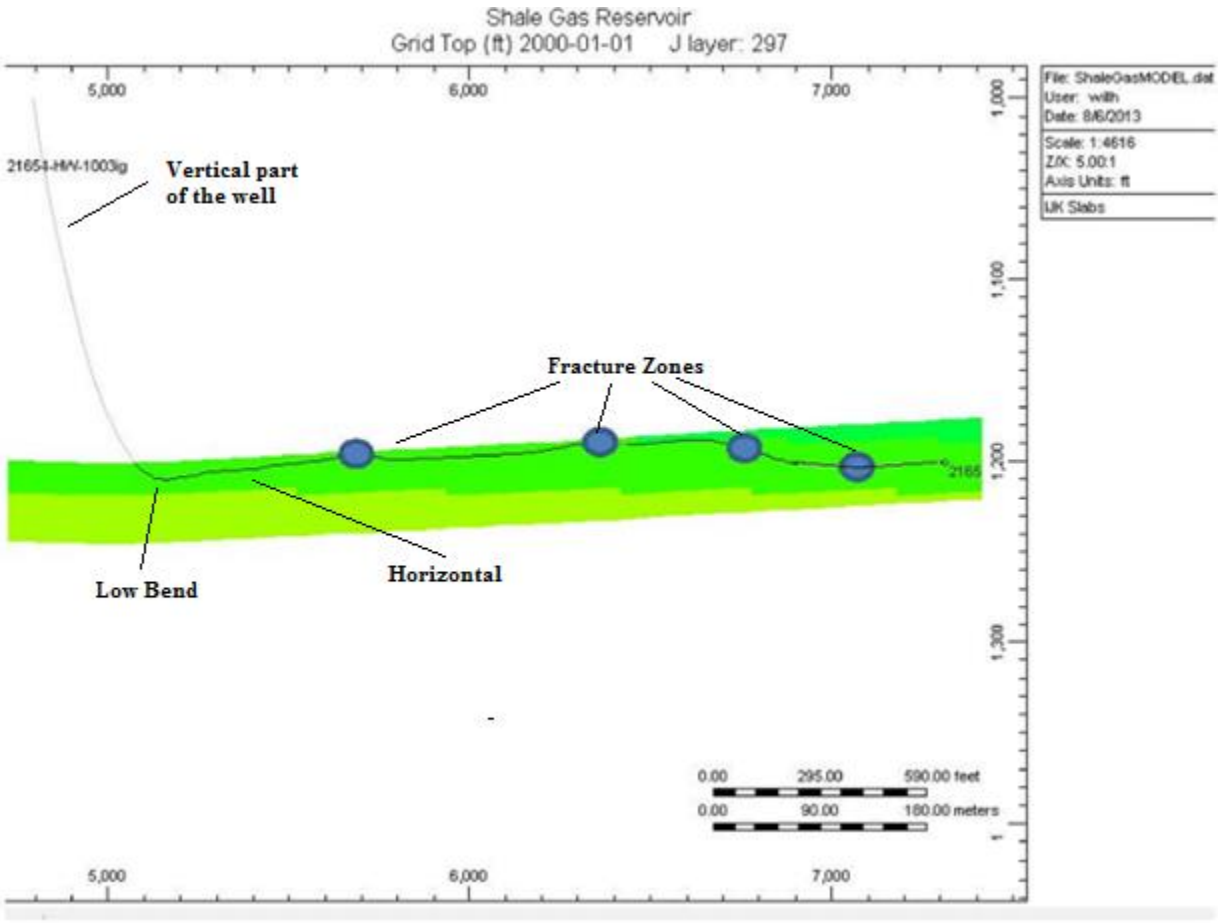

Figure 25: HW 1003 Petrel model of the well

4. METHOD DEVELOPMENT

In preparation for injection, the piping in the well had been removed and the well had been taken offline. The purpose of the piping is to extract the water at the base of the well. Figure 25 does not conceptualize fully that the lowest part of the well is curved before the horizontal as well as at the tail end of the well. The well and the surrounding water table should reach equilibrium before the injection of CO_2, which should be dissipated into the reservoir by the

gaseous CO_2. The resulting well fixture on the surface contains a gate valve and a ball valve which leads to an annulus. To minimize noise in the acoustic test, the ball valve was placed in line with the well head. With the removal of the some major causes of background interference, such as piping, the acoustic reflection is simplified significantly. While the reflection horizon becomes clearer and further analysis of the well is required to obtain more accurate and meaningful data from this method. A further detailed description of the location of the gun is seen in the Appendix on page 164. A gas composition summary is required to calculate the acoustic velocity of the gas column. This is achieved through gas chromography after injection of over 99% CO_2. This is the optimum way of determining the liquid level due to the lack of reflection surfaces. Alternate methods include: collar counting, horizon mapping, and/or historical mapping. Figure 26 is the flow sheet of this setup. The user is charging the instrument with compressed CO_2 for an acoustic liquid level test. Figure 27 shows the basic setup of the echometer on the well.

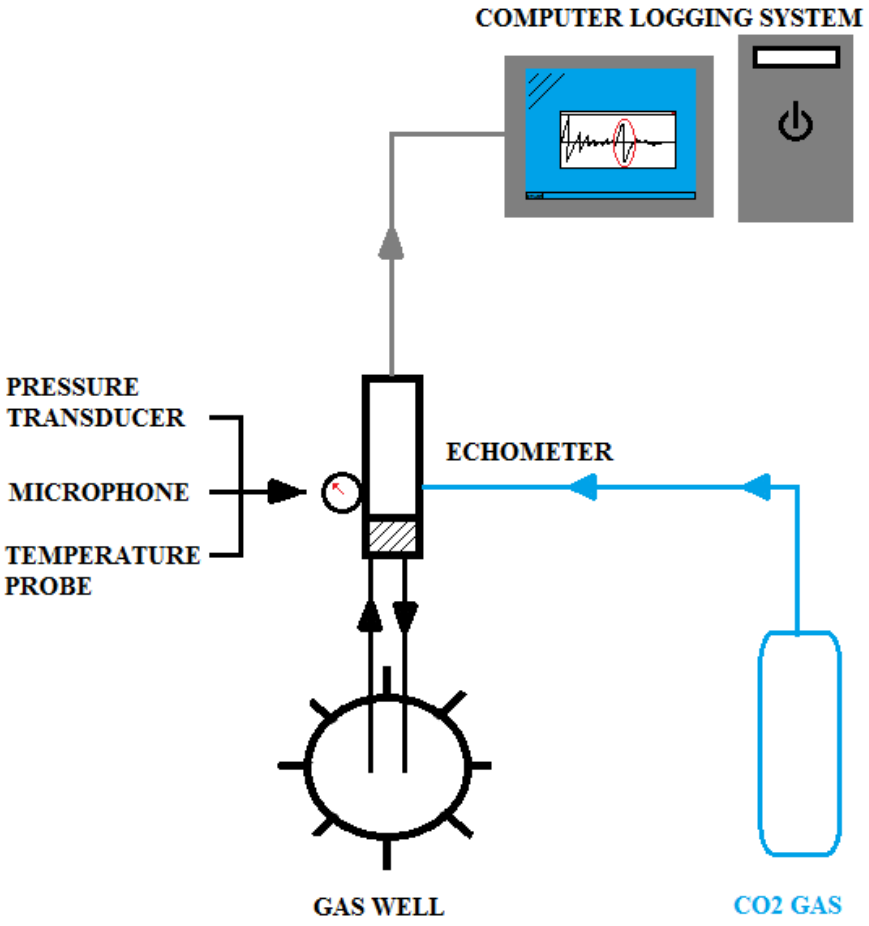

Figure 26: Simplified Logging Schematic

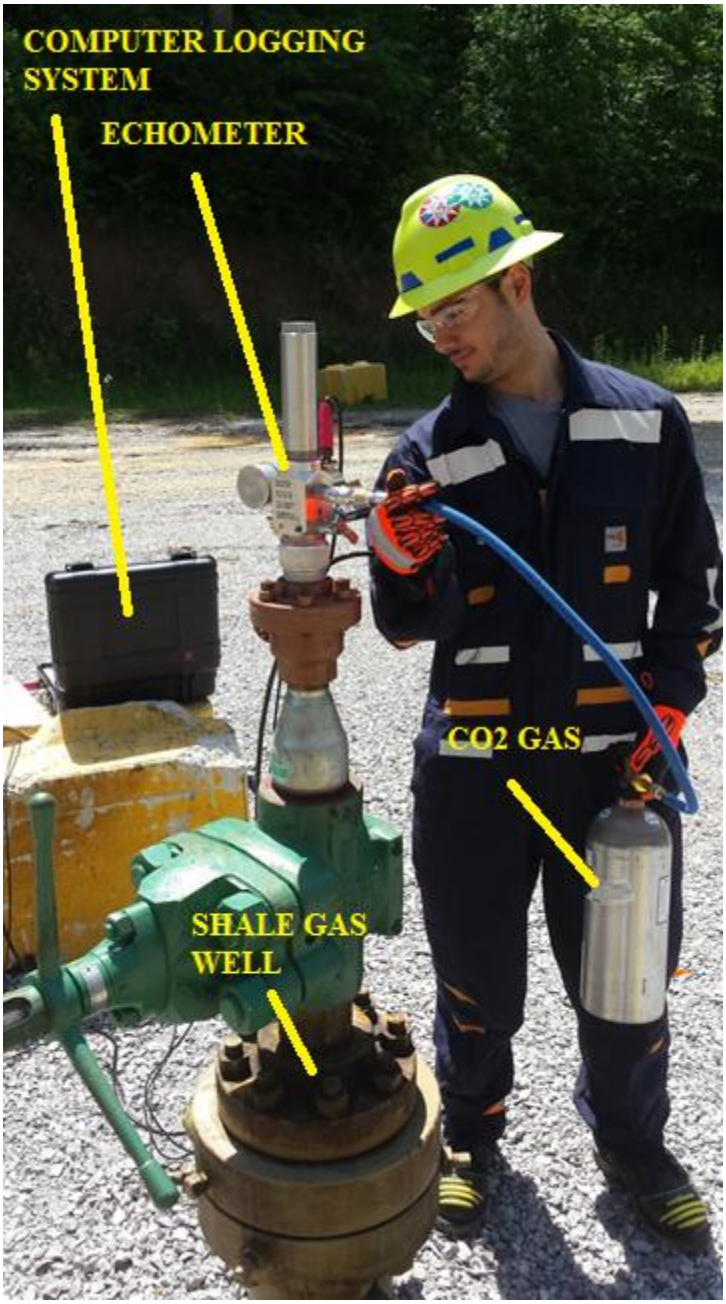

Figure 27: User Charging the Echometer for an Acoustic Test

While the setup for an echometer shot is relatively simple, a few basic steps should be taken and understood to provide the user with precise information. Arguably, the most important step in the echometer liquid level process is the location of the echometer in relation to the well head. The optimal location would be in line with the direction of travel of the acoustic wave. This is not

always possible and the results from field testing indicate the level of noise cancelation required negates the accuracy needed and makes the event horizontal nearly impossible to distinguish. The pressure of the echometer gun requires that it be greater than that of the well to propagate a wave through the well. The echometer manual states that the minimum pressure of the gun should be 150- 200 psi over the pressure of the well. If this operating pressure is increased an order of magnitude to 300-400 psi above the well pressure, the level of precision does not increase. This increase causes early reflections, making the detection of an event horizon more difficult.

5. RAW DATA INTERPRETATION

The echometer records the microphone noise from the shot and converts it to data in real time. This data is displayed on a graph with time on the X axis and millivolts on the Y axis. The values of the Y axis are meaningless in terms of amplitude; the magnitude of the axis is an indicator of markers, a reflection surface, a collar, or an opening in the wellbore. Figure 28 demonstrates a high pass unfiltered rendering of the acoustic data. The liquid level, circled in red, is the first and only marker in the well. This represents the round trip travel time for the wave to travel down the well and return to the microphone. In this test the time was 6.846 seconds. This coupled with the acoustic velocity yields the total distance traveled.

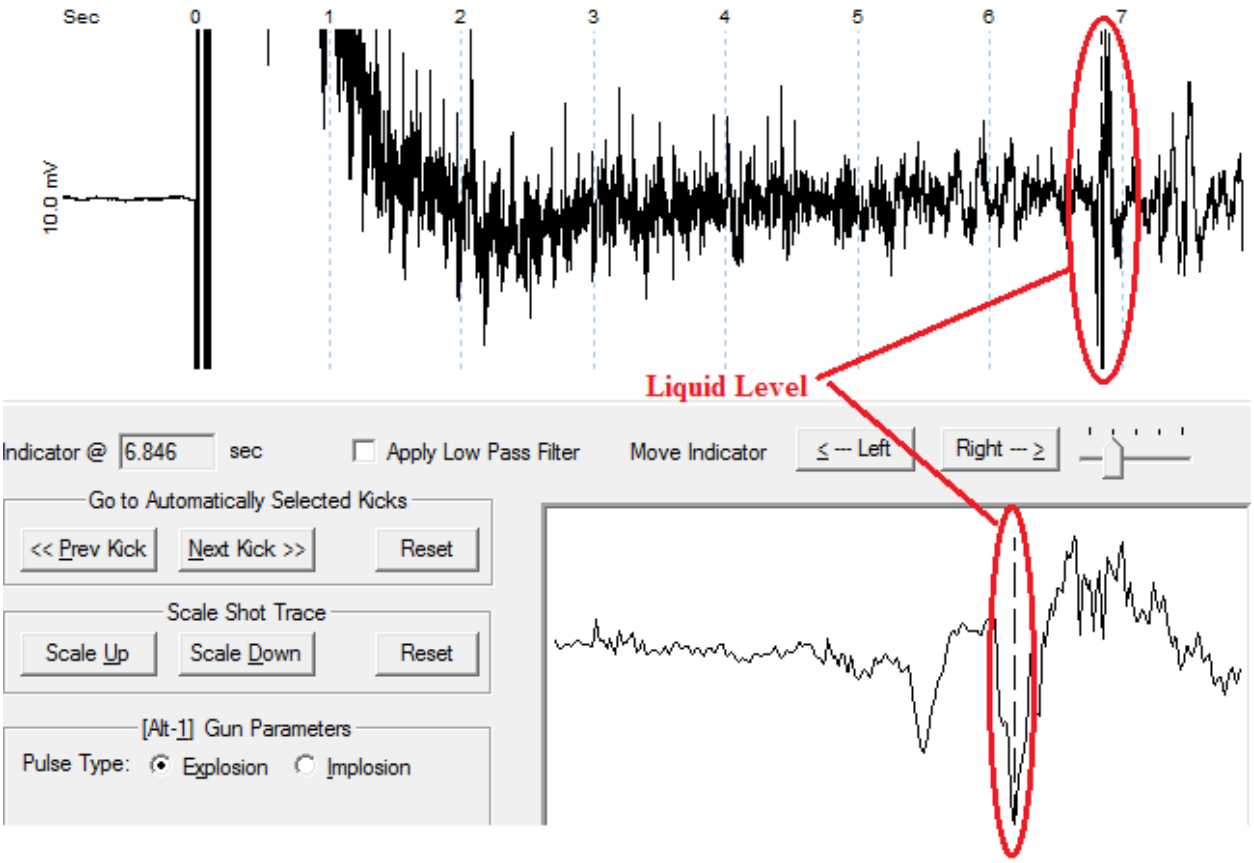

Figure 28: HW 1003 Acoustic Test with reflection surface

Acoustic velocity is measured by two techniques in this study: collar counting and gas composition. Gas composition is used by in conjunction with gas chromatography provided by another graduate student, Andrew Kyle Louk seen in the appendix. The results can then be calculated into an acoustic velocity using the equation below.

$$v_{sound} = \sqrt{\frac{\gamma RT}{M}}$$

$$v_{sound} = velocity\ of\ sound$$

$$\gamma = abiabatic\ constant$$

$$R = gas\ constant$$

$$M = molar\ mass\ of\ the\ gas\ composition$$

This method is the only method used to calculate the liquid level during the CO_2 soaking period due to the lack of tubing collars in the wellbore and the gas composition exceeding 99% CO_2 making the calculation extremely simple. The acoustic velocity was between 780-790 feet per second depending on the small percentage of heavier hydrocarbon in the system. The second method utilizes tubing collars that are set at predefined intervals of 32 feet. This can be seen in Figure 29 which is rendered by the Echometer program. Each of the peaks, in Figure 29, represent a reflection surface of the collars that connect the tubing together.

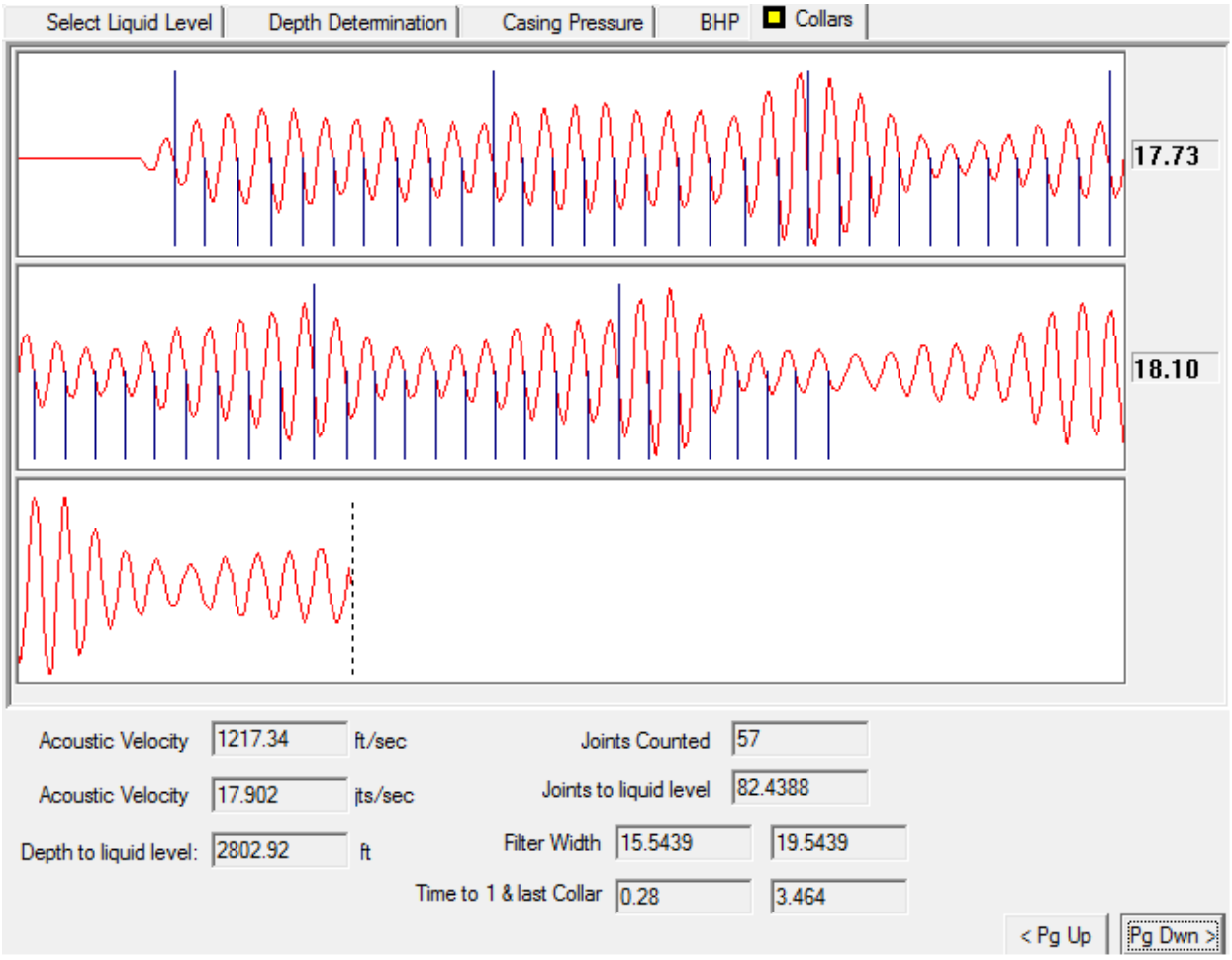

Figure 29: Collar counting in HW 1003 for depth

The illustration above demonstrates the technique of even spacing per collar. The distance is then extrapolated to the reflection surface seen as the dotted line. In this example, the reflection

surface was the end of the tubing which was set at 2804 feet. The accuracy of this method is suggested by an error of 0.0385% from 3 tests in this test from the measure distance of 2802.94 feet to the installed distance of 2804 feet which was provided by the installer. More difficulties and uncertainty enter the equation when the distance extrapolated is greater. This method allows the user to tune the shot signal to a known horizon and utilize it to achieve greater accuracy for liquid level testing. Figure 30 is the January 15, 2015 echometer shot after the tubing was reinstalled and the water was extracted from the well.

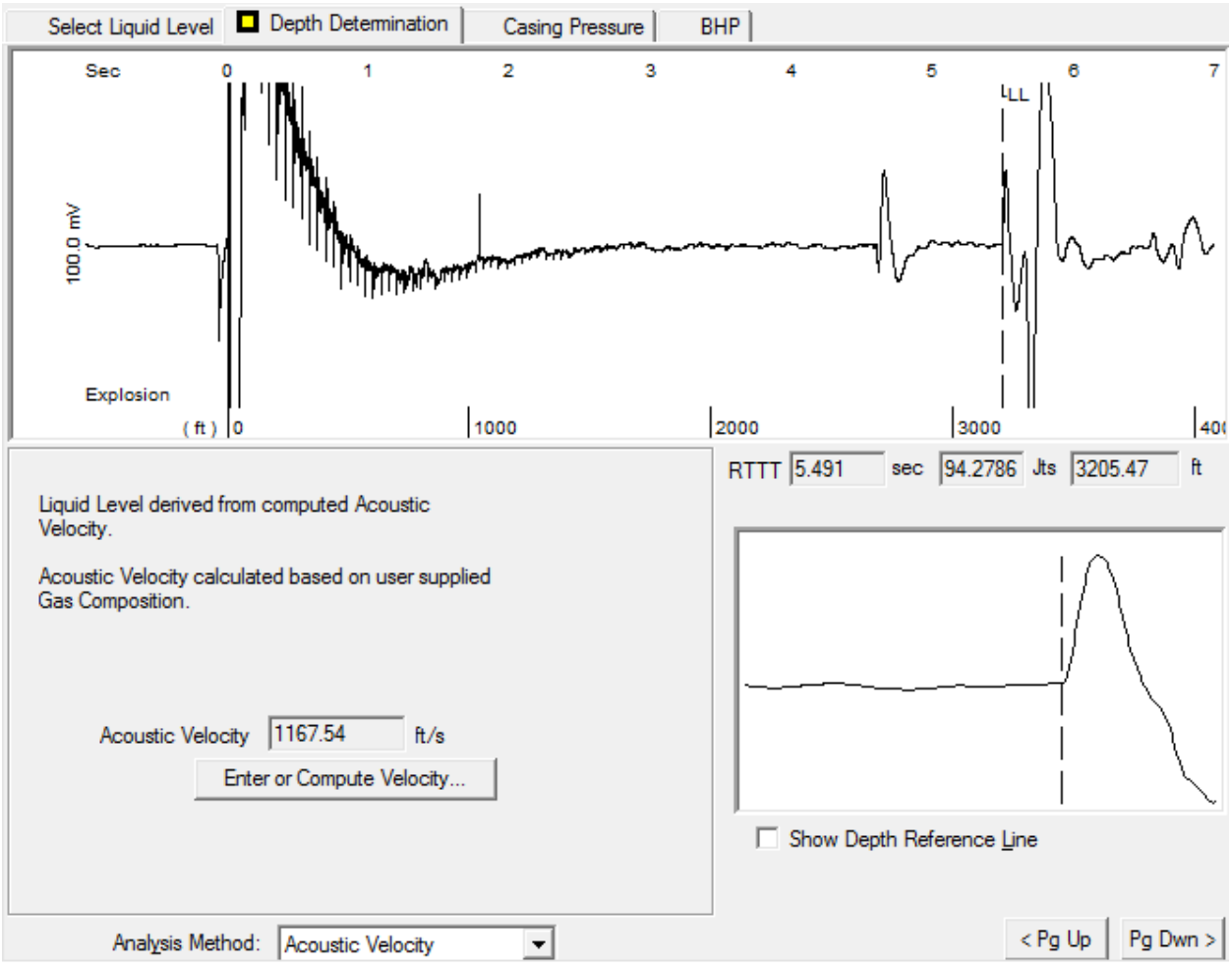

Figure 30: HW 1003 1/15/2015

6. DISCUSSION AND RESULTS

To quantify the precision of the instrument the first two tests on the well contain multiple acoustic shoots at varying gas gun pressures. The data for all the test is shown in Table E. The standard deviations for the first two test are ± 0.526' and 0.189' respectively. This suggests the testing parameters are precise and repeatable regardless of the detonation pressure of the gun.

Table E: Echometer Results from HW 1003

	Date	Time	Total Distance (ft.)	Acoustic Velocity (ft./s)
Test 1	**4/28/2014**	12:03:15	2676.2	781.813
	4/28/2014	12:05:07	2676.6	781.839
	4/28/2014	12:06:34	2676.2	781.844
	4/28/2014	12:13:09	2676.4	781.774
	4/28/2014	12:15:50	2676.7	781.853
	4/28/2014	12:19:53	2677.1	781.863
	4/28/2014	12:22:12	2675.2	781.424
	4/28/2014	12:26:03	2676.7	781.865
Test 2	**5/19/2014**	11:38:11	2704.4	793.201
	5/19/2014	11:40:47	2704.0	793.077
	5/19/2014	11:41:57	2704.0	793.077
	5/19/2014	11:43:01	2704.4	793.077
	5/19/2014	11:44:05	2704.4	793.077
	5/19/2014	11:46:07	2704.4	793.080
	5/19/2014	11:48:41	2704.4	793.080
	5/19/2014	11:50:01	2704.4	793.080
	5/19/2014	11:51:29	2704.0	793.080
Test 3	**6/17/2014**	12:46:40	2676.8	792.552
	6/17/2014	12:47:44	2698.2	793.230
	6/17/2014	12:48:42	2697.8	793.230
Test 4	**7/28/2014**	11:49:16	2670.7	792.733
	7/28/2014	11:49:16	2671.6	792.893
Test 5	**1/15/2015**		3205.5	1167.54

The averages of the distance traveled to the liquid level before the tubing was reinstalled is around 2690 feet total. With the high level of precision, there is a reflection point at this distance as the carbon dioxide was in the soaking period. The pressure over injection shows that the injected carbon dioxide never reached the liquid state as seen in the appendix and the horizon is assumed to be ground water that has reentered the well bore. Referring back to the well completion diagram (Figure 25), the bend between the vertical and the horizontal is the lowest elevation point until the second perforation, which can kill the well if in production. It is interesting to note that the well head pressure continued to decrease throughout the soaking period and leveled off at a period of three months. This indicates that the CO_2 is migrating in the simulated reservoir volume and reaching an equilibrium in a closed system.

With the pressure declining at a steady rate for a short period of time, the CO_2 is assumed to be adsorbing to the shale or migrating in the reservoir. No CO_2 nor tracer have been observed at the offset wells (Louk 2015). While 35% in volume of CO_2 has been reproduced, the shale has shown potential for a long term storage and enhanced gas recovery. The cost effectiveness and the enhanced recovery for the project is shown in the defense of Andrew Louk, 2015.

7. CONCLUSIONS

The purpose of this study was to gauge the effectiveness of the echometer for monitoring and verification of surface results of sequestration type projects. The echometer type liquid level sensor is ideal for sequestration type projects where little or no known reflection horizons are known due to the simplistic calculation of an acoustic velocity. The echometer provides accurate detection of liquid levels at low cost to the user, while maintaining the ability to service multiple

wells with varying completions and stages of production cycles. The echometer allows the ability to calculate bottom hole pressure from the liquid level detection with the surface gauge reading. This provides a low cost analysis of the current pumping cycles, effectiveness of dewatering of the reservoir, and information about sequestration events that have little to no monitoring instrumentation down the hole.

8. REFERENCES

de Sa Neto, Abelardo, and Abraham S. Grader. "Echo-Meter Buildup Tests: The Effects of Fluid Hydraulics and Thermodynamics." *Proceedings of SPE*56617 (1999): 267-278.

Louk, Andrew K. Monitoring For Enhanced Gas and Liquids Recovery From CO2 'Huff-and-Puff' Injection Test in a Horizontal Chattanooga Shale Well. Thesis. Virginia Polytechnic Institute and State University, 2015. N.p.: n.p., n.d. Print.

McCoy, James N., Augusto L. Podio, and Ken L. Huddleston. "Acoustic Determination of Producing Bottomhole Pressure." *SPE formation evaluation*3.03 (1988): 617-621

Podio, A. L. "Computerized Well Analysis by AL Podio*-UNIVERSITY OF TEXAS AT AUSTIN and J. N. McCoy*-ECHOMETER CENTER." (1990).

Rowlan, O. Lynn, et al. "Advanced techniques for acoustic liquid-level determination." *SPE Production and Operations Symposium*. Society of Petroleum Engineers, 2003.

CONCLUSIONS AND RECOMMENDATIONS

The results from the initial test with the micro computed tomography, environmental scanning electron microscope, and inductively coupled mass spectrometer have concluded that chemical transport is likely to occur with the addition of gaseous carbon dioxide to the reservoir environment. While laboratory testing indicated a 25 percent increase in permeability, the levels in the field may not reflect this significant of a change due to the in-situ stresses on the system. Water levels as of 4/29/2015 from the Echometer Liquid Level tests indicate that the injection wells currently have water levels values between the Pocahontas 9 and 7, roughly 1300 feet. This creates the potential for a slightly acidic solution to contact the five seams and create a potential for increased permeability as seen in Chapter 1.

The results from core hole C1 show that the various seams in the reservoir are heterogeneous in terms of chemical composition, cleat structure, gas content, and desorption rate. The gas content and desorption rates are correlated to the cleat porosity per seam and show trends of higher maximum desorption slopes with higher cleat porosity and gas not desorbed from the matrix during the three month desorption analysis with smaller cleat porosity. Which concludes that the cleats dominate the permeability in coal seams. Further study on the cleat structure is need to predict both sequestration and total recoverable gas in place. This level of testing suggests that field tests should be used to produce real world results.

Preliminary results from the echometer testing are very promising and have shown the ability to locate the liquid level within a reservoir in both vertical producing CBM wells and a CO_2 filled horizontal shale gas well. I suggest the following echometer tests for future work:

1. Water build up test: The coal bed methane wells are characterized by thin coal seams at various elevations. The gas from all of these seams comingles and is produced to pipeline. In theory, one seam could be producing larger quantities of gas then the others and should be the focus in hydraulic fracturing for that zone. The water build up test is similar to killing a natural gas well but done in a much slower, more controlled method. Water will be pumped into a well and echometer liquid level detections will provide the elevation of the water level. Gas composition and flows will be measured for each range of seams and help quantify the gas production by seam.
2. Pressure buildup test: The pressure build up test is already mentioned and described in this thesis. Over a large scale and time period the buildup tests have the potential to provide the permeability evolution in the immediate reservoir area.

The data presented in this thesis represents a qualitative and semi quantitative analysis (lack of in-situ constraints) of the coal seams in Central Appalachia. The results shown are for laboratory testing from a single well do not fully encompass the complexity of the system but help to provide insight into geochemical evolution in CO_2 sequestration events. The imaging through computed tomography provides another layer of information about various seams in a nondestructive manner. This new data will allow researchers and companies to make more informed decisions about the reservoirs they exploit without sacrificing expensive core samples.

APPENDIX FOR RAW DATA AND EQUIPMENT OPERATION

A. µCT SCANS

The following section contains the raw computed tomography imagines of various seams from C-1. The images are unfiltered and considered raw. Thousands of images are rendered per scan.

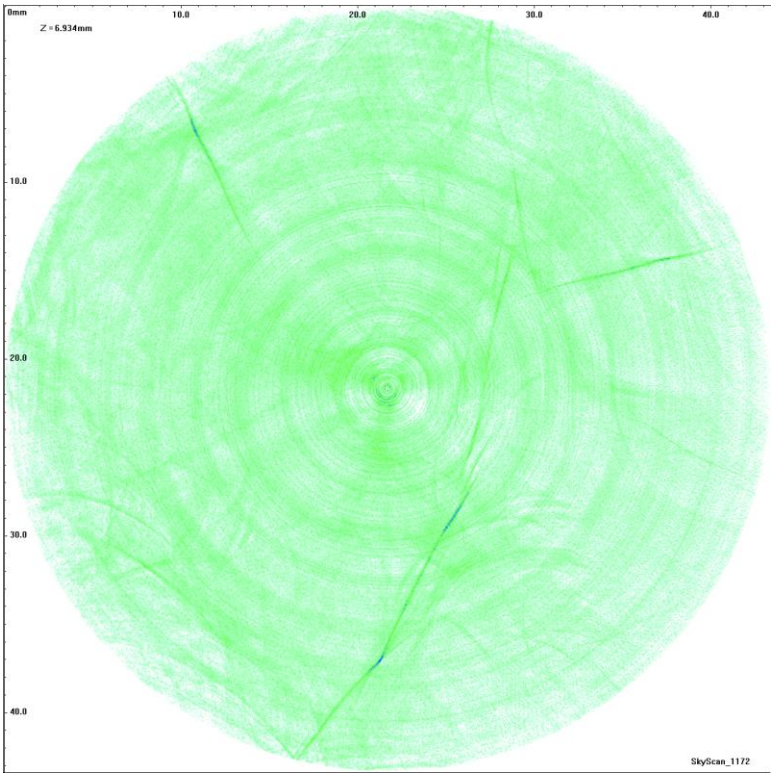

Figure 31: Elevation 892

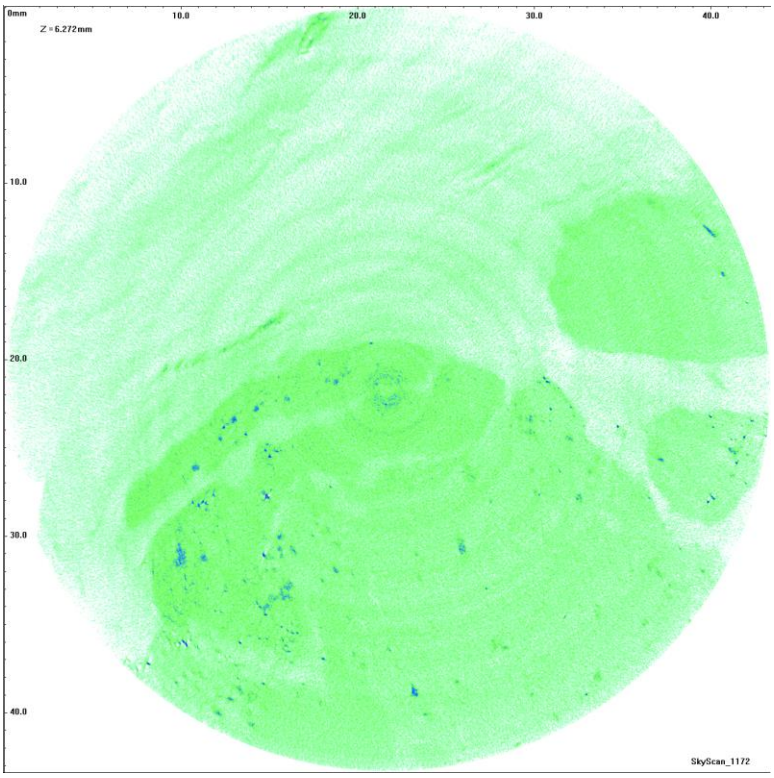

Figure 32: Elevation 1152 Boundary

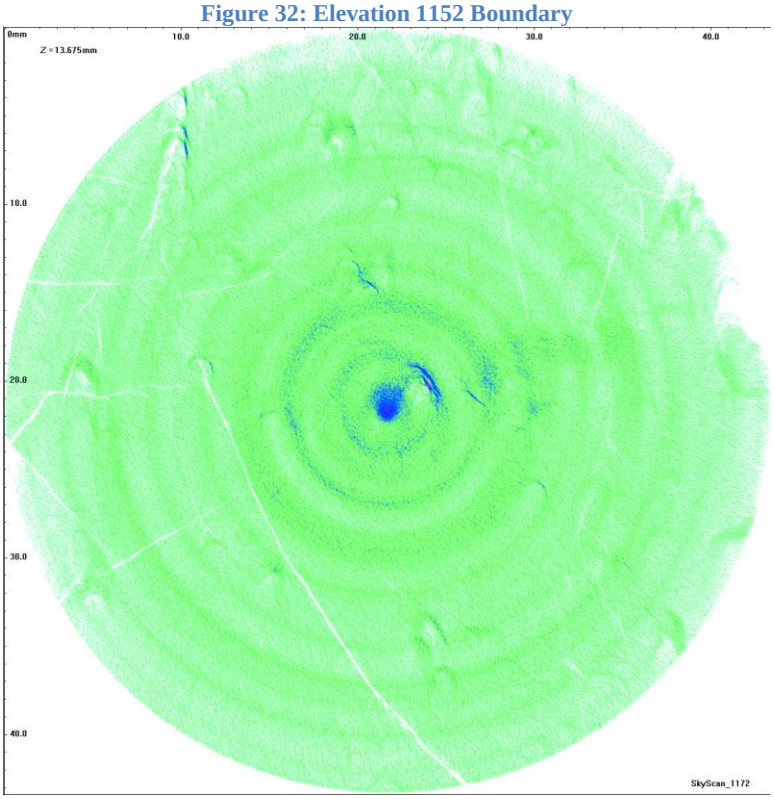

Figure 33: Elevation 1158

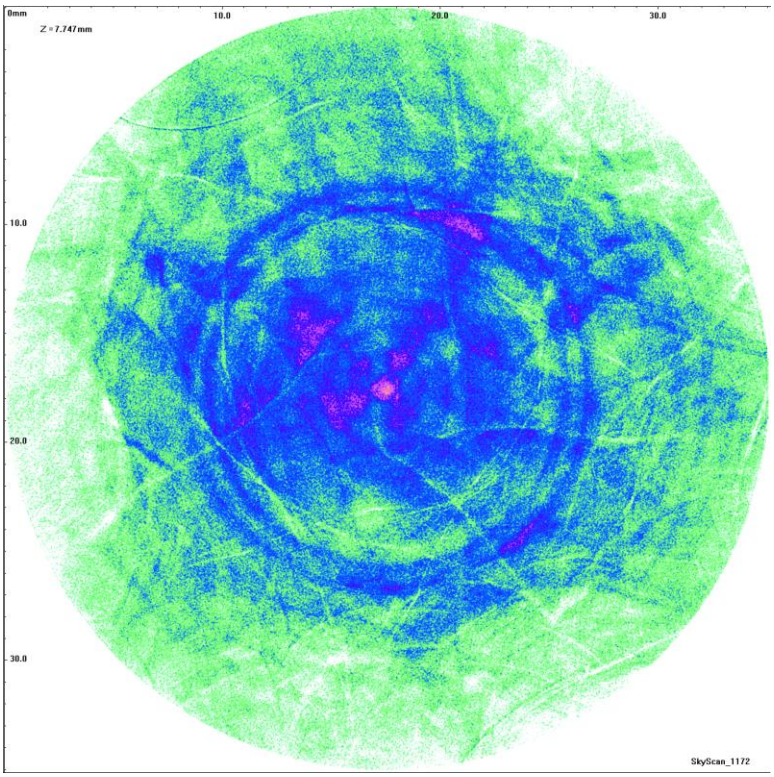

Figure 34: Elevation 1159.75

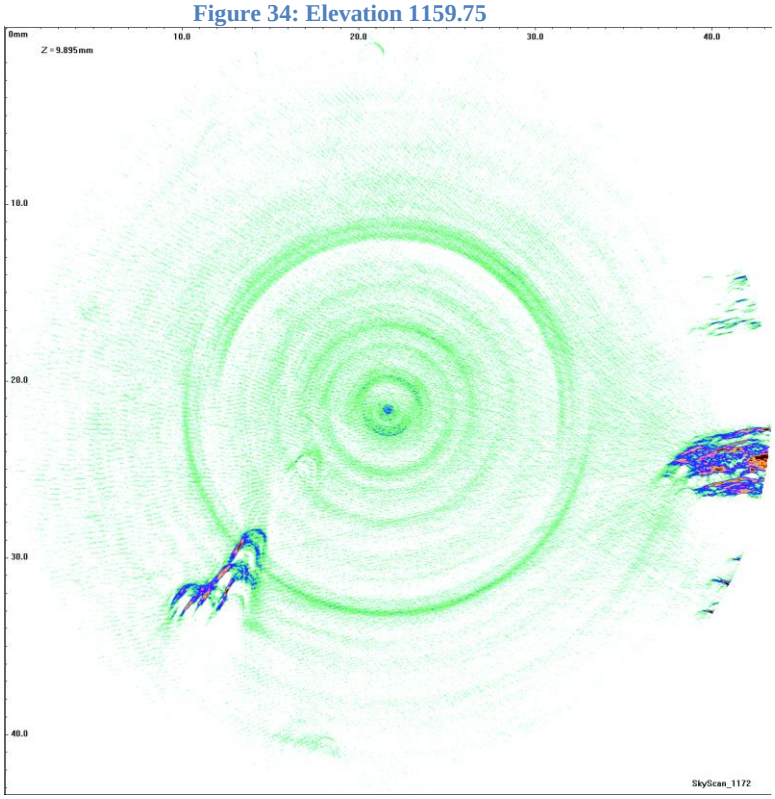

Figure 35: Elevation 1194

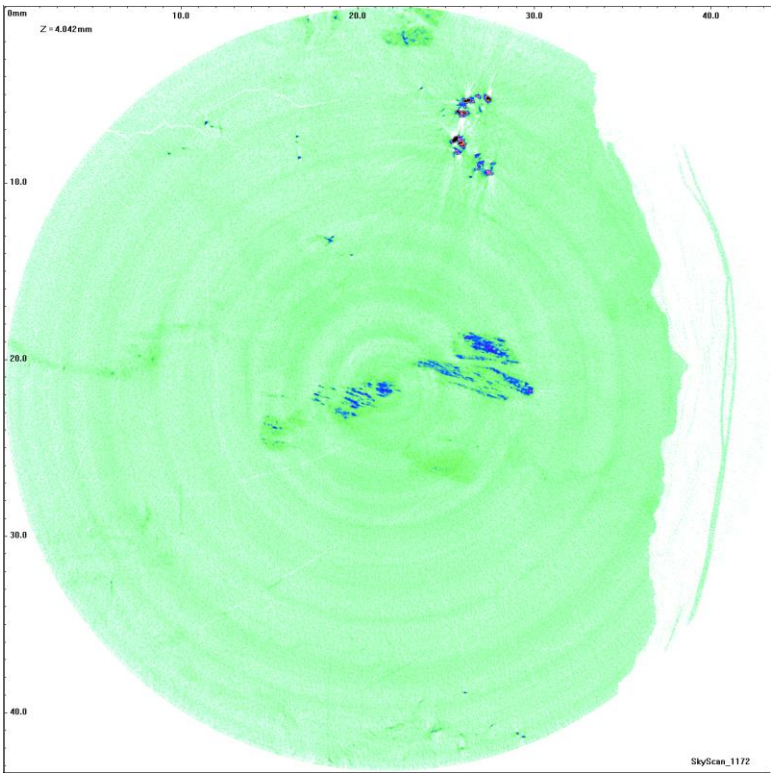

Figure 36: Elevation 1297.42

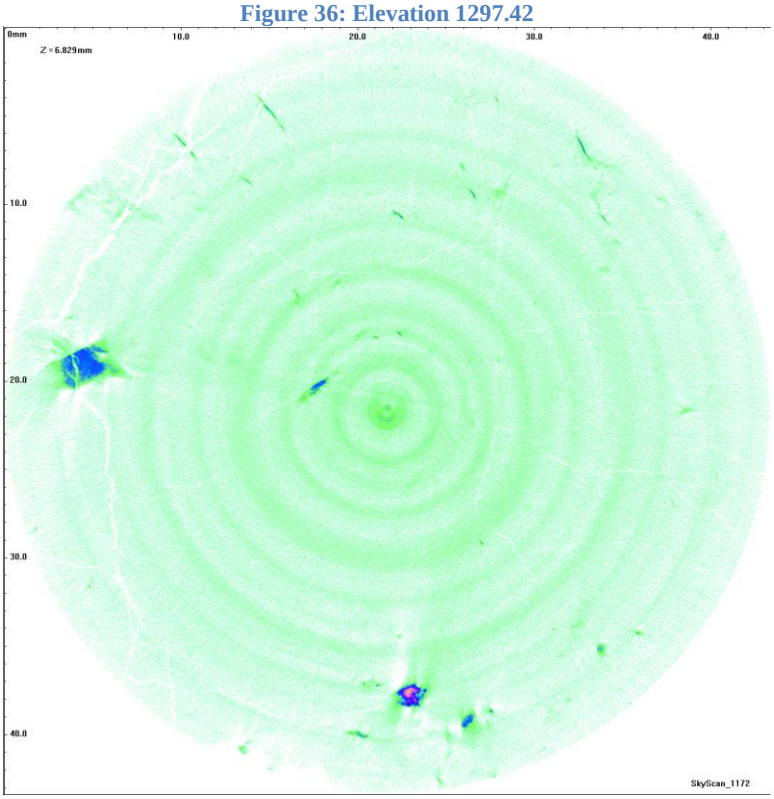

Figure 37: Elevation 1558

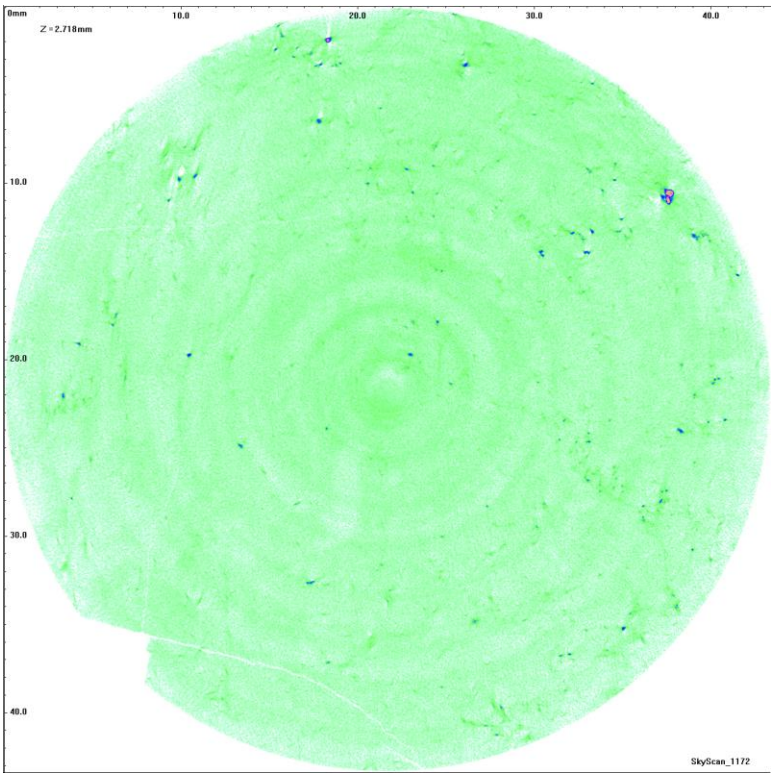

Figure 38: Elevation 1746.8

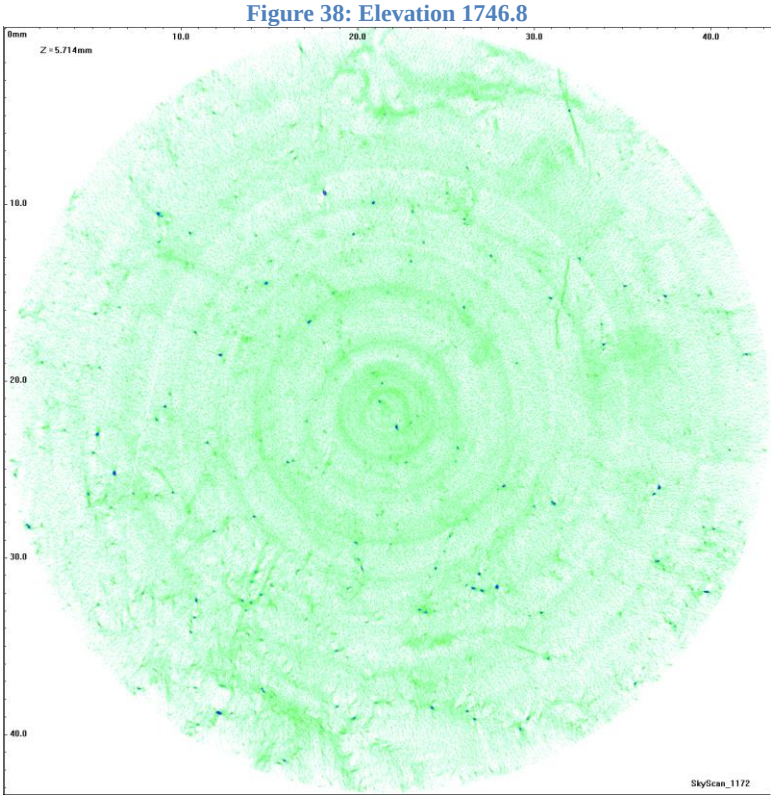

Figure 39: Elevation 1758

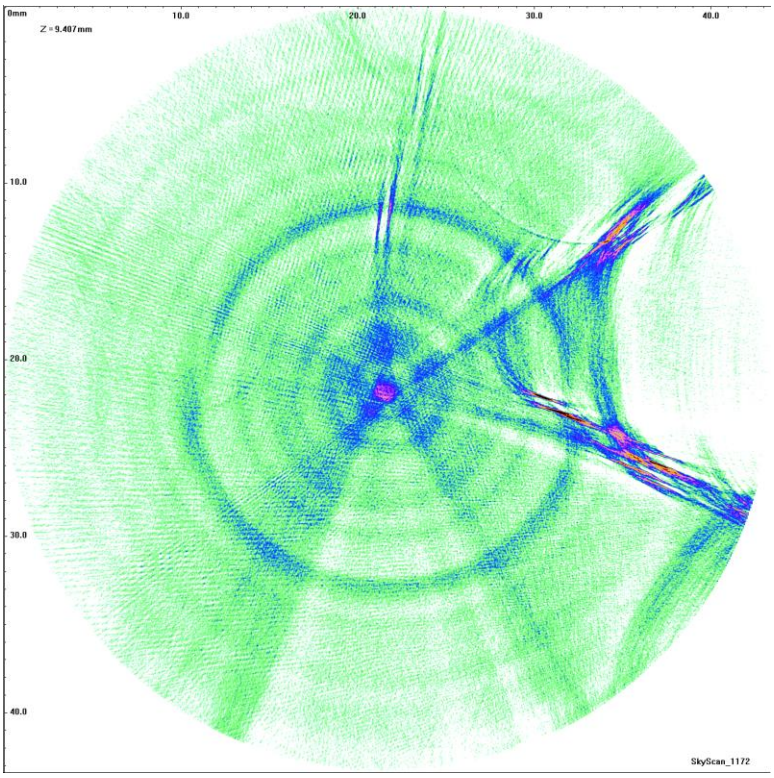

Figure 40: Elevation 1994

B. µCT SCANS CLEAT POROSITY

The following figures were used to cleat the representative cleat porosity for each of the seam. Only one of the images is listed, but multiple images from multiple location from within the seam were used to calculate the cleat porosity listed under the figure. Certain sections with increased levels of pyrite were avoided due to the lack of resolution of the cleat structure such as Elevation 1758.

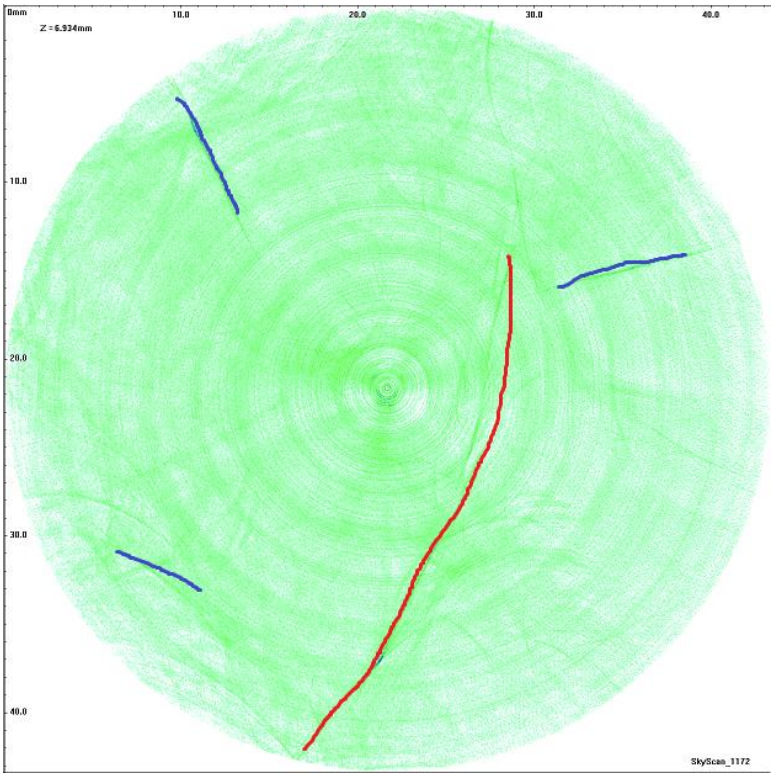

Figure 41: Elevation 892 Cleat Porosity (0.29%)

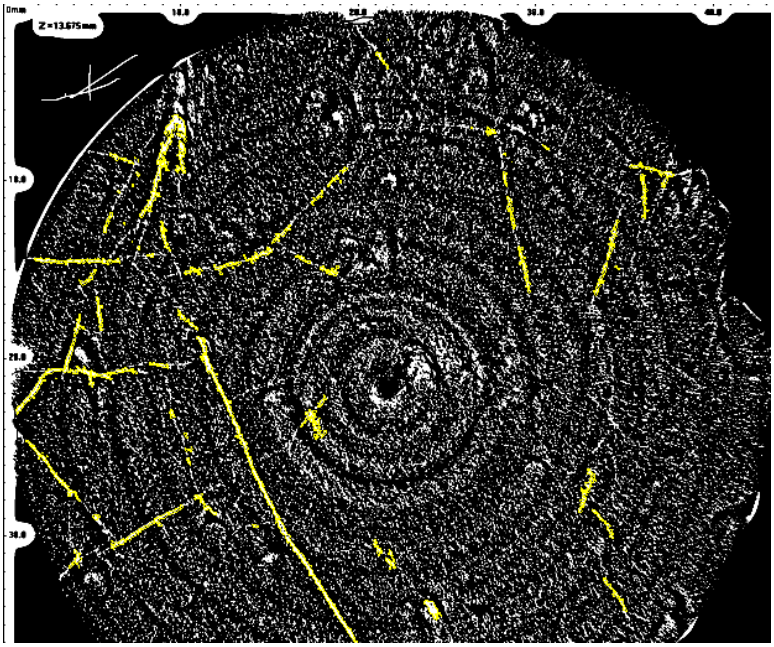

Figure 42: Elevation 1158 Cleat Porosity (1.22%)

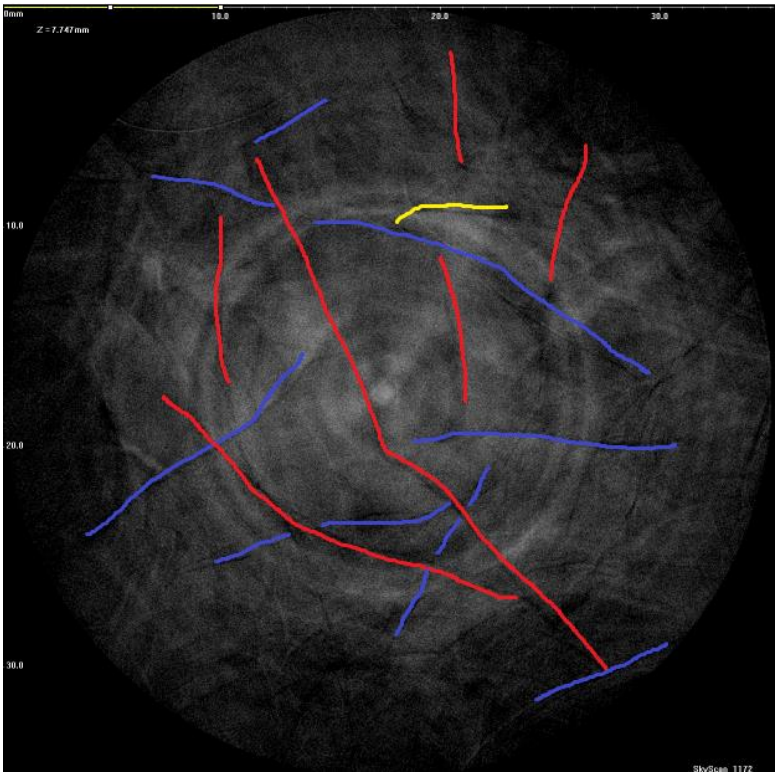

Figure 43: Elevation 1159 Cleat Porosity (0.13%)

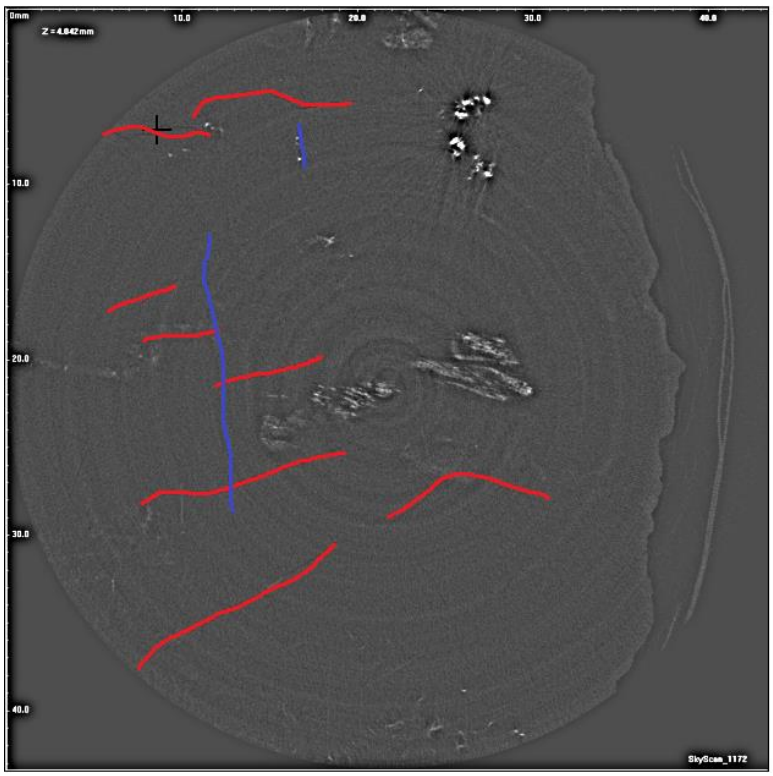

Figure 44: Elevation 1297 Cleat Porosity (0.09%)

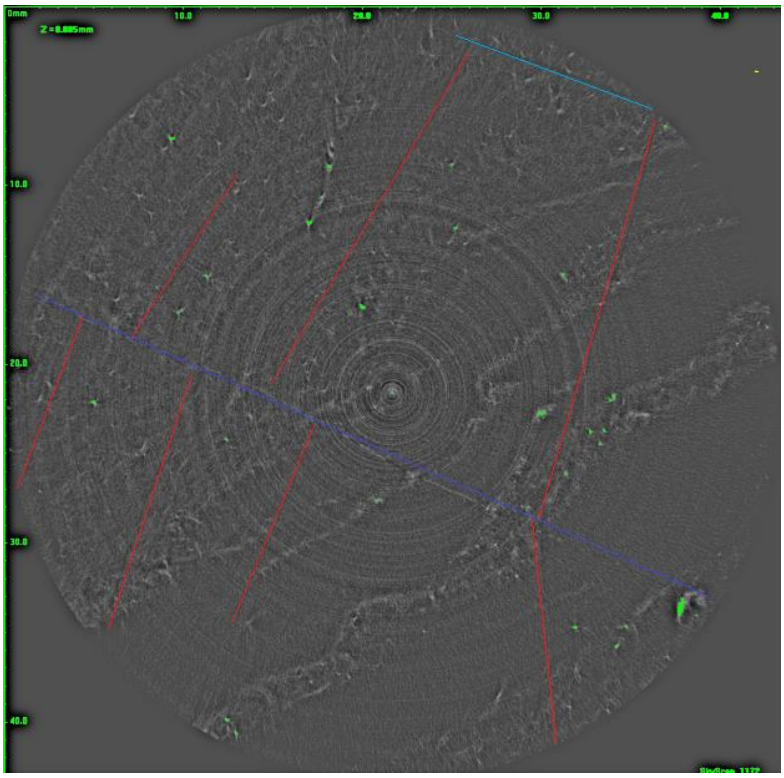

Figure 45: Elevation 1413 Cleat Porosity (1.45%)

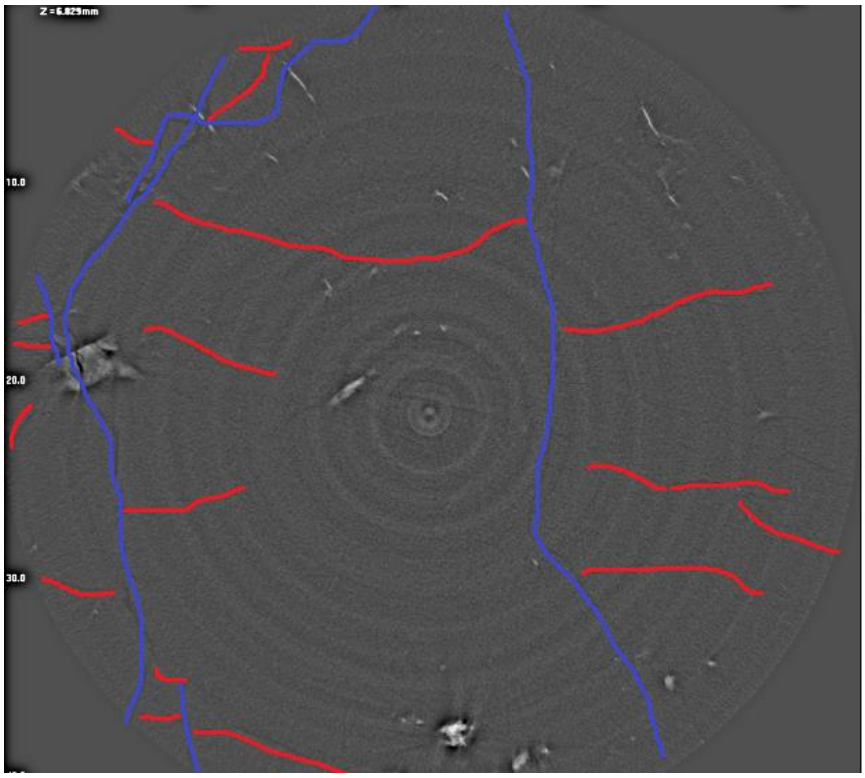

Figure 46: Elevation 1558 Cleat Porosity (0.22%)

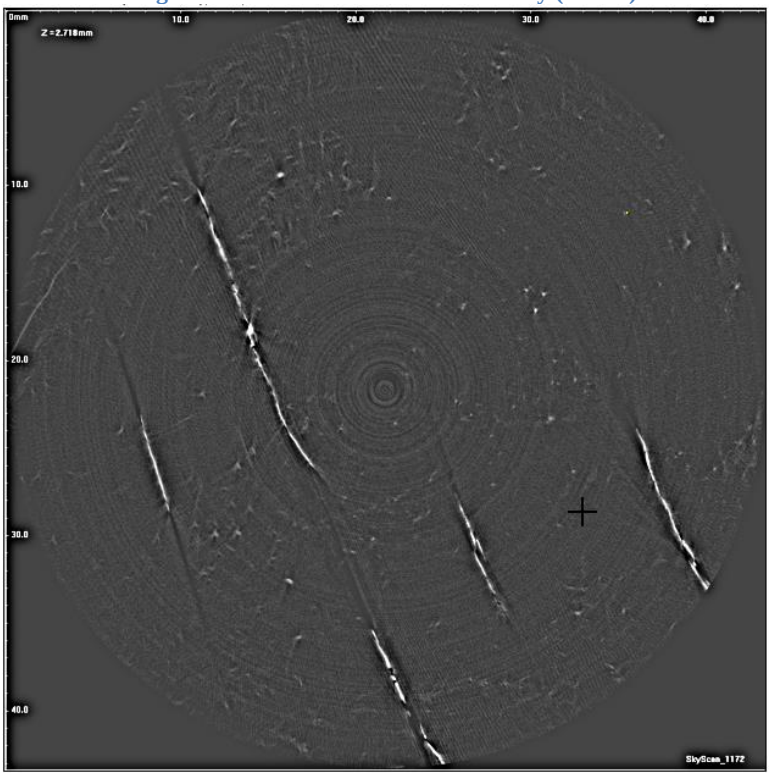

Figure 47: Elevation 1624 Cleat Porosity (1.96%)

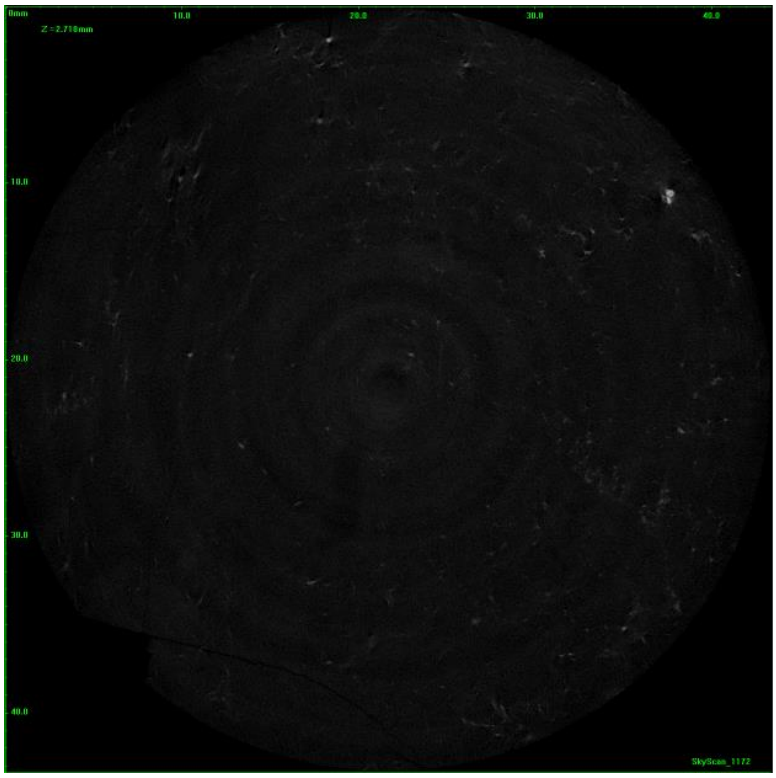

Figure 48: Elevation 1746 Cleat Porosity (0.05%)

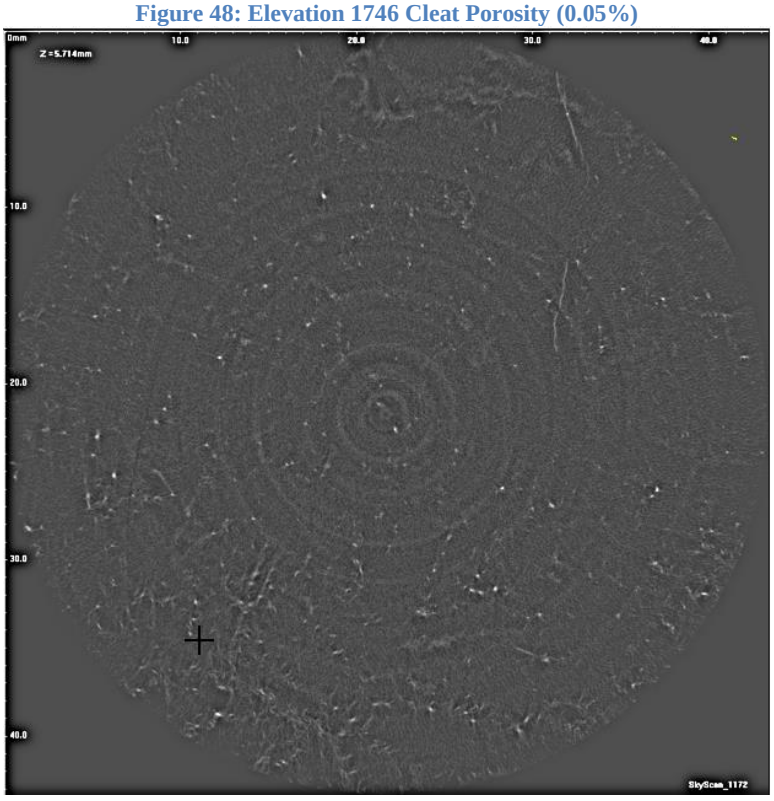

Figure 49: Elevation 1758 Cleat Porosity (N/A)

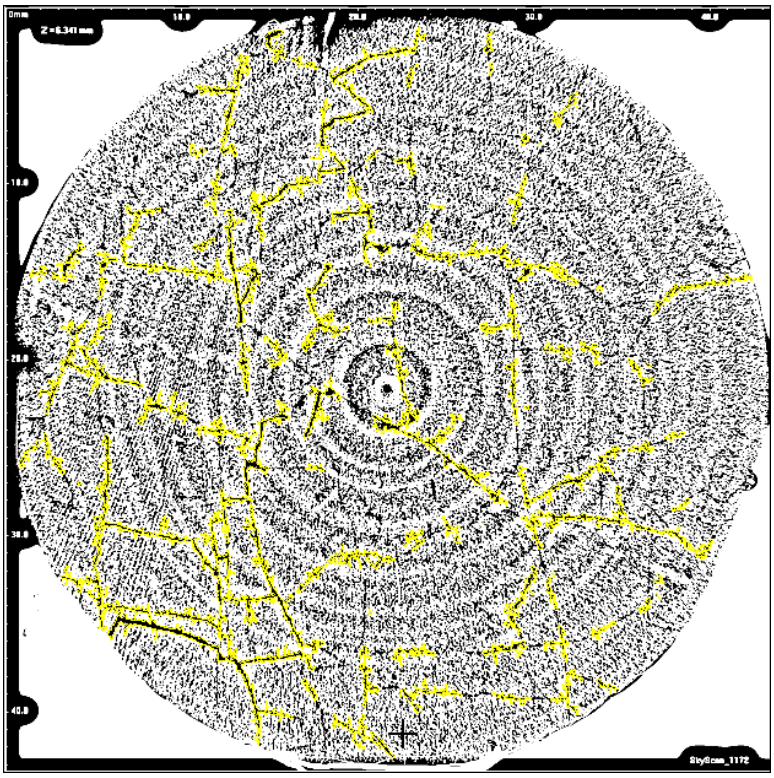

Figure 50: Elevation 1727 Cleat Porosity (4.30%)

C. CO2 SHALE INJECTION PHASE DIAGRAM AND GAS COMPOSITION

The data rendered in shows the transistion of the carbon dioxide between liquid and gasoues phase. The data and interruption can been seen in Andrew Louk's Master of Science Defense for Mining and Mineral Engineering " Monitoring For Enchanced Gas and Liquids Recovery From a CO2 'Huff-And-Puff' Injection Test In A Horizontal Chattanooga Shale Well".

Analyzed By:
Meter ID: C10
Analysis Time: 01/15/2015 10:23 Sample Type: Spot
Flowing Temp.: 0 Deg. F Flowing Pressure: 0 psig

Comp	UnNorm %	Normal %	Liquids (USgal/MCF)	Ideal (Btu/SCF)	Rel. Density
Propane	2.76395	2.77631	0.76719	69.85470	0.04227
Hydrogen Sulfide	0.00000	0.00000	0.00000	0.00000	0.00000
IsoButane	0.14475	0.14539	0.04772	4.72808	0.00292
Butane	0.49850	0.50073	0.15834	16.33524	0.01005
NeoPentane	0.00103	0.00103	0.00038	0.04140	0.00003
IsoPentane	0.05185	0.05208	0.01910	2.08363	0.00130
Pentane	0.08522	0.08560	0.03112	3.43131	0.00213
Hexane+	0.06725	0.06755	0.00000	0.00000	0.00000
Nitrogen	2.02817	2.03724	0.22481	0.00000	0.01970
Methane	64.58236	64.87125	11.03099	655.19952	0.35933
Carbon Dioxide	18.36845	18.45062	3.15835	0.00000	0.28036
Ethylene	0.00000	0.00000	0.00000	0.00000	0.00000
Ethane	10.96317	11.01221	2.95400	194.88303	0.11433
Hexane	0.00000	0.06755	0.02786	3.21249	0.00201
Heptane	0.00000	0.00000	0.00000	0.00000	0.00000
Heptane	0.00000	0.00000	0.00000	0.00000	0.00000
Octane	0.00000	0.00000	0.00000	0.00000	0.00000
Nonane	0.00000	0.00000	0.00000	0.00000	0.00000
Nonane	0.00000	0.00000	0.00000	0.00000	0.00000
Decane	0.00000	0.00000	0.00000	0.00000	0.00000
Undecane	0.00000	0.00000	0.00000	0.00000	0.00000
Ethane-	0.00000	0.00000	0.00000	0.00000	0.00000
Propane +	0.00000	0.00000	0.00000	0.00000	0.00000
Oxygen	0.00000	0.00000	0.00000	0.00000	0.00000
Water	0.00000	1.74067	0.00000	0.00000	0.00000
Helium	0.00000	0.00000	0.00000	0.00000	0.00000
Hydrogen	0.00000	0.00000	0.00000	0.00000	0.00000
Total	99.55469	100.00000	18.41988	949.76941	0.83686

Inferior Wobbe 1028.1858 (Btu/SCF) Superior Wobbe 1044.0488 (Btu/SCF)
Compressibility 0.9967 Density 0.0640 (lbm/ft3)
Real Rel. Density 0.8369 Ideal CV 949.7694 (Btu/SCF)
Wet CV 938.5260 (Btu/SCF) Dry CV 955.0963 (Btu/SCF)
Contract Temp. 60.0000 (deg F) Contract Press. 14.7300 (psia)
Number of Cycles 1 Connected Stream 1
Atmospheric Pressure 14.65

Figure 51: 12/1/2014 Gas Composition used for Acoustic Velocity

Analyzed By:
Meter ID: C4
Analysis Time: 01/15/2015 10:29 Sample Type: Spot
Flowing Temp.: 0 Deg. F Flowing Pressure: 0 psig

Comp	UnNorm %	Normal %	Liquids (USgal/MCF)	Ideal (Btu/SCF)	Rel. Density
Propane	2.76972	2.77512	0.76687	69.82472	0.04225
Hydrogen Sulfide	0.00000	0.00000	0.00000	0.00000	0.00000
IsoButane	0.14457	0.14485	0.04754	4.71027	0.00291
Butane	0.49573	0.49670	0.15707	16.20385	0.00997
NeoPentane	0.00094	0.00095	0.00035	0.03787	0.00002
IsoPentane	0.05156	0.05166	0.01895	2.06682	0.00129
Pentane	0.08520	0.08536	0.03104	3.42202	0.00213
Hexane+	0.06595	0.06608	0.00000	0.00000	0.00000
Nitrogen	1.48324	1.48613	0.16400	0.00000	0.01437
Methane	65.21670	65.34370	11.11151	659.97137	0.36194
Carbon Dioxide	18.44532	18.48124	3.16365	0.00000	0.28083
Ethylene	0.00000	0.00000	0.00000	0.00000	0.00000
Ethane	11.04671	11.06822	2.96908	195.87433	0.11491
Hexane	0.00000	0.06608	0.02725	3.14249	0.00197
Heptane	0.00000	0.00000	0.00000	0.00000	0.00000
Heptane	0.00000	0.00000	0.00000	0.00000	0.00000
Octane	0.00000	0.00000	0.00000	0.00000	0.00000
Nonane	0.00000	0.00000	0.00000	0.00000	0.00000
Nonane	0.00000	0.00000	0.00000	0.00000	0.00000
Decane	0.00000	0.00000	0.00000	0.00000	0.00000
Undecane	0.00000	0.00000	0.00000	0.00000	0.00000
Ethane-	0.00000	0.00000	0.00000	0.00000	0.00000
Propane +	0.00000	0.00000	0.00000	0.00000	0.00000
Oxygen	0.00000	0.00000	0.00000	0.00000	0.00000
Water	0.00000	1.74067	0.00000	0.00000	0.00000
Helium	0.00000	0.00000	0.00000	0.00000	0.00000
Hydrogen	0.00000	0.00000	0.00000	0.00000	0.00000
Total	99.80563	100.00000	18.45731	955.25372	0.83503

Inferior Wobbe	1035.2576 (Btu/SCF)	Superior Wobbe	1051.2450 (Btu/SCF)
Compressibility	0.9967	Density	0.0639 (lbm/ft3)
Real Rel. Density	0.8350	Ideal CV	955.2537 (Btu/SCF)
Wet CV	943.9605 (Btu/SCF)	Dry CV	960.6270 (Btu/SCF)
Contract Temp.	60.0000 (deg F)	Contract Press.	14.7300 (psia)
Number of Cycles	1	Connected Stream	1
Atmospheric Pressure	14.65		

Figure 52: 12/4/2014 Gas Composition used for Acoustic Velocity

Analyzed By:
Meter ID: C10
Analysis Time: 01/15/2015 10:23 Sample Type: Spot
Flowing Temp.: 0 Deg. F Flowing Pressure: 0 psig

Comp	UnNorm %	Normal %	Liquids (USgal/MCF)	Ideal (Btu/SCF)	Rel. Density
Propane	2.76395	2.77631	0.76719	69.85470	0.04227
Hydrogen Sulfide	0.00000	0.00000	0.00000	0.00000	0.00000
IsoButane	0.14475	0.14539	0.04772	4.72808	0.00292
Butane	0.49850	0.50073	0.15834	16.33524	0.01005
NeoPentane	0.00103	0.00103	0.00038	0.04140	0.00003
IsoPentane	0.05185	0.05208	0.01910	2.08363	0.00130
Pentane	0.08522	0.08560	0.03112	3.43131	0.00213
Hexane+	0.06725	0.06755	0.00000	0.00000	0.00000
Nitrogen	2.02817	2.03724	0.22481	0.00000	0.01970
Methane	64.58236	64.87125	11.03099	655.19952	0.35933
Carbon Dioxide	18.36845	18.45062	3.15835	0.00000	0.28036
Ethylene	0.00000	0.00000	0.00000	0.00000	0.00000
Ethane	10.96317	11.01221	2.95400	194.88303	0.11433
Hexane	0.00000	0.06755	0.02786	3.21249	0.00201
Heptane	0.00000	0.00000	0.00000	0.00000	0.00000
Heptane	0.00000	0.00000	0.00000	0.00000	0.00000
Octane	0.00000	0.00000	0.00000	0.00000	0.00000
Nonane	0.00000	0.00000	0.00000	0.00000	0.00000
Nonane	0.00000	0.00000	0.00000	0.00000	0.00000
Decane	0.00000	0.00000	0.00000	0.00000	0.00000
Undecane	0.00000	0.00000	0.00000	0.00000	0.00000
Ethane-	0.00000	0.00000	0.00000	0.00000	0.00000
Propane +	0.00000	0.00000	0.00000	0.00000	0.00000
Oxygen	0.00000	0.00000	0.00000	0.00000	0.00000
Water	0.00000	1.74067	0.00000	0.00000	0.00000
Helium	0.00000	0.00000	0.00000	0.00000	0.00000
Hydrogen	0.00000	0.00000	0.00000	0.00000	0.00000
Total	99.55469	100.00000	18.41988	949.76941	0.83686

Inferior Wobbe	1028.1858 (Btu/SCF)	Superior Wobbe	1044.0488 (Btu/SCF)
Compressibility	0.9967	Density	0.0640 (lbm/ft3)
Real Rel. Density	0.8369	Ideal CV	949.7694 (Btu/SCF)
Wet CV	938.5260 (Btu/SCF)	Dry CV	955.0963 (Btu/SCF)
Contract Temp.	60.0000 (deg F)	Contract Press.	14.7300 (psia)
Number of Cycles	1	Connected Stream	1
Atmospheric Pressure	14.65		

Figure 53: 1/15/2015 Gas Composition used for Acoustic Velocity

D. GAS DESORPTION TABLES FROM CARDNO

Gas Desorption data was performed by Cardno in their Bluefield Office.

Table F: Desorption Computation 765

Coal Sample Gas Desorption Computation

Bureau of Mines Direct Method Test

General Data

Company:	VCER	*Hole No.:*	CH-1-2014 (C-1)
Contact Person:		*Coalbed:*	Greasy Creek
Hole Location:		*Sample ID #:*	212
		MM&A Project #:	VCER101
Quadrangle:		***Coordinates***	
Core Collected by:	Tom Keim	*East:*	
Type of Drilling:		*North:*	
Drilling Contractor:		*Surface Elevation:*	
Sidewall Coring Contractor:		*Drilling Media:*	Water

Core Data

As-Rec'd, Whole Sample Wt. (g):	1282.90	*Core Length:*	1.87'
As-Rec'd, Crushed Sample Wt. (g):	1066.20	*Core Diameter:*	NQ
DMMF, Whole Sample Wt. (g):	1050.06	*Depth of Cored Interval:*	765.05'
DMMF, Crushed Sample Wt. (g):	872.69		766.92'

Time Data

	Day/Hr./ Min.		Day/Hr./Min.
Coalbed Encountered (A):	7/24/14 2:55 PM	*Core Reached Surface (C):*	7/24/14 3:34 PM
Hole Filled with Water (E):	NA	*Core Sealed in Canister (D):*	7/24/14 3:41 PM
Core Started Out of Hole (B):	7/24/14 3:30 PM		7/24/14 15.68333 333

Gas Volume Data

	Drilled with Air	***Drilled with Water***	

Lost Gas Volume	Not Performed		119.81 cc	
		Desorbed Gas Volume from Canister @ STP:	5097.52 cc	
		Residual Gas Volume from Crushed Core @ STP:	2463.26 cc	

Gas Content

Gas Content @ STP =(Lost Gas + Desorbed Gas Volumes)/Whole Sample Weight

Air, As-Received	***Air, DMMF***	***Water, As-Received***	***Water, DMMF***
Not Performed	Not Performed	4.07 cc/g	4.97 cc/g
Not Performed	Not Performed	130.29 ft³/ton	159.18 ft³/ton

Residual Gas Content @ STP =Residual Gas Volume/Crushed Sample Weight

As-Received	***DMMF***
2.31 cc/g	2.82 cc/g
74.02 ft³/ton	90.43 ft³/ton

Total Gas Content @ STP =Gas Content + Residual Gas Content

Air, As-Received	***Air, DMMF***	***Water, As-Received***	***Water, DMMF***
Not Performed	Not Performed	6.38 cc/g	7.79 cc/g
Not Performed	Not Performed	204.30 ft³/ton	249.61 ft³/ton

Table G: Gas Desorption Time Sheet 765

Coal Sample Gas Desorption Computation

Coal Desorption Data

Drill Hole: C-1 Canister #: 212

Number of Readings	Date	Time (Hrs./Min)	Desorbed Gas	Temp	F/C	Pressure (In.)	Inc. Adj. Volume	Cum. Adj. Volume
1	7/24/2014	3:51 PM	50.00	72.0	F	28.15	45.98	165.79
2	7/24/2014	4:01 PM	36.00	72.0	F	28.15	33.10	198.89
3	7/24/2014	4:11 PM	36.00	73.0	F	28.15	33.04	231.94
4	7/24/2014	4:21 PM	30.00	73.0	F	28.15	27.54	259.47

5	7/24/2014	4:31 PM	32.00	74.0	F	28.15	29.32	288.79
6	7/24/2014	4:52 PM	46.00	74.0	F	28.15	42.14	330.93
7	7/24/2014	5:12 PM	45.00	73.0	F	28.15	41.30	372.23
8	7/24/2014	5:52 PM	68.00	73.0	F	28.15	62.41	434.65
9	7/24/2014	7:54 PM	181.00	72.0	F	27.65	163.49	598.14
10	7/28/2014	6:25 PM	1310.00	70.0	F	27.57	1,184.28	1,782.42
11	7/29/2014	9:34 AM	160.00	68.0	F	27.60	145.35	1,927.77
12	7/30/2014	5:20 PM	209.00	70.0	F	27.68	189.70	2,117.47
13	7/31/2014	8:52 AM	105.00	66.0	F	27.73	96.20	2,213.67
14	8/1/2014	6:59 AM	150.00	69.0	F	27.73	136.65	2,350.32
15	8/2/2014	8:27 AM	145.00	70.0	F	27.70	131.70	2,482.02
16	8/3/2014	9:05 AM	107.00	70.0	F	27.70	97.19	2,579.21
17	8/4/2014	1:38 PM	111.00	70.0	F	27.71	100.86	2,680.07
18	8/5/2014	7:43 AM	72.00	69.0	F	27.71	65.54	2,745.61
19	8/6/2014	7:42 AM	89.00	69.0	F	27.67	80.90	2,826.52
20	8/7/2014	8:47 AM	91.00	70.0	F	27.68	82.60	2,909.11
21	8/8/2014	7:08 AM	86.00	70.0	F	27.70	78.11	2,987.23
22	8/9/2014	11:55 AM	95.00	70.0	F	27.68	86.23	3,073.45
23	8/10/2014	9:25 AM	57.00	70.0	F	27.66	51.70	3,125.15
24	8/11/2014	9:54 AM	64.00	70.0	F	27.67	58.07	3,183.22
25	8/12/2014	8:24 AM	92.00	70.0	F	27.53	83.05	3,266.27
26	8/13/2014	8:05 AM	56.00	70.0	F	27.56	50.61	3,316.88
27	8/14/2014	6:52 AM	39.00	70.0	F	27.66	35.37	3,352.25
28	8/15/2014	8:26 AM	58.00	70.0	F	27.64	52.57	3,404.82
29	8/16/2014	8:35 AM	57.00	69.0	F	27.63	51.74	3,456.56
30	8/17/2014	8:37 AM	58.00	70.0	F	27.62	52.53	3,509.08
31	8/18/2014	10:11 AM	71.00	70.0	F	27.50	64.02	3,573.11
32	8/19/2014	10:21 AM	10.00	70.0	F	27.50	9.02	3,582.13
33	8/20/2014	9:08 AM	65.00	70.0	F	27.60	58.83	3,640.95
34	8/22/2014	9:00 AM	69.00	70.0	F	26.50	59.96	3,700.91
35	8/25/2014	11:16 AM	86.00	68.0	F	27.71	78.44	3,779.35
36	8/27/2014	1:27 PM	59.00	69.0	F	27.72	53.73	3,833.08
37	8/29/2014	9:35 AM	69.00	68.0	F	27.71	62.93	3,896.01
38	9/2/2014	2:09 PM	153.00	73.0	F	27.69	138.14	4,034.15
39	9/5/2014	7:36 AM	87.00	69.0	F	27.80	79.46	4,113.60
40	9/8/2014	6:10 PM	93.00	70.0	F	27.74	84.59	4,198.20
41	9/10/2014	9:03 AM	54.00	69.0	F	27.70	49.14	4,247.34
42	9/12/2014	10:22 AM	64.00	70.0	F	27.70	58.13	4,305.47
43	9/15/2014	10:07 AM	44.00	67.0	F	27.78	40.31	4,345.78
44	9/17/2014	9:02 AM	54.00	66.0	F	27.62	49.28	4,395.06
45	9/19/2014	12:04 PM	49.00	68.0	F	27.74	44.74	4,439.80

46	9/23/2014	9:29 AM	54.00	66.0	F	27.87	49.72	4,489.52
47	9/25/2014	5:54 PM	77.00	70.0	F	27.80	70.19	4,559.71
48	9/30/2014	3:16 PM	107.00	69.0	F	27.53	96.77	4,656.49
49	10/7/2014	2:22 PM	91.00	69.0	F	27.59	82.48	4,738.97
50	10/13/2014	5:30 PM	96.00	70.0	F	27.69	87.17	4,826.13
51	10/22/2014	7:51 AM	71.00	63.0	F	27.63	65.19	4,891.32
52	10/28/2014	7:47 PM	112.00	70.0	F	27.62	101.44	4,992.76
53	11/4/2014	6:33 PM	30.00	65.0	F	27.75	27.56	5,020.32
54	11/11/2014	5:44 PM	193.00	72.0	F	27.50	173.38	5,193.70
55	11/14/2014	10:36 AM	26.00	70.0	F	27.72	23.63	5,217.33
Residual "A"	**11/14/2014**	**1:09 PM**	**1050.00**	**70.0**	**F**	**27.72**	**954.40**	**6,171.73**
Residual "B"	**11/14/2014**	**2:03 PM**	**1660.00**	**70.0**	**F**	**27.72**	**1,508.86**	**7,680.59**

Table H: Desorption Computation 905

Coal Sample Gas Desorption Computation

Bureau of Mines Direct Method Test

General Data

Company:	VCER	*Hole No.:*	CH-1-2014 (C-1)
Contact Person:		*Coalbed:*	Lower Seaboard (20 Bench)
Hole Location:		*Sample ID #:*	G-17
		MM&A Project #:	VCER101
Quadrangle:		***Coordinates***	
Core Collected by:	T. Keim	*East:*	
Type of Drilling:		*North:*	
Drilling Contractor:		*Surface Elevation:*	
Sidewall Coring Contractor:		*Drilling Media:*	Water

Core Data

As-Rec'd, Whole Sample Wt. (g):	497.10	*Core Length:*	0.73'
As-Rec'd, Crushed Sample Wt. (g):	462.70	*Core Diameter:*	
DMMF, Whole Sample Wt. (g):	476.83	*Depth of Cored Interval:*	905.00'
DMMF, Crushed Sample Wt. (g):	443.83		905.73'

Time Data

	Day/Hr./ Min.		Day/Hr./Min.

Coalbed Encountered (A):	7/28/14 3:55 PM	*Core Reached Surface (C):*	7/28/14 4:44 PM
Hole Filled with Water (E):	NA	*Core Sealed in Canister (D):*	7/28/14 4:50 PM
Core Started Out of Hole (B):	7/28/14 4:41 PM		
			7/28/2014
			16.83

Gas Volume Data

	Drilled with Air	***Drilled with Water***
Lost Gas Volume	Not Performed	189.83 cc

Desorbed Gas Volume from Canister @ STP:	5418.07 cc
Residual Gas Volume from Crushed Core @ STP:	688.99 cc

Gas Content

Gas Content @ STP =(Lost Gas + Desorbed Gas Volumes)/Whole Sample Weight

Air, As-Received	***Air, DMMF***	***Water, As-Received***	***Water, DMMF***
Not Performed	Not Performed	11.28 cc/g	11.76 cc/g
Not Performed	Not Performed	361.42 ft³/ton	376.78 ft³/ton

Residual Gas Content @ STP =Residual Gas Volume/Crushed Sample Weight

As-Received	***DMMF***
1.49 cc/g	1.55 cc/g
47.70 ft³/ton	49.73 ft³/ton

Total Gas Content @ STP =Gas Content + Residual Gas Content

Air, As-Received	***Air, DMMF***	***Water, As-Received***	***Water, DMMF***
Not Performed	Not Performed	12.77 cc/g	13.31 cc/g
Not Performed	Not Performed	409.12 ft³/ton	426.51 ft³/ton

Table I: Gas Desorption Time Sheet 905

Coal Sample Gas Desorption Computation

Coal Desorption Data

Drill Hole: CH-1-2014 (C-1) Canister #: G-17

Number of Readings	Date	Time (Hrs./Min)	Desorbed Gas	Temp	F/C	Pressure (In.)	Inc. Adj. Volume	Cum. Adj. Volume
1	7/28/2014	5:00 PM	84.00	74.0	F	28.05	76.68	266.51
2	7/28/2014	5:10 PM	74.00	74.0	F	28.05	67.55	334.06
3	7/28/2014	5:20 PM	61.00	76.0	F	28.05	55.48	389.54
4	7/28/2014	5:30 PM	57.00	76.0	F	28.05	51.84	441.38
5	7/28/2014	5:40 PM	44.00	77.0	F	28.05	39.94	481.32
6	7/28/2014	5:50 PM	43.00	77.0	F	28.05	39.03	520.35
7	7/28/2014	7:57 PM	289.00	65.0	F	27.45	262.61	782.96
8	7/29/2014	9:36 AM	631.00	68.0	F	27.60	573.23	1,356.19
9	7/30/2014	5:24 PM	640.00	70.0	F	27.68	580.89	1,937.08
10	7/31/2014	8:55 AM	238.00	66.0	F	27.73	218.06	2,155.14
11	8/1/2014	6:08 AM	300.00	69.0	F	27.73	273.30	2,428.44
12	8/2/2014	8:32 AM	255.00	70.0	F	27.70	231.62	2,660.06
13	8/3/2014	9:07 AM	205.00	70.0	F	27.70	186.20	2,846.26
14	8/4/2014	1:42 PM	192.00	70.0	F	27.71	174.46	3,020.71
15	8/5/2014	7:44 AM	120.00	69.0	F	27.71	109.24	3,129.96
16	8/6/2014	7:44 AM	140.00	69.0	F	27.67	127.26	3,257.22
17	8/7/2014	8:49 AM	133.00	70.0	F	27.68	120.72	3,377.94
18	8/8/2014	7:11 AM	120.00	70.0	F	27.70	109.00	3,486.93
19	8/9/2014	11:56 AM	132.00	70.0	F	27.68	119.81	3,606.74
20	8/10/2014	9:26 AM	82.00	70.0	F	27.66	74.37	3,681.11
21	8/11/2014	9:55 AM	86.00	70.0	F	27.67	78.03	3,759.14
22	8/12/2014	8:25 AM	103.00	70.0	F	27.53	92.98	3,852.12
23	8/13/2014	8:07 AM	91.00	70.0	F	27.56	82.24	3,934.36
24	8/14/2014	6:53 AM	49.00	70.0	F	27.66	44.44	3,978.80
25	8/15/2014	8:28 AM	76.00	70.0	F	27.64	68.88	4,047.68
26	8/16/2014	8:36 AM	65.00	69.0	F	27.63	59.00	4,106.68
27	8/17/2014	8:38 AM	68.00	70.0	F	27.62	61.59	4,168.27
28	8/18/2014	10:10 AM	75.00	70.0	F	27.50	67.63	4,235.90
29	8/19/2014	10:30 AM	10.00	70.0	F	27.50	9.02	4,244.92
30	8/20/2014	9:09 AM	81.00	70.0	F	27.60	73.31	4,318.22
31	8/22/2014	9:02 AM	79.00	70.0	F	26.50	68.65	4,386.87
32	8/25/2014	11:18 AM	98.00	68.0	F	27.71	89.38	4,476.25
33	8/27/2014	1:29 PM	65.00	69.0	F	27.72	59.19	4,535.45
34	8/29/2014	9:37 AM	76.00	68.0	F	27.71	69.32	4,604.77

35	9/2/2014	2:12 PM	140.00	73.0	F	27.69	126.40	4,731.16
36	9/5/2014	7:38 AM	88.00	69.0	F	27.80	80.37	4,811.54
37	9/8/2014	6:12 PM	84.00	70.0	F	27.74	76.41	4,887.94
38	9/10/2014	9:05 AM	36.00	69.0	F	27.70	32.76	4,920.70
39	9/12/2014	10:44 AM	53.00	70.0	F	27.70	48.14	4,968.84
40	9/15/2014	10:10 AM	31.00	67.0	F	27.78	28.40	4,997.24
41	9/17/2014	9:09 AM	43.00	66.0	F	27.62	39.24	5,036.48
42	9/19/2014	12:05 PM	38.00	68.0	F	27.74	34.70	5,071.18
43	9/23/2014	9:30 AM	31.00	66.0	F	27.87	28.55	5,099.72
44	9/25/2014	5:58 PM	56.00	70.0	F	27.80	51.05	5,150.77
45	9/30/2014	3:18 PM	81.00	69.0	F	27.53	73.26	5,224.03
46	10/7/2014	6:00 AM	71.00	69.0	F	27.59	64.35	5,288.39
47	10/13/2014	7:40 AM	75.00	70.0	F	27.69	68.10	5,356.48
48	10/22/2014	7:54 AM	43.00	63.0	F	27.63	39.48	5,395.96
49	10/28/2014	11:45 AM	70.00	70.0	F	27.62	63.40	5,459.36
50	11/4/2014	6:34 PM	10.00	65.0	F	27.75	9.19	5,468.55
51	11/11/2014	5:45 PM	145.00	72.0	F	27.50	130.26	5,598.81
52	11/14/2014	11:10 AM	10.00	70.0	F	27.72	9.09	5,607.90
Residual	**11/14/2014**	**12:39 PM**	**758.00**	**70.0**	**F**	**27.72**	**688.99**	**6,296.88**

Table J: Desorption Computation 974

Coal Sample Gas Desorption Computation

Bureau of Mines Direct Method Test

General Data

Company:	VCER	*Hole No.:*	CH-1-2014 (C-1)
Contact Person:		*Coalbed:*	U. Horsepen (10 Bench)
Hole Location:		*Sample ID #:*	H-54
		MM&A Project #:	VCER101
Quadrangle:		***Coordinates***	
Core Collected by:	T. Keim	*East:*	
Type of Drilling:		*North:*	
Drilling Contractor:		*Surface Elevation:*	
Sidewall Coring Contractor:		*Drilling Media:*	Water

Core Data

As-Rec'd, Whole Sample Wt. (g):	901.30	*Core Length:*	1.31'
As-Rec'd, Crushed Sample Wt. (g):	716.20	*Core Diameter:*	

DMMF, Whole Sample Wt. (g):	717.69	*Depth of Cored Interval:*	974.95'
DMMF, Crushed Sample Wt. (g):	570.30		976.26'

Time Data

	Day/Hr./Min.		Day/Hr./Min.
Coalbed Encountered (A):	7/29/14 9:08 AM	*Core Reached Surface (C):*	7/29/14 9:47 AM
Hole Filled with Water (E):	NA	*Core Sealed in Canister (D):*	7/29/14 9:57 AM
Core Started Out of Hole (B):	7/29/14 9:42 AM		7/29/2014 9.95

Gas Volume Data

	Drilled with Air	***Drilled with Water***
Lost Gas Volume	Not Performed	438.63 cc

Desorbed Gas Volume from Canister @ STP:	8302.94 cc
Residual Gas Volume from Crushed Core @ STP:	898.83 cc

Gas Content

Gas Content @ STP =(Lost Gas + Desorbed Gas Volumes)/Whole Sample Weight

Air, As-Received	***Air, DMMF***	***Water, As-Received***	***Water, DMMF***
Not Performed	Not Performed	9.70 cc/g	12.18 cc/g
Not Performed	Not Performed	310.72 ft³/ton	390.22 ft³/ton

Residual Gas Content @ STP =Residual Gas Volume/Crushed Sample Weight

As-Received	***DMMF***
1.26 cc/g	1.58 cc/g
40.21 ft³/ton	50.49 ft³/ton

Total Gas Content @ STP =Gas Content + Residual Gas Content

Air, As-Received	***Air, DMMF***	***Water, As-Received***	***Water, DMMF***

Not Performed	Not Performed	10.95 cc/g	13.76 cc/g
Not Performed	Not Performed	350.93 ft³/ton	440.71 ft³/ton

Table K:Gas Desorption Time Sheet 974

Coal Desorption Data

Drill Hole: CH-1-2014 (C-1) Canister #: H-54

Number of Readings	Date	Time (Hrs./Min)	Desorbed Gas	Temp	F/C	Pressure (In.)	Inc. Adj. Volume	Cum. Adj. Volume
1	7/29/2014	10:07 AM	142.00	75.0	F	28.20	130.08	568.71
2	7/29/2014	10:17 AM	111.00	75.0	F	28.20	101.68	670.39
3	7/29/2014	10:27 AM	107.00	76.0	F	28.20	97.83	768.22
4	7/29/2014	10:37 AM	88.00	76.0	F	28.20	80.46	848.69
5	7/29/2014	10:47 AM	89.00	78.0	F	28.20	81.07	929.76
6	7/29/2014	11:07 AM	133.00	78.0	F	28.20	121.15	1,050.91
7	7/29/2014	11:27 AM	129.00	81.0	F	28.20	116.86	1,167.77
8	7/29/2014	11:47 AM	119.00	72.0	F	28.25	109.82	1,277.59
9	7/29/2014	12:17 PM	159.00	72.0	F	28.25	146.73	1,424.32
10	7/29/2014	12:37 PM	121.00	72.0	F	28.25	111.66	1,535.98
11	7/29/2014	1:07 PM	152.00	74.0	F	28.25	139.75	1,675.73
12	7/29/2014	1:37 PM	145.00	72.0	F	28.25	133.81	1,809.54
13	7/29/2014	2:07 PM	130.00	72.0	F	28.25	119.97	1,929.51
14	7/29/2014	2:37 PM	126.00	72.0	F	28.25	116.28	2,045.79
15	7/29/2014	3:07 PM	113.00	72.0	F	28.25	104.28	2,150.07
16	7/29/2014	4:07 PM	177.00	72.0	F	28.25	163.34	2,313.42
17	7/29/2014	5:37 PM	213.00	72.0	F	28.25	196.57	2,509.98
18	7/29/2014	7:15 PM	216.00	69.0	F	27.70	196.56	2,706.55
19	7/30/2014	5:29 PM	940.00	70.0	F	27.68	853.18	3,559.73
20	7/31/2014	8:57 AM	480.00	66.0	F	27.73	439.78	3,999.51
21	8/1/2014	6:10 AM	561.00	69.0	F	27.73	511.07	4,510.58
22	8/2/2014	8:37 AM	452.00	70.0	F	27.70	410.55	4,921.13
23	8/3/2014	9:09 AM	341.00	70.0	F	27.70	309.73	5,230.86
24	8/4/2014	1:45 PM	305.00	70.0	F	27.71	277.13	5,507.99
25	8/5/2014	7:46 AM	206.00	69.0	F	27.71	187.53	5,695.52
26	8/6/2014	7:45 AM	221.00	69.0	F	27.67	200.90	5,896.41
27	8/7/2014	8:51 AM	213.00	70.0	F	27.68	193.33	6,089.74
28	8/8/2014	7:13 AM	153.00	70.0	F	27.70	138.97	6,228.71
29	8/9/2014	11:58 AM	177.00	70.0	F	27.68	160.65	6,389.36

30	8/10/2014	9:27 AM	112.00	70.0	F	27.66	101.58	6,490.95
31	8/11/2014	9:52 AM	117.00	70.0	F	27.67	106.16	6,597.10
32	8/12/2014	8:27 AM	139.00	70.0	F	27.53	125.48	6,722.58
33	8/13/2014	8:08 AM	121.00	70.0	F	27.56	109.35	6,831.93
34	8/14/2014	6:55 AM	87.00	70.0	F	27.66	78.91	6,910.84
35	8/15/2014	8:29 AM	99.00	70.0	F	27.64	89.73	7,000.56
36	8/16/2014	8:37 AM	76.00	69.0	F	27.63	68.99	7,069.55
37	8/17/2014	8:39 AM	81.00	70.0	F	27.62	73.36	7,142.91
38	8/18/2014	10:12 AM	95.00	70.0	F	27.50	85.67	7,228.57
39	8/19/2014	10:30 AM	10.00	70.0	F	27.50	9.02	7,237.59
40	8/20/2014	9:10 AM	103.00	70.0	F	27.60	93.22	7,330.81
41	8/22/2014	9:04 AM	92.00	70.0	F	26.50	79.94	7,410.75
42	8/25/2014	11:20 AM	111.00	68.0	F	27.71	101.24	7,511.99
43	8/27/2014	1:32 PM	71.00	69.0	F	27.72	64.66	7,576.65
44	8/29/2014	9:39 AM	86.00	68.0	F	27.71	78.44	7,655.09
45	9/2/2014	2:13 PM	156.00	73.0	F	27.69	140.85	7,795.93
46	9/5/2014	7:40 AM	96.00	69.0	F	27.80	87.68	7,883.61
47	9/8/2014	6:14 PM	95.00	70.0	F	27.74	86.41	7,970.02
48	9/10/2014	9:06 AM	53.00	69.0	F	27.70	48.23	8,018.25
49	9/12/2014	10:46 AM	61.00	70.0	F	27.70	55.41	8,073.66
50	9/15/2014	10:12 AM	25.00	67.0	F	27.78	22.90	8,096.56
51	9/17/2014	9:11 AM	50.00	66.0	F	27.62	45.63	8,142.19
52	9/19/2014	12:06 PM	35.00	68.0	F	27.74	31.96	8,174.15
53	9/23/2014	9:31 AM	32.00	66.0	F	27.87	29.47	8,203.61
54	9/25/2014	5:59 PM	60.00	70.0	F	27.80	54.69	8,258.31
55	9/30/2014	3:19 PM	79.00	69.0	F	27.53	71.45	8,329.76
56	10/7/2014	2:28 PM	71.00	69.0	F	27.59	64.35	8,394.11
57	10/13/2014	5:33 PM	71.00	70.0	F	27.69	64.47	8,458.58
58	10/22/2014	7:56 AM	38.00	63.0	F	27.63	34.89	8,493.47
59	10/28/2014	7:50 PM	76.00	70.0	F	27.62	68.83	8,562.30
60	11/4/2014	6:35 PM	10.00	65.0	F	27.75	9.19	8,571.49
61	11/11/2014	5:47 PM	161.00	72.0	F	27.50	144.63	8,716.12
62	11/14/2014	1:45 PM	28.00	70.0	F	27.72	25.45	8,741.57
Residual	**11/14/2014**	**3:34 PM**	**987.00**	**69.0**	**F**	**27.72**	**898.83**	**9,640.40**

Table L: Desorption Computation 1165

Coal Sample Gas Desorption Computation

Bureau of Mines Direct Method Test

General Data

Company:	VCER	*Hole No.:*	CH-1-2014 (C-1)
Contact Person:		*Coalbed:*	Pocahontas 11
Hole Location:		*Sample ID #:*	219
		MM&A Project #:	VCER101
Quadrangle:		***Coordinates***	
Core Collected by:	T. Keim	*East:*	
Type of Drilling:		*North:*	
Drilling Contractor:		*Surface Elevation:*	
Sidewall Coring Contractor:		*Drilling Media:*	Water

Core Data

As-Rec'd, Whole Sample Wt. (g):	538.20	*Core Length:*	0.74'
As-Rec'd, Crushed Sample Wt. (g):	511.30	*Core Diameter:*	
DMMF, Whole Sample Wt. (g):	493.23	*Depth of Cored Interval:*	1165.03'
DMMF, Crushed Sample Wt. (g):	468.57		1165.77'

Time Data

	Day/Hr./Min.		Day/Hr./Min.
Coalbed Encountered (A):	7/30/14 12:40 PM	*Core Reached Surface (C):*	7/30/14 1:50 PM
Hole Filled with Water (E):	NA	*Core Sealed in Canister (D):*	7/30/14 1:56 PM
Core Started Out of Hole (B):	7/30/14 1:44 PM		07/30/14 13.93333333

Gas Volume Data

	Drilled with Air	***Drilled with Water***
Lost Gas Volume	Not Performed	107.93 cc

Desorbed Gas Volume from Canister @ STP:	4157.53 cc
Residual Gas Volume from Crushed Core @ STP:	1109.20 cc

Gas Content

Gas Content @ STP =(Lost Gas + Desorbed Gas Volumes)/Whole Sample Weight

Air, As-Received	*Air, DMMF*	*Water, As-Received*	*Water, DMMF*
Not Performed	Not Performed	7.93 cc/g	8.65 cc/g
Not Performed	Not Performed	253.91 ft³/ton	277.06 ft³/ton

Residual Gas Content @ STP =Residual Gas Volume/Crushed Sample Weight

As-Received	*DMMF*
2.17 cc/g	2.37 cc/g
69.50 ft³/ton	75.84 ft³/ton

Total Gas Content @ STP =Gas Content + Residual Gas Content

Air, As-Received	*Air, DMMF*	*Water, As-Received*	*Water, DMMF*
Not Performed	Not Performed	10.09 cc/g	11.02 cc/g
Not Performed	Not Performed	323.41 ft³/ton	352.89 ft³/ton

Table M: Gas Desorption Time Sheet 1165

Coal Sample Gas Desorption Computation

Coal Desorption Data

Drill Hole: CH-1-2014 (C-1) Canister #: 219

Number of Readings	Date	Time (Hrs./Min)	Desorbed Gas	Temp	F/C	Pressure (In.)	Inc. Adj. Volume	Cum. Adj. Volume
1	7/30/2014	2:06 PM	41.00	72.0	F	28.25	37.84	145.76
2	7/30/2014	2:16 PM	37.00	72.0	F	28.25	34.15	179.91
3	7/30/2014	2:31 PM	41.00	72.0	F	28.25	37.84	217.74
4	7/30/2014	2:46 PM	42.00	72.0	F	28.25	38.76	256.50
5	7/30/2014	3:01 PM	32.00	72.0	F	28.25	29.53	286.03
6	7/30/2014	3:34 PM	63.00	72.0	F	28.25	58.14	344.17
7	7/30/2014	4:13 PM	78.00	72.0	F	28.25	71.98	416.16
8	7/30/2014	4:38 PM	47.00	72.0	F	28.25	43.37	459.53
9	7/30/2014	5:08 PM	53.00	70.0	F	28.25	49.10	508.63
10	7/30/2014	5:38 PM	48.00	70.0	F	28.25	44.46	553.09
11	7/30/2014	7:33 PM	97.00	68.0	F	27.70	88.44	641.53
12	7/31/2014	8:59 AM	271.00	67.0	F	27.73	247.82	889.35
13	8/1/2014	6:12 AM	327.00	69.0	F	27.73	297.90	1,187.24
14	8/2/2014	8:40 AM	255.00	70.0	F	27.70	231.62	1,418.86
15	8/3/2014	9:11 AM	195.00	70.0	F	27.70	177.12	1,595.98

16	8/4/2014	1:47 PM	175.00	70.0	F	27.71	159.01	1,754.99
17	8/5/2014	7:47 AM	110.00	69.0	F	27.71	100.14	1,855.13
18	8/6/2014	7:46 AM	123.00	69.0	F	27.67	111.81	1,966.94
19	8/7/2014	8:54 AM	118.00	70.0	F	27.68	107.10	2,074.04
20	8/8/2014	7:15 AM	94.00	70.0	F	27.70	85.38	2,159.42
21	8/9/2014	12:01 PM	104.00	70.0	F	27.68	94.39	2,253.81
22	8/10/2014	9:28 AM	76.00	70.0	F	27.66	68.93	2,322.74
23	8/11/2014	9:58 AM	78.00	70.0	F	27.67	70.77	2,393.51
24	8/12/2014	8:29 AM	86.00	70.0	F	27.53	77.63	2,471.15
25	8/13/2014	8:10 AM	81.00	70.0	F	27.56	73.20	2,544.35
26	8/14/2014	6:52 AM	43.00	70.0	F	27.66	39.00	2,583.35
27	8/15/2014	8:31 AM	66.00	70.0	F	27.64	59.82	2,643.17
28	8/16/2014	8:38 AM	53.00	69.0	F	27.63	48.11	2,691.28
29	8/17/2014	8:40 AM	59.00	70.0	F	27.62	53.43	2,744.71
30	8/18/2014	10:14 AM	70.00	70.0	F	27.50	63.12	2,807.83
31	8/19/2014	10:30 AM	10.00	70.0	F	27.50	9.02	2,816.85
32	8/20/2014	9:11 AM	76.00	70.0	F	27.60	68.78	2,885.63
33	8/22/2014	9:06 AM	76.00	70.0	F	26.50	66.04	2,951.67
34	8/25/2014	11:22 AM	100.00	68.0	F	27.71	91.21	3,042.88
35	8/27/2014	1:34 PM	61.00	69.0	F	27.72	55.55	3,098.43
36	8/29/2014	9:41 AM	64.00	68.0	F	27.71	58.37	3,156.80
37	9/2/2014	2:15 PM	136.00	73.0	F	27.69	122.79	3,279.59
38	9/5/2014	7:41 AM	80.00	69.0	F	27.80	73.06	3,352.65
39	9/8/2014	6:16 PM	86.00	70.0	F	27.74	78.23	3,430.88
40	9/10/2014	9:07 AM	47.00	69.0	F	27.70	42.77	3,473.65
41	9/12/2014	10:47 AM	59.00	70.0	F	27.70	53.59	3,527.24
42	9/15/2014	10:12 AM	33.00	67.0	F	27.78	30.23	3,557.47
43	9/17/2014	9:12 AM	51.00	66.0	F	27.62	46.54	3,604.01
44	9/19/2014	12:07 PM	36.00	68.0	F	27.74	32.87	3,636.88
45	9/23/2014	9:32 AM	35.00	66.0	F	27.87	32.23	3,669.11
46	9/25/2014	6:01 PM	61.00	70.0	F	27.80	55.61	3,724.72
47	9/30/2014	3:20 PM	88.00	69.0	F	27.53	79.59	3,804.31
48	10/7/2014	2:29 PM	88.00	69.0	F	27.59	79.76	3,884.07
49	10/13/2014	5:34 PM	86.00	70.0	F	27.69	78.09	3,962.16
50	10/22/2014	7:58 AM	63.00	63.0	F	27.63	57.84	4,020.00
51	10/28/2014	7:51 PM	81.00	70.0	F	27.62	73.36	4,093.36
52	11/4/2014	6:36 PM	18.00	65.0	F	27.75	16.54	4,109.89
53	11/11/2014	5:50 PM	159.00	72.0	F	27.50	142.84	4,252.73
54	11/14/2014	2:36 PM	14.00	70.0	F	27.72	12.73	4,265.46
Residual	**11/14/2014**	**4:20 PM**	**1218.00**	**69.0**	**F**	**27.72**	**1,109.20**	**5,374.66**

Table N: Desorption Computation 1200

Coal Sample Gas Desorption Computation

Bureau of Mines Direct Method Test

General Data

Company:	VCER	*Hole No.:*	CH-1-2014 (C-1)
Contact Person:		*Coalbed:*	Pocahontas 10 (20 Bench)
Hole Location:		*Sample ID #:*	G-46
		MM&A Project #:	VCER101
Quadrangle:		***Coordinates***	
Core Collected by:	T. Keim	*East:*	
Type of Drilling:		*North:*	
Drilling Contractor:		*Surface Elevation:*	
Sidewall Coring Contractor:		*Drilling Media:*	Water

Core Data

As-Rec'd, Whole Sample Wt. (g):	494.30	*Core Length:*	1.15'
As-Rec'd, Crushed Sample Wt. (g):	391.30	*Core Diameter:*	
DMMF, Whole Sample Wt. (g):	446.26	*Depth of Cored Interval:*	1200.25'
DMMF, Crushed Sample Wt. (g):	353.27		1201.64'

Time Data

	Day/Hr./ Min.		Day/Hr./Min.
Coalbed Encountered (A):	7/30/14 2:48 PM	*Core Reached Surface (C):*	7/30/14 3:16 PM
Hole Filled with Water (E):	NA	*Core Sealed in Canister (D):*	7/30/14 3:24 PM
Core Started Out of Hole (B):	7/30/14 3:10 PM		7/30/2014 15.4

Gas Volume Data

	Drilled with Air	***Drilled with Water***
Lost Gas Volume	Not Performed	257.80 cc

Desorbed Gas Volume from Canister @ STP:	5781.95 cc
Residual Gas Volume from Crushed Core @ STP:	895.05 cc

Gas Content

Gas Content @ STP	=(Lost Gas + Desorbed Gas Volumes)/Whole Sample Weight			
Air, As-Received	***Air, DMMF***		***Water, As-Received***	***Water, DMMF***
Not Performed	Not Performed		12.22 cc/g	13.53 cc/g
Not Performed	Not Performed		391.45 ft³/ton	433.60 ft³/ton
Residual Gas Content @ STP	=Residual Gas Volume/Crushed Sample Weight			
	As-Received		***DMMF***	
	2.29 cc/g		2.53 cc/g	
	73.28 ft³/ton		81.17 ft³/ton	
Total Gas Content @ STP	=Gas Content + Residual Gas Content			
Air, As-Received	***Air, DMMF***		***Water, As-Received***	***Water, DMMF***
Not Performed	Not Performed		14.51 cc/g	16.07 cc/g
Not Performed	Not Performed		464.73 ft³/ton	514.77 ft³/ton

Table O: Gas Desorption Time Sheet 1200

Coal Sample Gas Desorption Computation

Coal Desorption Data

Drill Hole: CH-1-2014 (C-1) Canister #: G-46

Number of Readings	Date	Time (Hrs./Min)	Desorbed Gas	Temp	F/C	Pressure (In.)	Inc. Adj. Volume	Cum. Adj. Volume
1	7/30/2014	3:34 PM	72.00	72.0	F	28.25	66.44	324.24
2	7/30/2014	3:44 PM	86.00	74.0	F	28.25	79.07	403.31
3	7/30/2014	3:54 PM	64.00	72.0	F	28.25	59.06	462.37
4	7/30/2014	4:17 PM	116.00	72.0	F	28.25	107.05	569.42
5	7/30/2014	4:37 PM	93.00	72.0	F	28.25	85.82	655.25
6	7/30/2014	5:07 PM	125.00	70.0	F	28.25	115.79	771.04
7	7/30/2014	5:37 PM	101.00	70.0	F	28.25	93.56	864.60
8	7/30/2014	7:31 PM	225.00	68.0	F	27.70	205.14	1,069.74

9	7/31/2014	9:01 AM	790.00	68.0	F	27.73	721.06	1,790.79
10	8/1/2014	6:14 AM	510.00	69.0	F	27.73	464.61	2,255.40
11	8/2/2014	8:45 AM	366.00	70.0	F	27.70	332.44	2,587.84
12	8/3/2014	9:14 AM	260.00	70.0	F	27.70	236.16	2,824.00
13	8/4/2014	1:50 PM	231.00	70.0	F	27.71	209.89	3,033.89
14	8/5/2014	7:49 AM	135.00	69.0	F	27.71	122.90	3,156.79
15	8/6/2014	7:49 AM	175.00	69.0	F	27.67	159.08	3,315.87
16	8/7/2014	8:56 AM	164.00	70.0	F	27.68	148.85	3,464.72
17	8/8/2014	7:16 AM	145.00	70.0	F	27.70	131.70	3,596.42
18	8/9/2014	12:02 PM	144.00	70.0	F	27.68	130.70	3,727.12
19	8/10/2014	9:29 AM	92.00	70.0	F	27.66	83.44	3,810.57
20	8/11/2014	9:59 AM	87.00	70.0	F	27.67	78.94	3,889.50
21	8/12/2014	8:31 AM	107.00	70.0	F	27.53	96.59	3,986.09
22	8/13/2014	8:11 AM	103.00	70.0	F	27.56	93.08	4,079.18
23	8/14/2014	6:58 AM	68.00	70.0	F	27.66	61.67	4,140.85
24	8/15/2014	8:33 AM	86.00	70.0	F	27.64	77.94	4,218.80
25	8/16/2014	8:39 AM	66.00	69.0	F	27.63	59.91	4,278.70
26	8/17/2014	8:41 AM	70.00	70.0	F	27.62	63.40	4,342.10
27	8/18/2014	10:15 AM	83.00	70.0	F	27.50	74.84	4,416.95
28	8/19/2014	10:30 AM	10.00	70.0	F	27.50	9.02	4,425.96
29	8/20/2014	9:12 AM	90.00	70.0	F	27.60	81.45	4,507.41
30	8/22/2014	9:08 AM	82.00	70.0	F	26.50	71.25	4,578.67
31	8/25/2014	11:24 AM	104.00	68.0	F	27.71	94.86	4,673.52
32	8/27/2014	1:35 PM	69.00	69.0	F	27.72	62.84	4,736.36
33	8/29/2014	9:43 AM	73.00	68.0	F	27.71	66.58	4,802.94
34	9/2/2014	2:16 PM	150.00	73.0	F	27.69	135.43	4,938.37
35	9/5/2014	7:42 AM	75.00	69.0	F	27.80	68.50	5,006.87
36	9/8/2014	6:18 PM	88.00	70.0	F	27.74	80.05	5,086.91
37	9/10/2014	12:00 PM	49.00	69.0	F	27.70	44.59	5,131.50
38	9/12/2014	10:48 AM	61.00	70.0	F	27.70	55.41	5,186.91
39	9/15/2014	10:14 AM	41.00	67.0	F	27.78	37.56	5,224.47
40	9/17/2014	9:13 AM	54.00	66.0	F	27.62	49.28	5,273.75
41	9/19/2014	12:08 PM	47.00	68.0	F	27.74	42.91	5,316.66
42	9/23/2014	9:33 AM	42.00	66.0	F	27.87	38.67	5,355.34
43	9/25/2014	6:03 PM	68.00	70.0	F	27.80	61.99	5,417.32
44	9/30/2014	5:21 PM	96.00	69.0	F	27.53	86.83	5,504.15
45	10/7/2014	2:30 PM	89.00	69.0	F	27.59	80.67	5,584.82
46	10/13/2014	5:35 PM	90.00	70.0	F	27.69	81.72	5,666.54
47	10/22/2014	7:59 AM	61.00	63.0	F	27.63	56.01	5,722.54
48	10/28/2014	7:53 PM	96.00	70.0	F	27.62	86.94	5,809.49
49	11/4/2014	6:37 PM	31.00	65.0	F	27.75	28.48	5,837.97

50	11/11/2014	5:51 PM	175.00	72.0	F	27.50	157.21	5,995.18
51	11/14/2014	3:11 PM	49.00	70.0	F	27.74	44.57	6,039.75
Residual	**11/14/2014**	**4:55 PM**	**984.00**	**70.0**	**F**	**27.74**	**895.05**	**6,934.80**

Table P: Desorption Computation 1297

Coal Sample Gas Desorption Computation

Bureau of Mines Direct Method Test

General Data

Company:	VCER	*Hole No.:*	CH-1-2014 (C-1)
Contact Person:		*Coalbed:*	Pocahontas 9 (10 Bench)
Hole Location:		*Sample ID #:*	F-26
		MM&A Project #:	
Quadrangle:		***Coordinates***	
Core Collected by:	T. Keim	*East:*	
Type of Drilling:		*North:*	
Drilling Contractor:		*Surface Elevation:*	
Sidewall Coring Contractor:		*Drilling Media:*	Water

Core Data

As-Rec'd, Whole Sample Wt. (g):	855.40	*Core Length:*	1.60'
As-Rec'd, Crushed Sample Wt. (g):	783.50	*Core Diameter:*	
DMMF, Whole Sample Wt. (g):	778.47	*Depth of Cored Interval:*	1297.42'
DMMF, Crushed Sample Wt. (g):	713.04		1299.02'
		0.10' Lost coal	

Time Data

	Day/Hr./Min.		Day/Hr./Min.
Coalbed Encountered (A):	7/30/14 11:03 AM	*Core Reached Surface (C):*	7/31/14 11:43 AM
Hole Filled with Water (E):	NA	*Core Sealed in Canister (D):*	7/31/14 11:51 AM
Core Started Out of Hole (B):	7/31/14 11:37 AM		07/31/14 11.85

Gas Volume Data

	Drilled with Air		***Drilled with Water***

Lost Gas Volume	Not Performed		144.14 cc

Desorbed Gas Volume from Canister @ STP:	4575.90 cc
Residual Gas Volume from Crushed Core @ STP:	755.54 cc

Gas Content

Gas Content @ STP =(Lost Gas + Desorbed Gas Volumes)/Whole Sample Weight

Air, As-Received	***Air, DMMF***	***Water, As-Received***	***Water, DMMF***
Not Performed	Not Performed	5.52 cc/g	6.06 cc/g
Not Performed	Not Performed	176.78 ft³/ton	194.25 ft³/ton

Residual Gas Content @ STP =Residual Gas Volume/Crushed Sample Weight

As-Received	***DMMF***
0.96 cc/g	1.06 cc/g
30.89 ft³/ton	33.95 ft³/ton

Total Gas Content @ STP =Gas Content + Residual Gas Content

Air, As-Received	***Air, DMMF***	***Water, As-Received***	***Water, DMMF***
Not Performed	Not Performed	6.48 cc/g	7.12 cc/g
Not Performed	Not Performed	207.67 ft³/ton	228.19 ft³/ton

Table Q: Gas Desorption Time Sheet 1297

Coal Sample Gas Desorption Computation

Coal Desorption Data

Drill Hole: CH-1-2014 (C-1) Canister #: F-26

Number of Readings	Date	Time (Hrs./Min)	Desorbed Gas	Temp	F/C	Pressure (In.)	Inc. Adj. Volume	Cum. Adj. Volume
1	7/31/2014	12:01 PM	55.00	72.0	F	28.35	50.94	195.08
2	7/31/2014	12:11 PM	42.00	72.0	F	28.35	38.90	233.98

3	7/31/2014	12:21 PM	40.00	72.0	F	28.35	37.04	271.02
4	7/31/2014	12:36 PM	43.00	72.0	F	28.35	39.82	310.84
5	7/31/2014	12:56 PM	55.00	72.0	F	28.35	50.94	361.78
6	7/31/2014	1:16 PM	54.00	72.0	F	28.35	50.01	411.79
7	7/31/2014	1:36 PM	48.00	72.0	F	28.35	44.45	456.24
8	7/31/2014	2:06 PM	64.00	72.0	F	28.35	59.27	515.51
9	7/31/2014	2:36 PM	68.00	74.0	F	28.35	62.74	578.25
10	7/31/2014	3:36 PM	101.00	72.0	F	28.35	93.54	671.79
11	7/31/2014	5:12 PM	91.00	72.0	F	28.35	84.28	756.07
12	7/31/2014	6:47 PM	89.00	67.0	F	27.75	81.45	837.51
13	8/1/2014	6:17 AM	284.00	69.0	F	27.73	258.72	1,096.24
14	8/2/2014	8:47 AM	340.00	70.0	F	27.70	308.82	1,405.06
15	8/3/2014	9:16 AM	226.00	70.0	F	27.70	205.28	1,610.33
16	8/4/2014	1:52 PM	200.00	70.0	F	27.71	181.72	1,792.06
17	8/5/2014	7:50 AM	128.00	69.0	F	27.71	116.52	1,908.58
18	8/6/2014	7:51 AM	143.00	69.0	F	27.67	129.99	2,038.57
19	8/7/2014	8:58 AM	151.00	70.0	F	27.68	137.05	2,175.63
20	8/8/2014	7:18 AM	121.00	70.0	F	27.70	109.90	2,285.53
21	8/9/2014	12:03 PM	131.00	70.0	F	27.68	118.90	2,404.43
22	8/10/2014	9:30 AM	77.00	70.0	F	27.66	69.84	2,474.27
23	8/11/2014	9:59 AM	84.00	70.0	F	27.67	76.21	2,550.48
24	8/12/2014	8:32 AM	97.00	70.0	F	27.53	87.56	2,638.05
25	8/13/2014	8:13 AM	90.00	70.0	F	27.56	81.33	2,719.38
26	8/14/2014	6:59 AM	57.00	70.0	F	27.66	51.70	2,771.08
27	8/15/2014	8:34 AM	78.00	70.0	F	27.64	70.69	2,841.77
28	8/16/2014	8:40 AM	62.00	69.0	F	27.63	56.28	2,898.05
29	8/17/2014	8:42 AM	65.00	70.0	F	27.62	58.87	2,956.92
30	8/18/2014	10:16 AM	80.00	70.0	F	27.50	72.14	3,029.06
31	8/19/2014	10:30 AM	10.00	70.0	F	27.50	9.02	3,038.08
32	8/20/2014	9:13 AM	80.00	70.0	F	27.60	72.40	3,110.48
33	8/22/2014	9:10 AM	75.00	70.0	F	26.50	65.17	3,175.65
34	8/25/2014	11:26 AM	95.00	68.0	F	27.71	86.65	3,262.30
35	8/27/2014	1:37 PM	66.00	69.0	F	27.72	60.10	3,322.40
36	8/29/2014	9:45 AM	74.00	68.0	F	27.71	67.49	3,389.89
37	9/2/2014	2:18 PM	153.00	73.0	F	27.69	138.14	3,528.03
38	9/5/2014	7:45 AM	74.00	69.0	F	27.80	67.58	3,595.61
39	9/8/2014	6:20 PM	91.00	70.0	F	27.74	82.77	3,678.39
40	9/10/2014	9:10 AM	50.00	69.0	F	27.70	45.50	3,723.89
41	9/12/2014	10:49 AM	64.00	70.0	F	27.70	58.13	3,782.02
42	9/15/2014	10:15 AM	40.00	67.0	F	27.78	36.64	3,818.67
43	9/17/2014	9:14 AM	54.00	66.0	F	27.62	49.28	3,867.94

44	9/19/2014	12:09 PM	36.00	68.0	F	27.74	32.87	3,900.81
45	9/23/2014	9:34 AM	36.00	66.0	F	27.87	33.15	3,933.96
46	9/25/2014	6:04 PM	65.00	70.0	F	27.80	59.25	3,993.22
47	9/30/2014	3:22 PM	105.00	69.0	F	27.53	94.97	4,088.18
48	10/7/2014	2:32 PM	93.00	69.0	F	27.59	84.30	4,172.48
49	10/13/2014	5:37 PM	94.00	70.0	F	27.69	85.35	4,257.83
50	10/22/2014	8:01 AM	65.00	63.0	F	27.63	59.68	4,317.51
51	10/28/2014	7:54 PM	106.00	70.0	F	27.62	96.00	4,413.51
52	11/4/2014	6:39 PM	23.00	65.0	F	27.75	21.13	4,434.63
53	11/11/2014	5:52 PM	196.00	72.0	F	27.50	176.08	4,610.71
54	11/17/2014	10:30 AM	123.00	72.0	F	27.21	109.33	4,720.04
Residual	**11/17/2014**	**4:25 PM**	**850.00**	**72.0**	**F**	**27.21**	**755.54**	**5,475.58**

Table R: Desorption Computation 1413

Coal Sample Gas Desorption Computation

Bureau of Mines Direct Method Test

General Data

Company:	VCER	*Hole No.:*	CH-1-2014 (C-1)
Contact Person:		*Coalbed:*	Pocahontas 7 (10 Bench)
Hole Location:		*Sample ID #:*	F-68
		MM&A Project #:	VCER101
Quadrangle:		***Coordinates***	
Core Collected by:	T. Keim	*East:*	
Type of Drilling:		*North:*	
Drilling Contractor:		*Surface Elevation:*	
Sidewall Coring Contractor:		*Drilling Media:*	Water

Core Data

As-Rec'd, Whole Sample Wt. (g):	638.70	*Core Length:*	1.05'
As-Rec'd, Crushed Sample Wt. (g):	607.40	*Core Diameter:*	
DMMF, Whole Sample Wt. (g):	548.85	*Depth of Cored Interval:*	1413.50'
DMMF, Crushed Sample Wt. (g):	521.95		1414.55'

Time Data

	Day/Hr./ Min.		Day/Hr./Min.

Coalbed Encountered (A):	8/4/14 3:15 PM	*Core Reached Surface (C):*	8/4/14 4:06 PM
Hole Filled with Water (E):	NA	*Core Sealed in Canister (D):*	8/4/14 4:13 PM
Core Started Out of Hole (B):	8/4/14 4:00 PM		
			8/4/2014 16.21666667

Gas Volume Data

	Drilled with Air		***Drilled with Water***
Lost Gas Volume	Not Performed		229.81 cc
		Desorbed Gas Volume from Canister @ STP:	5599.36 cc
		Residual Gas Volume from Crushed Core @ STP:	912.87 cc

Gas Content

Gas Content @ STP =(Lost Gas + Desorbed Gas Volumes)/Whole Sample Weight

Air, As-Received	***Air, DMMF***	***Water, As-Received***	***Water, DMMF***
Not Performed	Not Performed	9.13 cc/g	10.62 cc/g
Not Performed	Not Performed	292.39 ft³/ton	340.26 ft³/ton

Residual Gas Content @ STP =Residual Gas Volume/Crushed Sample Weight

As-Received	***DMMF***
1.50 cc/g	1.75 cc/g
48.15 ft³/ton	56.03 ft³/ton

Total Gas Content @ STP =Gas Content + Residual Gas Content

Air, As-Received	***Air, DMMF***	***Water, As-Received***	***Water, DMMF***
Not Performed	Not Performed	10.63 cc/g	12.37 cc/g
Not Performed	Not Performed	340.54 ft³/ton	396.29 ft³/ton

Table S: Gas Desorption Timesheet 1413

Coal Sample Gas Desorption Computation

Coal Desorption Data

Drill Hole: CH-1-2014 (C-1) Canister #: F-68

Number of Readings	Date	Time (Hrs./Min)	Desorbed Gas	Temp	F/C	Pressure (In.)	Inc. Adj. Volume	Cum. Adj. Volume
1	8/4/2014	4:23 PM	102.00	72.0	F	28.30	94.30	324.10
2	8/4/2014	4:35 PM	82.00	72.0	F	28.30	75.81	399.91
3	8/4/2014	4:45 PM	66.00	72.0	F	28.30	61.02	460.93
4	8/4/2014	4:55 PM	55.00	72.0	F	28.30	50.85	511.77
5	8/4/2014	5:15 PM	85.00	72.0	F	28.30	78.58	590.35
6	8/4/2014	5:35 PM	70.00	72.0	F	28.30	64.71	655.07
7	8/4/2014	7:29 PM	260.00	69.0	F	27.70	236.60	891.67
8	8/5/2014	7:53 AM	491.00	69.0	F	27.71	446.98	1,338.65
9	8/6/2014	7:53 AM	647.00	69.0	F	27.67	588.14	1,926.79
10	8/7/2014	8:59 AM	509.00	70.0	F	27.68	461.99	2,388.78
11	8/8/2014	7:19 AM	10.00	70.0	F	27.70	9.08	2,397.86
12	8/9/2014	12:05 PM	310.00	70.0	F	27.68	281.37	2,679.23
13	8/10/2014	9:23 AM	198.00	70.0	F	27.66	179.58	2,858.82
14	8/11/2014	10:00 AM	204.00	70.0	F	27.67	185.09	3,043.91
15	8/12/2014	8:33 AM	189.00	70.0	F	27.53	170.61	3,214.52
16	8/13/2014	8:13 AM	175.00	70.0	F	27.56	158.15	3,372.67
17	8/14/2014	7:00 AM	119.00	70.0	F	27.66	107.93	3,480.60
18	8/15/2014	8:36 AM	146.00	70.0	F	27.64	132.32	3,612.93
19	8/16/2014	8:41 AM	117.00	69.0	F	27.63	106.20	3,719.13
20	8/17/2014	8:43 AM	111.00	70.0	F	27.62	100.53	3,819.66
21	8/18/2014	10:17 AM	125.00	70.0	F	27.50	112.72	3,932.38
22	8/19/2014	10:30 AM	95.00	71.0	F	27.50	85.50	4,017.88
23	8/20/2014	9:15 AM	79.00	70.0	F	27.60	71.50	4,089.38
24	8/22/2014	9:12 AM	125.00	70.0	F	26.50	108.62	4,197.99
25	8/25/2014	11:28 AM	152.00	68.0	F	27.71	138.63	4,336.63
26	8/27/2014	1:38 PM	99.00	69.0	F	27.72	90.16	4,426.79
27	8/29/2014	9:47 AM	96.00	68.0	F	27.71	87.56	4,514.34
28	9/2/2014	2:20 PM	189.00	73.0	F	27.69	170.64	4,684.98
29	9/5/2014	7:46 AM	126.00	69.0	F	27.80	115.08	4,800.06
30	9/8/2014	6:21 PM	112.00	70.0	F	27.74	101.88	4,901.94
31	9/10/2014	9:11 AM	60.00	69.0	F	27.70	54.60	4,956.54
32	9/12/2014	10:50 AM	72.00	70.0	F	27.70	65.40	5,021.93
33	9/15/2014	10:16 AM	37.00	67.0	F	27.78	33.90	5,055.83
34	9/17/2014	9:36 AM	58.00	66.0	F	27.62	52.93	5,108.76

35	9/19/2014	12:10 PM	39.00	68.0	F	27.74	35.61	5,144.37
36	9/23/2014	9:35 AM	30.00	66.0	F	27.87	27.62	5,171.99
37	9/25/2014	6:05 PM	62.00	70.0	F	27.80	56.52	5,228.51
38	9/30/2014	3:23 PM	89.00	69.0	F	27.53	80.49	5,309.01
39	10/7/2014	2:35 PM	71.00	69.0	F	27.59	64.35	5,373.36
40	10/13/2014	5:38 PM	82.00	70.0	F	27.69	74.45	5,447.81
41	10/22/2014	8:03 AM	33.00	63.0	F	27.63	30.30	5,478.11
42	10/28/2014	7:55 PM	82.00	70.0	F	27.62	74.27	5,552.38
43	11/4/2014	6:41 PM	10.00	65.0	F	27.75	9.19	5,561.56
44	11/11/2014	5:54 PM	193.00	72.0	F	27.50	173.38	5,734.94
45	11/17/2014	10:50 AM	106.00	72.0	F	27.21	94.22	5,829.16
Residual	**11/17/2014**	**3:05 PM**	**1027.00**	**72.0**	**F**	**27.21**	**912.87**	**6,742.04**

Table T: Gas Desorption Computation 1572

Coal Sample Gas Desorption Computation

Bureau of Mines Direct Method Test

General Data

Company:	VCER	*Hole No.:*	CH-1-2014 (C-1)
Contact Person:		*Coalbed:*	Pocahontas 5 (10 Bench)
Hole Location:		*Sample ID #:*	H-43
		MM&A Project #:	VCER101
Quadrangle:		***Coordinates***	
Core Collected by:	T. Keim	*East:*	
Type of Drilling:		*North:*	
Drilling Contractor:		*Surface Elevation:*	
Sidewall Coring Contractor:		*Drilling Media:*	Water

Core Data

As-Rec'd, Whole Sample Wt. (g):	580.40	*Core Length:*	1.00'
As-Rec'd, Crushed Sample Wt. (g):	510.40	*Core Diameter:*	
DMMF, Whole Sample Wt. (g):	534.30	*Depth of Cored Interval:*	1572.35'
DMMF, Crushed Sample Wt. (g):	469.86		1573.35'

Time Data

	Day/Hr./Min.		Day/Hr./Min.

Coalbed Encountered (A):	8/12/14 6:30 AM	*Core Reached Surface (C):*	8/12/14 8:45 AM
Hole Filled with Water (E):	NA	*Core Sealed in Canister (D):*	8/12/14 8:53 AM
Core Started Out of Hole (B):	8/12/14 8:32 AM		
			8/12/2014 8.883333333

Gas Volume Data

	Drilled with Air	***Drilled with Water***
Lost Gas Volume	Not Performed	161.19 cc

Desorbed Gas Volume from Canister @ STP:	6074.65 cc
Residual Gas Volume from Crushed Core @ STP:	653.96 cc

Gas Content

Gas Content @ STP =(Lost Gas + Desorbed Gas Volumes)/Whole Sample Weight

Air, As-Received	***Air, DMMF***	***Water, As-Received***	***Water, DMMF***
Not Performed	Not Performed	10.74 cc/g	11.67 cc/g
Not Performed	Not Performed	344.21 ft³/ton	373.91 ft³/ton

Residual Gas Content @ STP =Residual Gas Volume/Crushed Sample Weight

As-Received	***DMMF***
1.28 cc/g	1.39 cc/g
41.05 ft³/ton	44.59 ft³/ton

Total Gas Content @ STP =Gas Content + Residual Gas Content

Air, As-Received	***Air, DMMF***	***Water, As-Received***	***Water, DMMF***
Not Performed	Not Performed	12.03 cc/g	13.06 cc/g
Not Performed	Not Performed	385.25 ft³/ton	418.50 ft³/ton

Table U: Gas Desorption Time Sheet 1572

Coal Sample Gas Desorption Computation

Coal Desorption Data

Drill Hole: CH-1-2014 (C-1) Canister #: H-43

Number of Readings	Date	Time (Hrs./Min)	Desorbed Gas	Temp	F/C	Pressure (In.)	Inc. Adj. Volume	Cum. Adj. Volume
1	8/12/2014	9:03 AM	52.00	73.0	F	28.10	47.64	208.83
2	8/12/2014	9:13 AM	46.00	73.0	F	28.10	42.15	250.98
3	8/12/2014	9:23 AM	48.00	73.0	F	28.10	43.98	294.95
4	8/12/2014	9:43 AM	43.00	73.0	F	28.10	39.40	334.35
5	8/12/2014	10:05 AM	50.00	73.0	F	28.10	45.81	380.16
6	8/12/2014	10:25 AM	43.00	73.0	F	28.10	39.40	419.56
7	8/12/2014	10:55 AM	54.00	73.0	F	28.10	49.48	469.04
8	8/12/2014	11:25 AM	56.00	73.0	F	28.10	51.31	520.34
9	8/12/2014	12:25 PM	88.00	74.0	F	28.10	80.48	600.82
10	8/12/2014	1:25 PM	80.00	72.0	F	28.10	73.44	674.26
11	8/12/2014	3:25 PM	142.00	72.0	F	28.10	130.35	804.60
12	8/12/2014	5:23 PM	121.00	72.0	F	28.10	111.07	915.68
13	8/12/2014	7:44 PM	122.00	72.0	F	27.47	109.48	1,025.15
14	8/13/2014	8:14 AM	328.00	70.0	F	27.56	296.42	1,321.57
15	8/14/2014	7:01 AM	395.00	70.0	F	27.66	358.26	1,679.83
16	8/15/2014	8:37 AM	374.00	70.0	F	27.64	338.97	2,018.80
17	8/16/2014	8:45 AM	296.00	69.0	F	27.63	268.68	2,287.48
18	8/17/2014	8:46 AM	236.00	70.0	F	27.62	213.74	2,501.22
19	8/18/2014	10:19 AM	240.00	70.0	F	27.50	216.42	2,717.64
20	8/19/2014	10:32 AM	199.00	71.0	F	27.50	179.11	2,896.74
21	8/20/2014	9:16 AM	170.00	70.0	F	27.60	153.85	3,050.60
22	8/21/2014	9:20 AM	160.00	70.0	F	27.70	145.33	3,195.93
23	8/22/2014	9:14 AM	143.00	70.0	F	26.50	124.26	3,320.18
24	8/25/2014	11:30 AM	342.00	68.0	F	27.71	311.93	3,632.11
25	8/26/2014	9:13 AM	100.00	68.0	F	27.72	91.24	3,723.35
26	8/27/2014	1:41 PM	112.00	69.0	F	27.72	102.00	3,825.35
27	8/29/2014	9:49 AM	183.00	68.0	F	27.71	166.91	3,992.26
28	9/2/2014	2:21 PM	334.00	73.0	F	27.69	301.55	4,293.81
29	9/5/2014	7:48 AM	212.00	69.0	F	27.80	193.62	4,487.43
30	9/8/2014	6:23 PM	202.00	70.0	F	27.74	183.74	4,671.17
31	9/10/2014	9:12 AM	115.00	69.0	F	27.70	104.65	4,775.82
32	9/12/2014	10:51 AM	123.00	70.0	F	27.70	111.72	4,887.54
33	9/15/2014	10:17 AM	111.00	67.0	F	27.78	101.69	4,989.23
34	9/17/2014	9:38 AM	105.00	67.0	F	27.62	95.64	5,084.87
35	9/19/2014	12:11 PM	84.00	68.0	F	27.74	76.70	5,161.57

36	9/23/2014	9:36 AM	104.00	66.0	F	27.87	95.77	5,257.33
37	9/25/2014	6:06 PM	104.00	70.0	F	27.80	94.80	5,352.14
38	9/30/2014	3:25 PM	154.00	69.0	F	27.53	139.28	5,491.42
39	10/7/2014	2:37 PM	148.00	69.0	F	27.59	134.15	5,625.57
40	10/13/2014	5:39 PM	133.00	70.0	F	27.69	120.76	5,746.33
41	10/22/2014	8:04 AM	93.00	63.0	F	27.63	85.39	5,831.71
42	10/28/2014	7:57 PM	120.00	70.0	F	27.62	108.68	5,940.39
43	11/4/2014	6:43 PM	51.00	65.0	F	27.75	46.85	5,987.24
44	11/11/2014	5:55 PM	176.00	72.0	F	27.50	158.11	6,145.35
45	11/17/2014	2:28 PM	101.00	70.0	F	27.32	90.48	6,235.83
Residual	**11/17/2014**	**5:20 PM**	**730.00**	**70.0**	**F**	**27.32**	**653.96**	**6,889.79**

Table V: Gas Desorption Computation 1624

Coal Sample Gas Desorption Computation

Bureau of Mines Direct Method Test

General Data

Company:	VCER	*Hole No.:*	CH-1-2014 (C-1)
Contact Person:		*Coalbed:*	Pocahontas 5 (20 Bench)
Hole Location:		*Sample ID #:*	H-10
		MM&A Project #:	VCER101
Quadrangle:		***Coordinates***	
Core Collected by:	T. Keim	*East:*	
Type of Drilling:		*North:*	
Drilling Contractor:		*Surface Elevation:*	
Sidewall Coring Contractor:		*Drilling Media:*	Water

Core Data

As-Rec'd, Whole Sample Wt. (g):	479.90	*Core Length:*	0.86'
As-Rec'd, Crushed Sample Wt. (g):	471.80	*Core Diameter:*	
DMMF, Whole Sample Wt. (g):	439.66	*Depth of Cored Interval:*	1624.46'
DMMF, Crushed Sample Wt. (g):	432.24		1625.32'

Time Data

	Day/Hr./Min.		Day/Hr./Min.
Coalbed Encountered (A):	8/12/14 11:10 AM	*Core Reached Surface (C):*	8/12/14 11:36 AM
Hole Filled with Water (E):	NA	*Core Sealed in Canister (D):*	8/12/14 11:46 AM
Core Started Out of Hole (B):	8/12/14 11:29 AM		
			8/12/2014 11.76666667

Gas Volume Data

	Drilled with Air	***Drilled with Water***
Lost Gas Volume	Not Performed	160.86 cc

Desorbed Gas Volume from Canister @ STP:	4801.45 cc
Residual Gas Volume from Crushed Core @ STP:	706.17 cc

Gas Content

Gas Content @ STP =(Lost Gas + Desorbed Gas Volumes)/Whole Sample Weight

Air, As-Received	***Air, DMMF***	***Water, As-Received***	***Water, DMMF***
Not Performed	Not Performed	10.34 cc/g	11.29 cc/g
Not Performed	Not Performed	331.27 ft³/ton	361.59 ft³/ton

Residual Gas Content @ STP =Residual Gas Volume/Crushed Sample Weight

As-Received	***DMMF***
1.50 cc/g	1.63 cc/g
47.95 ft³/ton	52.34 ft³/ton

Total Gas Content @ STP =Gas Content + Residual Gas Content

Air, As-Received	***Air, DMMF***	***Water, As-Received***	***Water, DMMF***
Not Performed	Not Performed	11.84 cc/g	12.92 cc/g
Not Performed	Not Performed	379.22 ft³/ton	413.93 ft³/ton

Table W: Gas Desorption Time Sheet 1624

Coal Sample Gas Desorption Computation

Coal Desorption Data

Drill Hole: CH-1-2014 (C-1) Canister #: H-10

Number of Readings	Date	Time (Hrs./Min)	Desorbed Gas	Temp	F/C	Pressure (In.)	Inc. Adj. Volume	Cum. Adj. Volume
1	8/12/2014	11:56 AM	60.00	74.0	F	28.10	54.8702	215.7312
2	8/12/2014	12:06 PM	44.00	74.0	F	28.10	40.2381	255.9694
3	8/12/2014	12:21 PM	51.00	74.0	F	28.10	46.6397	302.6091
4	8/12/2014	12:36 PM	46.00	74.0	F	28.10	42.0672	344.6762
5	8/12/2014	12:56 PM	46.00	72.0	F	28.10	42.2255	386.9017
6	8/12/2014	1:26 PM	60.00	72.0	F	28.10	55.0767	441.9784
7	8/12/2014	1:56 PM	60.00	72.0	F	28.10	55.0767	497.0551
8	8/12/2014	3:26 PM	126.00	72.0	F	28.10	115.6611	612.7162
9	8/12/2014	5:23 PM	121.00	72.0	F	28.10	111.0714	723.7876
10	8/12/2014	7:50 PM	115.00	72.0	F	27.47	103.1970	826.9846
11	8/13/2014	8:22 AM	285.00	70.0	F	27.56	257.5563	1084.5408
12	8/14/2014	6:07 AM	325.00	70.0	F	27.66	294.7702	1379.3110
13	8/15/2014	8:44 AM	292.00	70.0	F	27.64	264.6482	1643.9592
14	8/16/2014	8:51 AM	224.00	69.0	F	27.63	203.3284	1847.2877
15	8/17/2014	8:50 AM	178.00	70.0	F	27.62	161.2099	2008.4976
16	8/18/2014	10:25 AM	186.00	70.0	F	27.50	167.7234	2176.2210
17	8/19/2014	10:34 AM	135.00	71.0	F	27.50	121.5052	2297.7262
18	8/20/2014	9:17 AM	117.00	70.0	F	27.60	105.8871	2403.6133
19	8/21/2014	9:22 AM	110.00	70.0	F	27.70	99.9127	2503.5260
20	8/22/2014	9:16 AM	100.00	70.0	F	26.50	86.8948	2590.4208
21	8/25/2014	11:33 AM	238.00	68.0	F	27.71	217.0728	2807.4936
22	8/26/2014	9:15 AM	69.00	68.0	F	27.72	62.9556	2870.4491
23	8/27/2014	1:42 PM	82.00	69.0	F	27.72	74.6752	2945.1243
24	8/29/2014	9:51 AM	137.00	68.0	F	27.71	124.9537	3070.0780
25	9/2/2014	2:23 PM	260.00	73.0	F	27.69	234.7417	3304.8197
26	9/5/2014	7:49 AM	158.00	69.0	F	27.80	144.3016	3449.1212
27	9/8/2014	6:24 PM	176.00	70.0	F	27.74	160.0911	3609.2123
28	9/10/2014	9:14 AM	90.00	69.0	F	27.70	81.9014	3691.1138
29	9/12/2014	10:53 AM	97.00	70.0	F	27.70	88.1048	3779.2186
30	9/15/2014	10:18 AM	82.00	67.0	F	27.78	75.1211	3854.3397
31	9/17/2014	9:39 AM	83.00	67.0	F	27.62	75.5993	3929.9390
32	9/19/2014	12:12 PM	68.00	68.0	F	27.74	62.0879	3992.0270
33	9/23/2014	9:38 AM	84.00	66.0	F	27.87	77.3496	4069.3766
34	9/25/2014	6:07 PM	90.00	70.0	F	27.80	82.0418	4151.4184

35	9/30/2014	3:26 PM	129.00	69.0	F	27.53	116.6716	4268.0900
36	10/7/2014	2:38 PM	121.00	69.0	F	27.59	109.6746	4377.7647
37	10/13/2014	5:40 PM	116.00	70.0	F	27.69	105.3244	4483.0891
38	10/22/2014	8:07 AM	88.00	63.0	F	27.63	80.7965	4563.8855
39	10/28/2014	7:58 PM	114.00	70.0	F	27.62	103.2468	4667.1323
40	11/4/2014	6:44 PM	36.00	65.0	F	27.75	33.0700	4700.2024
41	11/11/2014	5:56 PM	171.00	72.0	F	27.50	153.6170	4853.8194
42	11/17/2014	10:00 AM	111.00	70.0	F	27.32	99.4379	4953.2572
43	11/18/2014	11:37 AM	10.00	70.0	F	27.61	9.0535	4962.3107
Residual	**11/18/2014**	**11:58 AM**	**780.00**	**70.0**	**F**	**27.61**	**706.1697**	**5668.4803**

Table X: Gas Desorption Computation 1625

Coal Sample Gas Desorption Computation

Bureau of Mines Direct Method Test

General Data

Company:	VCER	*Hole No.:*	CH-1-2014 (C-1)
Contact Person:		*Coalbed:*	Carb Shale
Hole Location:		*Sample ID #:*	F-52
		MM&A Project #:	VCER101
Quadrangle:		***Coordinates***	
Core Collected by:	T. KEIM	*East:*	
Type of Drilling:		*North:*	
Drilling Contractor:		*Surface Elevation:*	
Sidewall Coring Contractor:		*Drilling Media:*	Water

Core Data

As-Rec'd, Whole Sample Wt. (g):	1150.60	*Core Length:*	0.77'
As-Rec'd, Crushed Sample Wt. (g):	67.50	*Core Diameter:*	
DMMF, Whole Sample Wt. (g):	Not Performed	*Depth of Cored Interval:*	1625.32'
DMMF, Crushed Sample Wt. (g):	Not Performed		1626.09'

Time Data

	Day/Hr./Min.		Day/Hr./Min.
Coalbed Encountered (A):	8/12/14 11:10 AM	*Core Reached Surface (C):*	8/12/14 11:36 AM

Hole Filled with Water (E):	NA	*Core Sealed in Canister (D):*	8/12/14 11:44 AM
Core Started Out of Hole (B):	8/12/14 11:29 AM		8/12/2014 11.73333 333

Gas Volume Data

	Drilled with Air	***Drilled with Water***
Lost Gas Volume	Not Performed	35.01 cc

Desorbed Gas Volume from Canister @ STP:	652.56 cc
Residual Gas Volume from Crushed Core @ STP:	119.55 cc

Gas Content

Gas Content @ STP =(Lost Gas + Desorbed Gas Volumes)/Whole Sample Weight

Air, As-Received	***Air, DMMF***	***Water, As-Received***	***Water, DMMF***
Not Performed	Not Performed	0.60 cc/g	Not Performed
Not Performed	Not Performed	19.14 ft³/ton	Not Performed

Residual Gas Content @ STP =Residual Gas Volume/Crushed Sample Weight

As-Received	***DMMF***
1.77 cc/g	Not Performed
56.74 ft³/ton	Not Performed

Total Gas Content @ STP =Gas Content + Residual Gas Content

Air, As-Received	***Air, DMMF***	***Water, As-Received***	***Water, DMMF***
Not Performed	Not Performed	2.37 cc/g	Not Performed
Not Performed	Not Performed	75.88 ft³/ton	Not Performed

Table Y: Gas Desorption Time Sheet 1625

Coal Sample Gas Desorption Computation

Coal Desorption Data

Drill Hole: CH-1-2014 (C-1) Canister #: F-52

Number of	Time	Desorbed	Inc. Adj.	Cum. Adj.

Readings	Date	(Hrs./Min)	Gas	Temp	F/C	Pressure (In.)	Volume	Volume
1	8/12/2014	11:54 AM	27.00	74.0	F	28.10	24.6916	59.7006
2	8/12/2014	12:04 PM	13.00	74.0	F	28.10	11.8885	71.5891
3	8/12/2014	12:19 PM	10.00	74.0	F	28.10	9.1450	80.7341
4	8/12/2014	12:34 PM	11.00	74.0	F	28.10	10.0595	90.7937
5	8/12/2014	12:54 PM	13.00	72.0	F	28.10	11.9333	102.7270
6	8/12/2014	1:24 PM	13.00	72.0	F	28.10	11.9333	114.6602
7	8/12/2014	1:54 PM	15.00	72.0	F	28.10	13.7692	128.4294
8	8/12/2014	3:24 PM	30.00	72.0	F	28.10	27.5384	155.9678
9	8/12/2014	5:20 PM	17.00	72.0	F	28.10	15.6051	171.5729
10	8/12/2014	7:52 PM	27.00	72.0	F	27.47	24.2289	195.8017
11	8/13/2014	8:25 AM	31.00	70.0	F	27.56	28.0149	223.8166
12	8/14/2014	6:09 AM	23.00	70.0	F	27.66	20.8607	244.6773
13	8/15/2014	8:45 AM	31.00	70.0	F	27.64	28.0962	272.7735
14	8/16/2014	8:53 AM	21.00	69.0	F	27.63	19.0620	291.8355
15	8/17/2014	8:52 AM	24.00	70.0	F	27.62	21.7362	313.5717
16	8/18/2014	10:27 AM	32.00	70.0	F	27.50	28.8556	342.4273
17	8/19/2014	10:37 AM	12.00	71.0	F	27.50	10.8005	353.2278
18	8/20/2014	9:18 AM	5.00	70.0	F	27.60	4.5251	357.7529
19	8/22/2014	9:18 AM	10.00	70.0	F	26.50	8.6895	366.4424
20	8/25/2014	11:35 AM	15.00	68.0	F	27.71	13.6811	380.1234
21	8/27/2014	1:44 PM	11.00	69.0	F	27.72	10.0174	390.1408
22	8/29/2014	9:53 AM	17.00	68.0	F	27.71	15.5052	405.6460
23	9/2/2014	2:25 PM	39.00	73.0	F	27.69	35.2113	440.8573
24	9/5/2014	7:50 AM	10.00	69.0	F	27.80	9.1330	449.9903
25	9/8/2014	6:25 PM	13.00	70.0	F	27.74	11.8249	461.8152
26	9/10/2014	9:15 AM	5.00	69.0	F	27.70	4.5501	466.3653
27	9/12/2014	10:55 AM	10.00	70.0	F	27.70	9.0830	475.4482
28	9/15/2014	10:19 AM	10.00	67.0	F	27.78	9.1611	484.6094
29	9/17/2014	9:40 AM	13.00	67.0	F	27.62	11.8409	496.4502
30	9/19/2014	12:13 PM	2.00	68.0	F	27.74	1.8261	498.2763
31	9/23/2014	9:39 AM	10.00	66.0	F	27.87	9.2083	507.4846
32	9/25/2014	6:07 PM	21.00	70.0	F	27.80	19.1431	526.6277
33	9/30/2014	3:27 PM	31.00	69.0	F	27.53	28.0374	554.6651
34	10/7/2014	2:40 PM	10.00	70.0	F	27.59	9.0469	563.7120
35	10/13/2014	5:42 PM	10.00	69.0	F	27.69	9.0969	572.8088
36	10/22/2014	8:08 AM	10.00	63.0	F	27.63	9.1814	581.9903
37	10/28/2014	7:59 PM	27.00	70.0	F	27.62	24.4532	606.4434
38	11/4/2014	6:46 PM	10.00	65.0	F	27.75	9.1861	615.6296
39	11/11/2014	5:58 PM	70.00	72.0	F	27.50	62.8841	678.5137
40	11/18/2014	11:37 AM	10.00	70.0	F	27.62	9.0567	687.5705

Residual	**11/18/2014**	**2:23 PM**	**132.00**	**70.0**	**F**	**27.62**	**119.5489**	**807.1194**

Table Z: Gas Desorption Computation 1648

Coal Sample Gas Desorption Computation

Bureau of Mines Direct Method Test

General Data

Company:	VCER	*Hole No.:*	CH-1-2014 (C-1)
Contact Person:		*Coalbed:*	Pocahontas 4
Hole Location:		*Sample ID #:*	G-45
		MM&A Project #:	VCER101
Quadrangle:		***Coordinates***	
Core Collected by:	T. KEIM	*East:*	
Type of Drilling:		*North:*	
Drilling Contractor:		*Surface Elevation:*	
Sidewall Coring Contractor:		*Drilling Media:*	Water

Core Data

As-Rec'd, Whole Sample Wt. (g):	926.00	*Core Length:*	1.37'
As-Rec'd, Crushed Sample Wt. (g):	Not Performed	*Core Diameter:*	
DMMF, Whole Sample Wt. (g):	Not Performed	*Depth of Cored Interval:*	1648.50'
DMMF, Crushed Sample Wt. (g):	Not Performed		1649.87'

Time Data

	Day/Hr./Min.		Day/Hr./Min.
Coalbed Encountered (A):	8/12/14 1:20 PM	*Core Reached Surface (C):*	8/12/14 2:50 PM
Hole Filled with Water (E):	NA	*Core Sealed in Canister (D):*	8/12/14 2:57 PM
Core Started Out of Hole (B):	8/12/14 2:40 PM		8/12/2014 14.95

Gas Volume Data

	Drilled with Air		*Drilled with Water*	
Lost Gas Volume	Not Performed		399.57 cc	

Desorbed Gas Volume from Canister @ STP:	8157.74 cc
Residual Gas Volume from Crushed Core @ STP:	Not Performed

Gas Content

Gas Content @ STP =(Lost Gas + Desorbed Gas Volumes)/Whole Sample Weight

Air, As-Received	*Air, DMMF*		*Water, As-Received*	*Water, DMMF*
Not Performed	Not Performed		9.24 cc/g	Not Performed
Not Performed	Not Performed		296.06 ft³/ton	Not Performed

Residual Gas Content @ STP =Residual Gas Volume/Crushed Sample Weight

As-Received		*DMMF*
Not Performed		Not Performed
Not Performed		Not Performed

Total Gas Content @ STP =Gas Content + Residual Gas Content

Air, As-Received	*Air, DMMF*		*Water, As-Received*	*Water, DMMF*
Not Performed	Not Performed		Not Performed	Not Performed
Not Performed	Not Performed		Not Performed	Not Performed

Table AA: Gas Desorption Time Sheet 1648

Coal Sample Gas Desorption Computation

Coal Desorption Data

Drill Hole: CH-1-2014 (C-1) Canister #: G-45

Number of	Time	Desorbed	Inc. Adj.	Cum. Adj.

Readings	Date	(Hrs./Min)	Gas	Temp	F/C	Pressure (In.)	Volume	Volume
1	8/12/2014	3:07 PM	152.00	72.0	F	28.10	139.5277	539.0987
2	8/12/2014	3:17 PM	104.00	72.0	F	28.10	95.4663	634.5650
3	8/12/2014	3:27 PM	101.00	72.0	F	28.10	92.7125	727.2775
4	8/12/2014	3:37 PM	84.00	72.0	F	28.10	77.1074	804.3849
5	8/12/2014	3:47 PM	73.00	72.0	F	28.10	67.0100	871.3949
6	8/12/2014	3:57 PM	70.00	72.0	F	28.10	64.2562	935.6510
7	8/12/2014	4:12 PM	86.00	72.0	F	28.10	78.9433	1014.5943
8	8/12/2014	4:32 PM	102.00	72.0	F	28.10	93.6304	1108.2247
9	8/12/2014	4:52 PM	103.00	72.0	F	28.10	94.5484	1202.7731
10	8/12/2014	5:19 PM	114.00	72.0	F	28.10	104.6458	1307.4189
11	8/12/2014	7:47 PM	366.00	72.0	F	27.47	328.4356	1635.8544
12	8/13/2014	8:17 AM	999.00	70.0	F	27.56	902.8025	2538.6569
13	8/14/2014	7:03 AM	1030.00	70.0	F	27.66	934.1948	3472.8518
14	8/15/2014	8:39 AM	837.00	70.0	F	27.64	758.5978	4231.4495
15	8/16/2014	8:47 AM	568.00	69.0	F	27.63	515.5828	4747.0323
16	8/17/2014	8:48 AM	440.00	70.0	F	27.62	398.4964	5145.5287
17	8/18/2014	10:22 AM	385.00	70.0	F	27.50	347.1694	5492.6981
18	8/19/2014	10:39 AM	301.00	71.0	F	27.50	270.9116	5763.6098
19	8/20/2014	9:19 AM	221.00	70.0	F	27.60	200.0089	5963.6187
20	8/21/2014	9:25 AM	200.00	70.0	F	27.70	181.6594	6145.2781
21	8/22/2014	9:20 AM	160.00	70.0	F	26.50	139.0317	6284.3098
22	8/25/2014	11:37 AM	310.00	68.0	F	27.71	282.7418	6567.0517
23	8/26/2014	9:17 AM	110.00	68.0	F	27.72	100.3640	6667.4156
24	8/27/2014	1:45 PM	110.00	69.0	F	27.72	100.1740	6767.5897
25	8/29/2014	9:55 AM	155.00	68.0	F	27.71	141.3709	6908.9606
26	9/2/2014	2:26 PM	287.00	73.0	F	27.69	259.1187	7168.0793
27	9/5/2014	7:53 AM	171.00	69.0	F	27.80	156.1745	7324.2538
28	9/8/2014	6:27 PM	159.00	70.0	F	27.74	144.6278	7468.8815
29	9/10/2014	9:16 AM	89.00	69.0	F	27.70	80.9914	7549.8730
30	9/12/2014	10:56 AM	97.00	70.0	F	27.70	88.1048	7637.9778
31	9/15/2014	10:20 AM	74.00	67.0	F	27.78	67.7923	7705.7700
32	9/17/2014	9:41 AM	69.00	67.0	F	27.62	62.8476	7768.6176
33	9/19/2014	12:14 PM	50.00	68.0	F	27.74	45.6529	7814.2705
34	9/23/2014	9:40 AM	60.00	66.0	F	27.87	55.2497	7869.5203
35	9/25/2014	6:08 PM	76.00	70.0	F	27.80	69.2798	7938.8000
36	9/30/2014	3:28 PM	109.00	69.0	F	27.53	98.5830	8037.3830
37	10/7/2014	2:41 PM	96.00	69.0	F	27.59	87.0146	8124.3976
38	10/13/2014	5:43 PM	96.00	70.0	F	27.69	87.1650	8211.5626
39	10/22/2014	8:09 AM	56.00	63.0	F	27.63	51.4159	8262.9786
40	10/28/2014	7:59 PM	86.00	69.0	F	27.62	78.0353	8341.0139

41	11/4/2014	6:47 PM	18.00	65.0	F	27.75	16.5350	8357.5489
42	11/11/2014	5:59 PM	164.00	72.0	F	27.50	147.3286	8504.8775
43	11/18/2014	1:45 PM	58.00	71.0	F	27.62	52.4300	8557.3075
Residual							**Not Performed**	

Table BB: Gas Desorption Computation 1727

Coal Sample Gas Desorption Computation

Bureau of Mines Direct Method Test

General Data

Company:	VCER	*Hole No.:*	CH-1-2014 (C-1)
Contact Person:		*Coalbed:*	Pocahontas 3 (10-20 Bench)
Hole Location:		*Sample ID #:*	H-35
		MM&A Project #:	VCER101
Quadrangle:		***Coordinates***	
Core Collected by:	T. KEIM	*East:*	
Type of Drilling:		*North:*	
Drilling Contractor:		*Surface Elevation:*	
Sidewall Coring Contractor:		*Drilling Media:*	Water

Core Data

As-Rec'd, Whole Sample Wt. (g):	0.00	*Core Length:*	3.62'
As-Rec'd, Crushed Sample Wt. (g):	Not Performed	*Core Diameter:*	
DMMF, Whole Sample Wt. (g):	Not Performed	*Depth of Cored Interval:*	1727.06'
DMMF, Crushed Sample Wt. (g):	Not Performed		1730.68'

Time Data

	Day/Hr./Min.		Day/Hr./Min.
Coalbed Encountered (A):	8/13/14 9:30 AM	*Core Reached Surface (C):*	8/13/14 11:01 AM
Hole Filled with Water (E):	NA	*Core Sealed in Canister (D):*	8/13/14 11:10 PM
Core Started Out of Hole (B):	8/13/14 10:52 AM		8/13/2014
			23.16666667

Gas Volume Data

	Drilled with Air		*Drilled with Water*
Lost Gas Volume	Not Performed		128.11 cc
		Desorbed Gas Volume from Canister @ STP:	3149.98 cc
		Residual Gas Volume from Crushed Core @ STP:	Not Performed / Recovered in Re-drill

Gas Content

Gas Content @ STP =(Lost Gas + Desorbed Gas Volumes)/Whole Sample Weight

Air, As-Received	*Air, DMMF*	*Water, As-Received*	*Water, DMMF*
Not Performed	Not Performed	Not Performed	Not Performed
Not Performed	Not Performed	Not Performed	Not Performed

Residual Gas Content @ STP =Residual Gas Volume/Crushed Sample Weight

As-Received	*DMMF*
Not Performed	Not Performed
Not Performed	Not Performed

Total Gas Content @ STP =Gas Content + Residual Gas Content

Air, As-Received	*Air, DMMF*	*Water, As-Received*	*Water, DMMF*
Not Performed	Not Performed	Not Performed	#VALUE!
Not Performed	Not Performed	Not Performed	#VALUE!

Table CC: Gas Desorption Time Sheet 1727

Coal Sample Gas Desorption Computation

Coal Desorption Data

Number of Readings	Drill Hole:	CH-1-2014 (C-1) Time (Hrs./Min)	Desorbed Gas	Temp	Canister #: F/C	H-35 Pressure (In.)	Inc. Adj. Volume	Cum. Adj. Volume
1	8/13/2014	11:21 AM	45.00	72.0	F	28.25	41.53	169.64
2	8/13/2014	11:31 AM	27.00	72.0	F	28.25	24.92	194.56
3	8/13/2014	11:41 AM	27.00	72.0	F	28.25	24.92	219.48
4	8/13/2014	12:01 PM	34.00	72.0	F	28.25	31.38	250.85
5	8/13/2014	12:31 PM	42.00	72.0	F	28.25	38.76	289.61
6	8/13/2014	1:01 PM	40.00	72.0	F	28.25	36.91	326.53
7	8/13/2014	3:01 PM	139.00	72.0	F	28.25	128.28	454.80
8	8/13/2014	4:01 PM	67.00	72.0	F	28.25	61.83	516.63
9	8/13/2014	5:32 PM	69.00	72.0	F	28.25	63.68	580.31
10	8/13/2014	7:06 PM	77.00	65.0	F	27.60	70.35	650.66
11	8/14/2014	7:11 AM	194.00	70.0	F	27.66	175.96	826.61
12	8/15/2014	8:47 AM	293.00	70.0	F	27.64	265.55	1,092.17
13	8/16/2014	8:55 AM	175.00	69.0	F	27.63	158.85	1,251.02
14	8/17/2014	8:54 AM	144.00	70.0	F	27.62	130.42	1,381.44
15	8/18/2014	10:29 AM	141.00	70.0	F	27.50	127.15	1,508.58
16	8/19/2014	10:41 AM	101.00	71.0	F	27.50	90.90	1,599.48
17	8/20/2014	9:22 AM	76.00	70.0	F	27.60	68.78	1,668.27
18	8/21/2014	9:26 AM	70.00	70.0	F	27.70	63.58	1,731.85
19	8/22/2014	9:22 AM	65.00	70.0	F	26.50	56.48	1,788.33
20	8/25/2014	11:39 AM	146.00	68.0	F	27.71	133.16	1,921.49
21	8/27/2014	1:47 PM	86.00	69.0	F	27.72	78.32	1,999.81
22	8/29/2014	9:57 AM	91.00	68.0	F	27.71	83.00	2,082.81
23	9/2/2014	2:28 PM	167.00	73.0	F	27.69	150.78	2,233.58

24	9/5/2014	7:55 AM	74.00	69.0	F	27.80	67.58	2,301.17
25	9/8/2014	6:29 PM	94.00	70.0	F	27.74	85.50	2,386.67
26	9/10/2014	9:17 AM	57.00	60.0	F	27.70	52.77	2,439.44
27	9/12/2014	10:57 AM	63.00	70.0	F	27.70	57.22	2,496.66
28	9/15/2014	10:21 AM	38.00	67.0	F	27.78	34.81	2,531.48
29	9/17/2014	9:43 AM	57.00	67.0	F	27.62	51.92	2,583.39
30	9/19/2014	12:15 PM	32.00	68.0	F	27.74	29.22	2,612.61
31	9/23/2014	9:42 AM	36.00	66.0	F	27.87	33.15	2,645.76
32	9/25/2014	6:09 PM	64.00	70.0	F	27.80	58.34	2,704.10
33	9/30/2014	6:57 AM	92.00	69.0	F	27.53	83.21	2,787.31
34	10/7/2014	2:42 PM	77.00	69.0	F	27.59	69.79	2,857.10
35	10/13/2014	5:44 PM	81.00	70.0	F	27.69	73.55	2,930.65
36	10/22/2014	8:10 AM	53.00	63.0	F	27.63	48.66	2,979.31
37	10/28/2014	8:01 PM	91.00	69.0	F	27.62	82.57	3,061.88
38	11/4/2014	6:48 PM	12.00	65.0	F	27.75	11.02	3,072.90
39	11/11/2014	5:59 PM	162.00	72.0	F	27.50	145.53	3,218.44
40	11/18/2014	2:15 PM	66.00	71.0	F	27.62	59.66	3,278.10
Residual							**Not Performed / Recovered in Re-drill**	

Table DD: Gas Desorption Computation 1728

Coal Sample Gas Desorption Computation

Bureau of Mines Direct Method Test

General Data

Company:	VCER	*Hole No.:*	CH-1R-2014 (C-1)
Contact Person:	(Wedged)	*Coalbed:*	Pocahontas 3 (10 Bench)
Hole Location:		*Sample ID #:*	H-60*

		MM&A Project #:	VCER101
Quadrangle:		***Coordinates***	
Core Collected by:	T Keim	*East:*	
Type of Drilling:		*North:*	
Drilling Contractor:		*Surface Elevation:*	
Sidewall Coring Contractor:		*Drilling Media:*	water

Core Data

As-Rec'd, Whole Sample Wt. (g):	1026.00	*Core Length:*	1.09'
As-Rec'd, Crushed Sample Wt. (g):	779.80	*Core Diameter:*	
DMMF, Whole Sample Wt. (g):	537.23	*Depth of Cored Interval:*	1727.06'
DMMF, Crushed Sample Wt. (g):	408.32		1728.15'

Time Data

	Day/Hr./ Min.		Day/Hr./Min.
Coalbed Encountered (A):	9/9/14 4:10 PM	*Core Reached Surface (C):*	9/9/14 5:10 PM
Hole Filled with Water (E):	NA	*Core Sealed in Canister (D):*	9/9/14 5:23 PM
Core Started Out of Hole (B):	9/9/14 4:56 PM		
			9/9/2014 17.38333333

Gas Volume Data

	Drilled with Air		***Drilled with Water***
Lost Gas Volume	Not Performed		74.94 cc
		Desorbed Gas Volume from Canister @ STP:	1827.48 cc
		Residual Gas Volume from Crushed Core @ STP:	1087.56 cc

Gas Content

Gas Content @ STP =(Lost Gas + Desorbed Gas Volumes)/Whole Sample Weight

Air, As-Received	***Air, DMMF***	***Water, As-Received***	***Water, DMMF***
Not Performed	Not Performed	1.85 cc/g	3.54 cc/g

Not Performed	Not Performed	59.40 ft³/ton	113.45 ft³/ton

Residual Gas Content @ STP =Residual Gas Volume/Crushed Sample Weight

	As-Received	***DMMF***
	1.39 cc/g	2.66 cc/g
	44.68 ft³/ton	85.33 ft³/ton

Total Gas Content @ STP =Gas Content + Residual Gas Content

Air, As-Received	***Air, DMMF***	***Water, As-Received***	***Water, DMMF***
Not Performed	Not Performed	3.25 cc/g	6.20 cc/g
Not Performed	Not Performed	104.08 ft³/ton	198.78 ft³/ton

Table EE: Gas Desorption Time Sheet 1728

Coal Sample Gas Desorption Computation

Coal Desorption Data

Drill Hole: CH-1R-2014 (C-1) Canister #: H-60*

Number of Readings	Date	Time (Hrs./Min)	Desorbed Gas	Temp	F/C	Pressure (In.)	Inc. Adj. Volume	Cum. Adj. Volume
1	9/9/2014	5:33 PM	30.00	72.0	F	28.35	27.78	102.72
2	9/9/2014	5:38 PM	15.00	72.0	F	28.35	13.89	116.61
3	9/9/2014	5:43 PM	15.00	72.0	F	28.35	13.89	130.50
4	9/9/2014	5:53 PM	20.00	72.0	F	28.35	18.52	149.02
5	9/9/2014	7:49 PM	96.00	74.0	F	27.70	86.54	235.57
6	9/10/2014	9:25 AM	160.00	69.0	F	27.70	145.60	381.17
7	9/11/2014	10:28 AM	186.00	69.0	F	27.63	168.84	550.00
8	9/12/2014	11:04 AM	10.00	70.0	F	27.70	9.08	559.09
9	9/13/2014	11:37 AM	88.00	70.0	F	27.73	80.02	639.10
10	9/14/2014	10:39 AM	44.00	66.0	F	27.77	40.37	679.48
11	9/15/2014	10:26 AM	55.00	67.0	F	27.78	50.39	729.86
12	9/16/2014	5:12 PM	94.00	69.0	F	27.64	85.36	815.22
13	9/17/2014	9:51 AM	41.00	67.0	F	27.62	37.34	852.56
14	9/19/2014	12:21 PM	85.00	68.0	F	27.74	77.61	930.17
15	9/23/2014	9:49 AM	10.00	66.0	F	27.87	9.21	939.38

16	9/25/2014	6:13 PM	88.00	70.0	F	27.80	80.22	1,019.60
17	9/30/2014	3:34 PM	139.00	69.0	F	27.53	125.72	1,145.31
18	10/7/2014	2:49 PM	124.00	69.0	F	27.59	112.39	1,257.71
19	10/13/2014	5:48 PM	109.00	70.0	F	27.69	98.97	1,356.68
20	10/22/2014	8:15 AM	74.00	63.0	F	27.63	67.94	1,424.62
21	10/28/2014	8:06 PM	95.00	69.0	F	27.62	86.20	1,510.82
22	11/4/2014	6:53 PM	22.00	65.0	F	27.75	20.21	1,531.03
23	11/11/2014	6:06 PM	150.00	72.0	F	27.50	134.75	1,665.78
24	11/18/2014	6:50 PM	56.00	70.0	F	27.68	50.83	1,716.61
25	11/25/2014	9:50 AM	79.00	71.0	F	27.65	71.49	1,788.10
26	12/1/2014	4:40 PM	48.00	71.0	F	27.82	43.70	1,831.81
27	12/10/2014	8:59 AM	51.00	70.0	F	27.58	46.12	1,877.93
28	12/15/2014	11:06 AM	27.00	69.0	F	27.61	24.49	1,902.42
Residual A	**12/15/2014**	**3:45 PM**	**459.00**	**69.0**	**F**	**27.61**	**416.34**	**2,318.76**
Residual B	**12/15/2014**	**4:17 PM**	**740.00**	**69.0**	**F**	**27.61**	**671.22**	**2,989.98**

Table FF: Gas Desorption Computation 1728.15

Coal Sample Gas Desorption Computation

Bureau of Mines Direct Method Test

General Data

Company:	VCER	*Hole No.:*	CH-1R-2014 (C-1)
Contact Person:	(Wedged)	*Coalbed:*	Pocahontas 3 (10-20 Bench)
Hole Location:		*Sample ID #:*	G-23*
		MM&A Project #:	VCER101
Quadrangle:		***Coordinates***	
Core Collected by:	T Keim	*East:*	
Type of Drilling:		*North:*	
Drilling Contractor:		*Surface Elevation:*	
Sidewall Coring Contractor:		*Drilling Media:*	Water

Core Data

As-Rec'd, Whole Sample Wt. (g):	1647.10	*Core Length:*	2.53'
As-Rec'd, Crushed Sample Wt. (g):	1168.80	*Core Diameter:*	
DMMF, Whole Sample Wt. (g):	1489.55	*Depth of Cored Interval:*	1728.15'
DMMF, Crushed Sample Wt. (g):	1057.00		1730.68'

Time Data

	Day/Hr./ Min.		Day/Hr./Min.
Coalbed Encountered (A):	9/9/14 4:10 PM	*Core Reached Surface (C):*	9/9/14 5:10 PM
Hole Filled with Water (E):	NA	*Core Sealed in Canister (D):*	9/9/14 5:25 PM
Core Started Out of Hole (B):	9/9/14 4:56 PM		9/9/2014
			17.41666667

Gas Volume Data

	Drilled with Air	***Drilled with Water***
Lost Gas Volume	Not Performed	55.45 cc

Desorbed Gas Volume from Canister @ STP:	3771.39 cc
Residual Gas Volume from Crushed Core @ STP:	1229.07 cc

Gas Content

Gas Content @ STP =(Lost Gas + Desorbed Gas Volumes)/Whole Sample Weight

Air, As-Received	***Air, DMMF***	***Water, As-Received***	***Water, DMMF***
Not Performed	Not Performed	2.32 cc/g	2.57 cc/g
Not Performed	Not Performed	74.43 ft³/ton	82.31 ft³/ton

Residual Gas Content @ STP =Residual Gas Volume/Crushed Sample Weight

As-Received	***DMMF***
1.05 cc/g	1.16 cc/g

	33.69 ft³/ton		37.25 ft³/ton	
Total Gas Content @ STP	=Gas Content + Residual Gas Content			
Air, As-Received	***Air, DMMF***		***Water, As-Received***	***Water, DMMF***
Not Performed	Not Performed		3.37 cc/g	3.73 cc/g
Not Performed	Not Performed		108.12 ft³/ton	119.56 ft³/ton

Table GG: Gas Desorption Time Sheet 1728.15

Coal Sample Gas Desorption Computation

Coal Desorption Data

Drill Hole: C-1 Canister #: G-23

Number of Readings	Date	Time (Hrs./Min)	Desorbed Gas	Temp	F/C	Pressure (In.)	Inc. Adj. Volume	Cum. Adj. Volume
1	9/9/2014	5:35 PM	46.00	72.0	F	28.35	42.60	98.05
2	9/9/2014	5:45 PM	36.00	72.0	F	28.35	33.34	131.39
3	9/9/2014	5:55 PM	32.00	72.0	F	28.35	29.64	161.02
4	9/9/2014	7:48 PM	170.00	74.0	F	27.70	153.25	314.28
5	9/10/2014	9:27 AM	304.00	69.0	F	27.70	276.64	590.92
6	9/11/2014	10:28 AM	313.00	69.0	F	27.63	284.12	875.04
7	9/12/2014	11:05 AM	213.00	70.0	F	27.70	193.47	1,068.50
8	9/13/2014	11:40 AM	156.00	70.0	F	27.73	141.85	1,210.35
9	9/14/2014	10:41 AM	93.00	66.0	F	27.77	85.33	1,295.68
10	9/15/2014	10:28 AM	95.00	67.0	F	27.78	87.03	1,382.71
11	9/16/2014	5:14 PM	149.00	69.0	F	27.64	135.30	1,518.01
12	9/17/2014	9:52 AM	53.00	67.0	F	27.62	48.27	1,566.28
13	9/19/2014	12:22 PM	148.00	68.0	F	27.74	135.13	1,701.42
14	9/23/2014	9:50 AM	205.00	66.0	F	27.87	188.77	1,890.19
15	9/25/2014	6:15 PM	178.00	70.0	F	27.80	162.26	2,052.45
16	9/30/2014	3:35 PM	226.00	69.0	F	27.53	204.40	2,256.85

17	10/7/2014	2:50 PM	215.00	69.0	F	27.59	194.88	2,451.73
18	10/13/2014	5:49 PM	198.00	70.0	F	27.69	179.78	2,631.50
19	10/22/2014	8:16 AM	172.00	63.0	F	27.63	157.92	2,789.42
20	10/28/2014	8:07 PM	187.00	69.0	F	27.62	169.68	2,959.11
21	11/4/2014	6:54 PM	98.00	65.0	F	27.75	90.02	3,049.13
22	11/11/2014	6:07 PM	257.00	72.0	F	27.50	230.87	3,280.00
23	11/18/2014	6:52 PM	147.00	70.0	F	27.68	133.42	3,413.43
24	11/25/2014	9:52 AM	139.00	71.0	F	27.65	125.79	3,539.22
25	12/1/2014	4:41 PM	120.00	71.0	F	27.82	109.26	3,648.48
26	12/10/2014	9:00 AM	123.00	70.0	F	27.58	111.24	3,759.71
27	12/15/2014	11:26 AM	74.00	69.0	F	27.61	67.12	3,826.84
Residual	**12/15/2014**	**4:52 PM**	**1355.00**	**69.0**	**F**	**27.61**	**1,229.07**	**5,055.90**

E. ECHOMETER LIQUID LEVEL DETECTION

The following figures are used to calculate the liquid level of shale natural gas well during a 'huff-and-puff' test. The data is given in both highpass and lowpass to allow for interruption.

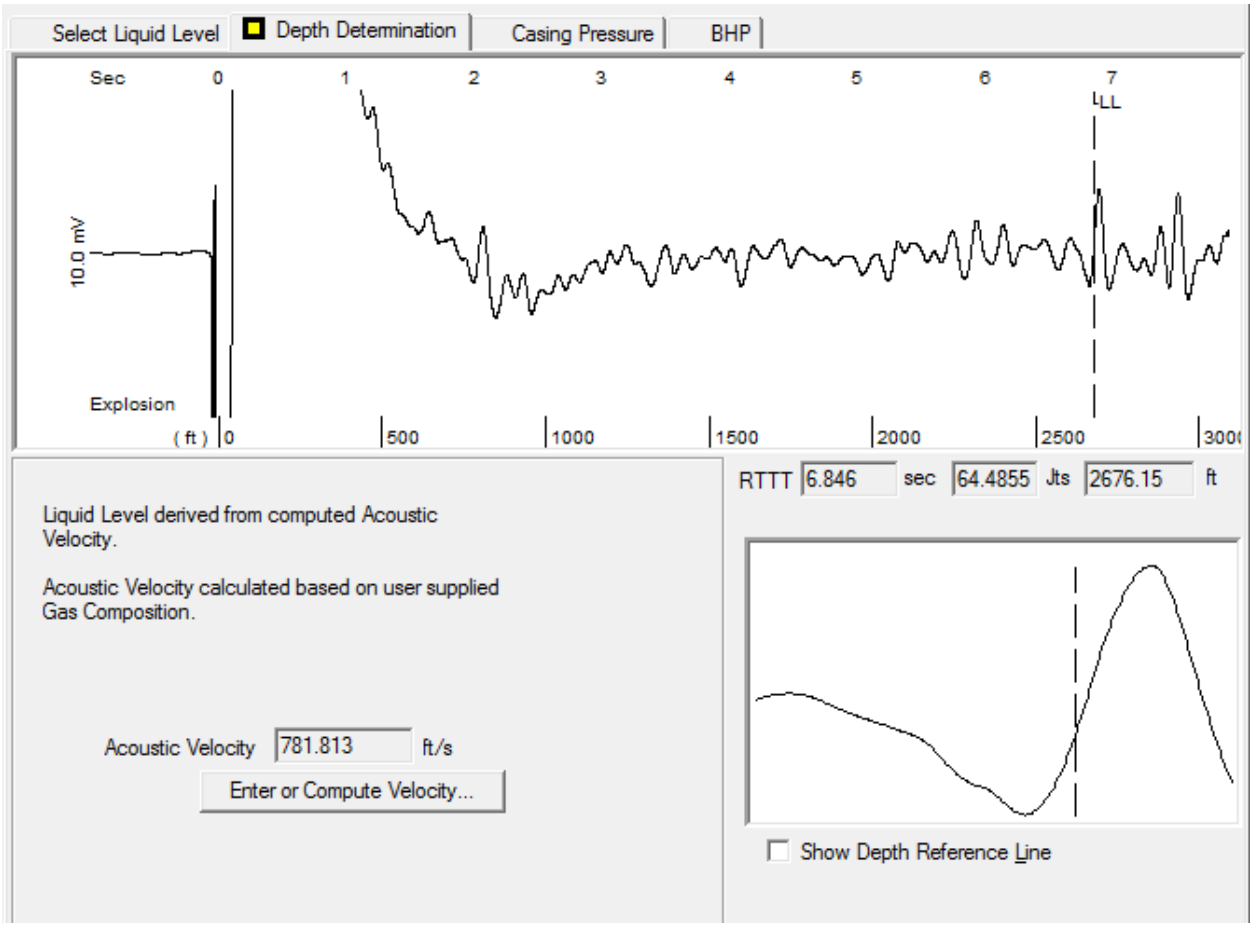

Figure 54: 4/28/2014 12:03:15 HW 1003 Acoustic Test

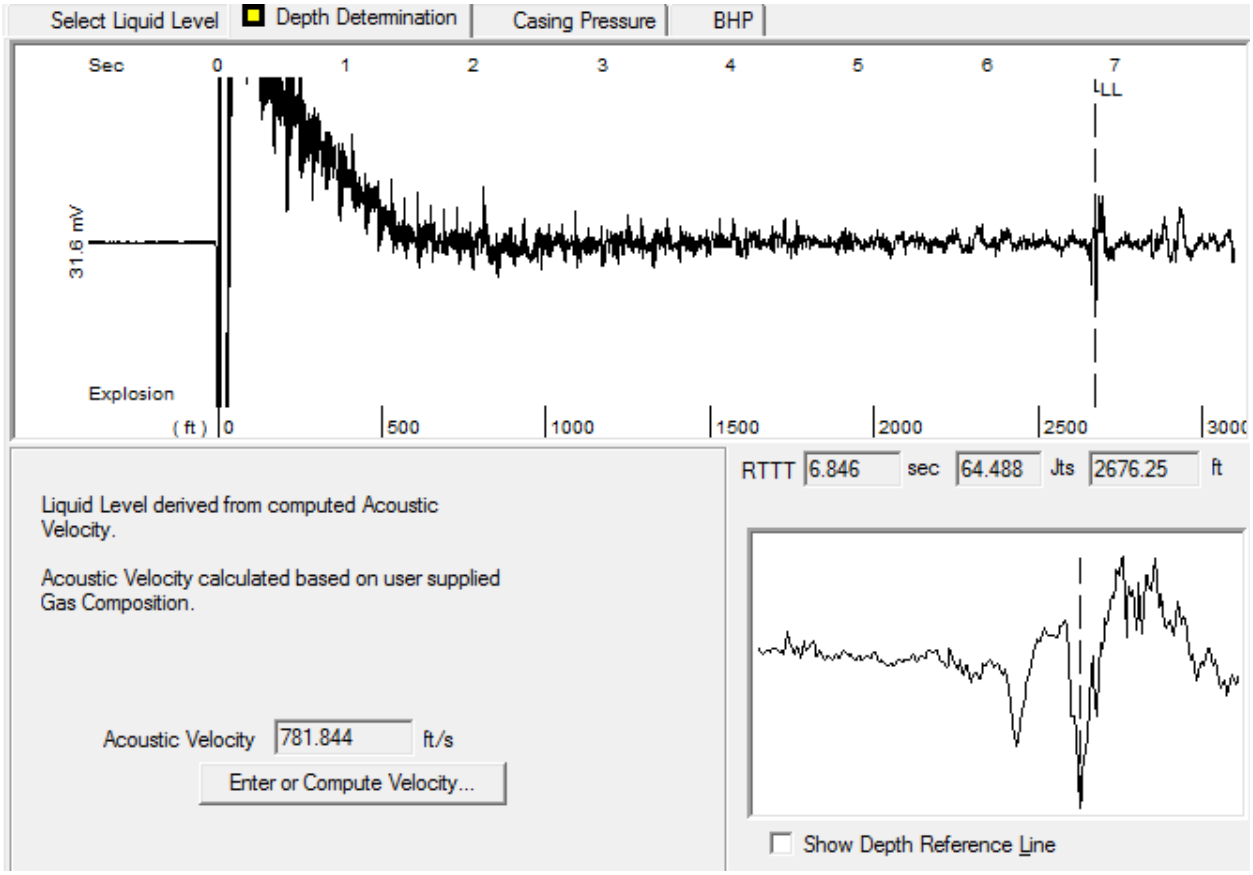

Figure 55: 4/28/2014 12:06:34 HW 1003 Acoustic Test

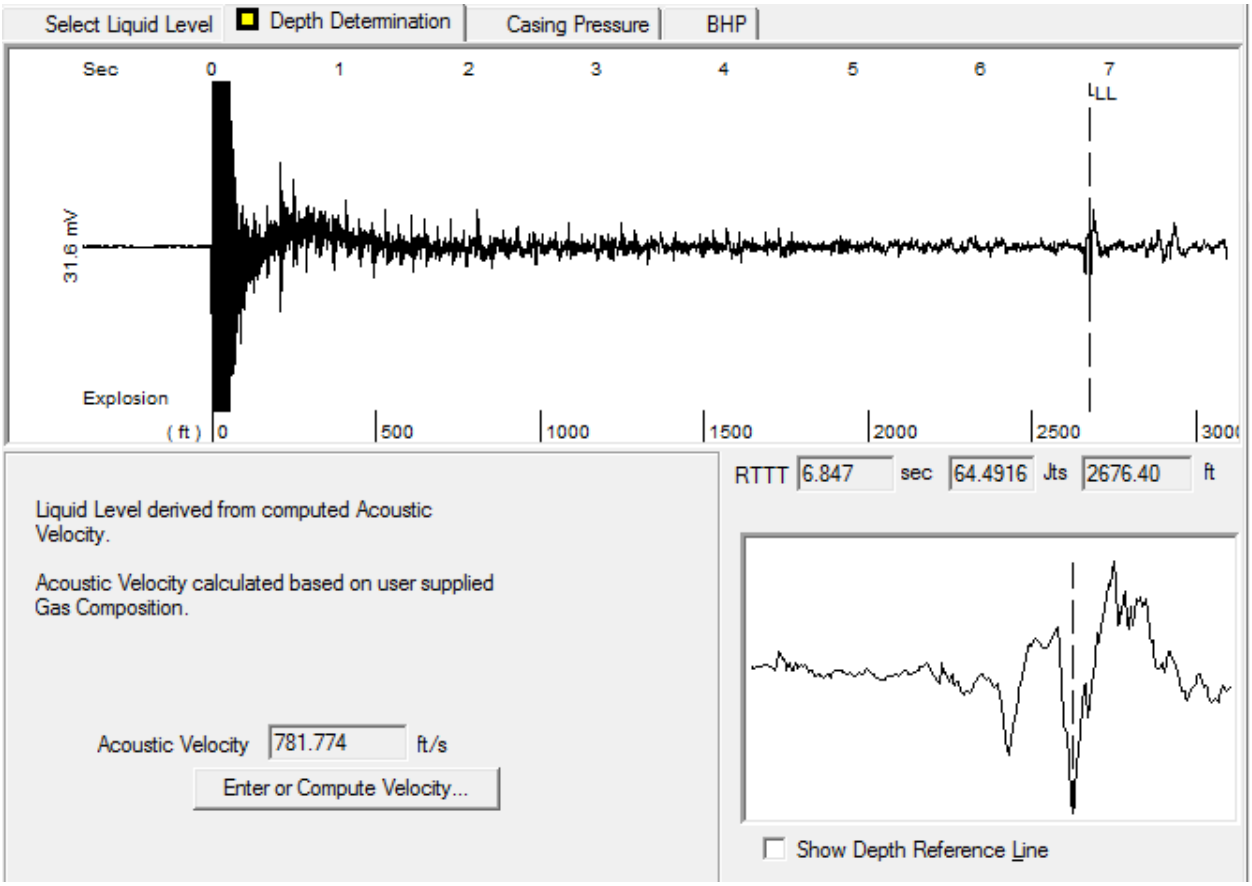

Figure 56: 4/28/2014 12:13:09 HW 1003 Acoustic Test

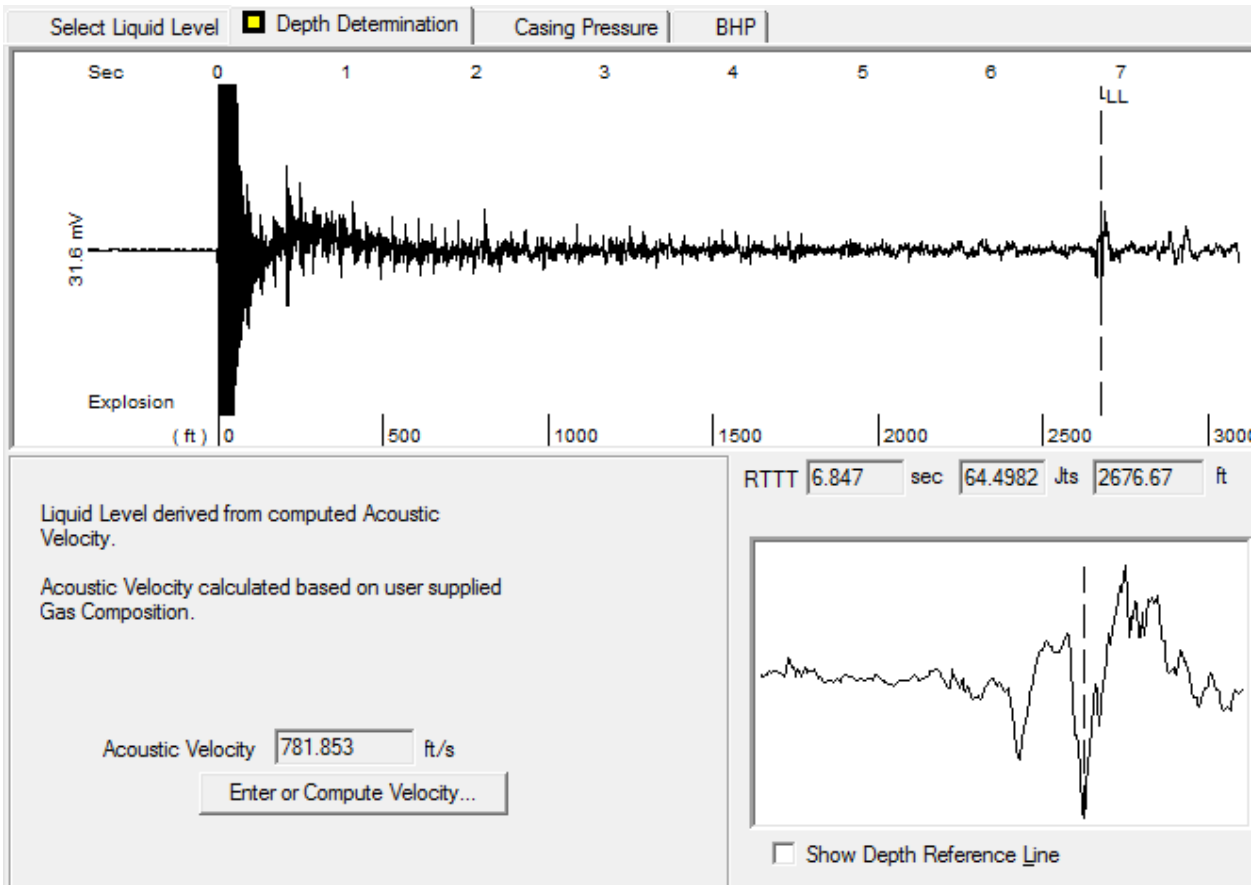

Figure 57: 4/28/2014 12:33:09 HW 1003 Acoustic Test

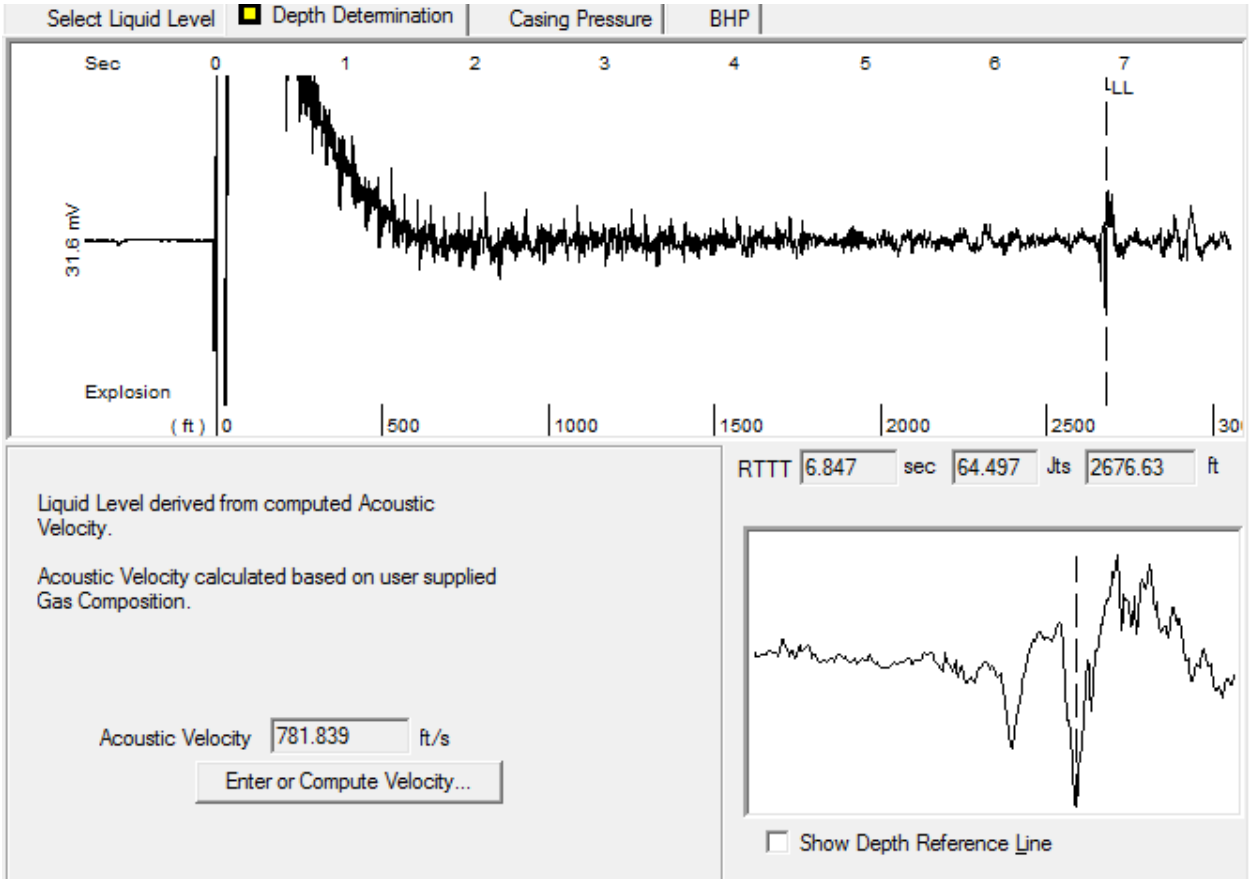

Figure 58: 4/28/2014 12:05:07 HW 1003 Acoustic Test

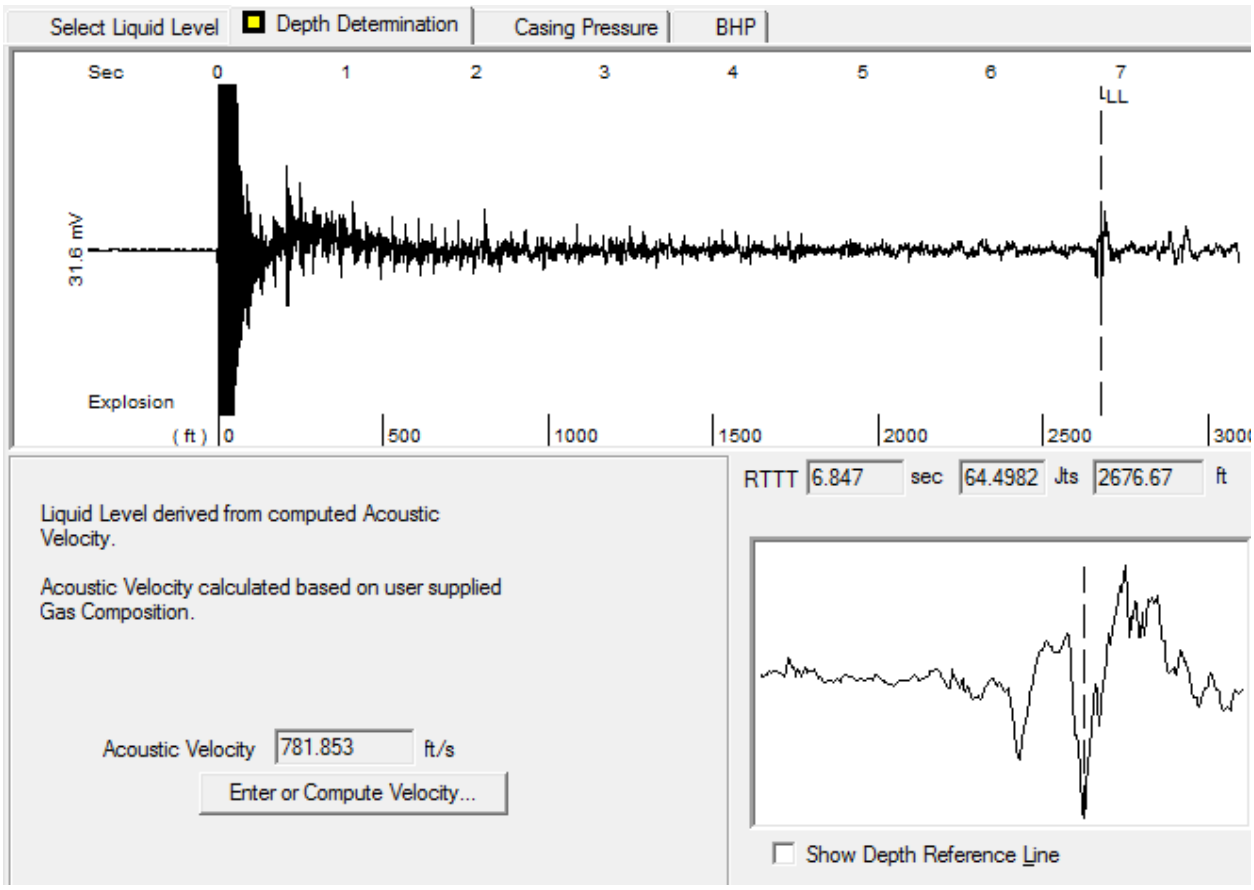

Figure 59: 4/28/2014 12:15:50 HW 1003 Acoustic Test

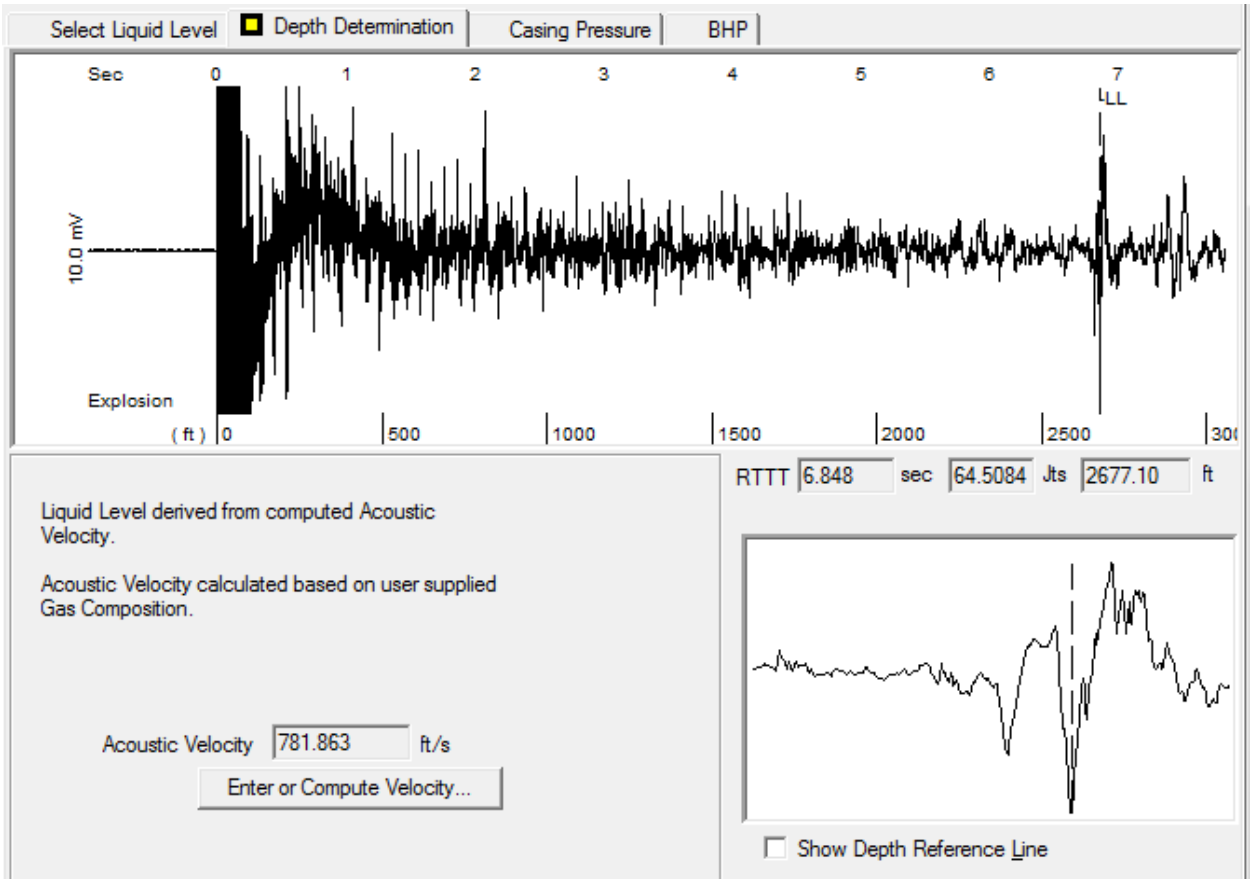

Figure 60 4/28/2014 12:19:53 HW 1003 Acoustic Test

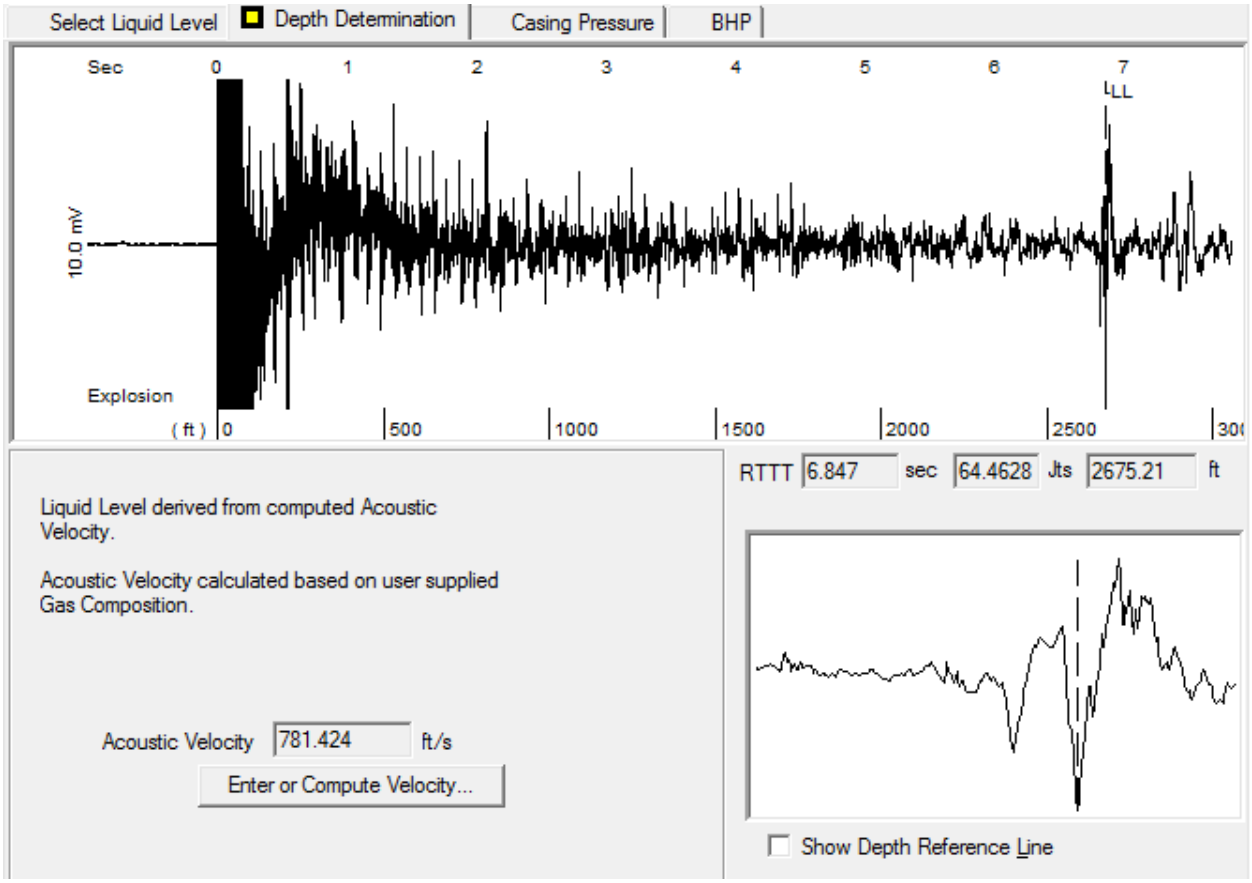

Figure 61: 4/28/2014 12:22:12 HW 1003 Acoustic Test

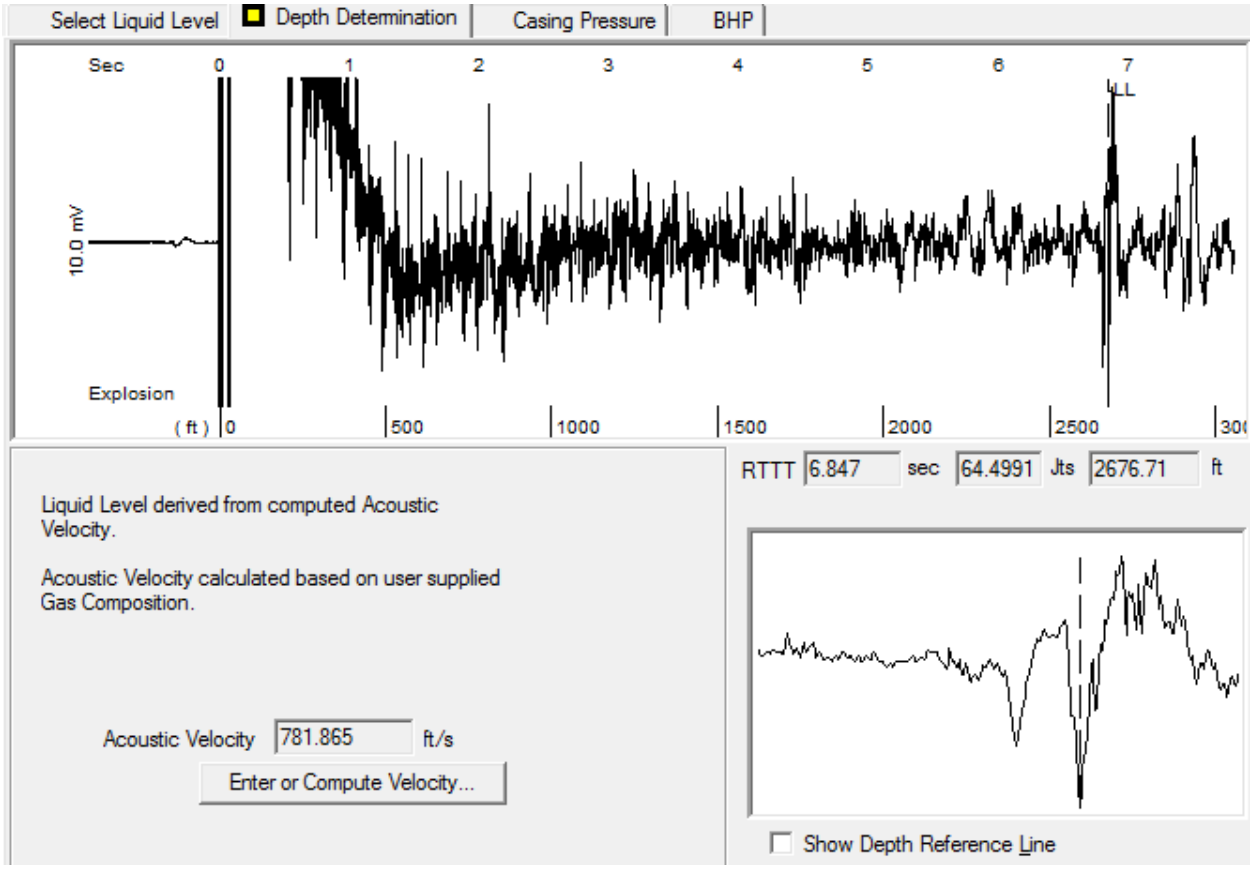

Figure 62: 4/28/14 12:26:03 HW 1003 Acoustic Test

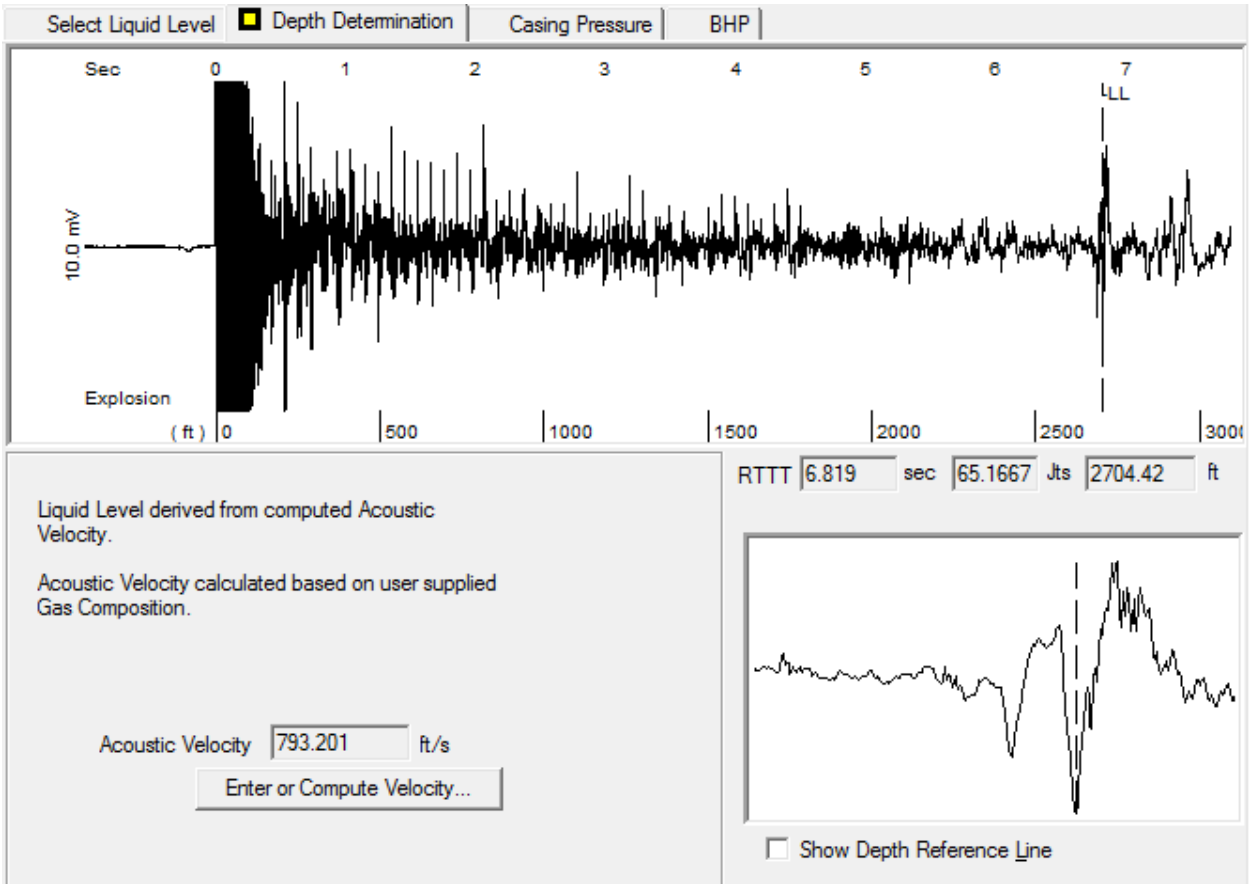

Figure 63: 5/19/2014 11:38:11 HW 1003 Acoustic Test

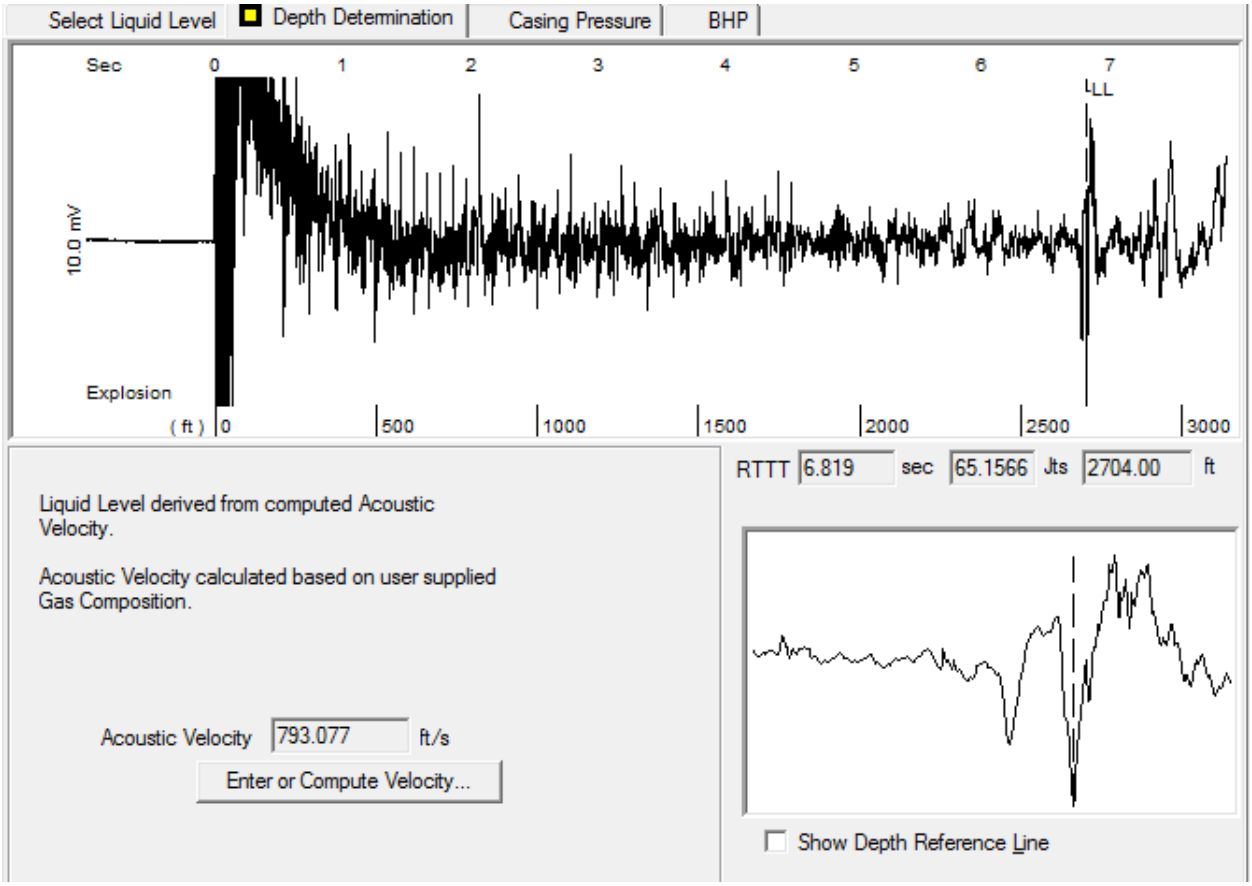

Figure 64: 5/19/2014 11:40:47 HW 1003 Acoustic Test

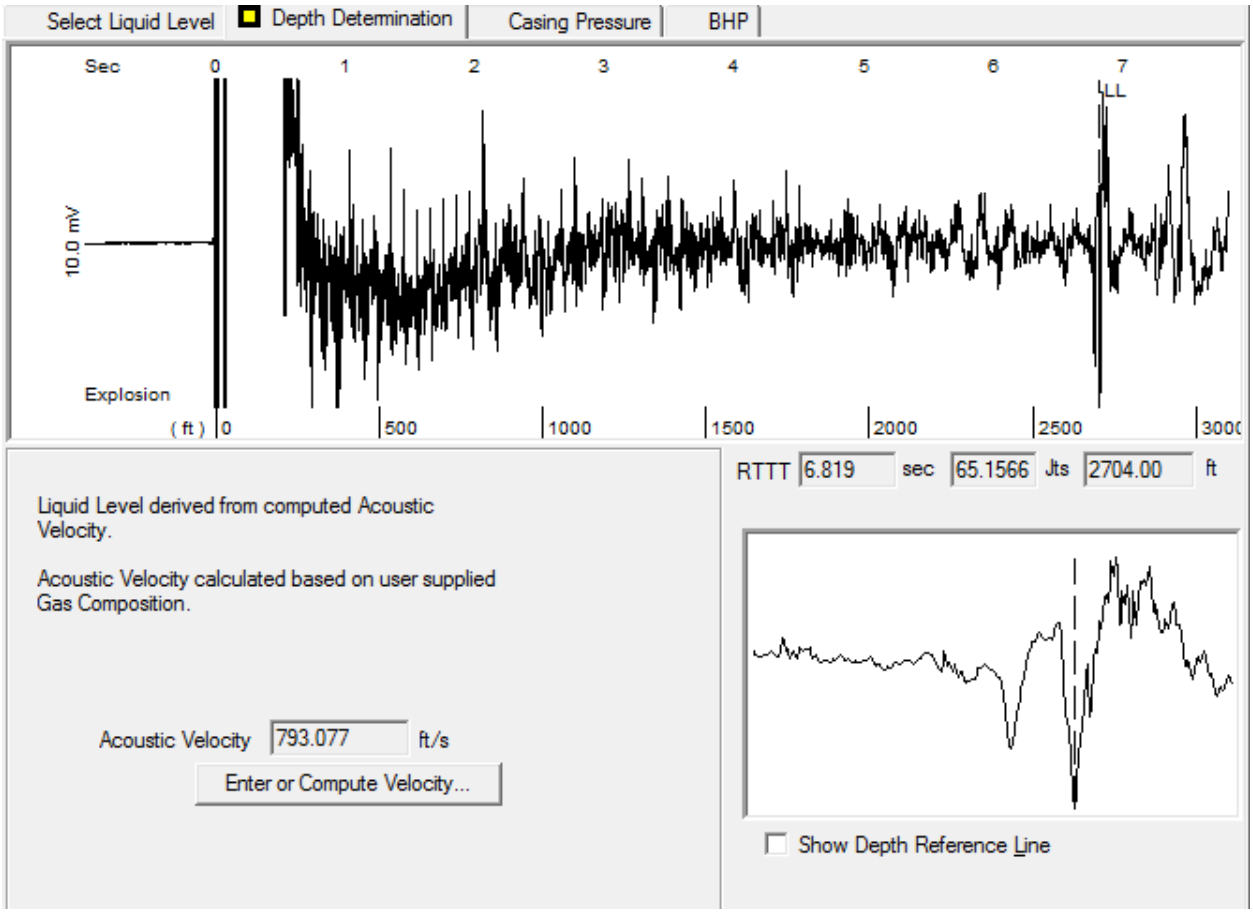

Figure 65: 5/19/2014 11:41:57 HW 1003 Acoustic Test

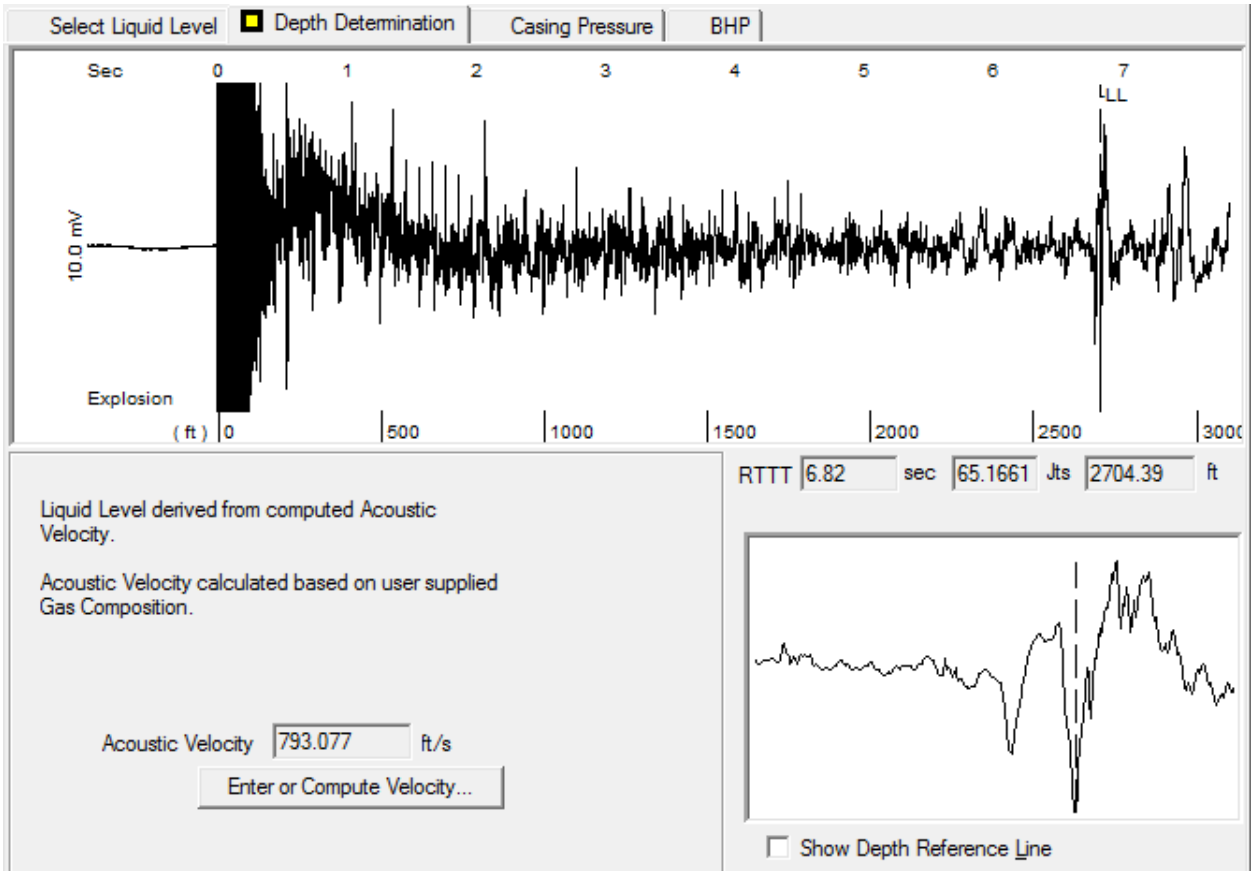

Figure 66: 5/19/2014 11:43:01 HW 1003 Acoustic Test

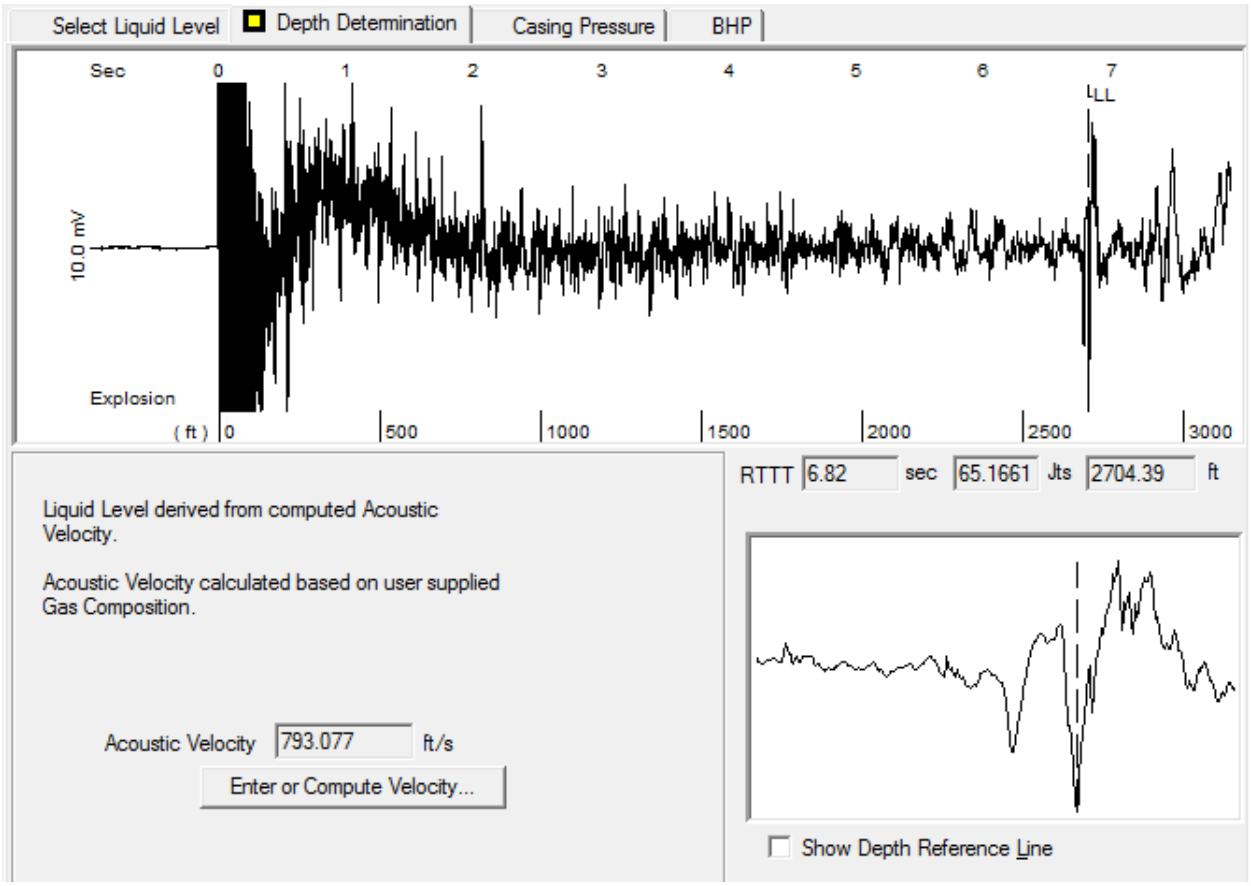

Figure 67: 5/19/2014 11:44:05 HW 1003 Acoustic Test

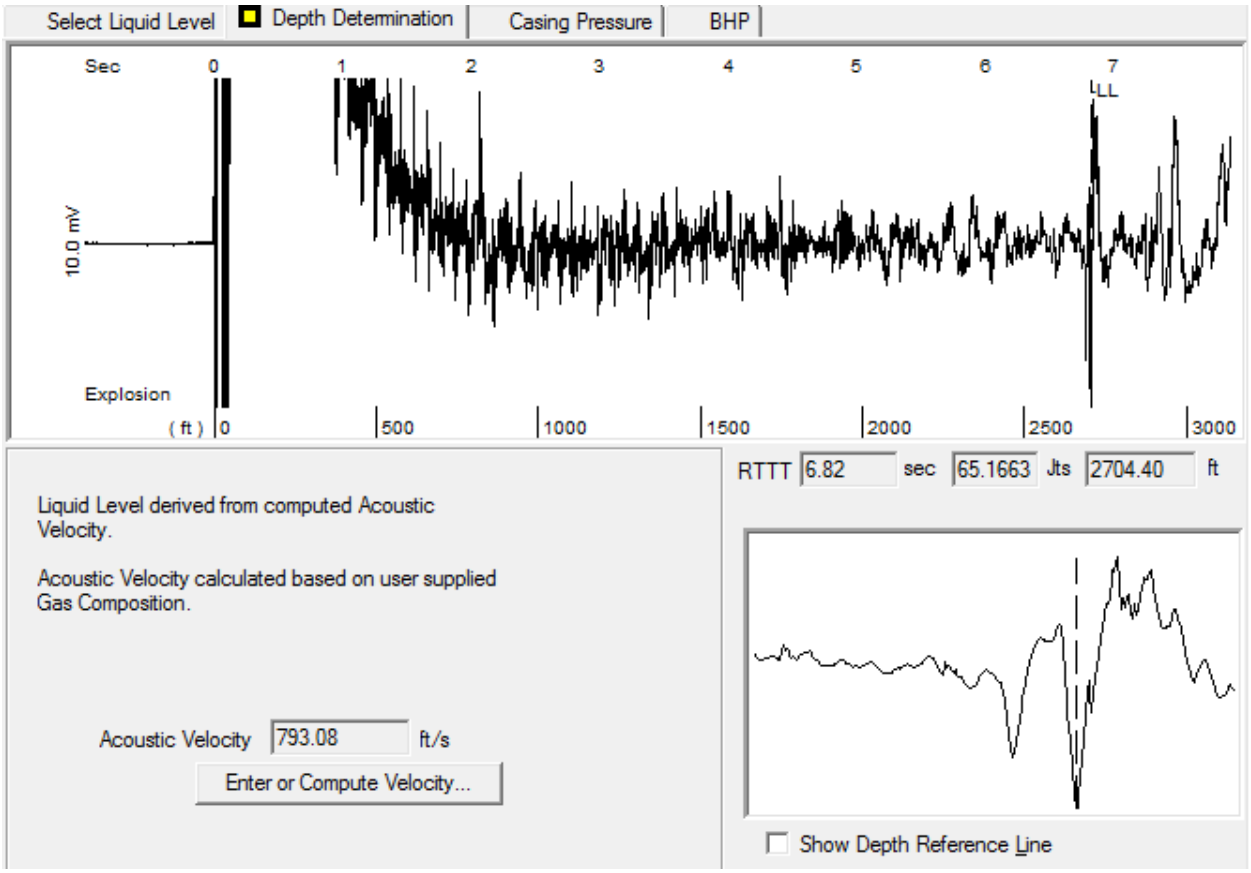

Figure 68: 5/19/2014 11:46:07 HW 1003 Acoustic Test

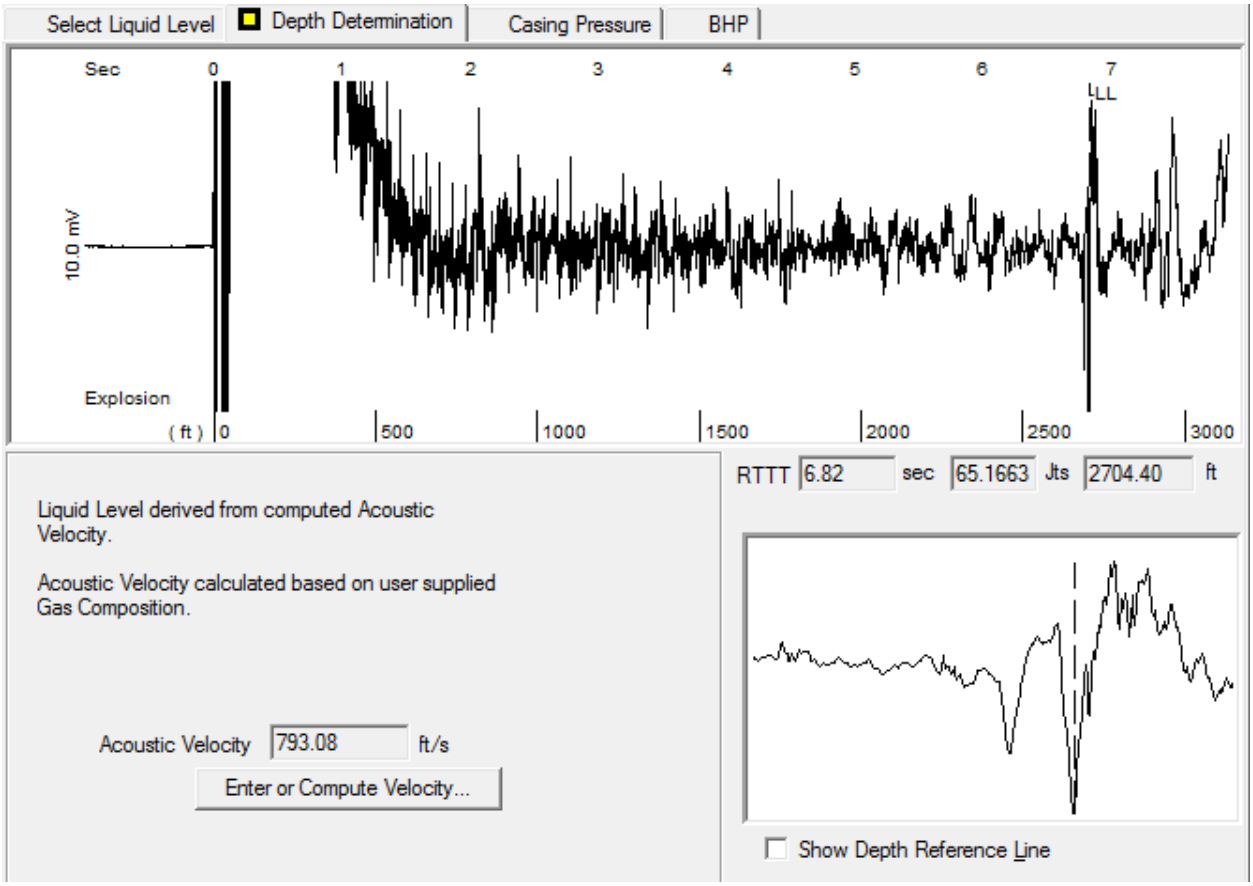

Figure 69: 5/19/14 11:48:41 HW 1003 Acoustic Test

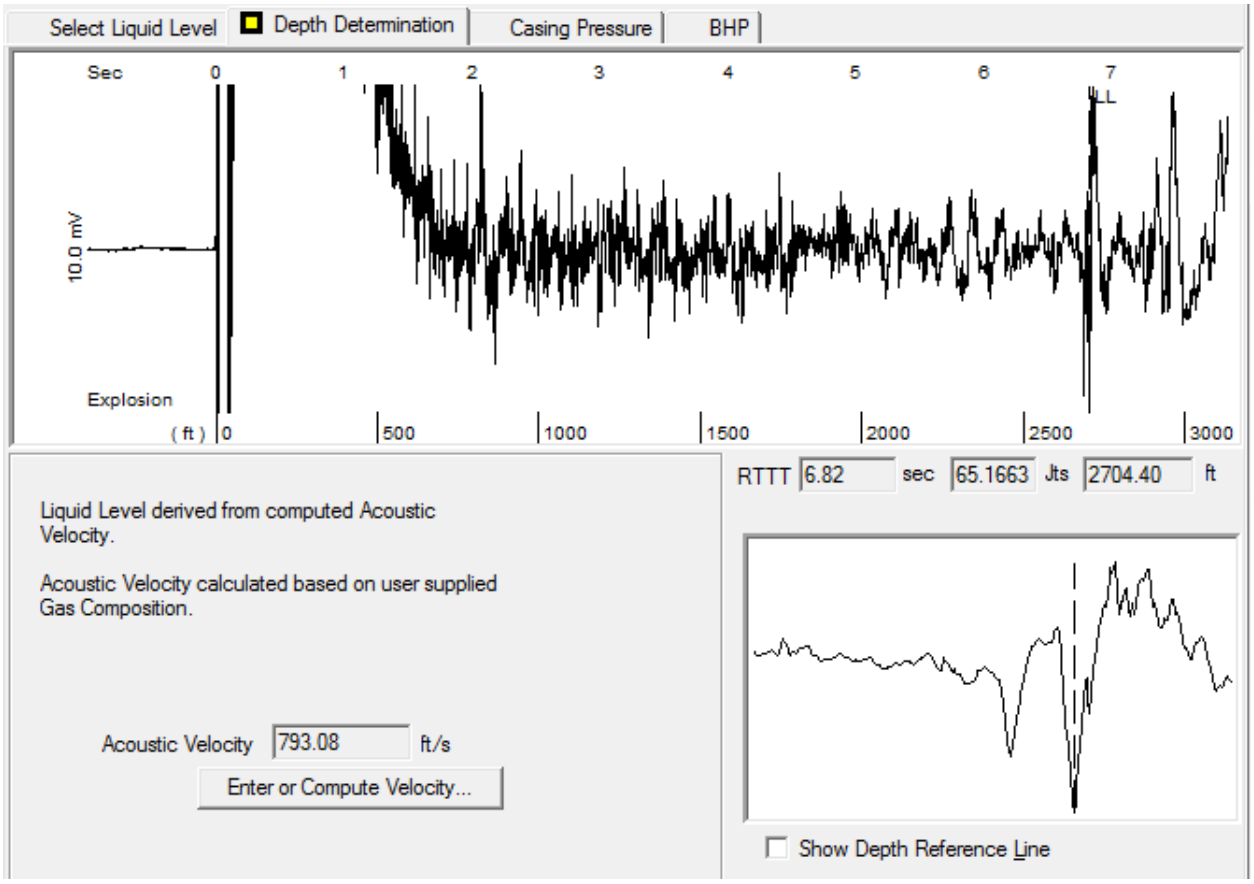

Figure 70: 5/19/2014 11:50:01 HW 1003 Acoustic Test

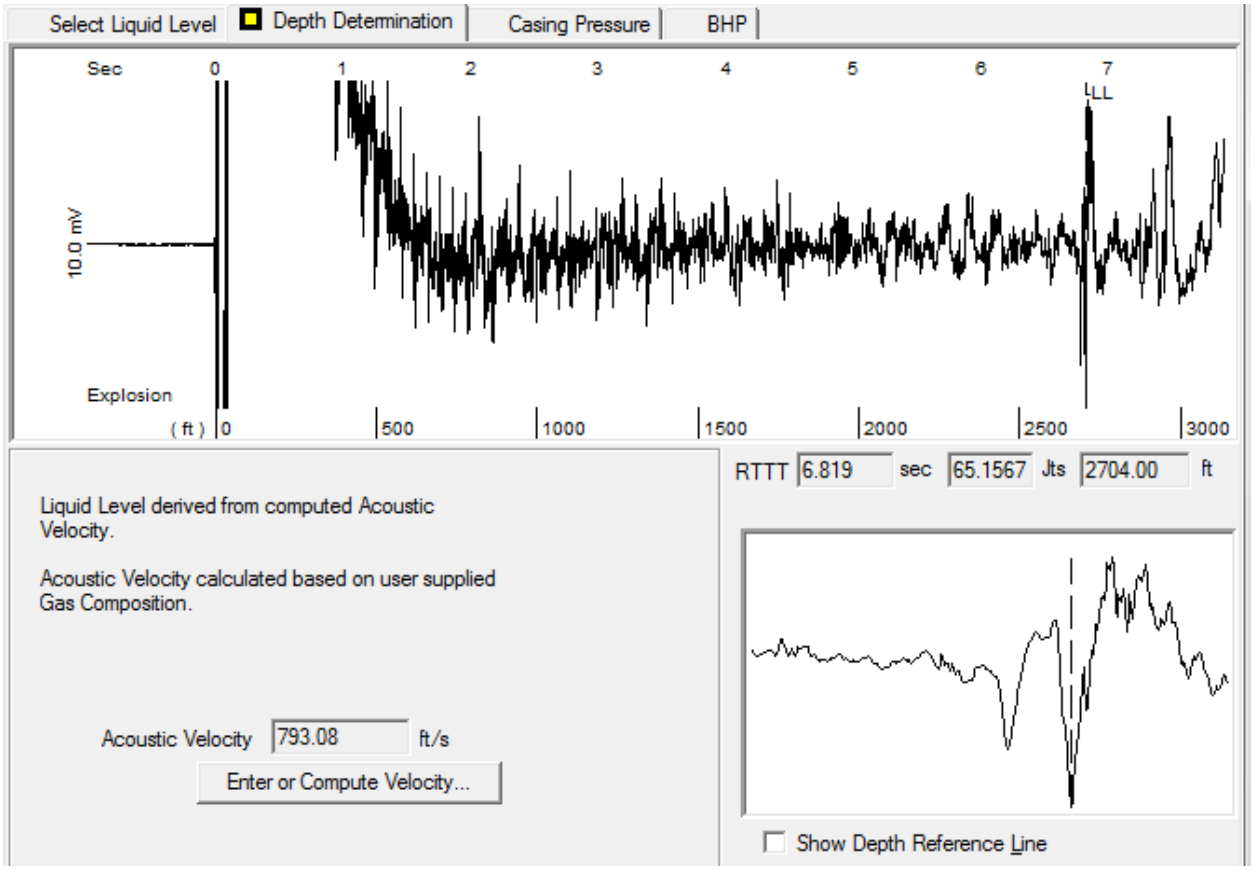

Figure 71: 5/19/2014 11:51:29 HW 1003 Acoustic Test

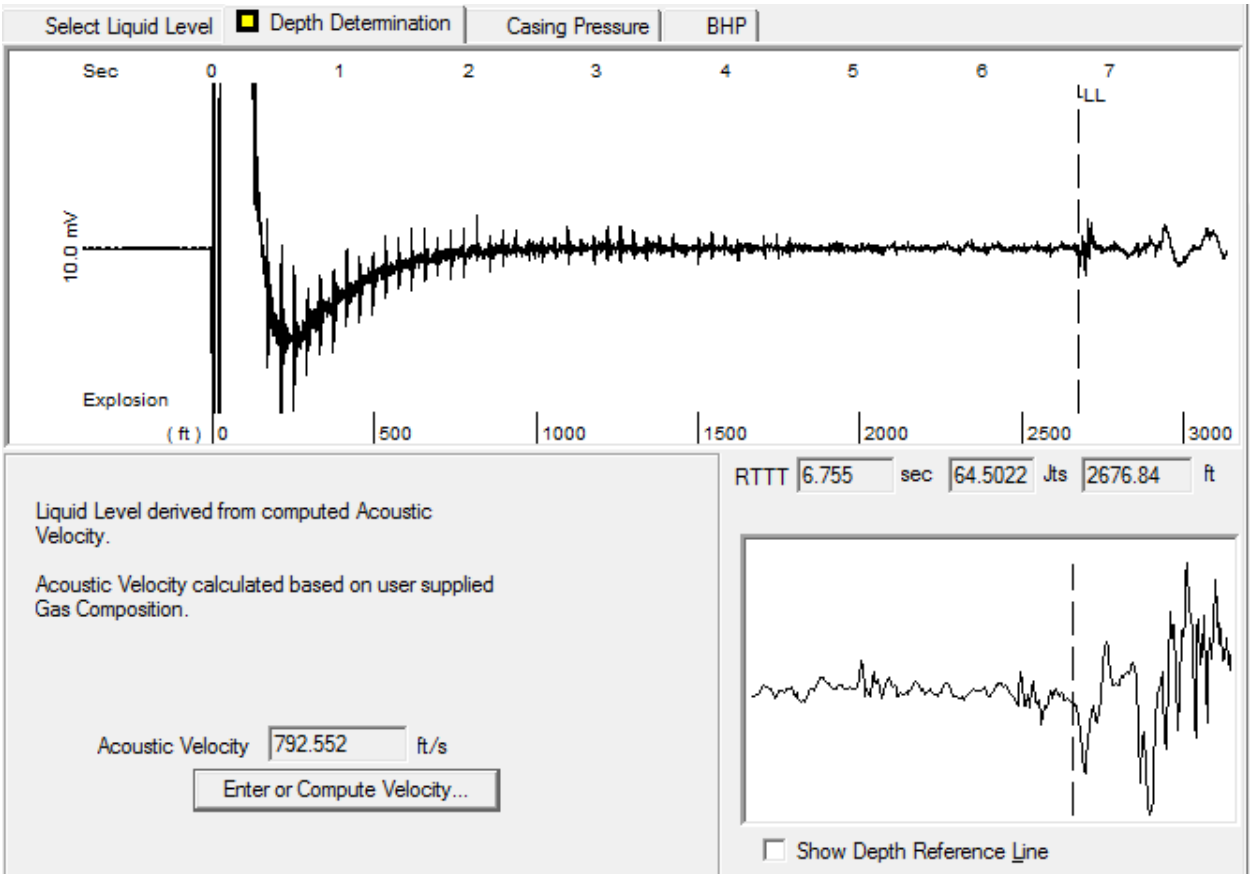

Figure 72: 6/17/2014 12:46:40 HW 1003 Acoustic Test

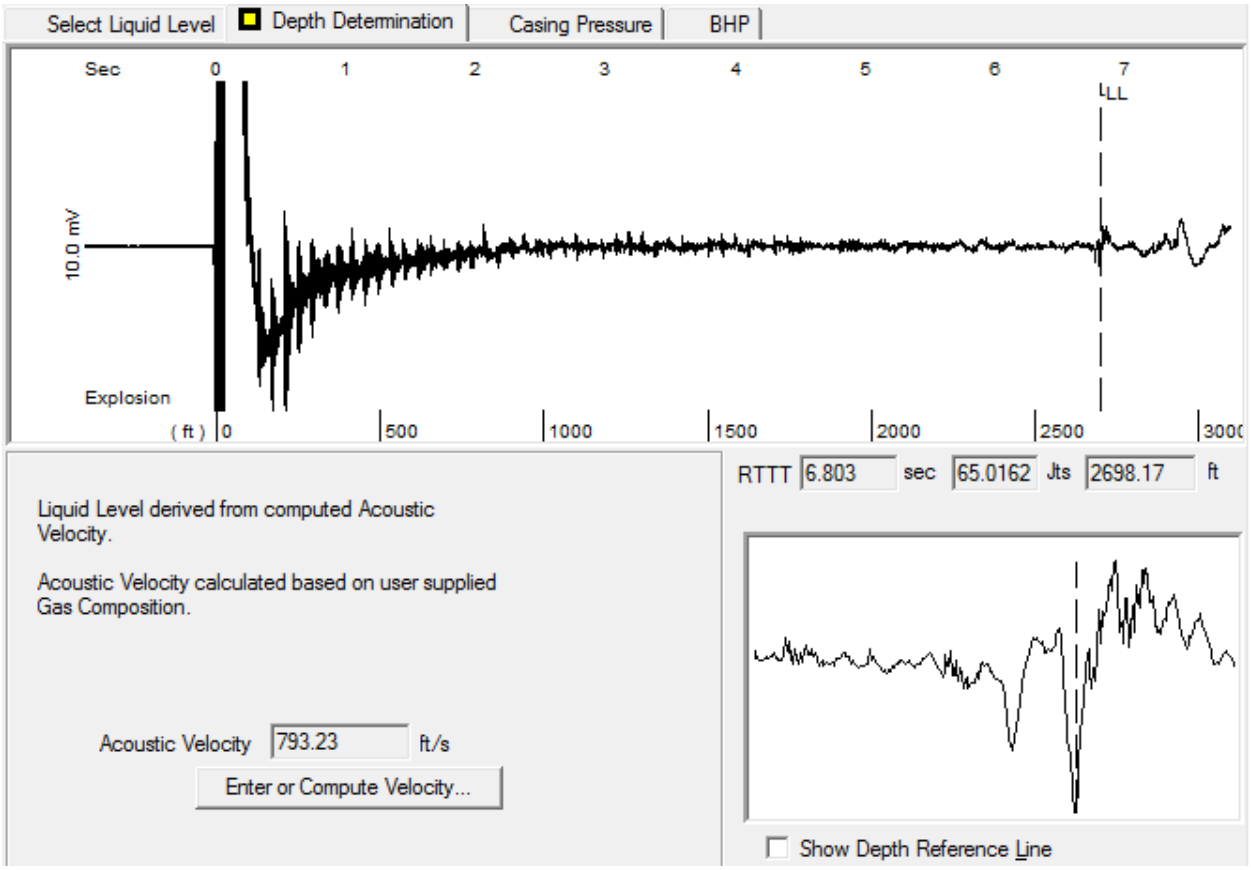

Figure 73: 6/17/2014 12:47:44 HW 1003 Acoustic Test

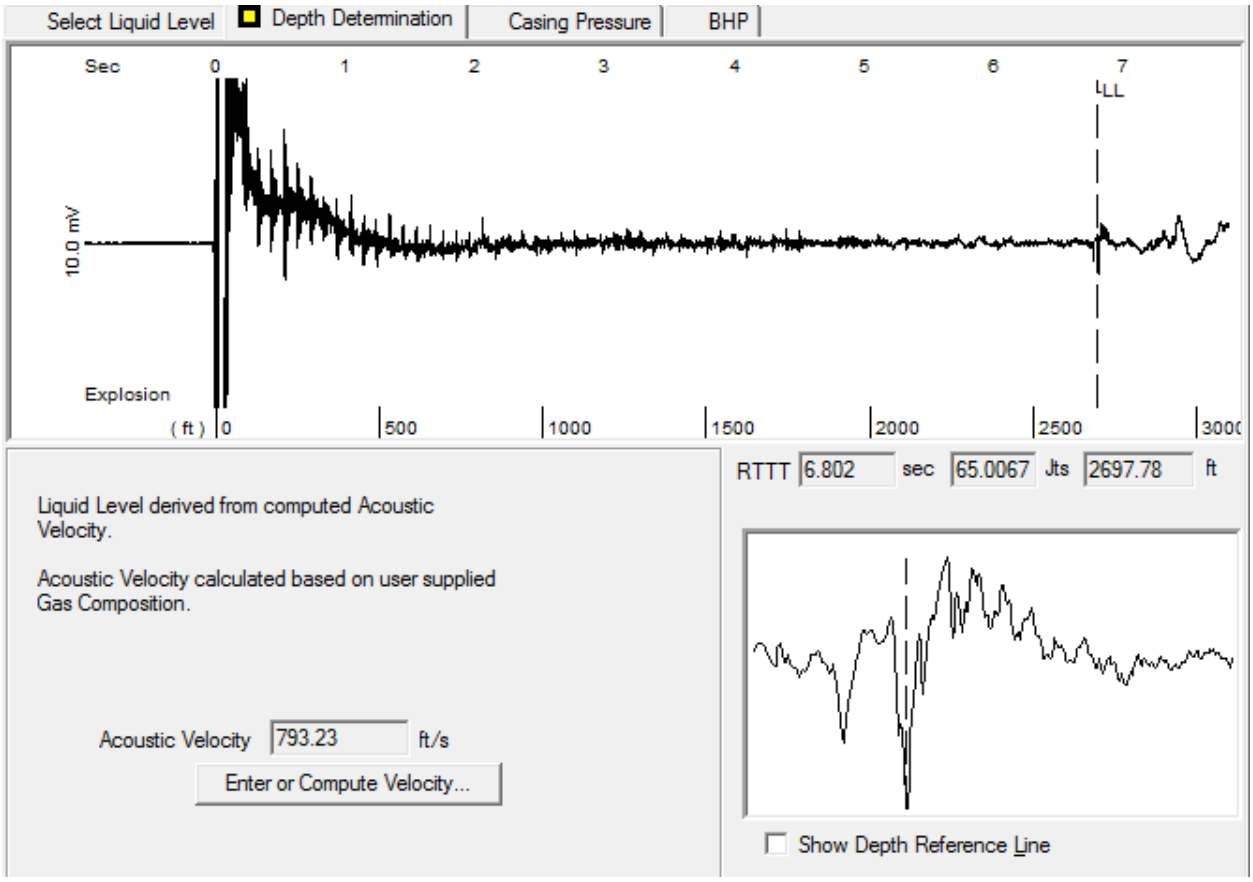

Figure 74: 6/17/14 12:48:42 HW 1003 Acoustic Test

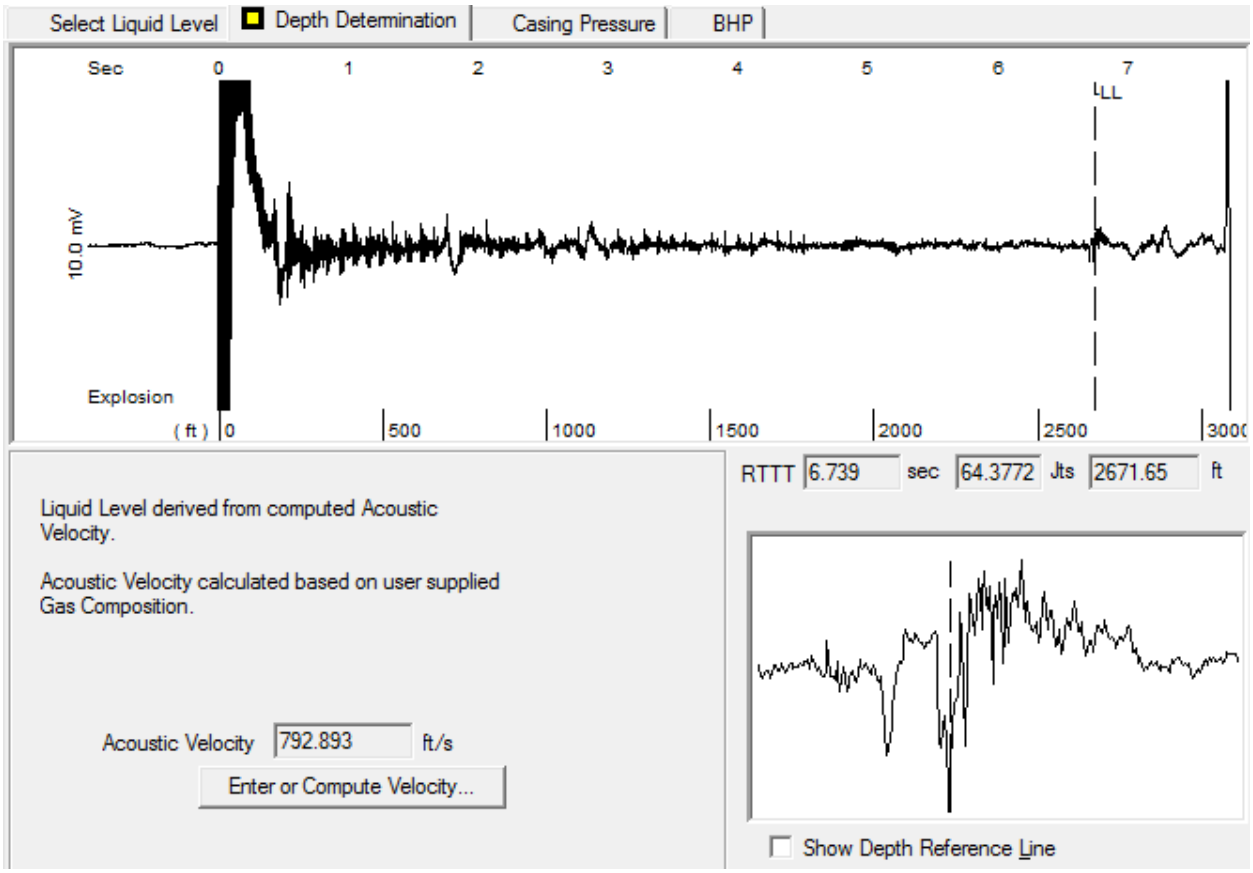

Figure 75: 7/28/14 11:57:13 HW 1003 Acoustic Test

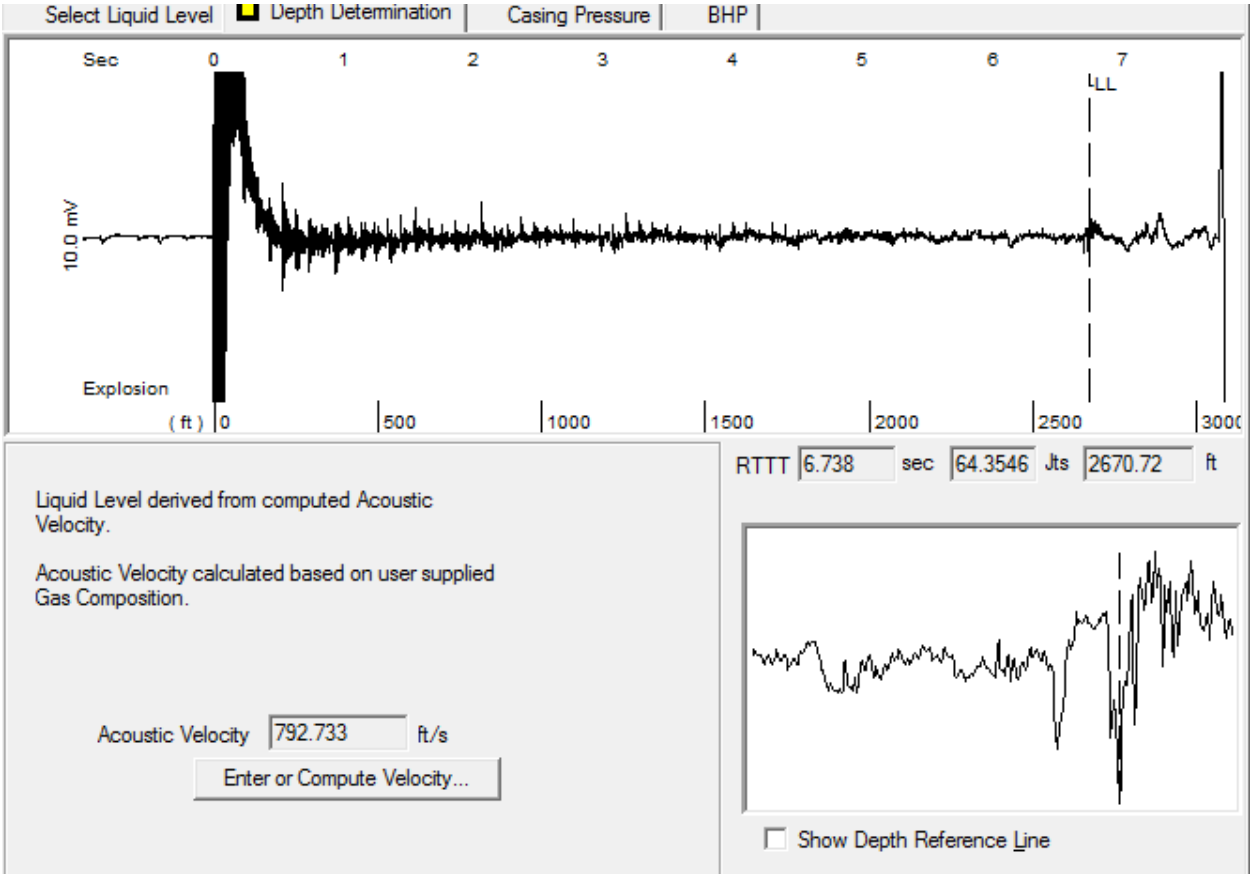

Figure 76: 7/28/2014 11:49:16 HW 1003 Acoustic Test

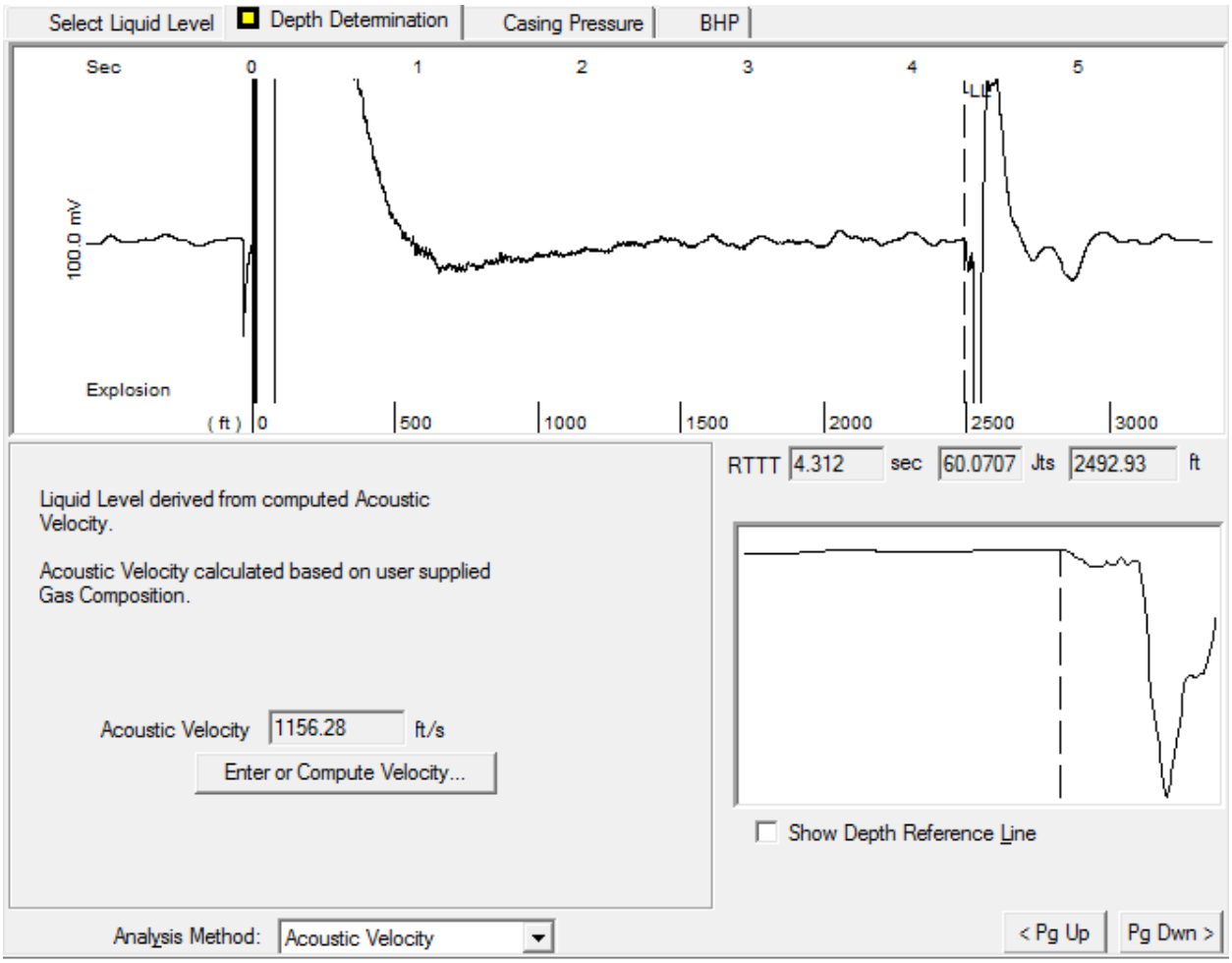

Figure 77: 12/3/14 HW 1003 Acoustic Test 1

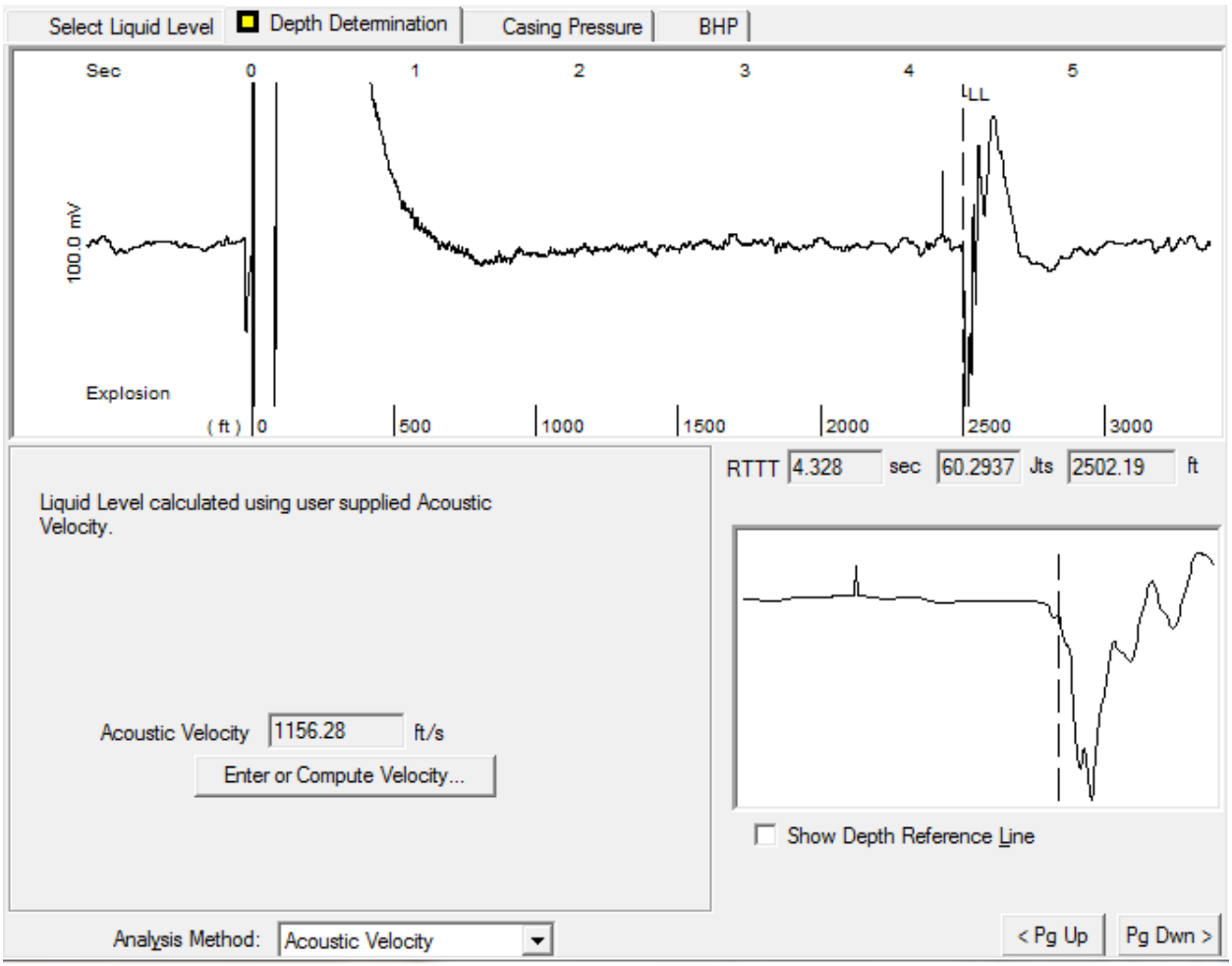

Figure 78: 12/3/14 HW 1003 Acoustic Test 2

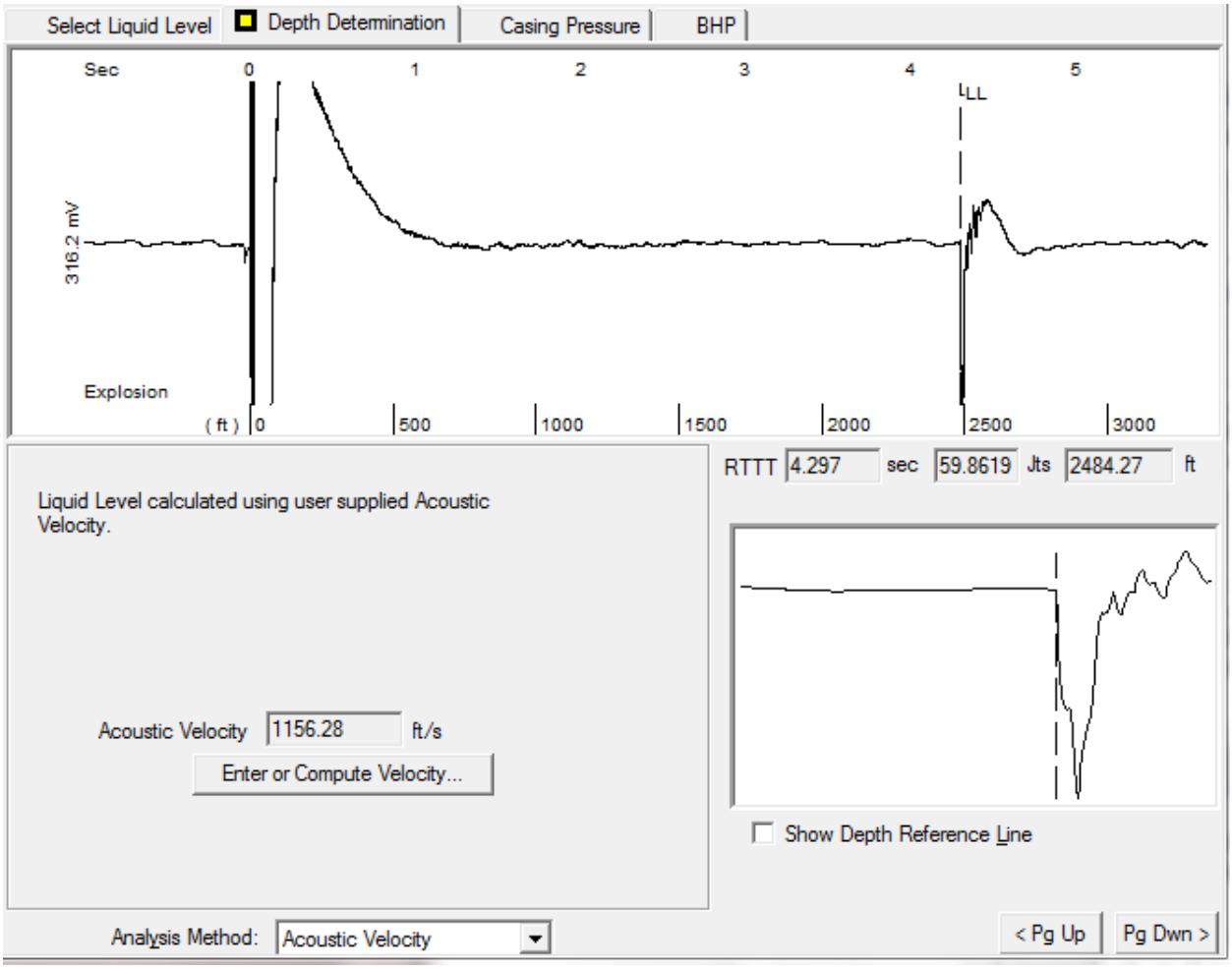

Figure 79: 12/3/14 HW 1003 Acoustic Test 2

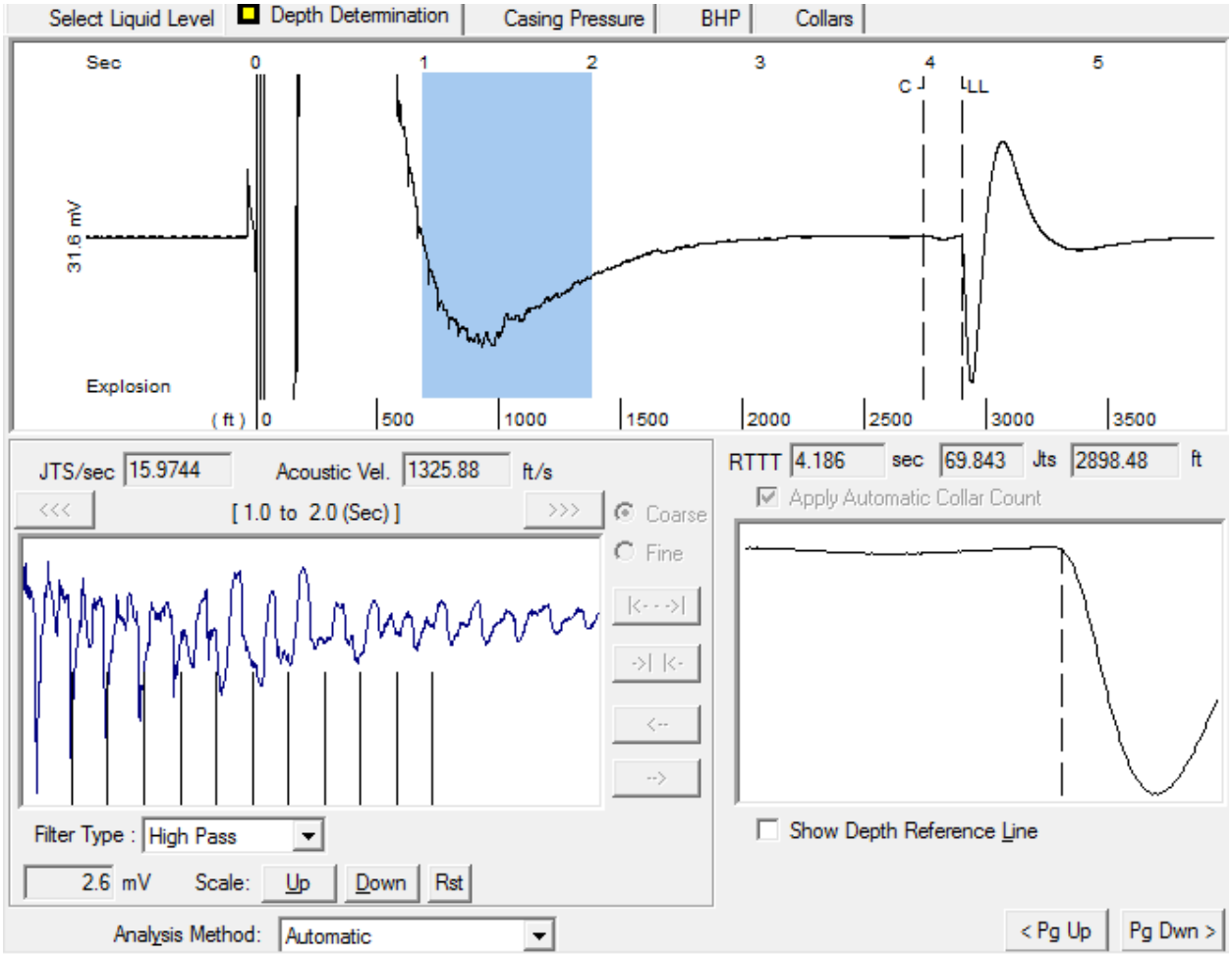

Figure 80: 12/05/2014 HW 1003 Acoustic Test Collars

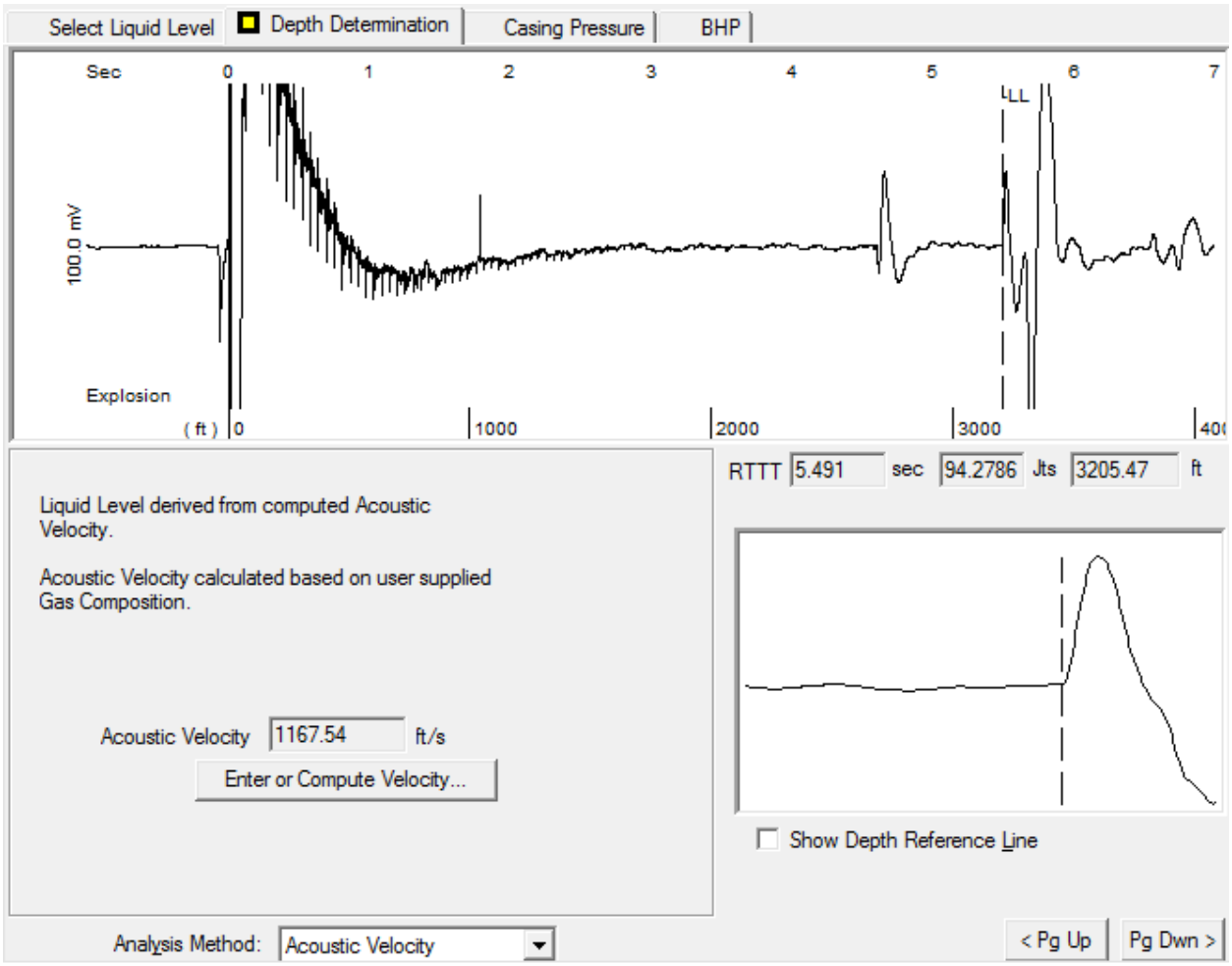

Figure 81: 01/15/2015 HW 1003 Acoustic Velocity

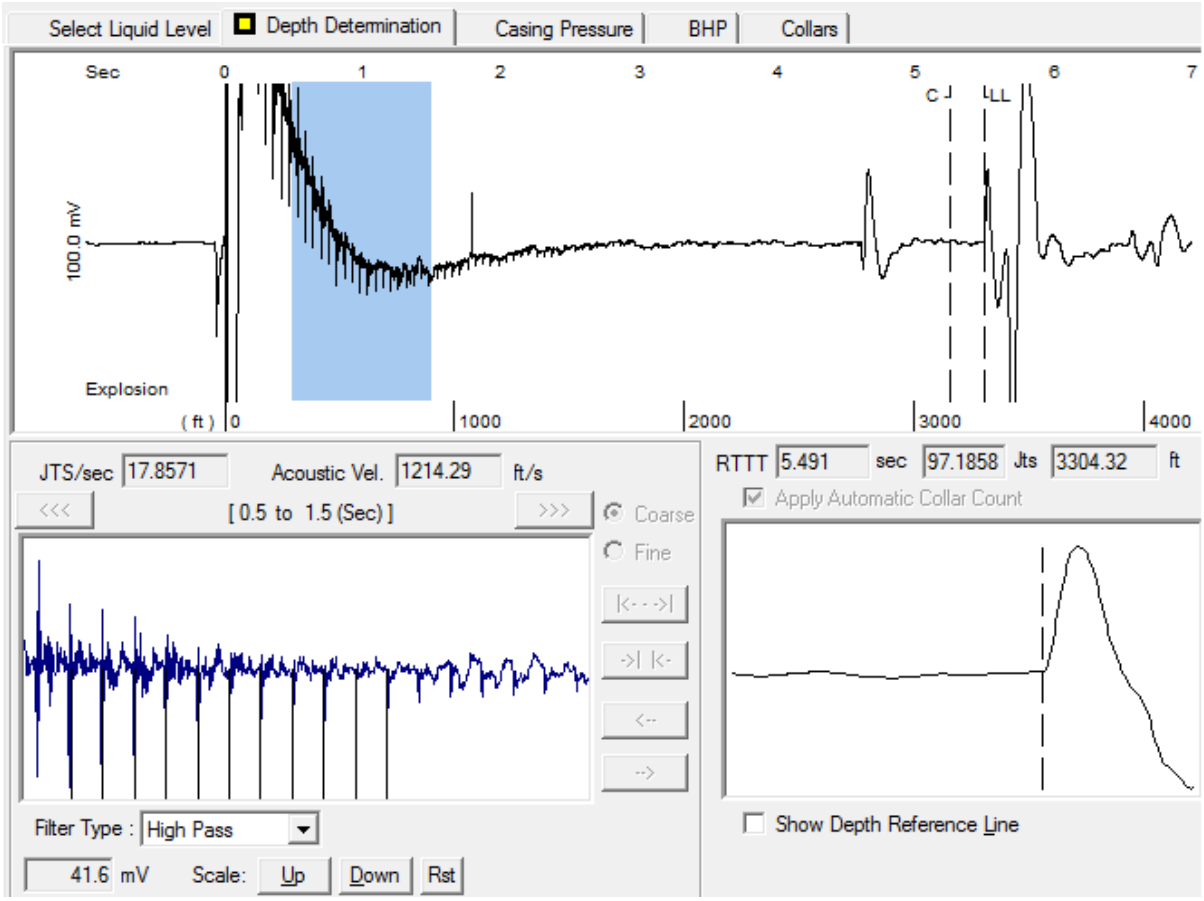

Figure 82: 01/15/2015 HW 1003 Acoustic Test Collars

F. FIELD OPERATION MANUAL ECHOMETER

LIQUID LEVEL TESTING

GUN LOCATION

The location on the well is extremely important to the resolution of the data and the longevity of the testing equipment. If possible the gun should be attached to the top of the well seen on this shale gas well.

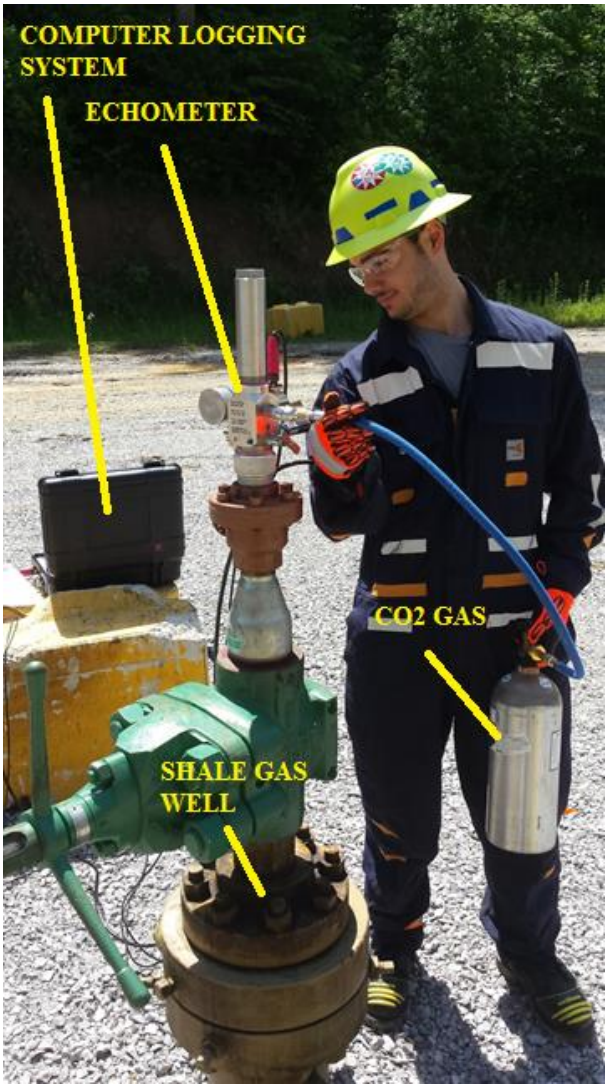

However, this is rarely the case and will have to find a bull plug on the side of the well.

It is important to minimize the distance between the tubing and the well.

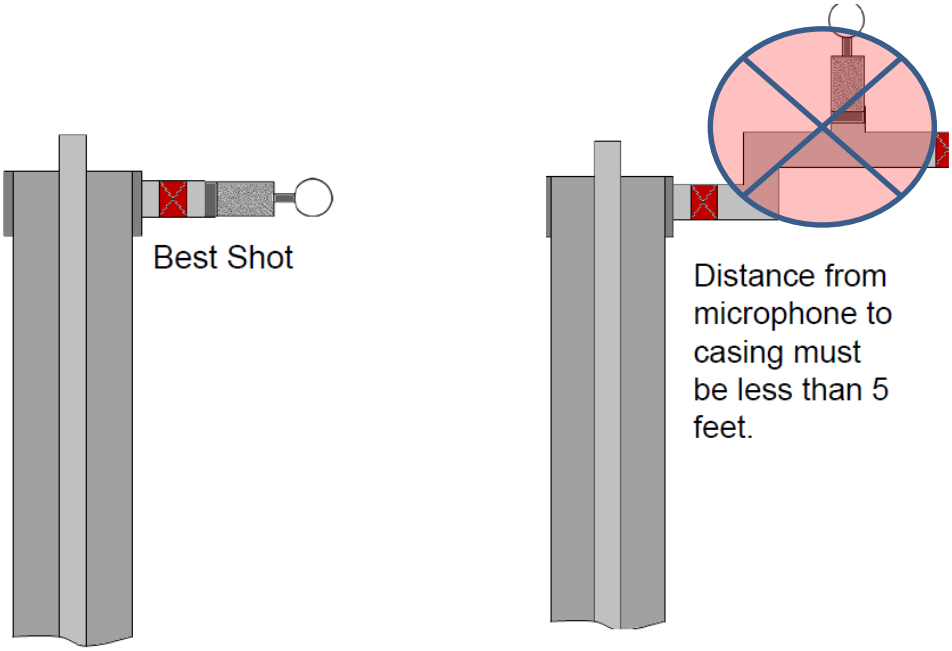

Equipment setup

Remove the bull plug and tighten the echometer gun to the threaded making sure it is clear of grease and debris. The connection should not be tested until the gun is charged! HAND TIGHTEN the pressure transducer only to the echometer gun! Connect all the wiring (echometer to main input on the outside of the box and the microphone from the echometer to the outside of the box). The echometer laptop should be connected to the echometer box by an USB cable. Turn the system on by flipping the switch on the box, a green LED should appear.

1. Start TWM. Select Acquire Mode on the connected laptop

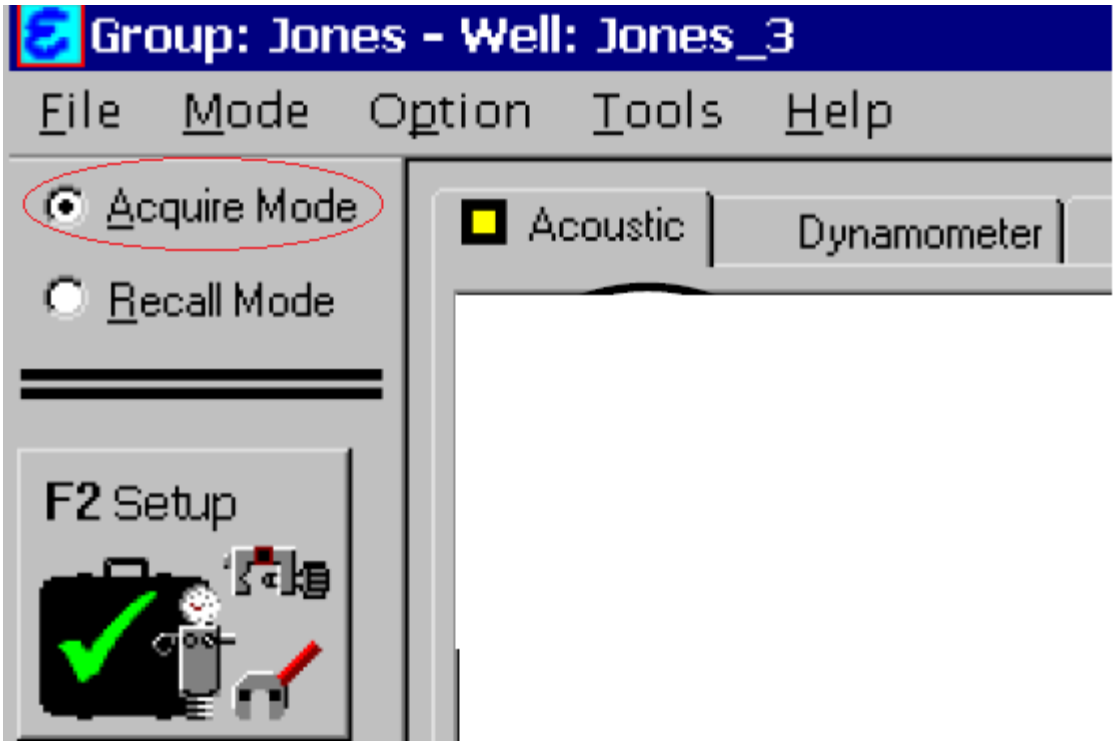

2. Select the serial number of the pressure transducer. It should be preset and there should be NO need to create another one. Use Create New…….if your serial number is not found in the list. Make sure all coefficients are entered as typed on transduce label. Also enter Gun Parameters at bottom (explosion).

This is what the pressure transducer looks like---

3. Start process of zeroing transducer by selecting Obtain Zero Offset button (Alt-3). Once the reading displayed in Present Zero Offset has stabilized press Update Zero Offset with Present Reading button to record this value. (THIS IS IMPORTANT for pressure build up tests)

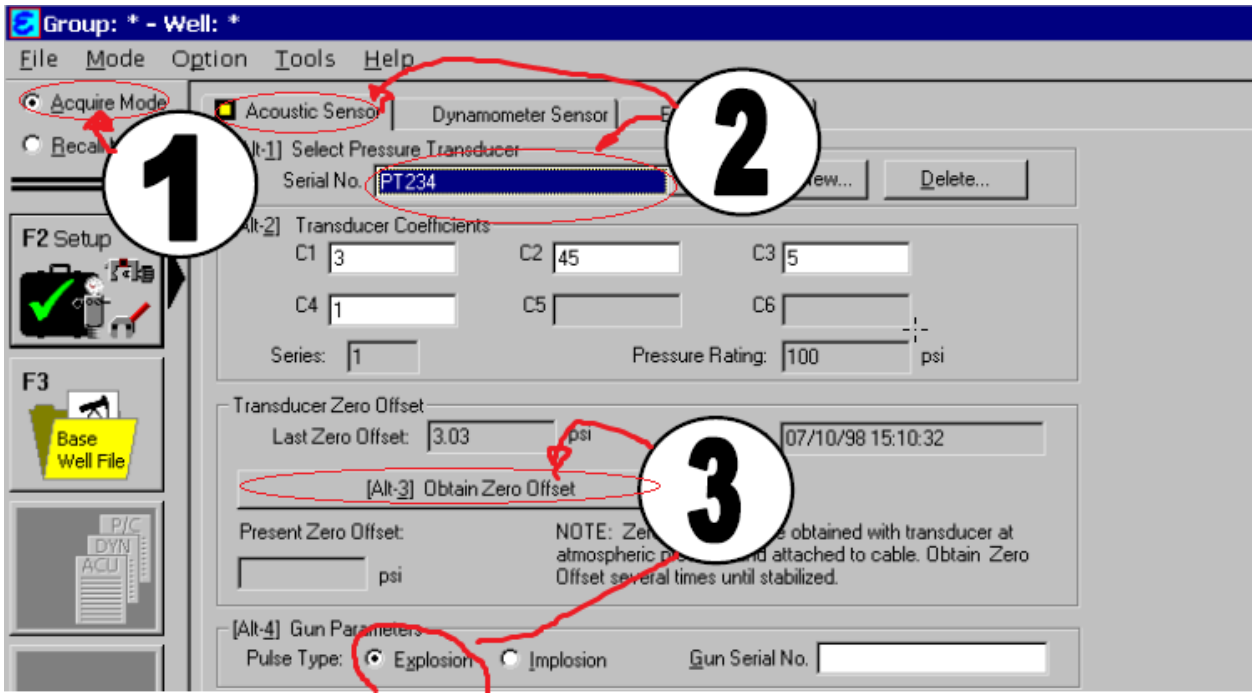

4. Open Base Well File for the well where data is to be acquired. Use New… to create a Base Well File if one does not exist. Be sure to enter at least pump and formation depths.

5. From the "F4" Select Test screen pick the Acoustic Tab to indicate that acoustic test data is to be acquired.

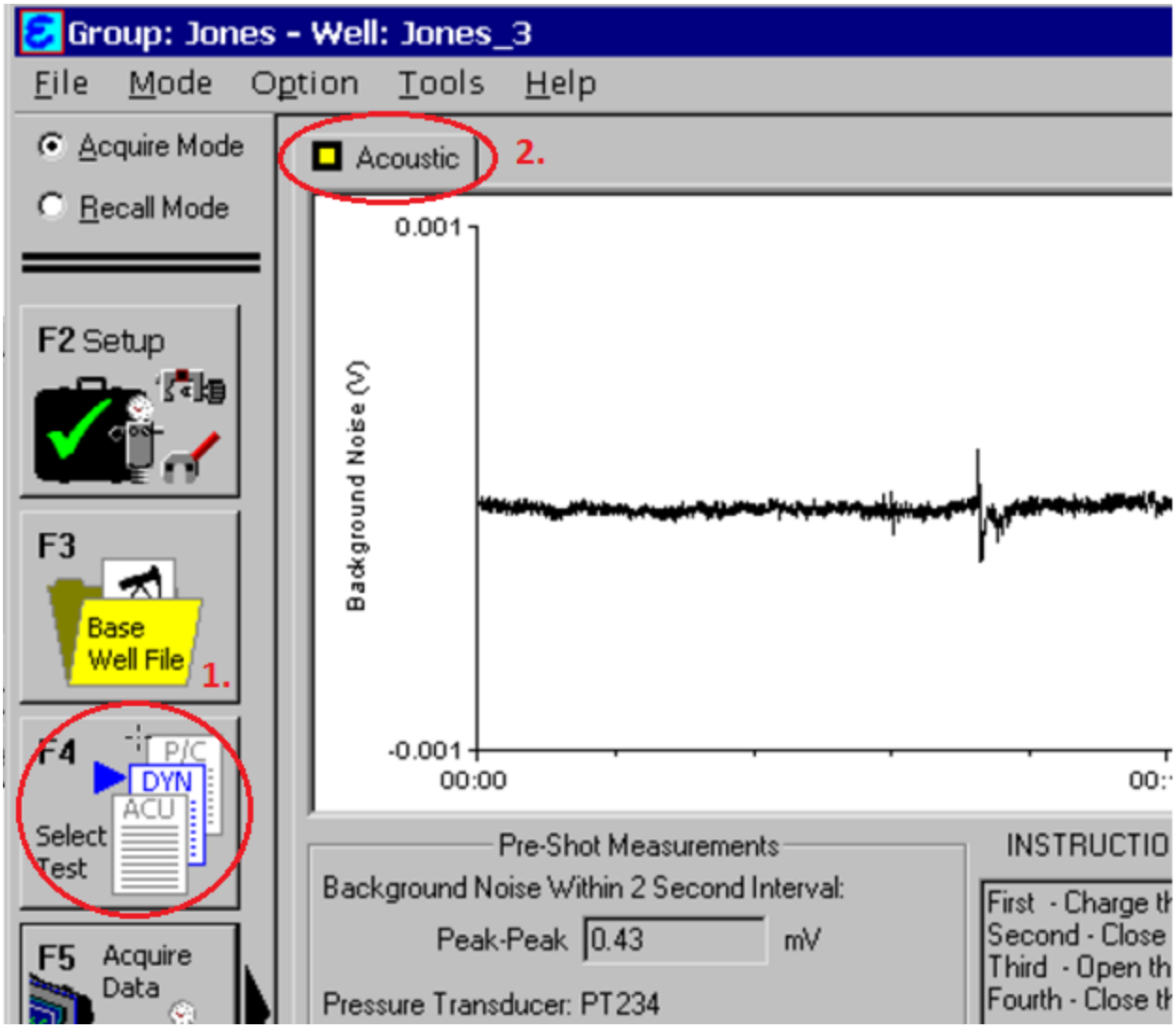

6. Prepare to Acquire Data "F5" by following steps detailed on INSTRUCTIONS panel.

First: Charge Gas Gun to 150 psi over the well pressure. (THIS IS IMPORTANT! If the well is opened to the gun before it is charged the condensates around the well will flow into the gun)

Second: Close the gas gun bleed valve.

(At this time the gun should be checked for leakage)

Third: Open the casing valve between the gas gun and well.
Fourth: Close the casing valve to flowline.

At this point the graph is displaying background noise.

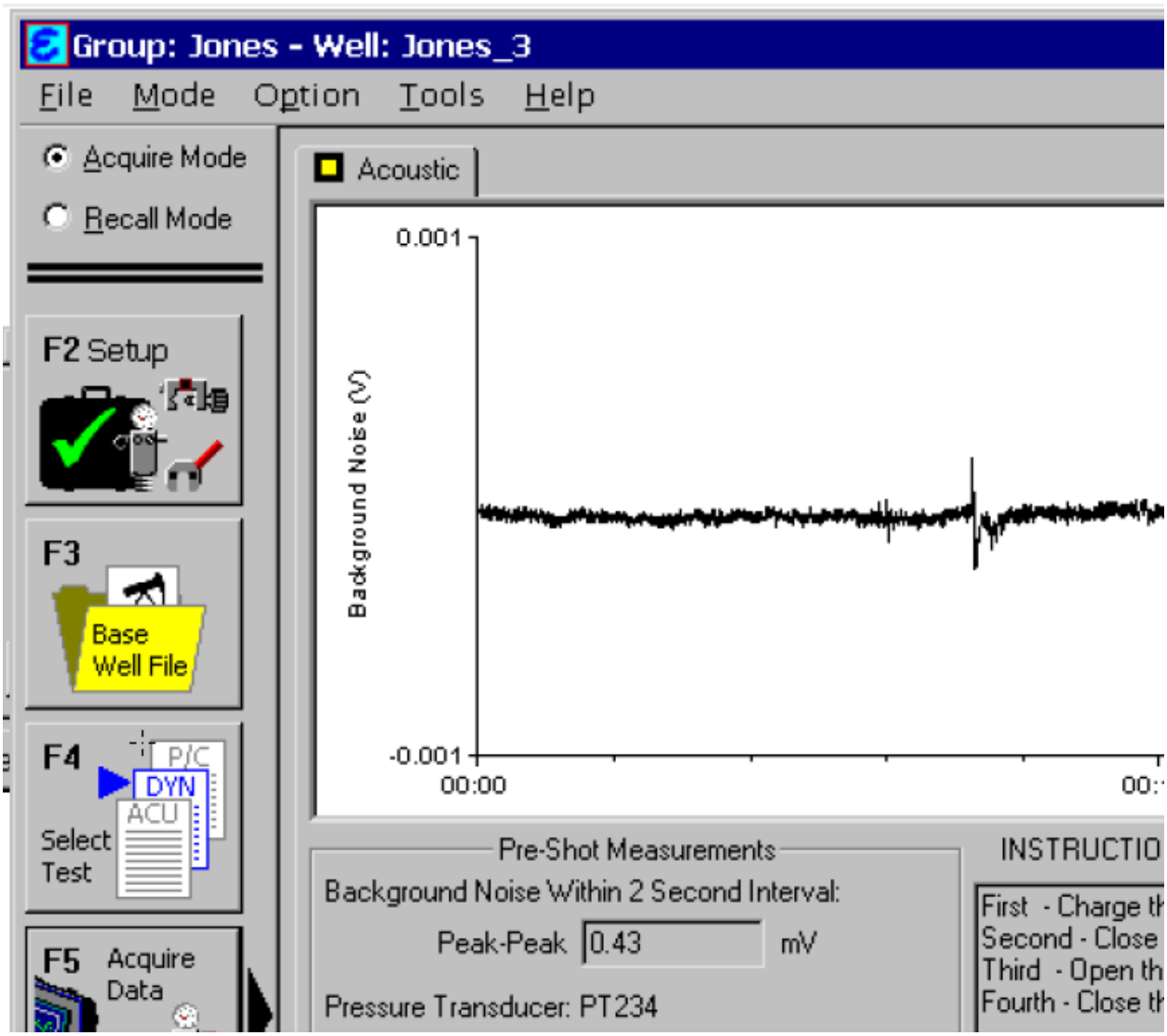

Acquire shot by pressing FIRE SHOT button (Alt-S). The graph will clear as TWM prepares to open the solenoid on the Remote Fire Gun. TWM displays the message “Automatic Gun has Been Fired “ along with a BEEP sound.

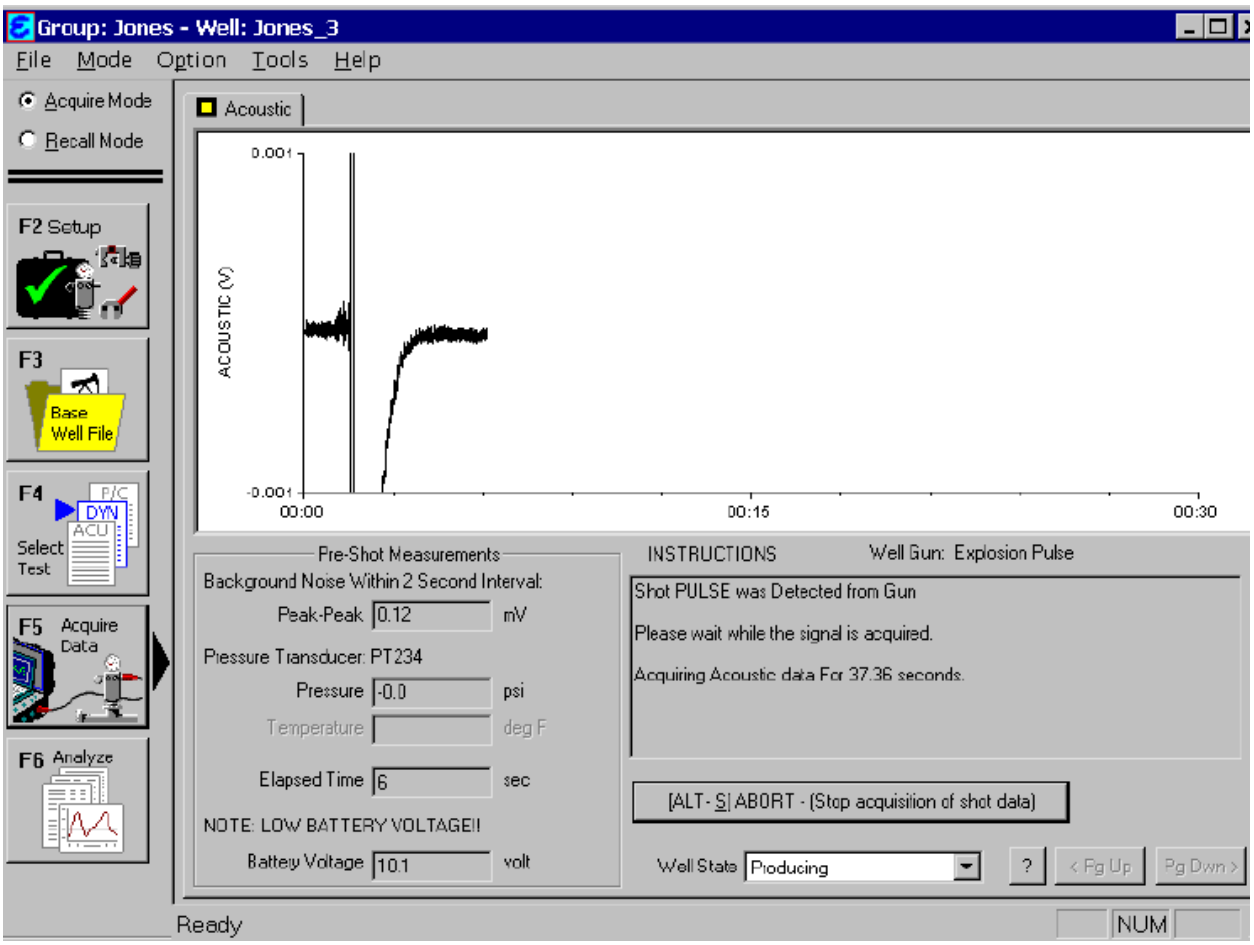

If shot pulse was not detected after the gun was fired press Abort (Stop acquisition of shot data) button, recharge at a higher pressure, go to step 6.

Once the shot has been acquired a Dialog appears. At this point the data can be saved or discarded so another shot can be taken. A brief comment can be entered into the description field. Otherwise, just Enter (press OK) to save the data set. Note once the shot is saved TWM continues to acquire casing pressure every 15 seconds for a maximum of 15 minutes or until manually stopped.

The program will then ask for a description of the shot and comments. Add comments on the psi of the shot and other comments

7. If you are just shooting a liquid and not rendered the data, you're done if the data look good. If not, we'll need to select the liquid level from the data.

Click the "Select Liquid Level" tab and a screen should appear.

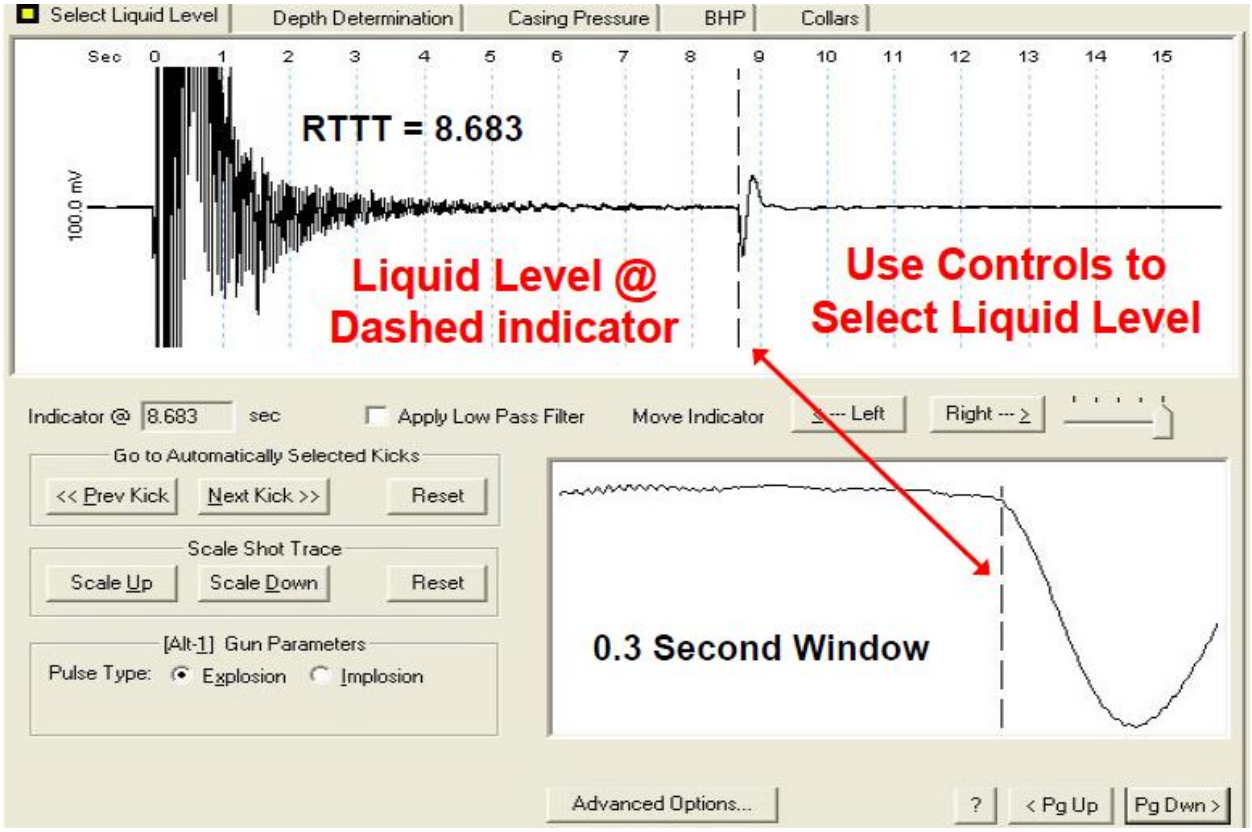

Most of the time, the software will select what it thinks the liquid level is located. To move the liquid level click the "Right ---- or ------Left" button. The slide bar to the right adjusts the magnitude of the movement. The viewing screen on the bottom is a magnified view of the top display

Important things to note----

- A reflection surface is a downward kick
- An enlargement in the well bore is an upward kick
- Reflection surfaces may echo in equal intervals
- Increasing the PSI of the gun does not increase resolution of the sample

Two methods for calculating the liquid level depth

- Acoustic velocity—uses the composition of the wellbore to calculate the propagation of the explosion wave to the liquid surface and back. On the bottom of the screen below, "Analysis method" to acoustic velocity. Then click, "enter or compute the velocity". The program will ask for various gas compositions of the well and then generate a velocity. This method is useful when the tubing has been removed from the well or the reflection surfaces of the collars are poor.

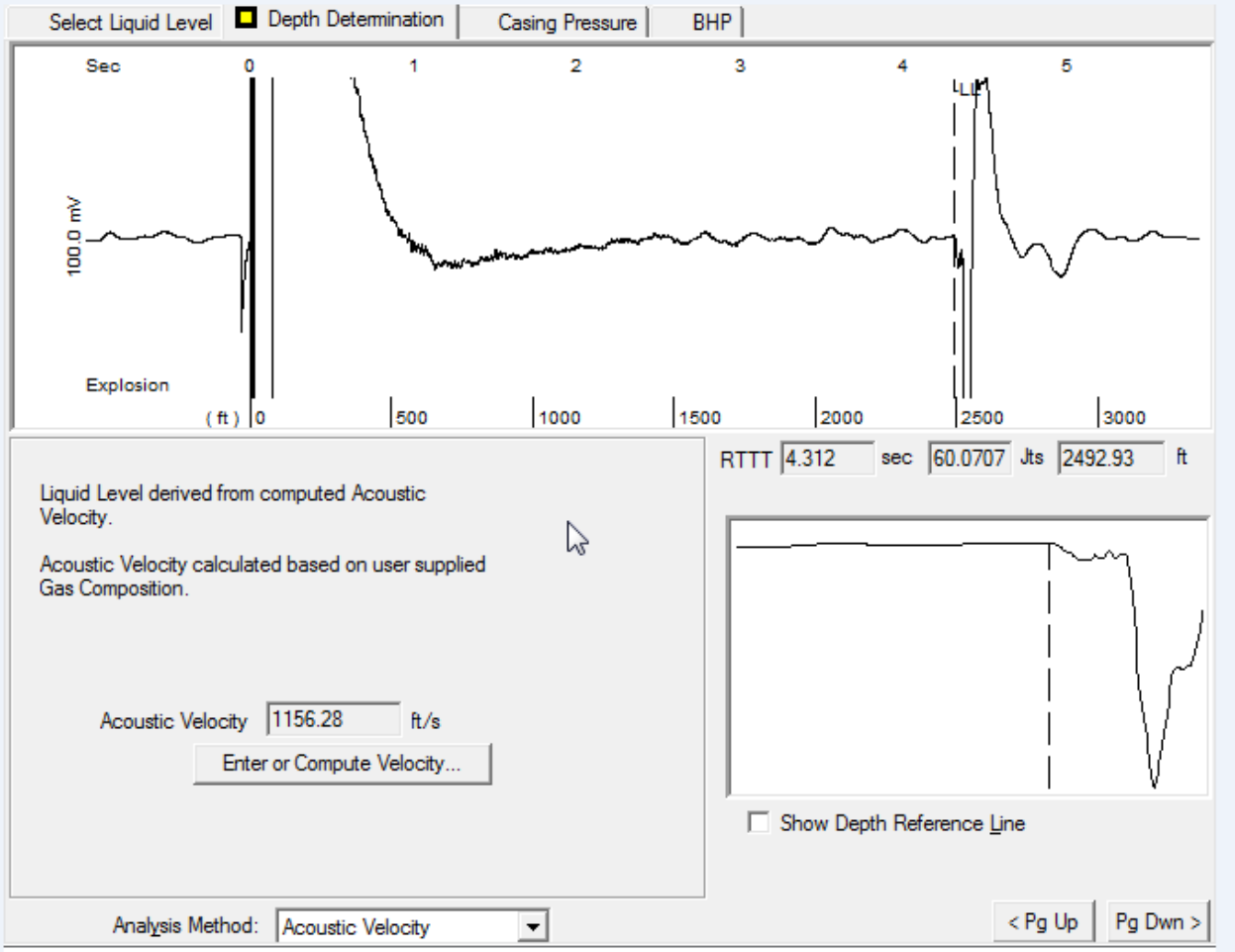

- Collar counting—utilizes the reflection surface between the tubing and the joints of a known distance over a known time to calculate a velocity. Below, the software has counted 61 joints of a known distance of 32

feet. It then extrapolates, the velocity to the reflection surface.

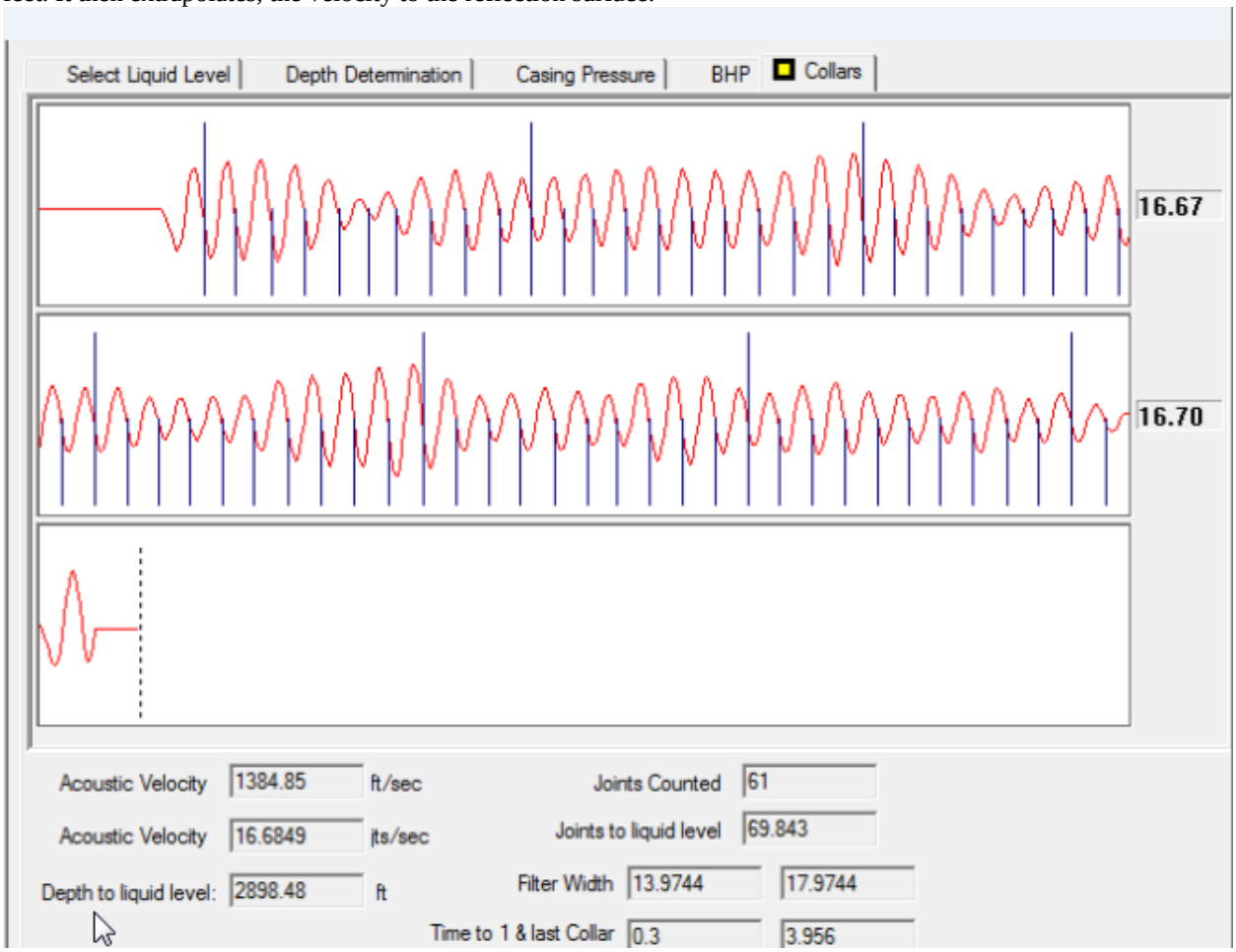

Some general tips and tricks.

- Make sure the well is closed to production and the value between the echometer and the well is open.
- Stepping on the microphone cable causes noise!
- Make sure the echometer is tight in the casing.
- Do not over tighten the pressure transducer
- The laptop that runs the software is set to never turn off. So if you close the lid, it will not turn off. The battery will die before you get to the field.
- Make sure your echometer box is charged and you have enough CO2 to complete all the testing in the field.

PRESSURE BUILD UP TEST

Connect all the wiring. HAND TIGHTEN the pressure transducer only! Turn the system on.

1). Start TWM. Select Acquire Mode.

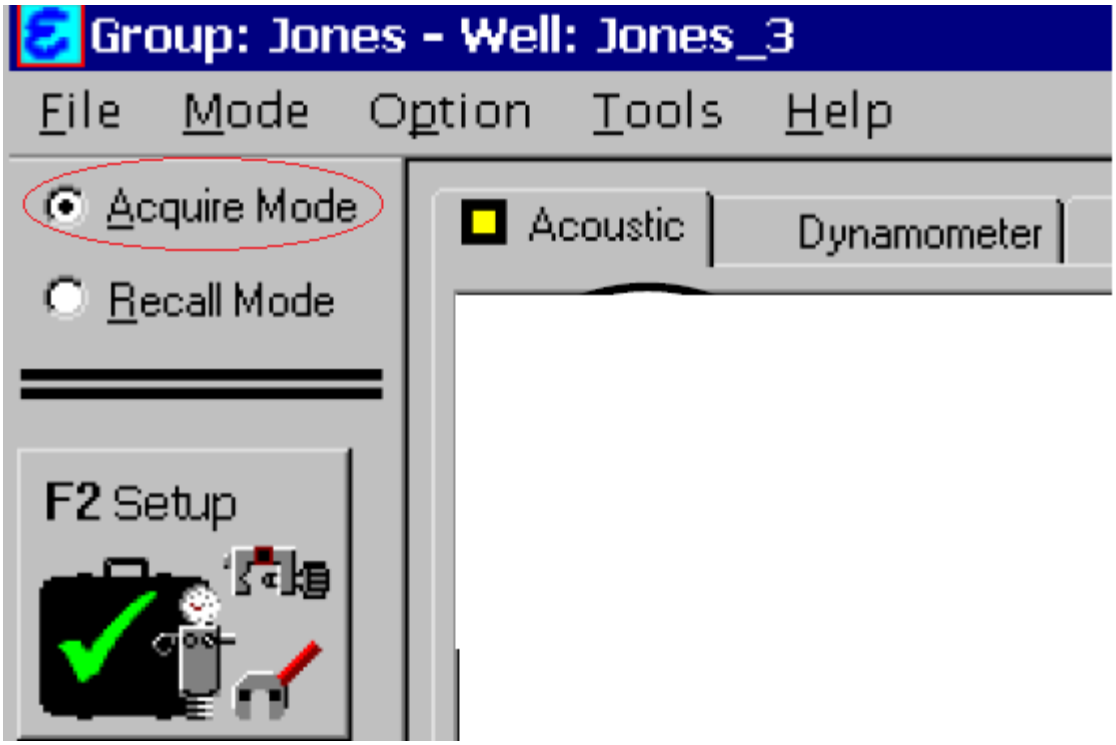

2) Select the serial number of the pressure transducer. It should be preset and there should be NO need to create another one. Use Create New…….if your serial number is not found in the list. Make sure all coefficients are entered as typed on transduce label. Also enter Gun Parameters at bottom (explosion).

This is what the pressure transducer looks like---

3) Start process of zeroing transducer by selecting Obtain Zero Offset button (Alt-3). Once the reading displayed in Present Zero Offset has stabilized press Update Zero Offset with Present Reading button to record this value. (THIS IS IMPORTANT for pressure build up tests)
4) Select the appropriate well file
5) Under the Select test tab---- click pressure transient. Make sure that "Apply Gaseous Liquid Column Correction factor" is checked

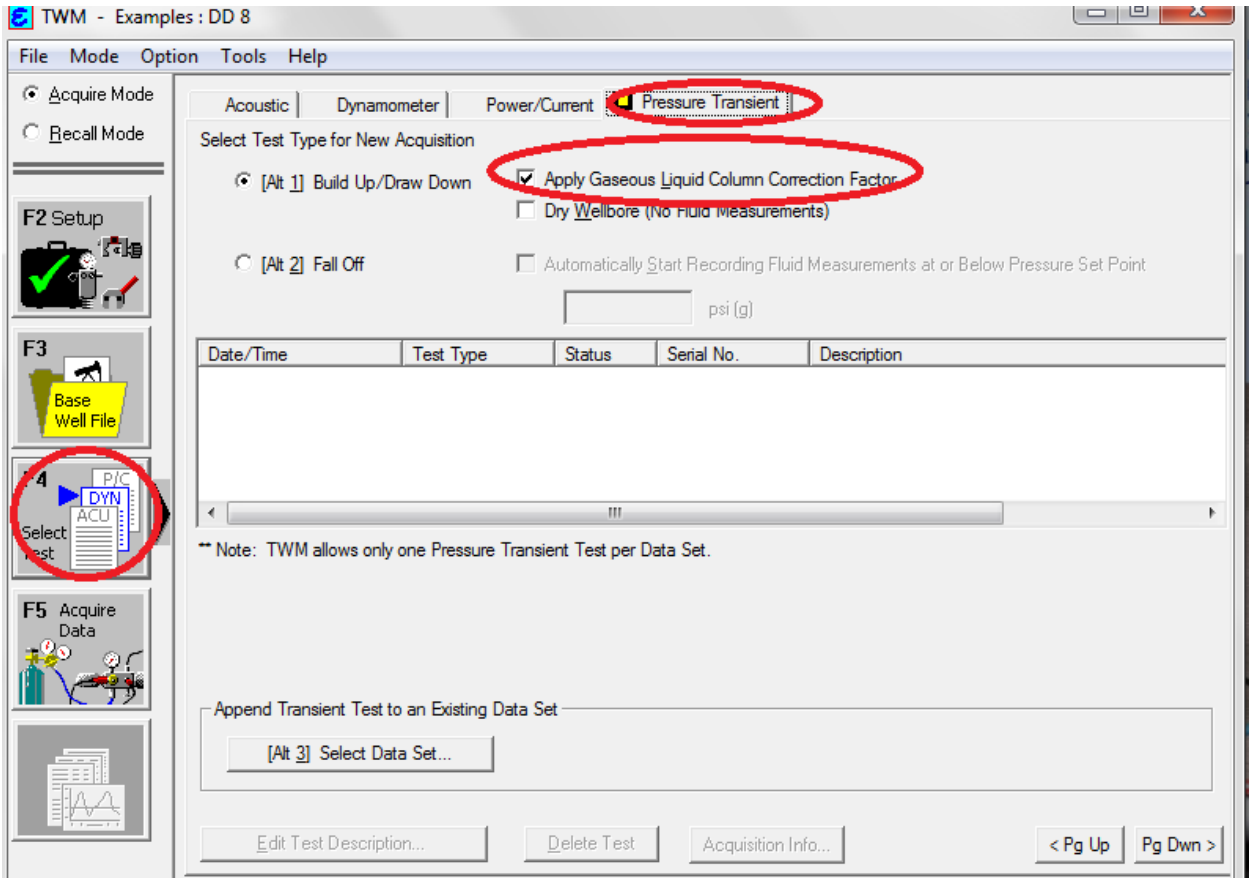

6) Click the acquire data. Now we have a couple of choices that need to be decided. First is the length of time required for the buildup test--- From the testing at Buchannan CNX wells 200 -300 minutes is enough to create a HORNER PLOT, which will be discussed later. The advantage of these well sites is that there is 3 phase power on all of the wells. Which translates to the power consumption of the echometer is not an issue over the testing period. Therefore, I prefer linear shot schedule. This is not the norm for a buildup test (log).

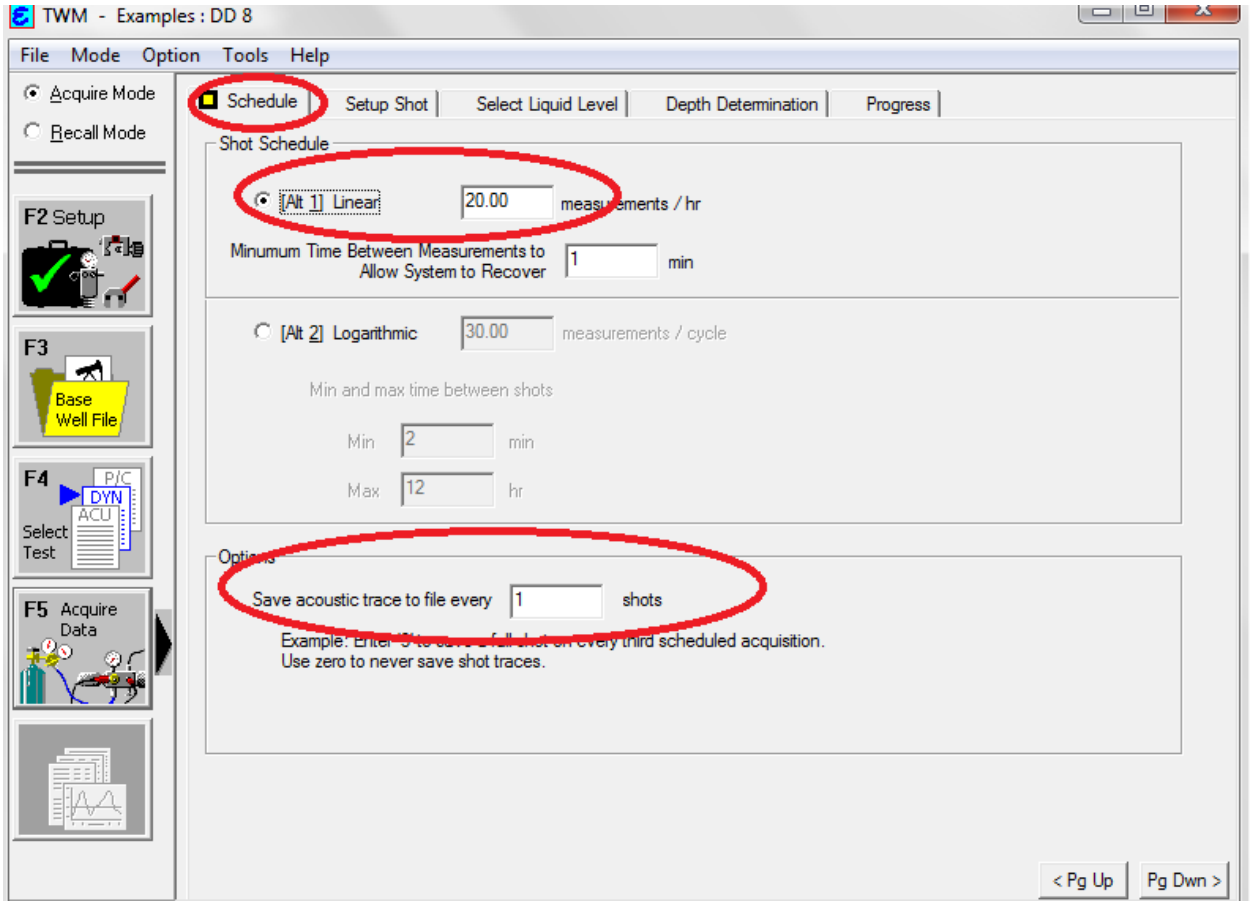

The other option is the acoustic trace or liquid level tracking. If you are sitting at the well the setting of 1 is perfectly fine, you just need to charge the gun when you want to the echometer to shot a liquid level. Liquid level tracking is important for a couple reasons. Let's look at the

buildup below.

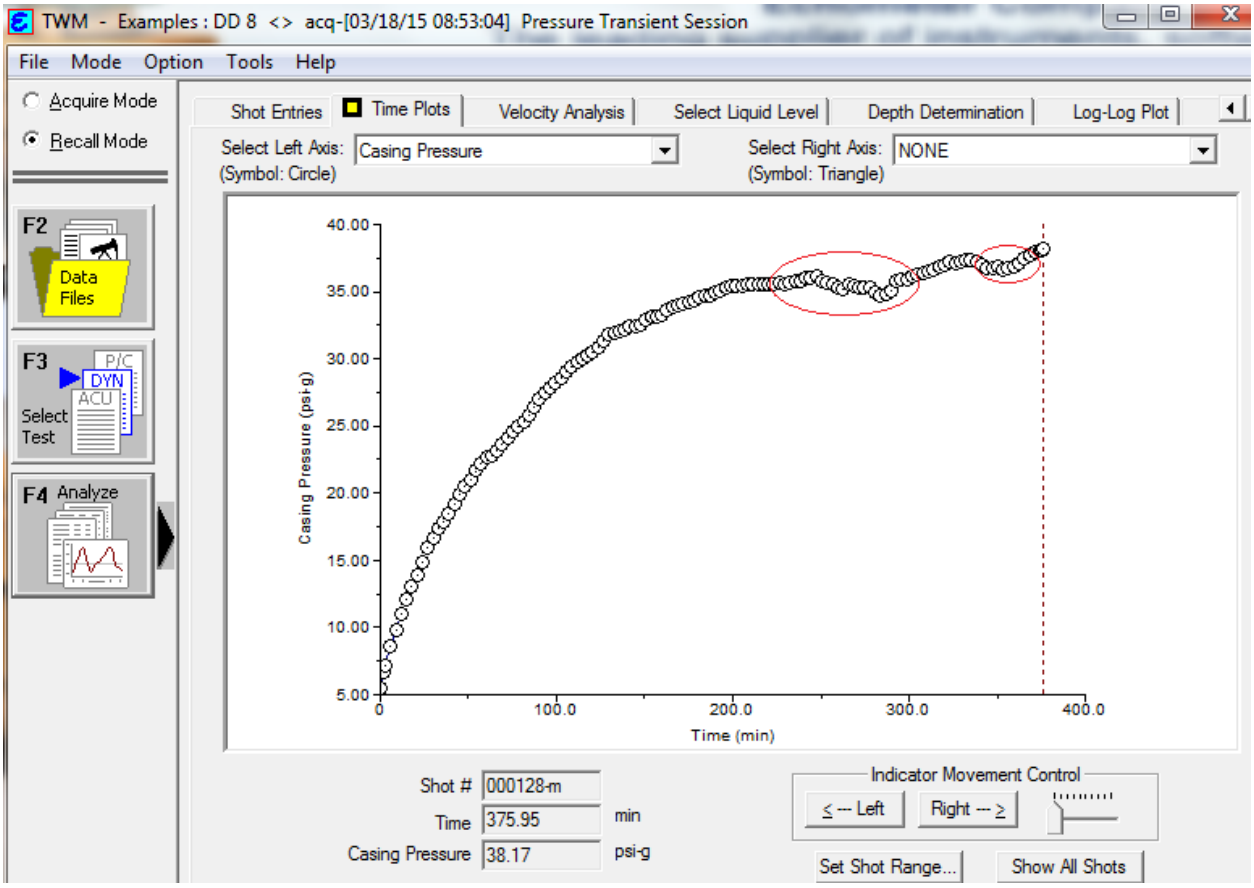

I've circled two regions on the buildup for examination. These are the pumping cycles of the well. If you want to shoot a liquid level every hour just change the scheduling and hook up the automatic gas hose and set the pressure of the gun.

7) A baseline liquid level will need to be shoot before the transient test can start. In the previous step, we have step the scheduling for the test. We need to follow the tabs over in that order.

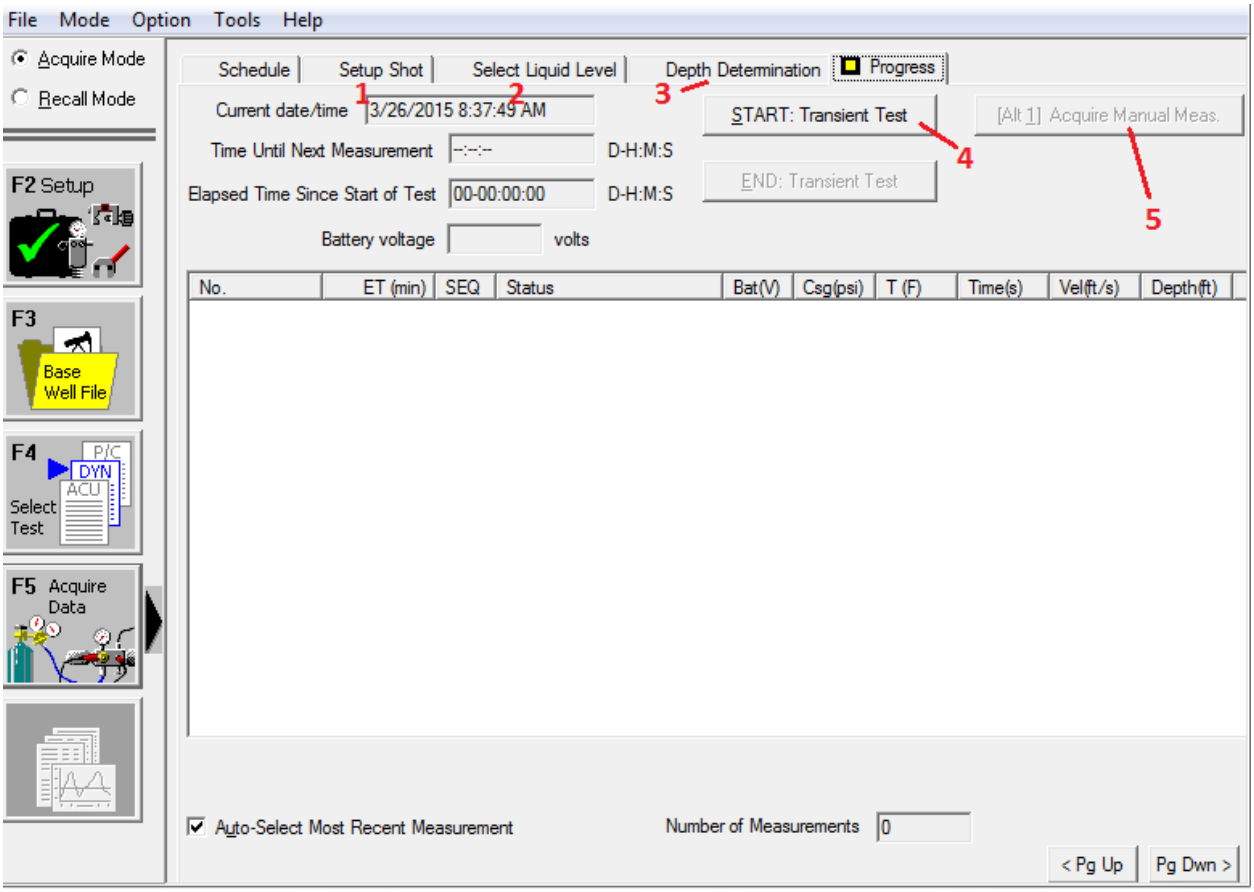

1) Setup the shot and shoot it just like you would the liquid level test
2) Select the liquid level and the software will attempt to match all the remaining shots to the reflection in that area
3) Depth determination is just a rendering of the depth and will give a basic layout of the well and parameters
4) Start the test
5) Allows you to manually acquire data. Just click the button if you see a major change in the pressure.

8) End the test and view the log log plot. We can calculate the permeability using the horner plot method.

$$k(md) = 162.6\,\frac{(Production\ STB)(Formation\ Volume\ Factor)(viscosity\ of\ the\ gas)}{(Thickness\ of\ the\ target\ areas\ ft)(slope\ of\ \frac{psi}{cylce})}$$

G. MICRO CT SCANNER FIELD OPERATION MANUAL

The coal received from Consol is in core sample boxes that contain samples of varying RQD (rock quality designation). Various samples from multiple seams were taken from multiple elevations. All of the grab samples are not intact enough to warrant testing. Choice samples were taken and cut to length with a diamond saw. The sample were then dried and wrapped in plastic wrap to protect against coal dust in the micro CT scanner.

The samples are then mounted on the staging area of brass. The machine, SkyScan 1172, is switched to the "on" position via the use of a key on the side of the machine and then to start like the action of starting a car after the computer is turned on and password "handlewithmorecare".

The shielded door can now be opened through the use of the Windows-based program SkyScan1172 which is located on the desktop of the computer to the right. If the computer is password protected. Enter "handlewithmorecare" to gain access to the desktop.

After the program is started, an initialization window should appear on the screen. The start image on the screen contains the main menu bar, the control bar in the top of the screen, and the status bar at the bottom.

A basic description of the major components used in the command bar is listed in the table below.

Basic Icons for SkyScan µCT scanner

	*Starts the X-ray Tubes*
	*Open/close the door (will stop other processes ie charging of the X-ray tubes)*
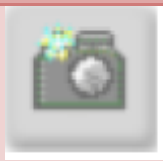 or 	*Get one image from the X-ray camera using the acquisition settings* *Continuous imaging from the X-ray camera*
	*Activates or deactivates the image from the visual camera inside the system in the object stage*

It is best to activate the internal camera, which is the light bulb, and then open the chamber to make sure that the chamber is in fact empty. The X-ray tubes need to be charged to apply the correct amount of energy to the specimen. This process normally takes 15 minutes if the machine has been used in the past two months. If not it will take 45 minutes. The charging process may not be interrupted or the charging cycle will start over.

Once the specimen is safely inside the chamber the voltage should be ramped up to 100 kV. This may be achieved through clicking the source indicator which will pop up the X-ray tube window.

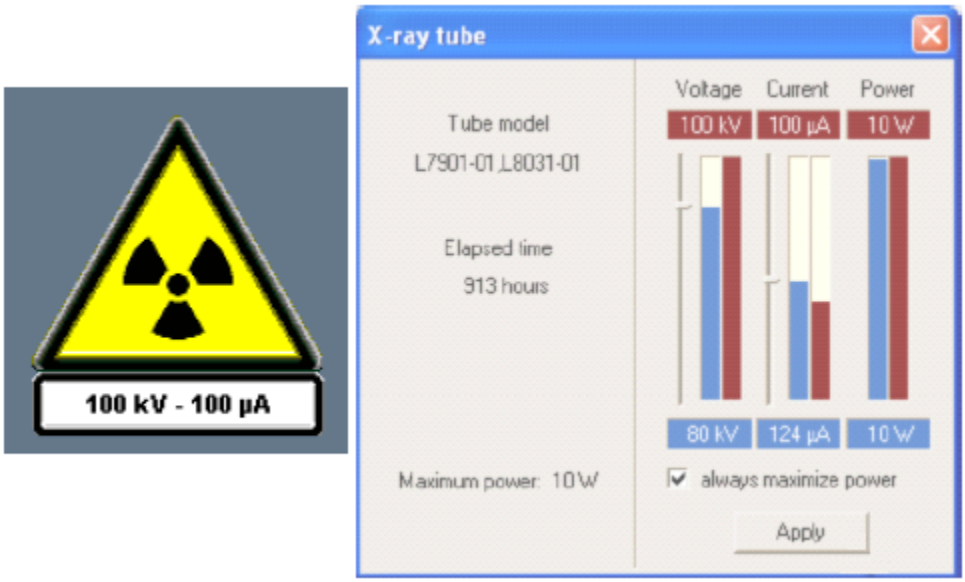

A greater voltage is applied to the sample to penetrate the oversized sample of the coal. It is larger than what is typically inserted into the machine and requires long scanning times and large amounts of energy.

With every scan there is an option of applying filters. When the object is positioned in the right place for scanning it is important to select the optimal filter. The selected filter will be placed in front of the camera. This allows changing the camera sensitivity for polychromatic X-

ray radiation from the source. The no filter option is typically used for objects with a low X-ray absorption, thus small samples or materials compositions with a low average atomic number. Different metal filters can be used to cut the low energy X-ray radiation, which will reduce the nonlinear X-ray absorption in dense materials which causes a phenomenon known as beam hardening (The surface layer of the dense sample works as an X-ray filter for the rest of the sample. This reduces information from the middle of the dense sample and distorts the reconstruction density distribution.). To counteract this process the addition of a 0.5 millimeter aluminum filter and copper filter is applied as seen in the figure below (figure is not representative of the machine in question).

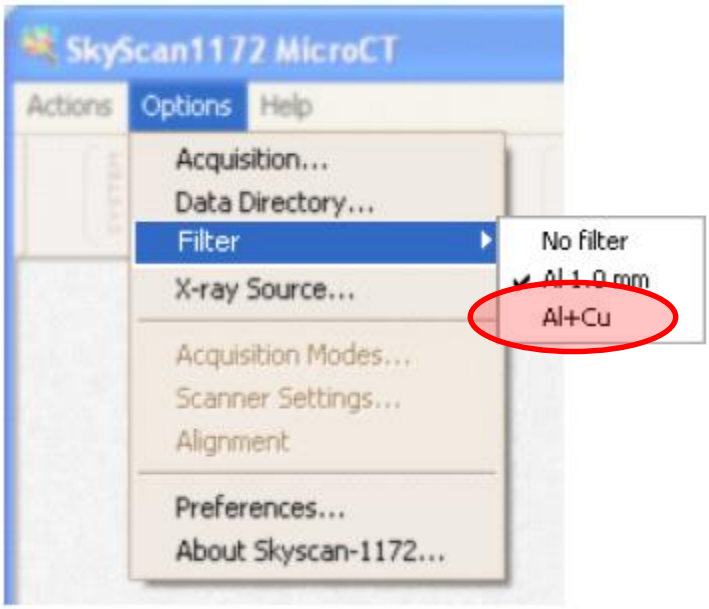

Filter selection

Now that all the appropriate measures were taken to ensure that the scan will yield useable results, we can start the scan setup. Under the “actions” tab, click “Start Oversize scan”. A dialog box will appear with most of the clickable options in grey. The only option available will be the start button at the top of the dialog box. Once clicked, Skyscan will start taking wide image photos of the sample in question. It will continue to down step photos until the maximum

length of travel is complete. The prefix box should now be open and blank. Fill in this box with the desired name for the scan followed by an underscore. For all of the samples of coal, the name corresponds with the elevation depth of the grab sample. The end of the name must be followed by an underscore otherwise the scan will not run correctly. For example a coal from elevation 2282 feet would be named, 2282_. Two more buttons ("top", followed immediately by "bottom") become available after the prefix has been named. The top of the scan and the bottom of the scan limits must now be selected for the sample. If the boundaries of the scan are too large for a single scan, the software will break up the scanning into segments. This is important in calculating scanning time. Click on the photo to the left to denote the top and bottom limits. Next, click "start scan" and this acquisition box should appear as seen in the figure below .

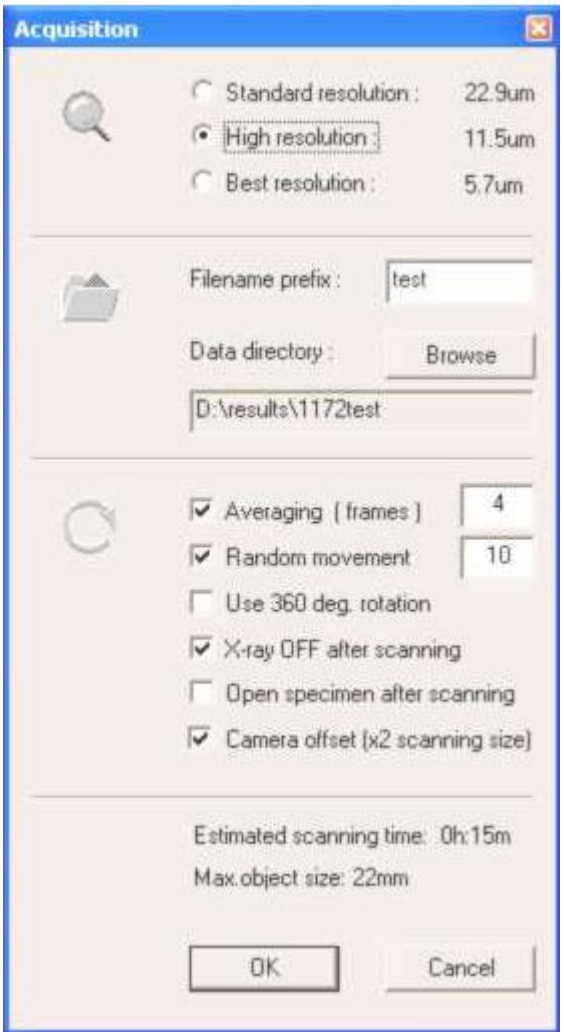

Acquisition Dialog box

The top most tier of the acquisition box is based on the resolution. NOTE: if you select a resolution less than 10µm the core (1.875" diameter) will come in contact with the X-ray plate. For most samples I set the initial distance to the X-ray to 22.9 µm and then the best resolution option is 11.4µm. To change the distance to the scanner you can double click on the bottom tool bar or slide the toggle as seen in the figure below.

Status bar

The file prefix name should be predetermined by the name you gave the oversize scan. Make sure you create a file to store all the .tin files. There will be a lot of files. The next section

is extremely important to understand what is actually going on in the scanner. Below is a table to explain each of the setting and the normal conditions I run samples at.

Rotation Step	*The change or movement in angular measurement between scans*	(0.2-0.8)
Averaging	Allows to improve the image quality by averaging of several images in every angular position. The value is given in number of frames and taken at the exposure time. Increasing the number of frames will increase the quality but makes the acquisition longer.	(8)
Random movement	Can reduce ring artifacts in the reconstruction cross sections, but will increase scanning time, especially in low magnifications.	(8)
Use 360 Degree	Rotation can reduce asymmetrical artifacts from dense objects across the surrounded low absorption material. This mode will increase the scanning time near twice.	(not checked)
X-ray off after scanning	Defines that the X-ray source will be switched off automatically after the acquisition cycle.	(checked)
Open specimen after scanning	The chamber will open after scanning cycles	(not checked)
Camera Offset	Allows to increase the horizontal field of view twice by scanning the object be two acquisition cycles with offset camera positions. It will take twice the scanning time and increase the size of the projection files into two views. After two acquisition cycles	(checked)

	with the camera offset in different positions the projection images will be created by combing all pairs of the images from identical projections angles to the wide projection images which are used in the reconstruction process.

The software will give you an estimated time for completion. This estimation is for each of the segments of the scan. Therefore, if multiple segments are present the estimated time of completion is number of segments multiplied by the time needed to scan.

Once the scan is complete, open NRecon. SkyScan's NRecon package is used to reconstruct cross-section images from tomography projection images, mainly the cone-beam X-ray projections. The algorithm implemented is the Feldkamp algorithm. The native SkyScan data are recognized automatically and can also reconstruct non-native tomography data. NRecon is used in conjunction with NReconServer, which will start automatically.

Upon starting, NRecon will ask for a data set. Find the folder that the data was saved in and double click any of the .tif files. NRecon will open the entire data set. In the tabs to the left are: the current position, which is the middle of the sample, top, bottom, and step. The first step should always be to preview the scan in question. The preview will determine if the sample needs a color ramp or the RU values need to be changed. The standard is color set one, on inverse, which will have the densest material in black and less dense material in blue and green tints. There are other optimizing options that include smoothing, misalignment, ring artifacts, beam-hardening, CS rotation, undersample, defect pixel masking, and reconstruct 180 +only. This may be optimized through the use of the preview tool.

Set the output to the desired folder and set the step size(in mm). The reconstruction may now be started.